DETERMINATION OF ATMOSPHERIC PARAMETERS BY ACOUSTIC MEANS

Progress Report No. 1

July, 1962

Prepared in partial fulfillment of

Grant Agreement DA-SIG-36-039-62-G17
Office of the Chief Signal Officer
Research and Development Division
Washington 25, D. C.

Under the Supervision of

THOMAS G. BARNES, Physicist
Principal Investigator

CARLOS McDONALD, Physicist
Project Director

SCHELLENGER RESEARCH LABORATORIES
TEXAS WESTERN COLLEGE EL PASO, TEXAS

DETERMINATION OF ATMOSPHERIC PARAMETERS BY ACOUSTIC MEANS

Progress Report No. 1

July, 1962

Prepared in partial fulfillment of
Grant Agreement DA-SIG-36-039-62-G17
Office of the Chief Signal Officer
Research and Development Division
Washington 25, D. C.

Under the Supervision of

THOMAS G. BARNES, Physicist
Principal Investigator

CARLOS McDONALD, Physicist
Project Director

SCHELLENGER RESEARCH LABORATORIES
TEXAS WESTERN COLLEGE EL PASO, TEXAS

CONTENTS

DETERMINATION OF ATMOSPHERIC PARAMETERS BY ACOUSTIC MEANS

Progress Report No. 1

July, 1962

INTRODUCTION

CARLOS MCDONALD, Physicist

Project Director

INTRODUCTION

This progress report is a summary of research studies and associated developmental activities performed by the Schellenger Research Laboratories, Texas Western College, El Paso, Texas, under the U. S. Army Signal Corps Grant Number DA-SIG-36-039-62-G17, "Determination of Atmospheric Parameters by Acoustic Means," during the period from November 14, 1961, to June 25, 1962.

In accordance with the proposed program, during this initial period of the studies emphasis was placed on

1. Survey of Literature (Sec. I-1);
2. Theoretical and experimental investigation of problems inherent in performing acoustic measurements in the upper atmosphere by means of devices on moving platforms (Secs. I-2, I-3, I-4, and I-5);
3. The theory, design, development, and testing of an air-borne acoustic interferometer (referred to as the "Sonotherm" in this report) for performing local acoustic measurements in the upper atmosphere (Secs. II-6, II-7, II-8, and III-10).

The air-borne acoustic interferometer, or Sonotherm system presently under development (Secs. II-7, II-8) is based on a theoretical study (Sec. II-6) and previous work performed at Schellenger Research Laboratories. Theoretical and experimental results (Secs. II-6, III-10) indicate that, with the Sonotherm system, local upper atmospheric acoustic measurements of sound velocity, sound absorption and acoustic impedance are

possible up to altitudes of at least 150,000 ft. From these measurements, atmospheric temperature, density or pressure, and viscosity effects can be determined. Also, due to its construction, its compactness, and its simple electronic circuitry requirements, it is suitable for either balloon-borne or rocketsonde applications.

In conjunction with the development of the Sonotherm system, theoretical and experimental studies were made on the various effects which could reduce the accuracy of the acoustic measurements by the Sonotherm or any other air-borne acoustic device. The effects investigated included:

1. Sound dispersion and non-ideal gas effects (Sec. I-2);

2. Thermal and radiation effects by the sound transducers on the acoustic measurements (Sec. I-3, I-4);

3. Thermal boundary layer effects on the acoustic interferometer measurements (Sec. I-5);

4. Wind and altitude effects (Sec. II-6, part 3).

From the above studies, not only were the magnitudes of the various effects on the performance of the Sonotherm determined, but they also indicated various ways by which the above effects could be minimized or eliminated.

Environmental testing of an experimental Sonotherm system was performed in the Schellenger Research Laboratories' climate chamber (Sec. III-10) in order to determine the Sonotherm's ability to measure the desired acoustic parameters under the expected environmental conditions, and also to verify and determine the various effects described previously. One of

the problems encountered in environmental testing was the need of a reference device to measure the air temperature accurately at low atmospheric pressures. As a result, an acoustic thermometer is under development (Sec. II-9) for use in the environmental chamber. At the same time, there is a possibility that it can be adapted for balloon-borne temperature measurements in the upper atmosphere.

The sections which follow contain detailed reports of the theoretical and experimental studies summarized above. An abstract of each report is included below:

Section I-1. Survey of Literature in the Field of Atmospheric Acoustics By Richard C. Montgomery.

A review of literature pertinent to the field of atmospheric acoustics is summarized. The historical development of acoustic means of investigating gas properties is discussed, and recent developments of acoustic devices for measuring temperature in the upper atmosphere are reviewed.

Section I-2. Nonideal Gas and Dispersion Effects on the Speed of Sound By E. Alan Dean.

The speed of sound in air is investigated. The nonideal gas effect and the dispersion due to vicsothermal and rotational absorption is formulated. The neglection of the effect of water vapor, due to both a change in molecular mass and the excitation of oxygen vibration, limits the formulation to low humidity regions above the tropopause.

Section I-3. Thermal and Radiation Effects on Acoustic Measurements in the Upper Atmosphere - By R. C. Montgomery.

A study is made of the heating effects of the transducers of airborne acoustic devices on moving platforms. It is assumed that the transducer can be treated as a flat plate, and the equations describing the boundary layer development and their heat transfer coefficient are derived. Computations are made for several different cases, to show the relations between the transducer temperature and altitude, reflection coefficient, and other parameters. Finally, equations are derived to find the variation of transducer temperature with the parameters generated by certain atmospheric models and fall rates.

Section I-4. Numerical Analysis of Heat Balance Equation - By H. Launspach, Jr.

The temperature history of the transducer element of the airborne acoustic interferometer (Sonotherm) was obtained from a differential equation representing the transducer temperature as a function of time. After investigation of simplified heat balance equations, the differential equation was solved numerically by the Runga-Kutta method with the aid of the Bendix G-15 digited computer. Results of simulated balloon flights up to 155,000 feet altitude and simulated parachute flights from 220,000 feet to 5,000 feet altitude are given in graphical and tabular form.

Section I-5. Thermal Boundary Layer Effects on the Sonotherm Acoustic Interferometer - By Eyung-Wha-Kang.

The sound propagation between the transducers of the Sonotherm acoustic Interferometer is analyzed when thermal boundary layers are present on the transducer faces. Exact and approximate expressions, in

terms of specific acoustic impedance, are derived for determining the maximum receiver sound pressure as a function of sound frequency, thermal boundary layer thickness, and the temperature difference between the air and the transducer faces. It is determined that a knowledge of the sound frequencies, corresponding to two successive sound pressure maximums on the receiver face can be used to determine the temperature of the undistributed air medium and the thermal boundary layer thickness.

Section II-6. Air-borne Acoustic Interferometer (Sonotherm) for Atmospheric Measurements - By Carlos McDonald.

An airborne acoustic interferometer (Sonotherm) for performing local acoustic measurements in the upper atmosphere is theoretically described. Unlike typical interferometers, the spacing between the sound transducers is held fixed while the sound frequency is varied. The standing wave sound pressure as a function of frequency is related to the speed of sound, sound absorption and acoustic impedance. Relations between the acoustic, mechanical and electrical characteristics are derived. Thermal, wind, and altitude effects on its operation and accuracy are analyzed and determined. Due to its inherent compactness and simplicity, it is suitable for balloon or rocketsonde applications. It is estimated that local speed of sound measurements, corresponding to a temperature determination to within one degree, can be made up to altitudes of 65km.

Section II-7. Preliminary Design and Development of the Sonotherm Flight Unit - By Paul Dano

The preliminary design and development of the Sonotherm flight

unit is summarized. It includes a description of the sound transducers, the associated electronic circuitry, and the overall operational characteristics. A description of the environmental testing procedure is also included.

Section II-8. Design and Development of the Sonotherm Ground Detection System - By T. L. Henderson and Carlos McDonald.

The telemetered signal from the Sonotherm flight unit will consist of a frequency-amplitude modulated waveform. In order to obtain information regarding the speed of sound, the antiresonant frequency, corresponding to the maximum amplitude of the Sonotherm signal has to be determined. This report summarizes the various electronic techniques, under development or investigation, by which the antiresonant frequency can be determined. Theoretical and experimental evidence indicates that the proposed electronic techniques will be reliable and capable of performing the desired measurements to any degree of accuracy required.

Section II-9. Acoustic Thermometer for Environmental Testing - By H. N. Ballard.

An acoustic thermometer was discussed in a Schellenger Research Laboratories publication, Response Time and Effects of Radiation on the Veco Bead Thermometer, April 7, 1961. The operation of the thermistor has been improved to the extent that the uncertainty in the determination of the time of travel of the sound pulse between the speaker and the microphone has been reduced to $\pm 1 \mu$sec, corresponding to an accuracy of ± 0.5°C in the determination of the chamber air temperature over a range from -85° to +25°C and at a pressure of 670 mm Hg.

Section III-10. Environmental Testing of the Sonotherm System -

By Paul Dano and Carlos McDonald.

This report summarizes the results of the environmental testing program of the Sonotherm system. The testing program consisted of various experiments performed in order to verify and determine the magnitude of air density, thermal, and wind effects on the accuracy and operation of the Sonotherm system. It is shown that the experimental results are in general agreement with theoretical predictions.

DETERMINATION OF ATMOSPHERIC PARAMETERS BY ACOUSTIC MEANS

Progress Report No. 1

July, 1962

Section I

SURVEY OF LITERATURE AND THEORETICAL INVESTIGATION

1. Survey of Literature in the Field of Atmospheric Acoustics - Richard C. Montgomery

2. Nonideal Gas Dispersion Effects on the Speed of Sound - E. Alan Dean

3. Thermal and Radiation Effects on Acoustic Measurements in the Upper Atmosphere - Richard C. Montgomery

4. Numerical Analysis of Heat Balance Equations - Henry H. Launspach, Jr.

5. Thermal Boundary Layer Effects on the Sonotherm Acoustic Interferometer - Eyung-Wha Kang

DETERMINATION OF ATMOSPHERIC PARAMETERS

BY ACOUSTIC MEANS

DA-SIG-36-039-62-G17

Progress Report No. 1

July, 1962

Section I

SURVEY OF LITERATURE AND THEORETICAL INVESTIGATION

-1-

Survey of Literature in the Field of Atmospheric Acoustics

Richard C. Montgomery
Physicist

S C H E L L E N G E R R E S E A R C H L A B O R A T O R I E S
Texas Western College El Paso, Texas

SURVEY OF LITERATURE IN THE FIELD OF ATMOSPHERIC ACOUSTICS

Acoustic means of measuring various physical parameters have been studied for many years.[20] Temperature and frequency dependence of the of the velocity of sound,[18] absorption characteristics,[19] specific heat [1,2], molecular structure[3,4,5], dispersion and heat capacity[6,7], and many other properties of solids, liquids and gases, have been probed, and many successful techniques have been evolved.

One of the earliest suggested uses of acoustic investigation was that of determining temperature, an idea usually credited to Mayer[8] in 1873. For a period of about fifty years following Mayer's suggestions, a number of experiments were performed in studying the velocity of sound in various media. In general, the trend of the research undertaken at the time was to more accurately determine the velocity of sound. Over a period of time the velocity of sound in dry air was thoroughly investigated, usually by resonant tube techniques, and interest in the use of acoustics slowly faded.

In 1925 G.W. Pierce[9] began an intensive investigation of the velocity and absorption of ultrasonic sound in various gases. Using a device consisting of a driven quartz crystal and a reflector, and detecting changes in resonant frequency and power loss, he observed a number of interesting phenomena.

Pierce's investigations led to a great revival of interest in the use of acoustics as a scientific tool. The reasons for this renewed interest is demonstrated in the following quotation[10], "The absorption of audible sound in a gas medium is very small. However it has long been

known that the absorption increases with increasing frequency of the sound. In 1911 Lebedew (Peter Lebedew, Ann. d. Physik 35, 71, 1911) published a paper in which the adsorption of high frequency sound in air was treated from a theoretical point of view. This article and one by Neklapajeff (Neklapajeff, Ann. d. Physik 35, 175, 1911) on an experimental determination of the adsorption helped suggest that more accurate data on adsorption might throw some light on molecular structure. In an unpublished investigation by G. E. Raburn it was discovered that CO_2 absorbs sound of frequency 100,000 to 300,000 cycles per sec. to such an extent that is almost opaque to it. This excessive absorption has since been verified by the author by two independent methods. G. W. Pierce (G. W. Pierce, Proc. Amer. Acad. Arts and Sciences 60, 271, 1925) and T. P. Abello (T. P. Abello, Proc. Nat. Acad. Sci. 13, 699, 1927; also Phys. Rev. 31, 1083, 1928) refer to it also.

It is a familiar fact that the velocity of sound varies with the intensity. Such a change in velocity was observed and recorded by Regnault in connection with his experiments in 1863 on the velocity of sound in the newly laid Paris water pipes. Regnault states that the velocity decreases as the intensity diminishes but that a limiting velocity of 330.6 m per sec. for feeble sounds is soon reached. A.L. Foley (A.L. Foley, Phys. Rev., 16, 449, 1920) observed a similar decrease in velocity in 1920. H.O. Taylor (H.O. Taylor, Phys. Rev., Vol. 2, 270, 1913) records a diminished wavelength in a highly absorbing tube. Hitchcock (R.C. Hitchcock, Proc. IRE., 15,907, 1927) reported that the velocity of the waves from a vibrating crystal is a function

of the energy which the crystal radiates and he obtained a value in air nearly twice the velocity of ordinary sound waves. No other record of a variation in the velocity with intensity for a continuous low or high frequency sound has been found by the author. Both Regnault's and Foley's observations were on sound pulses."

In the years following Pierce's original use of the interferometer a great deal of experimentation was done, and the operation of the interferometer was greatly improved. Such an extensive quantity of material was published in these years that it is impractical to describe the experiments performed and the apparatus built. Along with the experiments, a great deal of theoretical work was done, first on the single crystal Pierce-type interferometer,[17] and later on the double crystal variety. A most extensive theoretical discussion of the double crystal interferometer is given by Fry.[11]

An example of the more practical aspects of acoustic measurements in recent years was the use of this method by Livengood[12], Rona, and Baruch to measure the temperature of burning gases in an automobile engine. Using a pulse type system, consisting of two barium titanate transducers coupled through brass rods to the combustion chamber, to measure transit time through the combustion gases, Livengood, et. al., estimated that they had an accuracy of better than 5% under the following conditions:

(1) Pressure 15 to 700 PSIA

(2) $\frac{dp}{dt}$ in excess of 200,000 psia/sec.

(3) Temp 100°F to 4000°F.

(4) $\frac{dT}{dt}$ in excess of 100,000°F / sec.

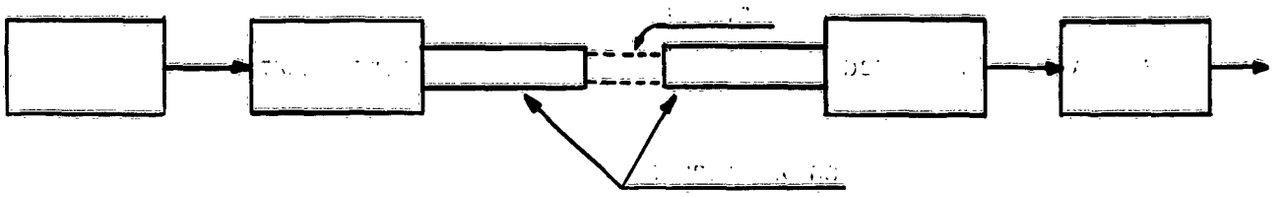

Of more direct interest is that work which has been done in the past 15 years on the determination of temperature, and other atmospheric parameters by acoustic means. In 1949, an acoustic thermometer was proposed, built and tested by Barrett and Suomi[13] at The University of Chicago. The device consisted essentially of a crystal transmitter and receiver, set up so that pulses incident on the receiver were amplified and applied to the transmitter. The transit time of the acoustic signal was determined by measuring the repetition rate of the pulses. Several of the problems which arise when using acoustic means are discussed in the article. The effect of finite amplitude on the velocity of sound was considered, but neglected, due to the very small amplitudes used. It was pointed out that γ, the ratio of specific heats, could not necessarily be considered constant, except over a small frequency range, and was definitely affected by gas composition and humidity.[15] The relation used to connect the speed of sound to temperature was an empirical one

$$c = 20.067 \left[T(1+0.3192\, e/p) \right]^{\frac{1}{2}}$$

e = vapor pressure
p = ambient pressure

from Ishii[14].

The conclusion of the article reads, "In summary, it may be safely concluded that the sonic technique of temperature measurement constitutes a major improvement over other precedures because of (a) its indifference toward radi-

ation, (b) its measurement of a property of the air directly related to air temperature, without the use of intermediate matter which must establish thermal equilibrium with the air, (c) its inherent freedom from the exponential time lag associated with ordinary thermometers, and (d) its utility in connection with space integrations of air temperature to obtain more representative values for synoptic studies."

Two other sources of acoustic measurement which have been found, but about which little information is available are: a "sonic temperature transducer" has been commercially produced by Cambridge Systems, Inc., Waltham, Mass., but enough information has not yet been released to make an evaluation of the device possible. Several groups have worked, in recent years, on the possibility of measuring the speed of sound by reflecting an electromagnetic wave from an acoustic wave. An excellent discussion of the results achieved can be found in "Design concept study for a wind profile instrument", Midwest Research Institute, Final Report, Contract No. DA-23-072-506-ORD-11.

In 1958 Mordukhovich[16], tested a different version of the acoustic thermometer, as a means of investigating the radiation errors in the standard radiosonde. The instrument consisted of a capacitive bi-directional transmitter, and two capacitive receivers, all placed along a common axis. The device transmitted a continuous signal over several wavelengths, and then compared the phase of the received signal to that of the transmitter, the duality of the system being used to reduce the effects of wind. The system was exceedingly complex, requiring a 35 tube flight unit, and continuous film recording of the signals.

The lack of pertinent information in the article is indicated by the

authors conclusion,

"Results of the preliminary tests of local acoustic method of measuring temperature of the lower stratosphere permit the formulation of a conclusion of its possible use for estimating the radiation and inertia errors of other device and an explanation of the detail of structure of a temperature field in the atmosphere to heights of 40 km."

Literature Cited

1. Kundt, Pogg. Ann. 135, 337 (1868).
2. John C. Beckerle, J. Chem. Phys. 21, 2034-2040 (1953).
3. W.T. Richards and J.A. Reid, J. Chem. Phys., 2, 206 (1934).
4. V.O. Knudsen and E. Fricke, J. Acous. Soc. Am., 12,225 (1940).
5. E. Fricke, J. Acous. Soc. Am., 12,245 (1940).
6. J.R. Partington and W.C. Schilling, Phil. Mag., 9,1020.
7. P.G. Corran, J.D. Lambert, R. Salter, and B. Worbuiton, Proc. Roy. Soc. A244, No1237, 212-219 (1958).
8. A.M. Mayer, Phil. Mag., Ser. 4, 45, 18-22 (1873).
9. G.W. Pierce, Proc. Amer. Acad. Arts and Sciences, 60, 271 (1925).
10. W.H. Pielemeier, Phys. Rev. 34, Oct. (1929).
11. William J. Fry, J. Acous. Soc. Am. 21, 17 (1949).
12. J.C. Livengood, T.P. Rona, and J.J. Baruch, J. Acous. Soc. Am. 26, 824 (1954).
13. E.W. Barrett and V.E. Suomi, J. Meteorol., 6, No. 4 (1949).
14. Ishii, Ch., 1935: Supersonic Velocity in Gases. Sci. Pap. Inst. Phys. Che. Res., Tokyo, 26, 201-207.
15. Kneser, H.O., 1933: Schallabsorption in Mehratomigen Gasen. Ann. Physik, 16, 337-349.
16. M.I. Mordukhovich, Bulletin, Academy of Sciences, USSR, Geophysics Series, March 1959, 329-335. English Edition published May 1960, National Academy of Sciences.
17. M. Greenspan and M.C. Thomson Jr. J. Acous. Soc. Am. 23, 627 (1951).
18. A. Lacam and R. Gergeon Phys. Abs. 4911 (1956).
19. D. Tabuchi, J. Chem. Phys. 23, 2033-2037 (1955).
20. Fitzmaurice, J.A., Nat. Bureau of Stds, Publication #3130, 13-15, (1954).

DETERMINATION OF ATMOSPHERIC PARAMETERS
BY ACOUSTIC MEANS

DA-SIG-36-039-62-G17

Progress Report No. 1

July, 1962

Section I:
SURVEY OF LITERATURE AND THEORETICAL INVESTIGATION

Nonideal Gas Dispersion Effects on the Speed of Sound

E. A. Dean
Physicist

SCHELLENGER RESEARCH LABORATORIES
Texas Western College El Paso, Texas

CONTENTS

TABLES

FIGURES

NONIDEAL GAS AND DISPERSION EFFECTS ON THE SPEED OF SOUND

1. Introduction

One might justly ask what is the meaning of the term "the speed of sound." Since the query is central to the problem of determining the temperature of a gas by measuring the speed of sound, it deserves a definitive answer. One use of the term, properly called the "phase velocity," is the velocity of the wave-front (equi-phase surface) along the wave normal. Another use, more correctly labeled the "group velocity," is the velocity of energy flow. In a nondissipative, stationary medium these two velocities are equal to one another and numerically equal to the so-called local sound speed c. This number is simply the constant in the wave equation, $c^2 \nabla^2\phi = \ddot{\phi}$.

If the medium is in motion with velocity $\underset{\sim}{u}_o$, the motion does not affect the direction $\underset{\sim}{n}$ of the wave normal but does change the magnitude of the phase velocity v_p such that it differs from the local sound speed by the component of $\underset{\sim}{u}_o$ in the direction of $\underset{\sim}{n}$. Thus, $\underset{\sim}{v}_p = (c + \underset{\sim}{u}_o \cdot \underset{\sim}{n})\underset{\sim}{n}$. The fact that the direction of the wave normal is not changed by motion of the medium does not alter the effect of $\underset{\sim}{u}_o$ on energy flow. The velocity of this flow v_g is simply the vector sum of the two velocities, $\underset{\sim}{v}_g = c\underset{\sim}{n} + \underset{\sim}{u}_o$ ..

The above nomenclature of phase and group velocities [1] * contrasts with the electromagnetic definitions; however, the terms are in keeping with the concept of differentiating detween phase and energy flow velocities. If the medium is also dissipative, there is associated absorption and dispersion. In this case, analogy with the electromagnetic definitions can be made if the acoustic wave is not monochromatic. For a pulse or a wave packet, the group velocity becomes [2].

$$\underset{\sim}{v}_g = \underset{\sim}{n}\left(\frac{dk}{d}\right)^{-1} + \underset{\sim}{u}_o ,$$

where $\omega = 2\pi f$ and $k = \omega/v_p$. Since dispersion causes $v_p = v_p(\omega)$, here the group velocity differs from the phase velocity even if the medium is stationary.

A standing wave is an interference phenomenon which is independent of energy transfer but dependent on phase. Therefore, a resonance measurement determines phase velocity. **

In contrast, a measurement of pulse transit time between fixed source and receiver is a determination of group velocity. However, the group velocity may be expressed in terms of the phase velocity by the above relation; consequently, only the phase velocity of sound

*Numbers in brackets refer to literature cited at end of this paper.

**It is assumed that to create a standing wave, one must first have a plane traveling wave. If the wave is not plane, a medium velocity normal to the wave normal may complicate matters.

need be determined. Excluding a moving medium, this requires the evaluation of what has been labeled the local speed, c (which is not identical to the constant in the wave equation if dissipation or nonhomogeneity is considered). The symbolic problem of using c both for the constant in the wave equation and the local sound speed is not unique in physics but is confusing. From this point hence, c will be used for the local sound speed only.

The inclusion of dispersion complicates the calculation of c ; however, $c(\omega)$ may be expanded by a power series $c(\omega) = a_0 + a_1\omega + a_2\omega^2 + \ldots$. The constant coefficient in this expansion is sometimes called the "zero-frequency" speed of sound. A more proper term might be the nondispersive speed of sound.

It is the purpose of this paper to determine the value of a_0 and c for air. It has been noted that c is a function of ω, and it will appear that it is also a function of ambient pressure P_0 , and composition. The value of $\frac{a_0}{\sqrt{T_0}}$ is dependent on P_0 and T_0 because of nonideal gas effects and variations in specific heats due to molecular vibration and rotation effects.

The dispersion of sound is closely tied with item (2) above, with additional dispersion due to viscous and thermal conductive energy losses. These effects depend on the molecular structure of a gas, rather than the normally assumed continuity involved in sound. As

such, the ratio of the wavelength to the mean free path is an important number. This number, in turn, depends on the frequency-to-pressure ratio. Considering a constant frequency, it would seem that dispersion depends only on pressure; however, the presence of trace gases such as H_2O and CO_2 strongly affect dispersion also.

There is some argument as to which of the two approaches, continuous fluid or molecular, is to be preferred. It is true that viscous and thermal conductive effects may be treated by the macroscopic coefficients of viscosity and thermal conductivity, and the effects believed to be due to rotation and vibration can be postulated as a bulk viscosity. However, the argument seems to be academic in light of the purpose of this paper; therefore, both concepts will be used as the occasion arises.

2. Derivation of the Nondispersive Speed of Sound

The determination of a_o is firmly based on the equation of continuity, Newton's second law of motion, and the conservation of energy principle. However, the solution of these three equations in the case of general fluid has not yet been achieved. The solutions which commonly find their way into sophomore texts are replete with unstated assumptions, and it is informative to examine these unstated assumptions to form a basis for correction of the familiar result $a_o = (\gamma RT/M)^{\frac{1}{2}}$.

The "exact" equations*[3] governing the propagation of sound in fluids have been developed. Rather than repeat these equations in full it will first be assumed that the fluid is perfect, i.e., that the fluid is non-viscous and will not conduct heat. The three equations are then simplified to:

$$\dot{\rho} + \nabla \cdot (\rho \underset{\sim}{u}) = 0$$

$$\rho \dot{\underset{\sim}{u}} = \rho \underset{\sim}{F} - \rho(\underset{\sim}{u} \cdot \nabla)\underset{\sim}{u} - \nabla P$$

$$\dot{T} + \underset{\sim}{u} \cdot \nabla T + \frac{\gamma - 1}{\beta} \nabla \cdot \underset{\sim}{u} + q(T - T_o) = 0 \ ,$$

where ρ, the density, $\underset{\sim}{F}$ is the external force per unit mass, P is the hydrostatic pressure, T is the absolute temperature, γ is the ratio of specific heats, β is the coefficient of thermal expansion, and q is a radiation coefficient taken from Newton's law of cooling. In the above and following, the dot above a variable will represent partial differentiation with respect to time.

Performing a change of variables defined by $\rho = \rho_o + \rho_1$, $\underset{\sim}{u} = \underset{\sim}{u}_o + \underset{\sim}{u}_1$, $P = P_o + P_1$, $T = T_o + T_1$, where the zero subscripts are used for constants and the unity subscripts are used for variables, enables some simplification. Now assume the variables are acoustic variables; i.e., ρ_1 = excess density, $\underset{\sim}{u}_1$ 2 particle velocity, P_1 = sound pressure, and T_1 = excess temperature. In

---

*See Hunt's qualifying remarks on page 3-32.

effect, this assumes the medium is homogeneous. Finally, assume the medium is stationary ($\underset{\sim}{u}_o = 0$) and there are no external forces such as those due to gravity* ($\underset{\sim}{F} = 0$). With this extremely simplified medium, the equations become:

$$\dot{\rho}_1 + \underset{\sim}{u}_1 \nabla \rho_1 + (\rho_o + \rho_1) \nabla \cdot \underset{\sim}{u}_1 = 0$$

$$(\rho_o + \rho_1) \dot{\underset{\sim}{u}}_1 = -(\rho_o + \rho_1)(\underset{\sim}{u}_1 \cdot \nabla)\underset{\sim}{u}_1 - \nabla P_1$$

$$\dot{T}_1 + \underset{\sim}{u}_1 \cdot \nabla T_1 + \frac{\gamma - 1}{\beta} \nabla \cdot \underset{\sim}{u}_1 + qT_1 = 0 ,$$

which are still unmanageable since they are nonlinear.

The "small-signal" approximation is now made. All acoustic variables are considered small in ratio to their ambient counterparts so that products of the variables and their derivatives are neglected. Thus, the linear equations,

$$\dot{\rho}_1 + \rho_o \nabla \cdot \underset{\sim}{u}_1 = 0$$

$$\rho_o \dot{\underset{\sim}{u}}_1 = -\nabla P_1$$

$$\dot{T}_1 + \frac{\gamma - 1}{\beta} \nabla \cdot \underset{\sim}{u}_1 = 0 ,$$

result.**

By differentiating the first equation with respect to time, and the second with respect to space, a substitution for $\nabla \cdot (\rho_o \dot{\underset{\sim}{u}}_1) = (\partial / \partial t)(\rho_o \nabla \cdot \underset{\sim}{u}_1)$ may be made so that

---

*The force due to gravity is balanced by a $\frac{\partial P}{\partial z}$ term if the gas is in gravitational equilibrium.

**The quantity q has also been considered small.

$$\nabla^2 P_1 = \ddot{\rho}_1 ,$$

or,*

$$\left(\frac{\partial P_1}{\partial \rho_1}\right) \nabla^2 P_1 = \ddot{P}_1 ,$$

the familiar wave equation, with phase velocity $(\partial P_1/\partial \rho_1)^{\frac{1}{2}}$, or $(\partial P/\partial \rho)^{\frac{1}{2}}$.

The evaluation of $\partial P/\partial \rho$ poses a problem. Physically, both P and ρ are state variables and their dependence on one another is defined by the kind of process involved. Mathematically, the third variable in the equation of state must be specified. The necessity of the conservation of energy equation is now apparent: it determines the type of physical process. The equation as written above states that there is no conversion of mechanical energy into thermal energy: all such processes have been neglected. Physically, this equation determines that the process is adiabatic. Mathematically, the third variable, the one held constant, must be entropy. Thus, consideration of the third equation determines that the solution for the set of three is

$$\left(\frac{\partial P}{\partial \rho}\right)_s \nabla^2 P_1 = \ddot{P}_1 ,$$

where the s subscript requires the entropy per mole to be constant. Therefore, since dispersion has been neglected,

---

* In effect, the assumption is made that $\partial \rho_1/\partial P_1$ does not vary with time. This would be a finite-amplitude effect.

$$a_o^2 = \left(\frac{\partial P}{\partial \rho}\right) .$$

This result may be cast in more familiar terms by introducing the molar volume, $v = M/\rho$, where M is the molecular mass. Thus $d\rho = -(\rho / v)\, dv$, or

$$a_o^2 = -\frac{v}{\rho}\left(\frac{\partial P}{\partial v}\right)_s = \frac{B_a}{\rho} ,$$

where the definition of the adiabatic bulk modulus has been used, $B_a = -v(\partial P/\partial v)_s$. Further manipulation of the partial derivative shows that*

$$B_a = -v\left(\frac{\partial P}{\partial v}\right)_s = +v\left(\frac{\partial s}{\partial v}\right)_\rho\left(\frac{\partial P}{\partial s}\right)_v = v\left(\frac{\partial s}{\partial T}\right)_\rho\left(\frac{\partial T}{\partial v}\right)_\rho\left(\frac{\partial T}{\partial s}\right)_v\left(\frac{\partial P}{\partial T}\right)_v$$

or

$$B_a = -v\left(\frac{\partial s}{\partial T}\right)_\rho\left(\frac{\partial T}{\partial s}\right)_v\left(\frac{\partial P}{\partial v}\right)_T .$$

Finally, from the following definitions, $C_P = T(\partial s/\partial T)_P$, $C_v = T(\partial s/\partial T)_v$, and $B_I = -v(\partial P/\partial v)_T$, where C_P and C_v are the molar heats at constant pressure and volume, respectively, and B_I is the isothermal bulk modulus, $B_a = (C_P/C_v)\, B_I$, or

$$a_o = \left(\frac{C_P B_I}{C_v \rho}\right)^{\frac{1}{2}} = \left(\frac{\gamma B_I}{\rho}\right)^{\frac{1}{2}} .$$

---

* See Callen [4] for partial derivative operations.

3. Nonideal Gas Effects

Thus far, nothing has been assumed regarding an equation of state, and the results are independent of which equation of state is chosen. If the gas is ideal, $\bar{P}v = \bar{R}T$ is the equation of state where $\bar{R}$ is the gas constant. For an ideal gas,

$$B_I = -v\left(\frac{\partial \bar{P}}{\partial v}\right)_T = (-v)\left(\frac{\bar{R}T}{v^2}\right) = \bar{P} ,$$

and

$$a_o^2 = \frac{\gamma \bar{P}}{\rho} = \frac{\gamma \bar{P} v}{M} = \frac{\gamma \bar{R} T}{M} .$$

A review of the assumptions made in this equation indicates that:

Assumption 1: the fluid must be nonviscous,

Assumption 2: the fluid must be nonconductive,

Assumption 3: the fluid must be homogeneous,

Assumption 4: the fluid must be stationary,

Assumption 5: the sound wave is of small amplitude,

Assumption 6: the radiation of heat is negligible, and

Assumption 7: the fluid is an ideal gas.

The fact that $a_o^2 = \gamma RT/M$ yields values in air that are accurate to four significant figures is remarkable considering such an emaciated theory.

A more accurate equation of state is all that is necessary to correct for the ideal gas restriction. Herzfeld and Litovitz [5] have

obtained the effect of a real gas in terms of the second virial coefficient $\bar{B}$, in the Kammerlingh-Onnes equation of state,

$$\frac{\bar{P}v}{RT} = 1 + \frac{\bar{B}}{v} + \frac{C}{v^2} + \ldots$$

The effect may be stated in terms of the following correction factor:

$$a_o = a_o^o \left[1 + P_o \left(\frac{\bar{B}}{RT} + \frac{1}{C_v^o} \frac{d\bar{B}}{dT} + \frac{1}{2} \frac{RT}{C_v^o C_p^o} \frac{d^2\bar{B}}{dT^2} \right)\right]$$

where the zero superscripts refer to the values of the quantity as P_o approaches zero. The pressure dependence of B_I, C_p, and C_v have been combined in this correction factor.

The value of a_o^o is simply the ideal-gas speed of sound,

$$a_o^o = \left(\frac{C_p^o B_I^o}{C_v^o \rho} \right)^{\frac{1}{2}} = \left(\frac{C_p^o}{C_v^o} \frac{RT}{M} \right)^{\frac{1}{2}} .$$

The fact that C_p^o and C_v^o both vary with temperature due to the dependence on temperature of rotational and vibrational heat capacities makes the value of a_o^o vary not exactly with the square root of temperature. The thermodynamic relation

$$C_v = C_p - Tv \beta^2 B_I ,$$

where β = coefficient of thermal expansion, $(1/v)(\partial v/\partial T)_P$ becomes in the special case of $P \longrightarrow 0$,

$$C_v^o = C_p^o - Tv\left(\frac{1}{T}\right)^2 P = C_p^o - R \ .$$

Thus, only knowledge of C_p^o (T) is necessary to determine the correction factor due to the ratio of specific heats.

The value of C_p^o for several gases has been calculated by the National Bureau of Standards [11]. The calculations are based on statistical mechanical equations and use spectroscopic data. Table 3-1 tabulates these values for the polyatomic constituents of dry air. Monatomic gases have classical equipartitional values of 2.5000 R for C_p^o, whereas other gases are affected by rotation and vibration. For the gases listed, the rotational heat capacities have approximately equipartitional values of R, and the vibrational heat capacities cause most of the temperature variation of C_p^o.

Table 3-2 tabulates the composition of dry air in terms of mole fractions given by Glueckauf [6]. The molecular mass (physical scale) of dry air is the weighted mean of the individual molecular masses and is 28.974 gm/mole. The same composition data has been used to calculate the weighted mean C_p^o which is tabulated in Table 3-1. The value of C_v^o is calculated similarly and the ratio of specific heats, $\gamma^o = C_p^o/C_v^o$ is tabulated in Table 3-3. The value of γ^o at the ice point (273.15°K) is 1.40054. This value is denoted by γ_o^o and the ratio γ^o/γ_o^o is tabulated in the next column. Both

Table 3-1
Molar heat at constant pressure as the pressure approaches zero for the constituent gases and dry air

T (°K)	C_p^o/R			
	N_2 (1)	O_2 (1)	CO_2 (1)	Dry Air (2)
180	3.5007	3.5020	3.7800	3.4917
190	3.5008	3.5025	3.8347	3.4919
200	3.5008	3.5032	3.8916	3.4921
210	3.5009	3.5042	3.9502	3.4924
220	3.5010	3.5056	4.0097	3.4927
230	3.5010	3.5073	4.0695	3.4931
240	3.5012	3.5095	4.1296	3.4938
250	3.5013	3.5122	4.1892	3.4944
260	3.5015	3.5155	4.2484	3.4953
270	3.5017	3.5193	4.3068	3.4963
273.15	3.5018	3.5207	4.3249	3.4966
280	3.5021	3.5238	4.3643	3.4975
290	3.5025	3.5288	4.4208	3.4989
300	3.5030	3.5344	4.4763	3.5005
310	3.5036	3.5407	4.5307	3.5023

(1) Taken from NBS circular 564 [11].

(2) Based on composition given in Table 3-2, C_p^o for monatomic gases = 2.5000 R.

Table 3-2
Composition and molecular weight of dry air

i	Gas	$\bar{X}_i$ (1)	M_i (2)
1	N_2	0.78085	28.023
2	O_2	0.20946	32.009
3	A	0.00934	39.995
4	CO_2	0.00032	44.020
5	Ne	0.00002	20.188
6	He	0.00001	4.004
	Dry Air	1.00000	28.974

(1) Data taken from Glueckauf [6].

(2) Based on physical scale (O^{16} = 16.00000).

Nitrogen isotopic composition, 14 : 15 = 9962:38 ;

Oxygen isotopic composition, 16 : 17 : 18 = 99757:39:204 ; taken from [6]. Isotopic molecular mass taken from Meggers [7], other gases based on chemical scale multiplied by 1.000272, see Dumond and Cohen [8]. The molecular mass for dry air is 28.966 on the chemical scale.

of these columns have been rounded off to five significant figures. The last column of Table 3-3 gives the correction to the speed of sound calculated from the formula

$$a_o^o = \sqrt{\frac{\gamma_o^o RT}{M}} = 20.051\sqrt{T} \quad ,$$

where the value $R = 8.31696$ has been used [8]. It can be seen that the correction is within 0.03% for the range 180°K to 310°K .

Table 3-3
Ratio of specific heats correction to the speed of sound in dry air

T (°K)	γ^o	γ^o/γ_o^o (1)	Correction (parts per 100,000) (2)
180	1.4013	1.0006	+ 28
190	1.4013	1.0005	+ 27
200	1.4013	1.0005	+ 26
210	1.4012	1.0005	+ 24
220	1.4012	1.0004	+ 22
230	1.4011	1.0004	+ 20
240	1.4010	1.0003	+ 16
250	1.4009	1.0003	+ 12
260	1.4008	1.0002	+ 7
270	1.4006	1.0000	+ 2
280	1.4004	.9999	- 5
290	1.4002	.9997	- 13
300	1.3999	.9996	- 22
310	1.3996	.9994	- 32

(1) Based on $\gamma_o^o = \gamma^o$ at 273.15°K = 1.40054.

(2) This column is more accurate than the other two due to rounding off for γ^o and γ^o/γ_o^o .

Returning to the equation of state correction, the second virial coefficient has been correlated to the compressibility, Joule-Thompson

coefficients, and other results of various investigators by the Bureau of Standards [11]. Table 3-4 tabulates these values, along with the first and second temperature derivatives of B. These derivatives

Table 3-4
The second virial coefficient and derivatives for air

T (°K)	$B^{(1)}$ (cm^3/mole)	dB/dT $\left(\frac{cm^3}{mole\ deg}\right)$	d^2B/dT^2 $\left(\frac{cm^3}{mole\ deg^2}\right)$
180	-49.32	+0.626	-.0083
190	-43.44	+0.552	-.0067
200	-38.24	+0.489	-.0057
210	-33.62	+0.437	-.0047
220	-29.48	+0.392	-.0043
230	-25.75	+0.354	-.0035
240	-22.39	+0.320	-.0032
250	-19.33	+0.292	-.0027
260	-16.54	+0.267	-.0024
270	-13.98	+0.245	-.0021
280	-11.64	+0.225	-.0019
290	- 9.48	+0.208	-.0015
300	- 7.48	+0.191	-.0016
310	- 5.63	+0.179	-.0012
320	- 3.91	+0.165	-.0013

(1) Taken from [11].

were obtained numerically from the tabulated values of B by using Newton's backward interpolation formula [12]:

$$\left(\frac{dB}{dT}\right)_i = \frac{1}{h}\left(\Delta^1 B_{i-1} + \frac{1}{2}\Delta^2 B_{i-2} + \frac{1}{3}\Delta^3 B_{i-3} + \frac{1}{4}\Delta^4 B_{i-4}\right)$$

and

$$\left(\frac{d^2B}{dT^2}\right)_i = \frac{1}{h^2}\left(\Delta^2 B_{i-2} + \Delta^3 B_{i-3} + \frac{11}{12}\Delta^4 B_{i-4}\right),$$

where i is the row number, h is the interval (in this case 10°K), and Δ^n is the nth finite difference. The fluctuation in $d^2\bar{B}/dT^2$ at high temperatures is believed to be due to the nature of this type of differentiation, which, at best, is inaccurate.

Using the values of Table 3-4, the corrections due to the equation of state may be calculated and are tabulated as Table 3-5. Here the corrections have arbitrarily been smoothed, since the fluctuation in $d^2\bar{B}/dT^2$ caused the corrections to fluctuate.

Table 3-5
Equation of state corrections to the speed of sound in dry air

Corrections are in parts per 100,000 and must be multiplied by the pressure in atmospheres.

T (°K)	Corrections (A) (Parts per 100,000 per atmosphere)
180	-133
190	- 98
200	- 73
210	- 52
220	- 36
230	- 22
240	- 10
250	+ 1
260	+ 10
270	+ 18
280	+ 24
290	+ 29
300	+ 33
310	+ 37

As an example in the use of this table, consider that the speed of sound at the ice point is given by $a_0^0 = 20.051\sqrt{273.15}$, since

there is no ratio of specific heat correction at this temperature. Thus $a_o^o = 331.38$ m/sec. To find the speed of sound at one atmosphere the correction of 20 parts per 100,000 is added, yielding $a_o = 331.45$ m/sec. Likewise, the speed of sound at 0.1 atmosphere (about 50,000 ft) would be 331.39 m/sec.

4. Vibrational Dispersion

When a gas is compressed adiabatically the temperature increases. The temperature increase is merely an indication of an increase in internal energy and the two concepts are related by the specific heat. For a monatomic gas, the only type of internal energy is that of translation; however, a polyatomic gas may also have rotational and vibrational energy. Since this type of energy is quantized rather than continuous, as translational energy is, one would expect the classical theory of equipartition of energy to fail. This failure causes the specific heats, and thus γ, to be functions of temperature, as was seen in the last section.

For the polyatomic constituents of dry air, N_2, O_2, and CO_2, the rotational quanta is small enough that the classical limit of quanta mechanics may be used in all but the very lowest temperatures (below 50°K or so). Thus, rotational energy may be treated in the same manner as translational energy, which will be investigated in the next section.

The vibrational quantum is large enough to require quantum mechanics, and therefore only a certain fraction of the molecules are at a specific vibrational energy level. These fractions depend on the total energy available, and thus the temperature. Under adiabatic compression, the temperature increase causes a readjustment of energy levels which requires a certain time, called the relaxation time τ. If the period of the sound wave causing the compression is much longer than τ, then the adjustment is complete and equilibrium among the various degrees of freedom exists. Thus the molar heat is equal to the static molar heat tabulated in Table 3-1. On the other hand, if the period of the sound wave is much less than τ, there is practically no adjustment of vibrational levels, negating this degree of freedom. Thus the dynamic molar heat includes no contribution from vibration, being equal to the static molar heat minus the vibrational molar heat. Assuming the equipartition of rotation, this would require $C_p^o = 3.50000\ R$ for linear molecules.

Since the speed of sound depends on C_p^o and C_v^o, there is a shift in speed between the low-frequency wave the the high-frequency wave. Between the two extremes there is dispersion. Figure 4-1 shows this dispersion plotted as a function of f/f_o where f_o is the frequency which corresponds to τ. The change in speed ($c_\infty - c_o$ in Figure 1) depends on the temperature and gas involved.

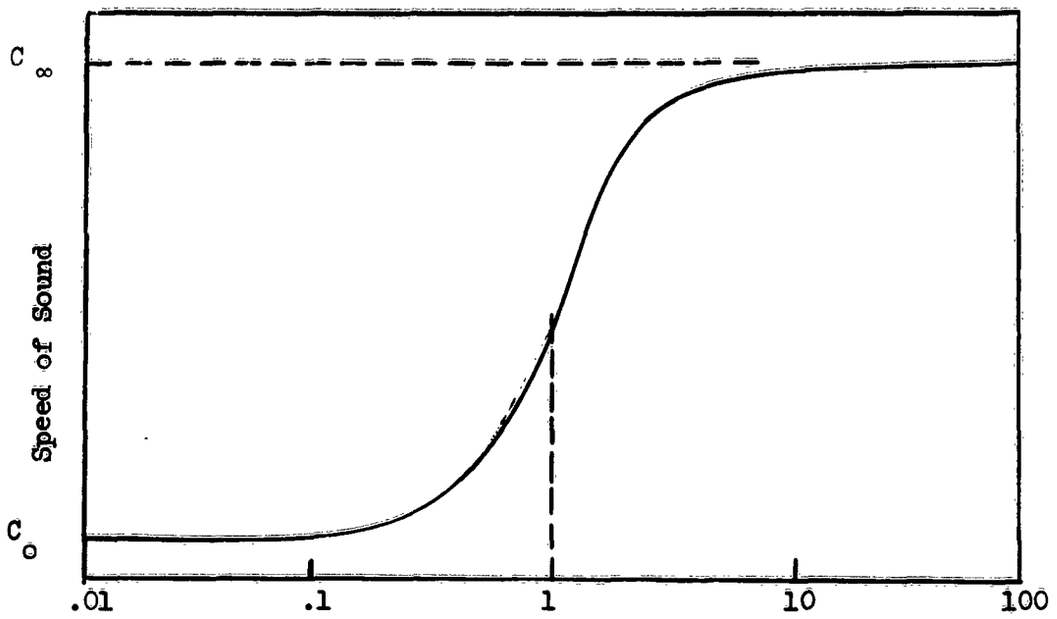

Figure 4-1. Ratio of f/f_o for a Particular Pressure. The dispersion of sound speed due to vibrational energy lag. The low-frequency speed c_o is determined by translational, rotational, and vibrational specific heats; c_∞ represents the high-frequency speed determined by only translational and rotational specific heats.

Unfortunately, it is difficult to make precise measurements of τ, and thus far theory has failed to predict accurate values [5]. To compound the problem, τ varies with pressure, temperature, and is sensitive to impurities. However, the high-frequency and low-frequency velocity limits are measurable and support the above theory closely.

The relaxation frequency for pure oxygen has been measured to be about 50 cps at atmospheric pressure and room temperature by Knotzel [14]. High-temperature shock measurements by Blackman [15] indicate that the relaxation frequency for nitrogen is even less than that of oxygen. Dry air has so little CO_2 that the dispersion due to this component will be considered unknown and will

introduce an error of from 1 to 2 parts per 100,000. Thus, at atmospheric pressure and room temperature, it is safe to assume that O_2 and N_2 are <u>not</u> in vibrational equilibrium if the frequency is over 500 cps, (approximately $10f_o$, see Figure 4-1) and a correction must be made to a_o^o to include this fact.

The temperature dependence of f_o may be inferred from shock measurements of τ. These measurements fall in a fairly straight line when τ is plotted logarithmically against $T^{-1/3}$. This indicates that as T decreases, τ increases or f_o decreases. Since most of the atmosphere is cooler than room temperature, this makes f_o even smaller than 50 cps, strengthening the thesis that there is no vibrational equilibrium for O_2 and N_2.

The pressure dependence of f_o may be derived from the following consideration: The relaxation time may be written $\tau = z\bar{\tau}$ where z is the number of collisions required for equilibrium and $\bar{\tau}$ is the mean time between collisions. Since z is only dependent on energy (temperature) the pressure dependence of τ comes only from $\bar{\tau}$, which varies inversely with pressure. Thus $\tau \propto P^{-1}$ and $f_o \propto P$, reducing f_o with increasing altitude, again strengthening the vibrational nonequilibrium thesis.

The relaxation frequency of O_2 is, however, strongly sensitive to small amounts of water vapor, f_o increasing as humidity increases. Fortunately, the air in the upper atmosphere is extremely dry.

The humidity at sea level might cause the O_2 to be in equilibrium, as it takes only 10% relative humidity to increase f_o to 5000 cps [16]. * The rapid decrease in temperature between the earth and the tropopause causes a reduction in water vapor content, which rapidly decreases f_o. For instance, the value of f_o above 8 km cannot be greater than 800 cps, even for air saturated with H_2O. Above the tropopause, there is not enough water vapor to cause equalization of vibrational freedom in O_2 at frequencies above 1 cps.

The necessary corrections to the speed of sound due to non-equilibrium in N_2 and O_2 and the error introduced by neglecting CO_2 dispersion is tabulated in Table 4-1. The corrections are based on C_p^o for O_2 and N_2 equal to 3.5000 R. This correction, when added to the γ correction in Table 3-3, gives a temperature-independent correction of +33 parts per 100,000. This should be independent of temperature since the assumption that O_2 and N_2 are not in vibrational equilibrium demands that C_p^o is independent of temperature. The correction applied to the speed of sound formula gives

$$a_o^o = 20.057\sqrt{T}$$

and the constant value of γ^o becomes

$$\gamma^o = 1.4015$$

* This affects calibration of air-borne sensors. The calibration should be done in dry air.

Table 4-1
Correction to speed of sound due to non-excitement of vibration in N_2 and O_2 and error due to lack of knowledge about the state of vibrational excitement of CO_2

T (°K)	Correction (parts per 100,000)	Error (parts per 100,000)
180	+ 5	1
190	+ 6	1
200	+ 7	1
210	+ 9	1
220	+12	1
230	+14	1
240	+16	1
250	+21	1
260	+25	1
270	+30	2
280	+38	2
290	+45	2
300	+54	2
310	+64	2

5. Viscothermal and Rotational Dispersion

When viscosity and thermal conductivity are included in the acoustic equations, the solution becomes that of an attenuated wave with associated dispersion. The first order approximation yields the so-called classical, or Stokes-Kirchhoff absorption, and a second order approximation shows dispersion. For a polyatomic gas, there is combined with the viscothermal absorption a rotational absorption due to the relaxation of the rotational degrees of freedom. The rotational dispersion is governed by the same equations as the vibrational dispersion except there is a difference in magnitude and in the number of collisions required for equilibrium. Although

the vibrational case may be handled separately from viscothermal effects, this is not true for rotation, and interaction must be considered because of the small number of collisions required for equilibrium.

The solution for absorption and dispersion may be accomplished through a power series expansion using $x = \omega\eta / P_o$ as variable, where η is the coefficient of viscosity. By the use of a "quasi-Burnett" expression for a diatomic gas, Greenspan [18] derives the following expression for the dimensionless ratios α / k_o where α is the absorption coefficient and $k_o = \omega / a_o$, the propagation constant,

$$\frac{\alpha}{k_o} = 0.6700x - 1.843x^3 + \ldots ,$$

and c/a_o

$$\frac{c}{a_o} = 1 + 0.9849x^2 .$$

By introducing the dimensionless ratios

$$\sigma = \frac{c_\infty}{a_o}$$

$$n = \frac{4}{5}\left[\frac{c_p'' \, c_v''}{c_p' \, c_v'}\right] Z ,$$

where c_∞ is the high-frequency speed (see Figure 4-1), the primed quantities refer to the equilibrium values, the double primed quantities refer to the non-equilibrium values, and Z is the number of collisions to establish equilibrium, Greenspan obtains the following expressions

for rotational relaxation:

$$\frac{\alpha}{k_o} = \frac{\sigma^2 - 1}{2\sigma} nx - \frac{\sigma^4 - 1}{4\sigma} n^3x^3 + \ldots$$

$$\frac{c}{a_o} = 1 + \frac{\sigma^2 - 1}{2} n^2x^2 + \ldots .$$

For a diatomic gas, $\sigma = 1.0911$ and $n = 0.5237Z$, which yields

$$\frac{\alpha}{k_o} = 0.0457Zx - 0.0137Z^3x^3 + \ldots$$

$$\frac{c}{a_o} = 1 + 0.0261Z^2x^2 .$$

The two types of dispersion do not combine linearly; however, if the gas is a Becker gas ($c_p \eta / K = 3/4$, where K is the thermal conductivity) Greenspan has shown [17] that

$$\frac{c}{a_o} = \left[\frac{a_o}{c_1} \frac{a_o}{c_2} - \frac{\alpha 1}{k_o} \frac{\alpha 2}{k_o} \right]^{-1},$$

where the unity subscripts refer to one mechanism and the two's refer to another. Air has values of $c_p \eta/K$ (Prandtl's number) of from .746 at 180°K to .703 at 320°K [11], so that to a fair approximation air is a Becker gas.

Using the above relation,

$$\frac{c}{a_o} = 1 + (0.9849 + 0.0261Z^2 + 0.0306Z)x^2 + \ldots$$

expresses the total dispersion due to viscosity, thermal conductivity and rotation. From absorption measurements, Greenspan determined the number of collisions for rotational equilibrium to be 4.82 ± 0.18. Substituting $Z = 4.82$,

$$\frac{c}{a_o} = 1 + 1.737x^2 + \ldots .$$

This value compares favorably with Greenspan's dispersion measurements, which seem to fit the expression

$$\frac{c}{a_o} = 1 + 1.7x^2 .$$

This fact seems to justify the quasi-Becker method of adding the viscothermal and molecular dispersions, since a direct sum, without absorption cross products, would yield*

$$\frac{c}{a_o} = 1 + 1.59x^2 .$$

The above expression has no x^3 term, so that the single correction term is fairly accurate (from Greenspan's dispersion data, the fit is good for corrections not greater than 4%). The temperature variation of the x^2 coefficient is unknown but x does vary with temperature through η. This variation is shown in Table 5-1, where the

* One must admit that this is not a sensitive test of the method. At higher f/P ratios, the dispersion deviates from Greenspan's theory, but this deviation also occurs in monatomic gases which have no molecular relaxation, so that the basic problem must be in the solution to the hydrodynamic equations.

coefficient $\bar{B}$ is defined as a correction factor to the speed of sound so that

$$c = a_o \left(1 + 10^{-5} \bar{B} \frac{f^2}{\bar{P}_o^2}\right) ,$$

with $\bar{P}_o$ in atmospheres and f in cycles per second.

Table 5-1
Viscothermal and rotational dispersion correction factor

$\bar{T}$ (°K)	$\bar{B}^*$ parts per 100,000/ $(\text{cps/atmos})^2 \times 10^{-15}$
180	98
190	108
200	118
210	129
220	139
230	150
240	161
250	172
260	183
270	195
280	206
290	217
300	229
310	241

*$\bar{B} = (1.737 \times 10^5)(2\pi\eta / 1.013 \times 10^6)^2$, viscosity data taken from Hilsenrath, et al [11] .

The error associated with $\bar{B}$ is about 8%. This is estimated considering that η is known only to within 2%, that Z is about 4% accurate, and there is some doubt as to the "quasi-Burnett" and "quasi-Becker" assumptions. Besides this error, which applies to all values, there is about 6% change in the Prandtl number

between 300°K and 200°K. There is also some theoretical justification to assume $\bar{Z}$ changes a like amount [19]. Together, these numbers are responsible for about half of $\bar{B}$ so that one may assume the value at 200°K may deviate by about 15%. This means that each of the numbers in Table 5-1 may be in error by about 18×10^{-15} parts per $100,000/(\text{cps/atmos})^2$.

6. Results and Conclusions

Of the assumptions listed in section 3, corrections to the phase velocity of sound have been obtained for Assumptions 1, 2, and 7. The fact that no heat radiation effect has ever been measured justifies Assumption 6, leaving the requirements that the medium must be stationary and homogeneous and that the sound wave must be of small amplitude. These assumptions must be investigated, but until such time, the velocity of sound may be expressed as

$$c = 20.057\sqrt{T}\ (1 + 10^{-5}\, AP_o + 10^{-5}\, Bf^2/P_o^2)\ ,$$

where A is the correction factor given in Table 3-5.

As long as the corrections remain small, the equation may readily be solved for T:

$$T = \left(\frac{c}{20.057}\right)^2 \left[1 - 2 \times 10^{-5}\ (AP_o + Bf^2/P_o^2)\right].$$

The values of A and B, both functions of T, may be obtained by first finding the uncorrected temperature, then using the corresponding value of A and B to obtain the corrected temperature. Alternately,

one may state

$$T = \frac{c^2}{402.28} + E(T)P_o + F(T)\frac{f^2}{P_o^2} ,$$

where the functions E and F are listed in Table 6-1.

Table 6-1
Temperature corrections to be applied to the determination of temperature by means of the speed of sound in dry air

T (°K)	E(T) (deg/atm)	F(T) (deg · atm^2 · sec^2) x 10^{-16}
180	+0.48	- 3.5
190	+0.37	- 4.1
200	+0.29	- 4.7
210	+0.22	- 5.3
220	+0.16	- 6.0
230	+0.10	- 6.8
240	+0.05	- 7.6
250	0.00	- 8.5
260	-0.05	- 9.4
270	-0.10	-10.4
280	-0.14	-11.4
290	-0.17	-12.5
300	-0.20	-13.6
310	-0.23	-14.8

The error in the determination of the constant 402.28 is about 10 parts per 100,000 due to uncertainties in C_p and the composition of air. This yields temperature errors of about 0.03°K. The error in E is probably not greater than 0.02° per atmosphere, whereas the error in F is about 0.5 x 10^{-16} deg atmosphere^2 sec^2. Thus the total temperature error is about

$$\epsilon = 0.03 + 0.02 P_o + 0.5 \times 10^{-16} f^2/P_o^2 \quad ,$$

where P_o is in atmospheres.

It is possible to reduce this error somewhat by a more thorough investigation of temperature effects on dispersion, but there is no need unless it appears feasible to measure temperature by this means at extremely high altitudes and other errors associated with the experiment are smaller than the dispersion error.

An example of corrections and errors for temperature measurements is given in Table 6-2. Two frequencies are assumed, 10,000 cps and 20,000 cps. It is apparent that large corrections and errors occur at high altitudes. This may be reduced by decreasing the frequency; however, since this also increases the size of the apparatus needed to obtain plane waves, there are some limitations.

Table 6-2
Example of corrections and errors for the measurement of temperature in the atmosphere(1)

Height (km)	20,000 cps Correction (°K)	20,000 cps Error (°K)	10,000 cps Correction (°K)	10,000 cps Error (°K)
10	+0.04	0.04	+0.04	0.04
20	+0.01	0.03	+0.01	0.03
30	0.00	0.03	0.00	0.03
40	-0.04	0.03	-0.01	0.03
50	-0.68	0.06	-0.17	0.04
60	-7.6	0.4	-1.9	0.1
70	---	---	- 20	2

(1) Atmospheric pressure and temperature taken from CIRA 1961 [20].

LITERATURE CITED

1. U. Ingard. 1958. Acoustics. Handbook of Physics, E. V. Condon and H. Odishaw, ed. McGraw-Hill: New York. p 3-112 to 3-113.

2. W. K. H. Panofsky and M. Phillips. 1955. Classical Electricity and Magnetism. Addison-Wesley: Reading, Mass.

3. F. V. Hunt. 1957. Propagation of sound in fluids. American Institute of Physics Handbook, D. E. Gray, ed. McGraw-Hill: New York. p 3-25 to 3-56.

4. H. B. Callen. 1960. Thermodynamics. John Wiley: New York. Appendix A.

5. K. F. Herzfeld and T. A. Litovitz. 1959. Absorption and Dispersion of Ultrasonic Waves. Academic Press: New York.

6. E. Glueckauf. 1951. The Composition of Atmospheric Air. Compendium of Meteorology, T. F. Malone, ed. American Meteorological Society: Boston. p 3-12.

7. W. F. Meggers. 1959. Key to the Periodic Chart of the Atoms. Welch Manufacturing Co.: Chicago.

8. J. W. M. Dumond and E. R. Cohen. 1958. Fundamental Constants of Atomic Physics. Handbook of Physics, E. V. Condon and H. Odishaw, ed. McGraw-Hill: New York. p 7-143.

9. G. Herzberg. 1950. Spectra of Diatomic Molecules. Van Nostrand: Princeton.

10. G. Herzberg and L. Herzberg. 1957. Constants of Polyatomic Molecules. American Institute of Physics Handbook. D. E. Gray, ed. McGraw-Hill: New York. p 7-145 to 7-161.

11. J. Hilsenrath, et al. 1955. Tables of Thermal Properties of Gases. NBS Circular 564: Washington.

12. F. B. Hilderbrand. 1956. Introduction to Numerical Analysis. McGraw-Hill: New York. p 134, 135.

13. E. H. Kennard. 1938. Kinetic Theory of Gases. McGraw-Hill: New York.

14. H. Knotzel and L. Knotzel. 1948. Shallabsorption and Dispersion in Sauerstoff. Ann. Physik. 2:393.

15. V. H. Blackman. 1955. Vibrational Relaxation in O_2 and N_2. Tech. Rept. Princeton University: Princeton.

16. E. A. Dean. 1959. Absorption of Low Frequency Sound in a Homogeneous Atmosphere. Tech. Rept. Texas Western College: El Paso.

17. M. Greenspan. 1954. Combined translational and relaxational dispersion of sound in gases. Jour. Acoust. Soc. Am. 26:70.

18. M. Greenspan. 1959. Rotational relaxation in nitrogen, oxygen, and air. Jour. Acoust. Soc. Am. 31:155.

19. J. G. Parker. 1959. Rotational and vibrational relaxation in diatomic gases. Phys. Fluids. 2:449.

20. Committee on Space Research. 1961. Cospar International Reference Atmosphere, 1961. H. Kallman-Bijl, et al, eds. North-Holland: Amsterdam.

DETERMINATION OF ATMOSPHERIC PARAMETERS

BY ACOUSTIC MEANS

DA-SIG-36-039-62-G17

Progress Report No. 1

July, 1962

Section I
SURVEY OF LITERATURE AND THEORETICAL INVESTIGATION

Thermal and Radiation Effects on Acoustic Measurements in the Upper Atmosphere

Richard C. Montgomery
Physicist

S C H E L L E N G E R R E S E A R C H L A B O R A T O R I E S

Texas Western College El Paso, Texas

C O N T E N T S

1. Introduction

Various sections included in this report are related to this study of convection and radiation heat effects on the performance of an airborne acoustic thermometer. Many simplifications have been made, but the results should be applicable to any body subject to radiation and laminar convection.

2. Derivation of the Equations Describing the Dynamic and Thermal Boundary Layers Due to Flow across a Flat Plate

If we assume that a flow of velocity U_s encounters a flat plate, we can determine the size and shape of the boundary layer which develops.

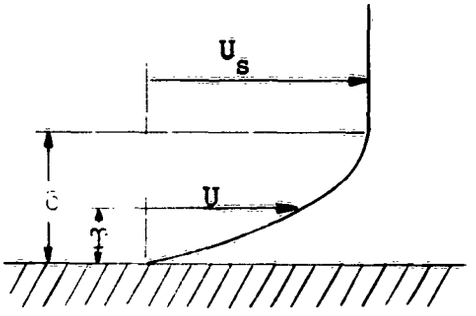

The flow will be determined from the space deviation of the momentum equation for boundary layers where U_s = stream velocity

U = local velocity

ρ = density

τ_ω = shear stress at the boundary

p = pressure

ℓ = layer thickness

$$\rho \frac{d}{dx} \int_o^\ell (U_s - U)\, U dy - \rho \frac{dU_s}{dx} \int_o^\ell U dy = \tau_\omega + \ell \frac{dp}{dx}$$

Since U_s is presumed to be constant, Bernoulli's equation states that the pressure p must be constant, and therefore the equation reduces to

$$\rho \frac{d}{dx} \int_0^{\ell} (U_s - U)\, U dy = \tau_\omega . \qquad (2\text{-}1)$$

The boundary conditions on this equation are

$$U = 0 \text{ for } y = 0,$$

$$U = U_s \text{ for } y = \delta .$$

From the equation governing two dimensional flow,

$$\rho \left(\frac{\partial U}{\partial \tau} + U \frac{\partial U}{\partial x} + V \frac{\partial U}{\partial y} \right) = - \frac{\partial P}{\partial x} + \mu \frac{\partial^2 U}{\partial y^2} .$$

Applied at $y = 0$, we find that

$$\frac{\partial^2 U}{\partial y^2} = 0 \quad \text{for } y = 0$$

and for a smooth fit of the curve to the free stream,

$$\frac{\partial U}{\partial y} = 0 \quad \text{at } y = \delta .$$

In order to satisfy these four conditions, we will assume that U can be represented as a four-term power series,

$$U = a + by + cy^2 + dy^3 .$$

From $U = 0$ when $y = 0$ we get $a = 0$.

From $\frac{\partial^2 U}{\partial y^2} = 0$ when $y = 0$ we get $c = 0$.

From $U = U_s$ at $y = \delta$, $U_s = b\delta + d\delta^3$.

From $\frac{\partial U}{\partial y} = 0$ at $y = \delta$, $0 = b + 3d\delta^2$.

Solving, we find $d = -\frac{1}{2} \frac{U_s}{\delta^3}$ and $b = \frac{3}{2} \frac{U_s}{\delta}$.

Thus, $$U = \frac{3}{2}\frac{U_s}{\delta} y - \frac{1}{2}\frac{U_s}{\delta^3} y^3 = \frac{3}{2} U_s\left(\frac{y}{\delta}\right) - \frac{1}{2} U_s\left(\frac{y}{\delta}\right)^3 ,$$

or $$\frac{U}{U_s} = \frac{3}{2}\left(\frac{y}{\delta}\right) - \frac{1}{2}\left(\frac{y}{\delta}\right)^3 .$$

Denoting the integrand as I, rearranging the left side of (2-1) and substituting (2-2) we get,

$$I = \rho \int_0^{\ell} (U_s - U)\, U\, dy$$

$$I = \rho\, U_s^2 \int_0^{\ell} \left(1 - \frac{U}{U_s}\right) \frac{U}{U_s}\, dy$$

$$I = \rho\, U_s^2 \int_0^{\ell} \left[1 - \frac{3}{2}\left(\frac{y}{\delta}\right) + \frac{1}{2}\left(\frac{y}{\delta}\right)^3\right]\left[\frac{3}{2}\left(\frac{y}{\delta}\right) - \frac{1}{2}\left(\frac{y}{\delta}\right)^3\right] dy$$

$$I = \rho\, U_s^2 \int_0^{\ell} \left[\frac{3}{2}\left(\frac{y}{\delta}\right) - \frac{9}{4}\left(\frac{y}{\delta}\right)^2 - \frac{1}{2}\left(\frac{y}{\delta}\right)^3 + \frac{3}{2}\left(\frac{y}{\delta}\right)^4 - \frac{1}{4}\left(\frac{y}{\delta}\right)^6\right] dy .$$

Since $U = U_s$ for $y \geq \delta$, the upper limit of the integral need only be taken to δ, where the integrand becomes and remains 0.

$$I = \rho\, U_s^2 \left[\frac{3}{4}\left(\frac{y}{\delta}\right) y - \frac{9}{12}\left(\frac{y}{\delta}\right)^2 y - \frac{1}{8}\left(\frac{y}{\delta}\right)^3 y - \frac{3}{10}\left(\frac{y}{\delta}\right)^4 y - \frac{1}{28}\left(\frac{y}{\delta}\right)^6 y\right]_0^{\delta}$$

$$= \rho\, U_s^2\, \delta\left[\frac{3}{4} - \frac{3}{4} - \frac{1}{8} + \frac{3}{10} - \frac{1}{28}\right]$$

$$= \rho U_s^2 \delta\left[\frac{3}{10} - \frac{1}{8} - \frac{1}{28}\right] = \rho\, U_s^2 \delta\left[\frac{39}{280}\right]. \qquad (2\text{-}3)$$

At the wall the velocity gradient is

$$\left(\frac{\partial U}{\partial y}\right)_{y=0} = \frac{3}{2}\frac{U_s}{\delta} ,$$

and

$$\tau_\omega = \mu \left(\frac{\partial U}{\partial y}\right)_{y=0} = \frac{3}{2} \mu \frac{U_s}{\delta} .$$

Therefore equation 2-1

$$\frac{d}{dx} I = \tau_\omega$$

reduces to

$$\frac{d}{dx}\left(\frac{39}{280} \rho U_s^2 \delta\right) = \frac{3}{2} \mu \frac{U_s}{\delta}$$

$$\delta \frac{d\delta}{dx} = \left(\frac{280}{39 \rho U_s^2}\right) \frac{3}{2} \mu U_s = \frac{140}{13} \frac{\mu}{\rho U_s} .$$

Separating variables,

$$\delta d\delta = \frac{140}{13} \frac{\mu}{\rho U_s} dx .$$

Integrating

$$\frac{\delta^2}{2} = \frac{140}{13} \frac{\mu}{\rho U_s} x + k ,$$

or

$$\delta = \sqrt{\frac{280}{13} \frac{\mu}{\rho U_s} x + 2k} .$$

If x is measured from the leading edges of the plate,

$$\delta = 4.64 \sqrt{\frac{\mu x}{\rho U_s}}$$

or

$$\frac{\delta}{x} = 4.64 \sqrt{\frac{\mu}{\rho U_s x}} = \frac{4.64}{\sqrt{\frac{\rho U_s x}{\mu}}} .$$

The term $\frac{\rho U_s x}{\mu}$ is known as the Reynolds number at a distance x, so that

$$\frac{\delta}{x} = 4.64 \, (Re_x)^{-\frac{1}{2}} . \qquad (2-4)$$

Using this value we will now introduce the heat-flow equation of boundary layers,

$$\frac{d}{dx}\int_0^{\ell} (t_s - t)\, U dy = \alpha \left(\frac{dt}{dy}\right)_{y=0} \qquad (2\text{-}5)$$

where t_s is the stream temperature, t is the local temperature, and α is the thermal conductivity divided by the product of density and specific heat, and solve it.

For boundary conditions we have

$$t = t_\omega \quad \text{for } y = 0,$$

$$t = t_s \quad \text{and} \quad \frac{\partial t}{\partial y} = 0 \quad \text{at } y = \delta_t ,$$

and

$$\frac{\partial^2 t}{\partial y^2} = 0 \quad \text{for } y = 0 .$$

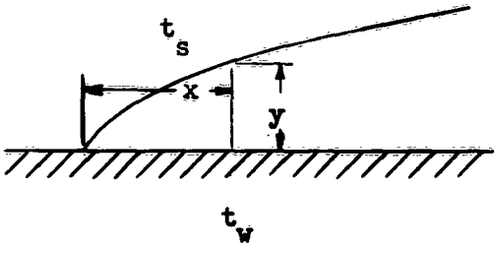

Again, using a four-term power series, we have

$$t = a + by + cy^2 + dy^3 .$$

If we introduce the variable $\theta = t - t_\omega$, we find $\theta = by + dy^3$, and

$$\theta' = \frac{\theta}{\theta_s} = \frac{3}{2}\left(\frac{y}{\delta_t}\right) - \frac{1}{2}\left(\frac{y}{\delta_t}\right)^3 ,$$

where

$$\theta_s = t_s - t_\omega .$$

The integral portion of (2-5)

$$I = \int_o^{\ell} (t_s - t)\, U dy = \int_o^{\ell} (\theta_s - \theta)\, U dy = \theta_s U_s \int_o^{\ell} (1 - \theta^1) \frac{U}{U_s}\, dy,$$

$$I = \theta_s U_s \int_o^{\ell} \left[1 - \frac{3}{2}\left(\frac{y}{\delta_t}\right) + \frac{1}{2}\left(\frac{y}{\delta_t}\right)^3\right]\left[\frac{3}{2}\left(\frac{y}{\delta}\right) - \frac{1}{2}\left(\frac{y}{\delta}\right)^3\right] dy .$$

Reducing the limit to δ_t we get

$$I = \theta_s U_s \int_o^{\delta_t} \left[\frac{3}{2}\left(\frac{y}{\delta}\right) - \frac{9}{4}\left(\frac{y}{\delta_t}\right)\left(\frac{y}{\delta}\right) - \frac{1}{2}\left(\frac{y}{\delta}\right)^3 + \frac{3}{4}\left(\frac{y}{\delta_t}\right)\left(\frac{y}{\delta}\right)^3 + \frac{3}{4}\left(\frac{y}{\delta_t}\right)^3\left(\frac{y}{\delta}\right) - \frac{1}{4}\left(\frac{y}{\delta_t}\right)^3\left(\frac{y}{\delta}\right)^3\right] dy$$

$$I = \theta_s U_s \left[\frac{3}{4}\left(\frac{y}{\delta}\right)y - \frac{3}{4}\left(\frac{y}{\delta_t}\right)\left(\frac{y}{\delta}\right)y - \frac{1}{8}\left(\frac{y}{\delta}\right)^3 y + \frac{3}{20}\left(\frac{y}{\delta_t}\right)\left(\frac{y}{\delta}\right)^3 y + \frac{3}{20}\left(\frac{y}{\delta_t}\right)^3\left(\frac{y}{\delta}\right)y - \frac{1}{28}\left(\frac{y}{\delta_t}\right)^3\left(\frac{y}{\delta}\right)^3 y\right]_o^{\delta_t}$$

$$I = \theta_s U_s \left[\frac{3}{4}\left(\frac{\delta_t}{\delta}\right)\delta_t - \frac{3}{4}\left(\frac{\delta_t}{\delta}\right)\delta_t - \frac{1}{8}\left(\frac{\delta_t}{\delta}\right)^3\delta + \frac{3}{20}\left(\frac{\delta_t}{\delta}\right)^3\delta + \frac{3}{20}\left(\frac{\delta_t}{\delta}\right)\delta_t - \frac{1}{28}\left(\frac{\delta_t}{\delta}\right)^3\delta_t\right]$$

$$= \theta_s U_s\, \delta_t \left[\left(\frac{3}{4} - \frac{3}{4} + \frac{3}{20}\right)\frac{\delta_t}{\delta} + \left(\frac{3}{20} - \frac{1}{8} - \frac{1}{28}\right)\left(\frac{\delta_t}{\delta}\right)^3\right].$$

Substituting $\zeta = \frac{\delta_t}{\delta}$, we have

$$I = \theta_s U_s \delta_t \left[\frac{3}{20}\zeta - \frac{3}{280}\zeta^3\right],$$

$$= \theta_s U_s \delta \left[\frac{3}{20}\zeta^2 - \frac{3}{280}\zeta^4\right].$$

If we assume that the thermal boundary layer equals the hydrodynamic boundary layer, i.e. $\zeta = 1$, the above equation becomes approximately

$$I = \theta_s U_s \delta\left(\frac{3}{20}\zeta^2\right),$$

that is, the fourth power term can be neglected.

Equation (2-5) then becomes

$$\frac{3}{20}\,\theta_s U_s \frac{d}{dx}\left(\delta\zeta^2\right) = \frac{3}{2}\,\alpha\frac{\theta_s}{\delta\zeta} ,$$

or

$$\frac{1}{10}\,U_s \left(\zeta^3\delta\frac{d\delta}{dx} + 2\zeta^2\delta^2\frac{d\zeta}{dx}\right) = \alpha .$$

Substituting for $\delta\frac{d\delta}{dx}$ and δ^2, we obtain

$$\frac{14}{13}\,\frac{\nu}{\alpha}\left(\zeta^3 + 4\times\zeta^2\frac{d\zeta}{dx}\right) = 1 ,$$

where ν, the kinematic viscosity, equals the viscosity divided by the density. Substituting $Pr = \frac{\nu}{\alpha}$, the Prandtl number

$$\zeta^3 + 4\left(\zeta^2\frac{d\zeta}{dx}\right) = \frac{13}{14\ Pr} .$$

Substituting $Z = \zeta^3$,

$$Z + \frac{4}{3}\left(\frac{dZ}{dx}\right) = \frac{13}{14\ Pr} .$$

Solution of this equation yields

$$Z = \frac{13}{14\ Pr} + Cx^{-3/4} .$$

When $x = 0$,

$$Z = \frac{13}{14\ Pr} ,$$

$$\zeta = \sqrt[3]{\frac{13}{14\ Pr}} ,$$

or

$$\zeta = \frac{1}{1.026\ \sqrt[3]{Pr}} \qquad (2\text{-}6)$$

$$\frac{\delta_t}{\delta} = \frac{1}{1.026\ \sqrt[3]{Pr}}$$

$$\delta_t = \frac{1}{1.026\sqrt[3]{Pr}} \; 4.64 \; (Re_x)^{-\frac{1}{2}} \; x$$

$$\delta_t = 4.53(Pr)^{-1/3} \; (Re_x)^{-\frac{1}{2}} \; x \; .$$

Since the Prandtl number of air is about .7, we find, from equation (2-6) that

$$\zeta = \frac{1}{.7234} = 1.08 \; .$$

Verifying the previous that $\zeta \doteq 1$, the final result gives

$$\delta_t = 4.53 \left(\frac{\nu}{\alpha}\right)^{-1\,3} \left(\frac{\nu}{U_s}\right)^{\frac{1}{2}} x^{\frac{1}{2}} \; .$$

3. Derivation of the Heat Transfer Coefficient.

The heat flow from the surface of a plate, such as that previously discussed, is given by

$$q = - k \; (d\theta / dy)_\omega \; ,$$

where k is the thermal conductivity of air. For convenience we shall derive a heat transfer coefficient h, such that

$$q = h \; (t_\omega - t_s) \; ,$$

where t_ω and t_s are the previously defined wall and stream temperatures. We have,

$$q = h \; (t_\omega - t_s) = - h\theta_s = - k(d\theta/dy)_\omega$$

or,

$$h = (k/\theta_s) \; (d\theta/dy)_w = k \; (d\theta^1/dy)_w = kd/dy \; \frac{3}{2}\left(\frac{y}{\delta_t}\right) - \frac{1}{2}\left(\frac{y}{\delta_t}\right)^3 \Big]_\omega$$

or,

$$h = \frac{k}{\delta_t}\left[\frac{3}{2} - \frac{3}{2}\left(\frac{y}{\delta_t}\right)^2\right]_{y=0} = \frac{3}{2}\frac{k}{\delta_t} .$$

Using the value previously obtained, we arrive at the equation,

$$h = 0.332 \frac{k}{x} \sqrt[3]{Pr}\ \sqrt{Re_x} .$$

Also of interest is the average heat transfer coefficient,

$$\underline{h} = \frac{1}{x}\int_0^x h\,dx = 2h = 0.664 \frac{k}{x} \sqrt[3]{Pr}\sqrt{Re_x} .$$

4. Variation of Heat Transfer Coefficient with Altitude.

Let us now consider the effect of temperature and pressure on the parameters of the heat transfer coefficient, k, Pr, and Re_x. The thermal conductivity k is independent of pressure over a wide range, but varies by approximately 80 percent from −100° to +200°F. The Prandtl number $Pr = \frac{\nu}{\alpha}$, where ν and α are both inversely proportional to density, thereby causes Pr to be independent of pressure (or density). From −100° to 200°F, the Prandtl number varies by approximately 7 percent. The Reynolds number $Re_x = \frac{U_\infty x}{\nu}$, varies inversely as ν, and therefore directly with pressure or density. In the range −100° to +200°F, ν and therefore Re_x vary by about 300 percent. The combined variation of the various parameters, with temperature, tend to cancel each other, so that h varies only 5 percent between −100° and +200°F. The heat transfer coefficient varies directly as the square root of density.

It should be noted that the previously derived expressions for heat transfer coefficient and temperature distribution are valid only for stream velocities well below the speed of sound. This necessity arises from two sources, the change in density due to local compression at high speeds,

and the heating effect which arises when a rapidly moving gas is slowed down. The change in density with velocity is given by the equation[1]

$$\frac{\Delta\rho}{\rho_o} = \frac{1}{2} M^2 ,$$

where M is the Mach number of the gas. The effect of frictional heating is described by the inequality[1]

$$T_\omega - T_s \gtrless \frac{\sqrt{Pr}\, U_s}{2gc} ,$$

where g is the gravitational constant and c is the specific heat, and where heat is transferred from the plate if the left side of the inequality is greater than the right side, and to the plate if the right side is greater than the left.

5. Temperature History.

In attempting to predict the temperature history of the transducer in flight, we will assume that it may be represented by a flat plate with an appropriate ratio of area to volume.

If we assume the proposed model, we can write the heat balance equation,

$$\rho c V \frac{dt}{d\tau} = -hA\,(t - t_f) + KA\epsilon - \epsilon\sigma A\,(t^4 - t_s^4)$$

or

$$\frac{dt}{d\tau} = \frac{-hA}{\rho c V}(t - t_f) + \frac{K\epsilon A}{\rho c V} - \frac{\epsilon\sigma A}{\rho c V}(t^4 - t_s^4) \qquad (2\text{-}7)$$

where

ρ = density

c = specific heat

V = Volume of body

A = surface area of body

h = heat transfer coefficient

K = solar radiation constant

ϵ = emissivity of body

σ = Stefan-Boltzmann constant

t = body temperature

t_f = air temperature

t_s = apparent radiation temperature of surroundings

τ = time.

In these equations, the terms involving h represent the heat lost or gained due to convection, the terms involving K represent the heat flux due to solar radiation, and the terms involving the fourth powers of temperature represent the heat lost or gained due to radiative exchange with the background.

Due to the difficulty involved in obtaining an exact solution to the differential equations, it is informative to study a series of simple cases, which yield some information about the processes occuring.

In the simplest instance, we may assume that the air temperature is constant and that there is no radiation of any kind. This assumption leads to the solution

$$\frac{t - t_f}{t_o - t_f} = \exp - (hA/\rho cV)_\tau ,$$

indicating an exponential approach to the air temperature.

As a second case, we will again assume that there is no radiation, and will assume that $t_f = B\tau$. That is, the air temperature is a linear function of time. In this instance we are lead to the solution,

$$t = B\tau - \frac{\rho cV}{hA} B \left[1 - e^{-(hA/\rho cV)\tau} \right] .$$

This solution indicates that the body temperature, after an initial transient state, lags behind the air temperature by a constant amount.

As a further step, let us consider the case in which we have linear air temperature combined with a constant radiation term K, or

$$\frac{dt}{d\tau} = \frac{-hA}{\rho cV} (t - t_f) + \frac{KA\epsilon}{\rho cV}$$

where

$$t_f = t_{fo} + B\tau .$$

This equation yields the solution,

$$t = B\tau + \frac{C - B}{\alpha} + \left(t_o - \frac{C - B}{\alpha} \right) e^{-\alpha\tau}$$

where

$$C = \frac{A}{\rho cV} (K\epsilon + ht_{fo})$$

and

$$\alpha = \frac{hA}{\rho cV} .$$

The solution indicates that for this case, after the initial transient has died out, the body temperature again follows the air temperature, but that the difference is modified by the radiation term.

With the above simplified solutions to form a basis for judgment, a computer program was prepared to solve equation (2-7) by increments. (See section I-4). Solutions have been run for the case of a body rising at the rate of 1000 ft per minute through the 1959 ARDC model atmosphere (simulated balloon flight) and falling at a variable rate (data for 4-6 lb

payload on a 15 ft parachute) through the same model atmosphere. For these calculations the ratio of volume to area was assumed to be .005 feet, and the body was assumed to be made of aluminum.

DETERMINATION OF ATMOSPHERIC PARAMETERS
BY ACOUSTIC MEANS

DA-SIG-36-039-62-G17

Progress Report No. 1

July, 1962

Section I:
SURVEY OF LITERATURE AND THEORETICAL INVESTIGATION

-4-

Numerical Analysis of Heat Balance Equations

Henry H. Launspach, Jr.
Physicist

SCHELLENGER RESEARCH LABORATORIES
Texas Western College El Paso, Texas

TABLE OF CONTENTS

1. Introduction

An airborne acoustic interferometer (See II-6), which has been designed to measure temperature and other atmospheric parameters, is to be carried through the atmosphere on a balloon (ascending) or on a parachute. Certain errors are caused in the measurements when the transducers are not in temperature equilibrium with the surrounding medium, as in the case when it is rising or falling through the atmosphere. The purpose of this study is to predict the transducer temperature at certain intervals during simulated flights so that an estimate of the errors may be obtained.

As given by Montgomery (See I-3), the variation of the transducer temperature with time may be represented by

$$\rho c V \frac{dt}{d\tau} = -hA(t - t_f) + KA\epsilon - \epsilon\sigma A(t^4 - t_s^4) \qquad (1\text{-}1)$$

where ρ = density of body,

c = specific heat of body,

V = volume of body,

A = surface area of body,

h = heat transfer coefficient,

K = solar radiation constant,

ϵ = emissivity of body,

σ = Stefan-Boltzmann constant,

t = body temperature,

t_f = air temperature,

t_s = apparent radiation temperature of surroundings,

and τ = time.

The three terms of the right member of the differential equation represent

convection, radiation absorption, and radiation emission, respectively. Because the third term contains a variable (temperature) raised to the fourth power, the equation does not lend itself to solution by ordinary means. Solutions were obtained numerically on the Bendix G-15 digital computer by the Runga-Kutta method.

2. Preliminary Studies

Before the Runga-Kutta solution was undertaken, preliminary studies were made to determine how the transducer would react under certain simplified conditions, and to evaluate and check coefficients, atmospheric parameters, and flight conditions. The solutions to three simplified versions of equation (1-1) were derived and after making certain assumptions about the transducer and its surrounding medium, numerical answers were obtained in tabular form on the computer. The derivation of the first simplified case is given in the following discussion.

Consider the heat balance equation with the convection term only

$$\rho c V \frac{dt}{d\tau} = - hA (t - t_f) \qquad (2\text{-}1)$$

For the case where the transducer is attached to a balloon rising at a constant rate through a region of the atmosphere where the temperature gradient, B, is constant, the atmospheric temperature may be represented as a function of time

$$t_f = B\tau + t_{f(o)} \qquad (2\text{-}2)$$

Substituting the value of t_f from equation (2-2) into equation (2-1) yields the solution

$$t = B\tau + \left[t_{f(o)} - \frac{\rho cV}{hA} B\right]\left[1 - \exp\left(-\frac{hA}{\rho cV}\tau\right)\right] + t_o\left[\exp\left(-\frac{hA\tau}{\rho cV}\right)\right]$$

(2-3)

where the initial conditions are $t = t_o$ and $t_f = t_{f(0)}$ when $\tau = 0$.

If the values of B or h should change during the time interval considered then equations (2-2) and (2-3) will not be valid. In the following discussion, expressions will be derived which will hold when the values of B and h are not constant. Consider an interval of time $\Delta\tau$ during which B and h are constant. From equation (2-3) the transducer temperature after this time is

$$t_1 = B\Delta\tau + \left[t_{f(o)} - \frac{\rho cV}{hA} B\right]\left[1 - \exp\left(-\frac{hA}{\rho cV}\Delta\tau\right)\right] + t_o\left[\exp\left(-\frac{hA}{\rho cV}\Delta\tau\right)\right]$$

and the air temperature is

$$t_{f(1)} = B\Delta\tau + t_{f(o)}$$

Now if t_1 and $t_{f(1)}$ are used as new initial conditions in equation (2-3), and if B and h are constant (but may have different values from the previous example), then the transducer and air temperatures after another increment of time are

$$t_2 = B\Delta\tau + \left[t_{f(1)} - \frac{\rho cV}{hA} B\right]\left[1 - \exp\left(-\frac{hA}{\rho cV}\Delta\tau\right)\right] + t_1\left[\exp\left(-\frac{hA}{\rho cV}\Delta\tau\right)\right]$$

$$t_{f(2)} = B\Delta\tau + t_{f(o)}$$

Following this same procedure, after n increments of time the temperatures are

$$t_n = B\Delta\tau + \left[t_{f(n-1)} - \frac{\rho cV}{hA}B\right]\left[1 - \exp\left(-\frac{hA}{\rho cV}\Delta\tau\right)\right] + t_{n-1}\left[\exp\left(-\frac{hA}{\rho cV}\Delta\tau\right)\right] \quad (2-4)$$

$$t_{f(n)} = B\Delta\tau + t_{f(n-1)} \quad (2-5)$$

Thus if the transducer or air temperatures are known at any time, the temperatures after an interval of time $\Delta\tau$ may be predicted provided the current values of B and h are known.

3. Balloon Flight Parameters

In order to simulate a balloon flight using equations (2-4) and (2-5) certain values were assigned to atmospheric and flight parameters. Based on the 1959 ARDC model atmosphere, the temperature gradients are

$$B = -3.6, \quad 0 \leq Z \leq 36$$

$$B = 0 \quad , \quad 36 < Z \leq 82$$

$$B = 1.6 \quad , \quad 82 < Z \leq 155$$

where B is the gradient in degrees F per 1000 feet and Z is the altitude in 1000 feet. The air density was assumed to decrease by a factor of 10 for each 50,000 feet, i.e.,

$$\rho \text{ (air)} = 0.08 \times 10^{-z/50} \text{ lb/cu ft} \quad (3-1)$$

The balloon ascent rate was given a value of 1000 feet per minute. This is based on past experience with neoprene balloons carrying 5 to 6 pound payloads up to about 70,000 feet. It is not known how well the assumed value

holds above this altitude. The transducer element was assumed to be a flat aluminum plate having a thickness of 0.005 feet (See II-7). Engineering units were used throughout the computation.

4. Preliminary Results

The computer was programmed to solve equations (2-4) and (2-5) simulating a balloon flight from mean sea level to 150,000 feet. The transducer and air temperatures and their differences were calculated and printed out for each minute of flight. This procedure was repeated for two other equations which had radiation terms. There is no direct comparison between the results obtained as certain parameters used in one equation were re-evaluated before solving the next equation, and therefore the data is not presented here. It was concluded that the best procedure in predicting the transducer temperature would be to find some way to solve equation (1-1). The Runga-Kutta method was chosen for this purpose.

5. The Runga-Kutta Method

Although the independent variable τ does not appear in the right member of equation (1-1), the parameters h and t_g can be expressed as functions of time, and therefore equation (1-1) may be written in the form

$$\frac{dt}{d\tau} = f(\tau, t) \qquad (5\text{-}1)$$

In general, such an equation having numerical coefficients and given initial conditions may be solved by a numerical method.. Suppose the solution to (5-1) is a smooth curve of the form $t = F(\tau)$. Starting with the initial values, the solution is constructed step by step for small (usually equal)

increments of the independent variable, i.e.,

$$\begin{aligned}
\tau_1 &= \tau_o + \Delta\tau, \; t_1 = t_o + \Delta t_o \\
\tau_2 &= \tau_1 \quad \Delta\tau, \; t_2 = t_1 + \Delta t_1 \\
&\cdots\cdots\cdots\cdots \\
\tau_{i+1} &= \tau_i + \Delta\tau, \; t_{i+1} = t_i + \Delta t_i
\end{aligned} \tag{5-2}$$

There are several methods of determining the increment of the dependent variable $\Delta\tau$ each one having its computational difficulties and inherent errors. The simplest of these is Euler's method, which requires extremely small increments of the independent variable to maintain sufficient accuracy

$$\Delta t_i = \left(\frac{dt}{d\tau}\right)_i \Delta\tau$$

where

$$\left(\frac{dt}{d\tau}\right)_i = f(\tau_i, t_i)$$

The Runga-Kutta method for finding $\Delta\tau_i$ is as follows

$$\Delta t_i = \frac{1}{6}(k_1 + 2k_2 + 2k_3 + k_4) \tag{5-3}$$

where

$$\begin{aligned}
k_1 &= \Delta\tau \, f(\tau_i, t_i) \\
k_2 &= \Delta\tau \, f\left(\tau_i + \frac{\Delta\tau}{2}, \; t_i + \frac{k_1}{2}\right) \\
k_3 &= \Delta\tau \, f\left(\tau_i + \frac{\Delta\tau}{2}, \; t_i + \frac{k_2}{2}\right) \\
k_4 &= \Delta\tau \, f\left(\tau_i + \Delta\tau, \; t_i + k_3\right)
\end{aligned}$$

The Runga-Kutta method, although more complicated than Euler's method, is more accurate. It does not require any special formulas to get the

solution started as does Milne's method[1], and is easily adapted for use on the digital computer. The increment of the independent variable can be easily changed, which proved to be a useful feature in solving the heat balance equation.

6. Flight Simulation Parameters

Computer programs were written to simulate flights of the acoustic interferometer ascending on a balloon or descending on a parachute through a model atmosphere.[2] The balloon flights were programmed from mean sea level to 155,000 feet whereas the parachute flights were started at 220,000 feet altitude and ended at 5,000 feet. The balloon ascent rate was given a constant value of 1000 feet per minute. The parachute descended at a variable rate, depending upon the altitude. The fall rates used (See Fig. 6-1) were based on several observations of 4 to 6 lb payloads attached to 15 foot parachutes which were ejected from Arcas missiles at altitudes of about 250,000 feet. The air density relation used in the preliminary studies, equation (3-1), was changed slightly to conform more closely to the model atmosphere, i.e.,

$$\rho \text{ (air)} = 0.08 \times 10^{-z/54} \quad \text{lb/cu ft}$$

where Z is the altitude in thousand feet. The value of the heat transfer

---

[1] For a detailed discussion on these and other numerical methods of solving differential equations see: F.B. Hildebrand, Introduction to Numerical Analysis, p. 188ff, McGraw-Hill, 1956; K.L. Nielsen, Methods in Numerical Analysis, p. 224ff, MacMillan, 1956.

[2] Air temperatures were based on the 1959 ARDC model atmosphere. Air density was obtained from a model described in Johnson, Satellite Environment Handbook, p. 20, Stanford University Press, 1961.

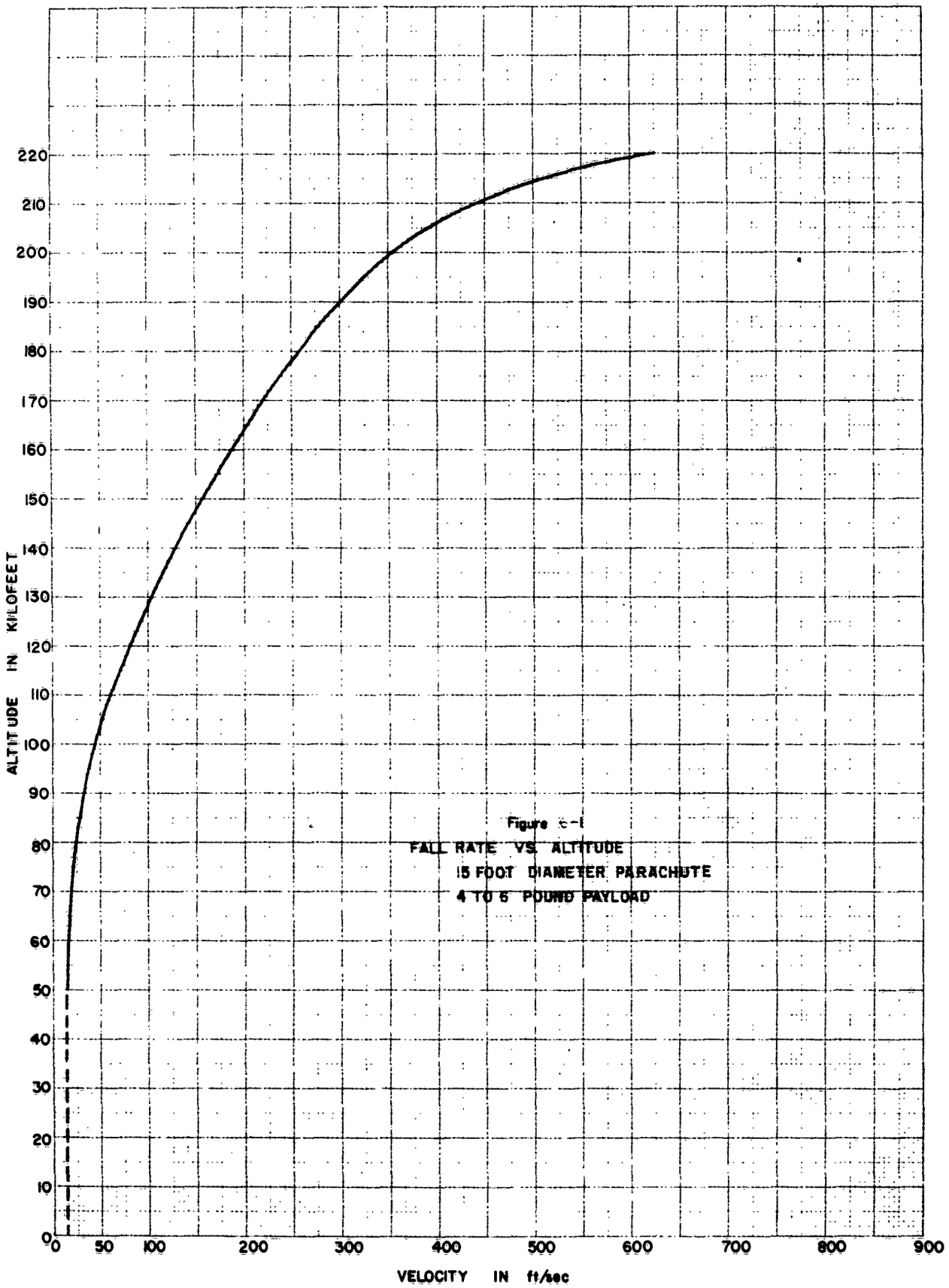

Figure c-1

FALL RATE VS. ALTITUDE

15 FOOT DIAMETER PARACHUTE

4 TO 5 POUND PAYLOAD

coefficient h is proportional to the square root of the air density

$$h = 2.1\sqrt{v}\left[10^{-z/108}\right] \text{ BTU/(hr ft}^2\ ^\circ\text{F)}$$

where v is ascent or descent rate in ft/sec. Other quantities used in the calculations were

$$\frac{A}{\rho c V} = 5.53\ ^\circ\text{F ft}^2\text{/BTU}$$

$$K = 200\ \text{BTU/ft}^2$$

$$\sigma = 0.173 \times 10^{-8}\ \text{BTU/(hr ft}^2\ ^\circ\text{R}^4\text{)}$$

The unit "R" is temperature expressed in degrees absolute Farenheit (Rankine).

7. The Computer Programs

The programs consisted essentially of the Runga-Kutta formulas, and several subroutines for evaluating the necessary parameters. Altitude was used as the independent variable instead of time, since most of the parameters were known as functions of altitude and also since the answers were desired every 5000 feet. Time and the time increment $\Delta\tau$ were calculated from the velocity vs. altitude function. For this reason it was necessary to include a simple sub-program to test whether the calculated $\Delta\tau$ had become large enough to make the solution unstable. The following method seemed to work satisfactorily. From the Runga-Kutta solution the k having the largest absolute value was selected. If it exceeded a certain value (5 degrees F was arbitrarily chosen) then the altitude increment (and hence the time increment $\Delta\tau$) was divided by X, a number proportional to the magnitude of the

k selected above.

The process of finding the solution to equation (1-1) on the computer is illustrated in the simplified flow diagram of the simulated parachute flight (Figure 7-1). The transducer was given an initial temperature of 90°F at 220,000 feet altitude. Two separate flights were run, corresponding to transducer emissivities of $\epsilon = 0$ (no radiation) and $\epsilon = 0.1$.

The balloon flight program is basically the parachute program with the velocity subroutine eliminated and a few other changes. The initial transducer temperature was 60°F at mean sea level. Two flights were made, as before, with $\epsilon = 0$ and $\epsilon = 0.1$.

In each of the above flights, the thermal boundary layer thickness at the transducer was calculated from the relation $\delta = 1/25h$ feet.

8. Results.

The difference between the predicted transducer temperatures and the standard atmosphere temperatures may be readily seen from the graphs (Figures 8-1 & 8-2). For the parachute flights (Figure 8-1), the predicted temperatures for $\epsilon = 0$ are closer to the air temperatures than those for $\epsilon = 0.1$, as expected. The difference between the two cases is about 10°F for most of the flight. Below 30,000 feet the curve for $\epsilon = 0$ lags the atmosphere by about 6°F whereas radiation ($\epsilon = 0.1$) brings the transducer almost in equilibrium with the air temperature. The predicted temperatures above 80,000 feet depend largely upon the initial transducer temperature. Based upon five samples, the average temperature inside the Arcas nose cone is about 110° - 120°F just before the instrument is ejected. A transducer having a temperature of 60°F on the ground would probably reach a maximum temperature of about 90°F or possibly less during the two minute missile

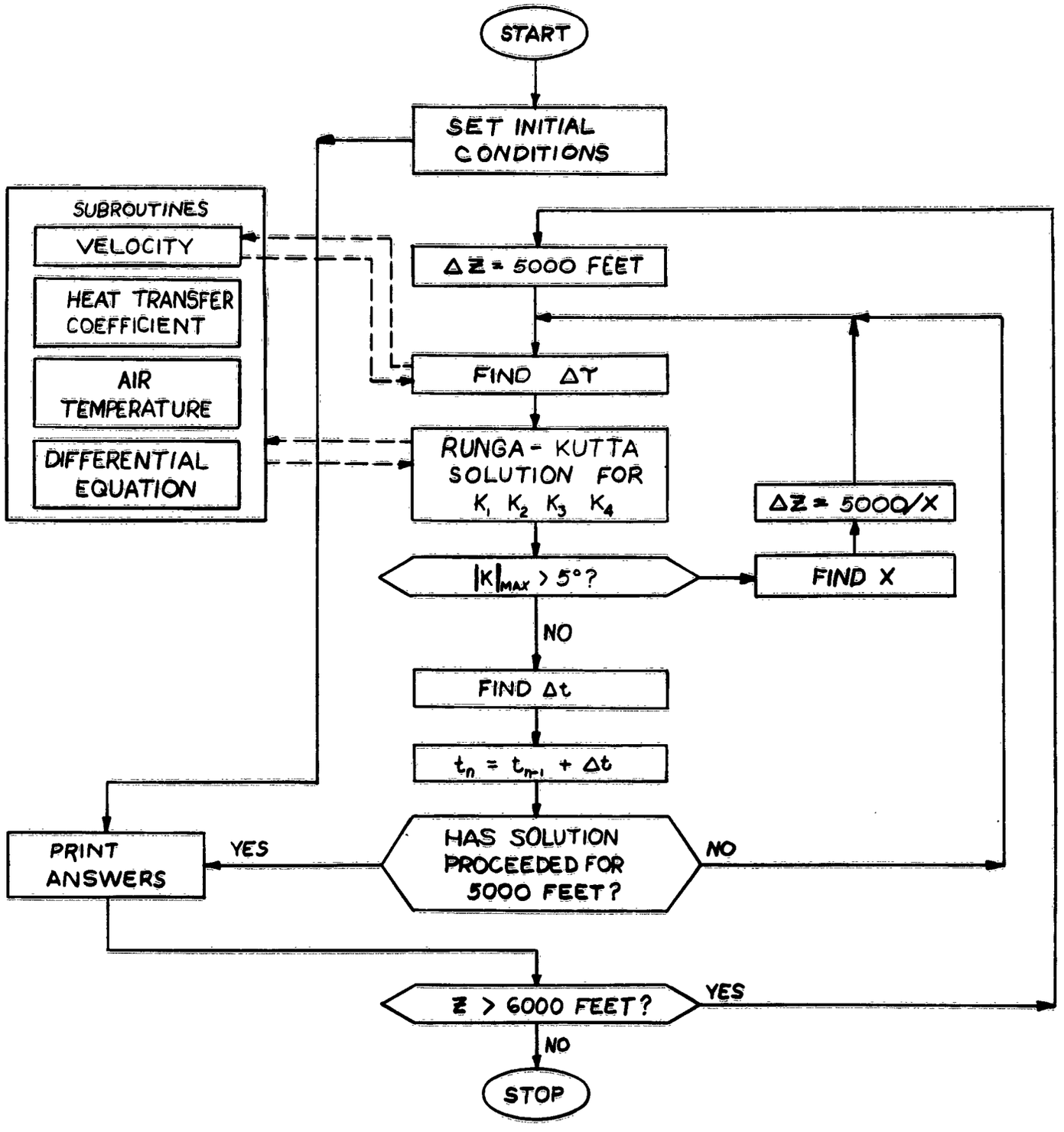

Fig. 7-1

Simplified Flow Diagram - Simulated Parachute Flight

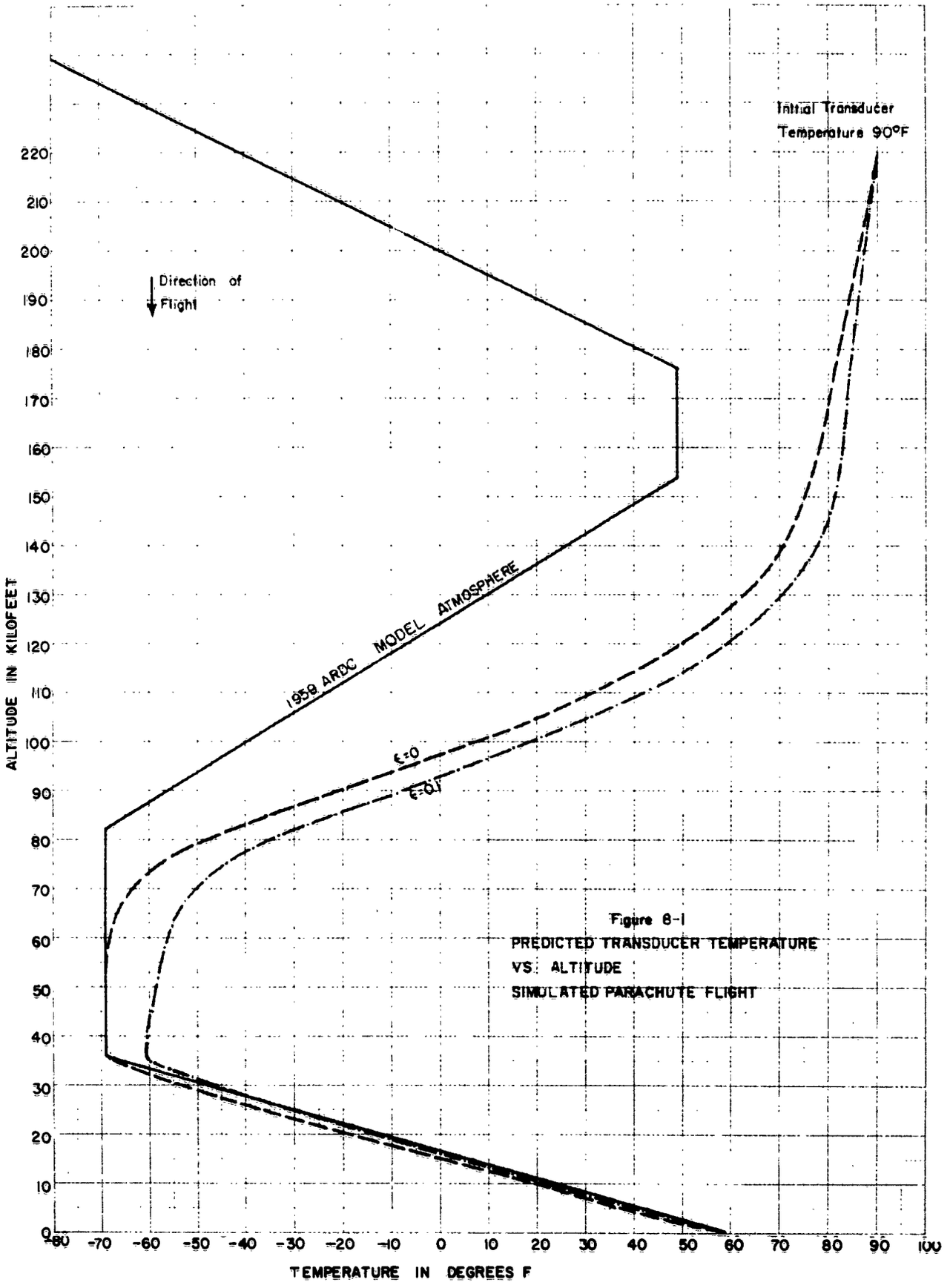

Figure 6-1
PREDICTED TRANSDUCER TEMPERATURE
VS. ALTITUDE
SIMULATED PARACHUTE FLIGHT

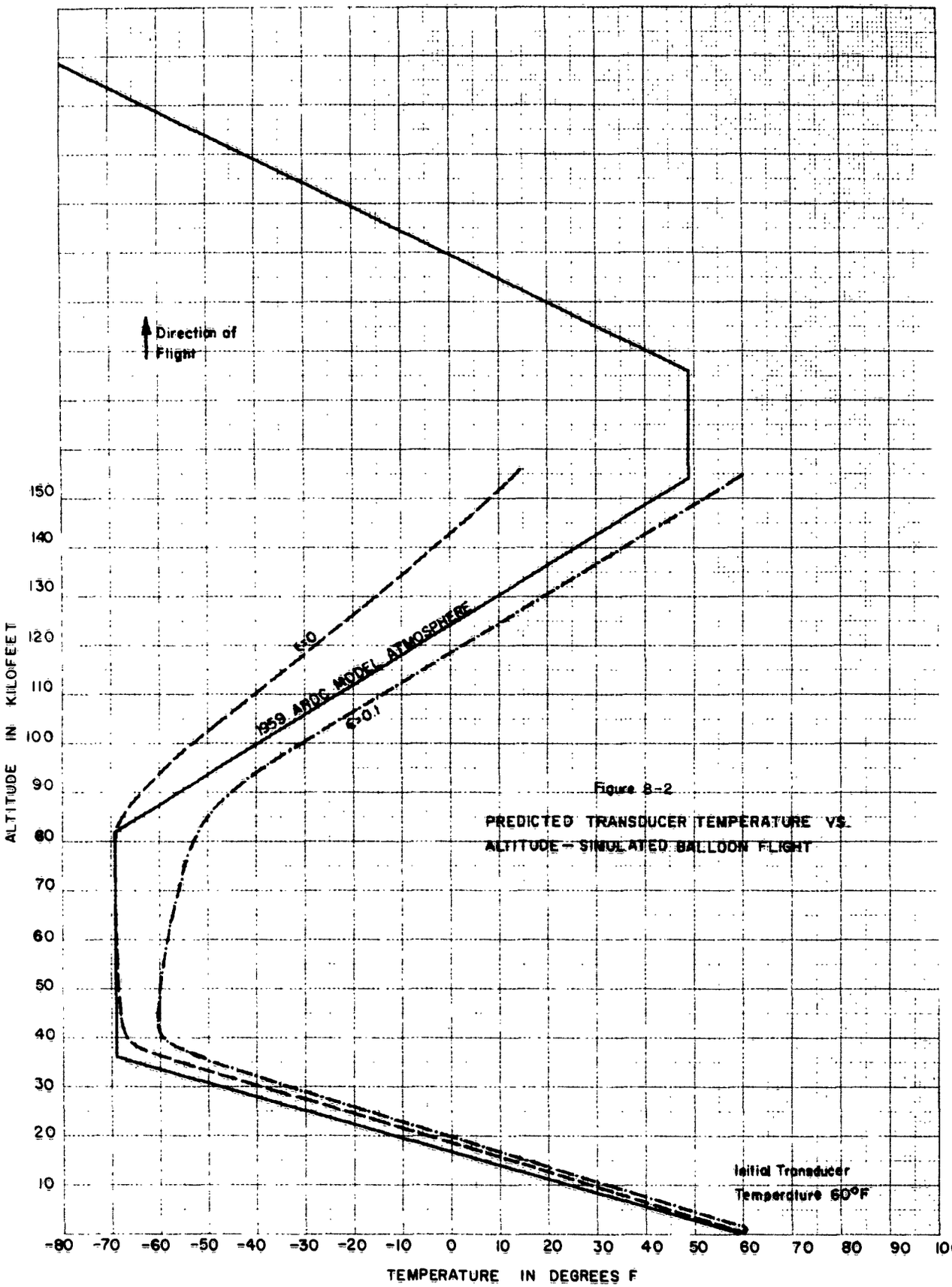

Figure 8-2

PREDICTED TRANSDUCER TEMPERATURE VS. ALTITUDE – SIMULATED BALLOON FLIGHT

flight. Complete results for the parachute flights as tabulated by the computer are given in Tables I & II.

The temperatures predicted for the balloon flight ($\epsilon = 0$) lag behind and finally reach the air temperature at about 70,000 feet (see Figure 8-2). After leaving the constant temperature region the transducer again lags the air temperature but the lag increases since the decreasing air density affects the heat transfer coefficient. For the flight with $\epsilon = 0.1$ the radiation effects predominate at about 50,000 feet and after leaving the constant temperature region the transducer leads the air temperature by about 10°F for the duration of the flight. Tables III & IV contain the computer output for the balloon flights.

In order to get a partial check on the above results, the program used to solve equation (2-4) in the preliminary studies (exact solution) was re-run using the same constants and parameters as in the Runga-Kutta solutions. These results differed from the corresponding Runga-Kutta solution (balloon flight, $\epsilon = 0$) by less than 0.5°F.

The results presented in this section are valid for a transducer element thickness of 0.005 feet. Since the quantity A/V appears in all the terms of the right member of equation (1-1) it is obvious that if a smaller plate thickness is used, the transducer will respond faster and the temperature difference between it and the atmosphere will be less.

TABLE I
TRANSDUCER TEMPERATURE vs AIR TEMPERATURE

Simulated Flight: Descent on Parachute

Transducer Emissivity = .000

ALTITUDE MSL (THSND FT)	TOTAL TIME (MIN)	LAYER TIME (SEC)	FALL RATE (FT/SEC)	BOUNDARY LAYER (FEET)	AIR TEMPERATURE (DEGREES F)	TRANSDUCER TEMPERATURE (DEGREES F)	TEMPERATURE DIFFERENCE (DEGREES F)
220.	.00	.00	625.	.082974	- 41.973	90.000	131.970
215.	.14	8.81	510.	.082565	- 31.635	89.177	120.810
210.	.32	10.52	440.	.079903	- 21.297	88.264	109.560
205.	.52	12.00	393.	.075996	- 10.959	87.285	98.245
200.	.74	13.33	357.	.071674	- .621	86.264	86.885
195.	.98	14.58	328.	.067163	9.716	85.221	75.504
190.	1.25	15.91	300.	.063175	20.054	84.179	64.125
185.	1.54	17.27	279.	.058885	30.392	83.168	52.777
180.	1.85	18.62	258.	.055043	40.730	82.227	41.498
175.	2.18	20.08	240.	.051299	49.000	81.375	32.375
170.	2.54	21.64	222.	.047945	49.000	80.523	31.523
165.	2.93	23.37	205.	.044766	49.000	79.565	30.565
160.	3.35	25.30	189.	.041929	49.000	78.493	29.493
155.	3.81	27.56	173.	.039418	49.000	77.296	28.296
150.	4.32	30.28	157.	.037220	42.444	75.803	33.359
145.	4.87	33.25	143.	.034965	34.250	73.746	39.496
140.	5.48	36.46	130.	.032986	26.056	70.971	44.915
135.	6.15	40.36	117.	.031281	17.861	67.340	49.479
130.	6.90	45.19	104.	.029856	9.666	62.699	53.032
125.	7.75	50.66	93.	.028304	1.472	56.904	55.432
120.	8.69	56.70	83.	.027003	- 6.722	49.863	56.585
115.	9.77	64.39	72.	.025971	- 14.916	41.445	56.362
110.	11.01	74.48	62.	.025244	- 23.111	31.548	54.659
105.	12.44	85.75	54.	.024148	- 31.305	20.252	51.558
100.	14.07	97.95	47.	.023304	- 39.500	7.761	47.262
95.	15.97	114.20	40.	.022756	- 47.694	- 5.769	41.925
90.	18.26	136.94	33.	.022590	- 55.889	- 20.113	35.776
85.	20.90	158.84	30.	.021297	- 64.083	- 34.527	29.557
80.	23.83	175.59	27.	.020179	- 69.000	- 47.960	21.040
75.	27.10	196.28	24.	.019239	- 69.000	- 57.561	11.439
70.	30.81	222.51	21.	.018488	- 69.000	- 63.442	5.557
65.	34.93	246.91	19.	.017246	- 69.000	- 66.596	2.403
60.	39.37	266.67	18.	.016135	- 69.000	- 68.080	.919
55.	44.20	289.85	16.	.015148	- 69.000	- 68.692	.307
50.	49.49	317.46	15.	.014281	- 69.000	- 68.909	.090
45.	55.05	333.33	15.	.012837	- 69.000	- 68.975	.024
40.	60.60	333.33	15.	.011539	- 69.000	- 68.993	.006
35.	66.16	333.33	15.	.010372	- 65.444	- 66.729	- 1.284
30.	71.71	333.33	15.	.009323	- 47.667	- 53.274	- 5.607
25.	77.27	333.33	15.	.008380	- 29.889	- 37.256	- 7.367
20.	82.83	333.33	15.	.007533	- 12.111	- 18.945	- 6.833
15.	88.38	333.33	15.	.006771	- 5.666	- .467	- 6.134
10.	93.94	333.33	15.	.006086	- 23.444	- 17.951	- 5.493
5.	99.49	333.33	15.	.005471	- 41.222	- 36.302	- 4.920

TABLE II
TRANSDUCER TEMPERATURE vs AIR TEMPERATURE

SIMULATED FLIGHT: DESCENT ON PARACHUTE

Transducer Emissivity = .100

ALTITUDE MSL (THSND FT)	TOTAL TIME (MIN)	LAYER TIME (SEC)	FALL RATE (FT/SEC)	BOUNDARY LAYER (FEET)	AIR TEMPERATURE (DEGREES F)	TRANSDUCER TEMPERATURE (DEGREES F)	TEMPERATURE DIFFERENCE (DEGREES F)
220.	.00	.00	625.	.082974	- 41.973	90.000	131.970
215.	.14	8.81	510.	.082565	- 31.635	89.403	121.040
210.	.32	10.52	440.	.079903	- 21.297	88.759	110.060
205.	.52	12.00	393.	.075996	- 10.959	88.086	99.046
200.	.74	13.33	357.	.071674	- .621	87.402	88.023
195.	.98	14.58	328.	.067163	9.716	86.724	77.008
190.	1.25	15.91	300.	.063175	20.054	86.076	66.022
185.	1.54	17.27	279.	.058885	30.392	85.485	55.094
180.	1.85	18.62	258.	.055043	40.730	84.987	44.258
175.	2.18	20.08	240.	.051299	49.000	84.600	35.600
170.	2.54	21.64	222.	.047945	49.000	84.233	35.232
165.	2.93	23.37	205.	.044766	49.000	83.777	34.777
160.	3.35	25.30	189.	.041929	49,000	83.224	34.224
155.	3.81	27.56	173.	.039418	49.000	82.561	33.561
150.	4.32	30.28	157.	.037220	42.444	81.619	39.175
145.	4.87	33.25	143.	.034965	34.250	80.125	45.875
140.	5.48	36.46	130.	.032986	26.056	77.917	51.861
135.	6.15	40.36	117.	.031281	17.861	74.859	56.998
130.	6.90	45.19	104.	.029856	9.666	70.802	61.135
125.	7.75	50.63	93.	.028304	1.472	65.607	64.135
120.	8.69	56.70	83.	.027003	- 6.722	59.149	65.871
115.	9.77	64.39	72.	.025971	- 14.916	51.317	66.233
110.	11.01	74.48	62.	.025244	- 23.111	42.025	65.135
105.	12.44	85.75	54.	.024148	- 31.305	31.334	62.639
100.	14.07	97.94	47.	.023304	- 39.500	19.420	58.919
95.	15.97	114.20	40.	.022756	- 47.694	6.449	54.144
90.	18.26	136.94	33.	.022590	- 55.889	- 7.304	48.584
85.	20.90	158.84	30.	.021297	- 64.083	- 21.244	42.839
80.	23.83	175.59	27.	.020179	- 69.000	- 34.479	34.521
75.	27.10	196.28	24.	.019239	- 69.000	- 44.123	24.877
70.	30.81	222.51	21.	.018488	- 69.000	- 50.233	18.767
65.	34.93	246.91	19.	.017246	- 69.000	- 53.862	15.138
60.	39.37	266.67	18.	.016135	- 69.000	- 56.046	12.954
55.	44.20	289.85	16.	.015148	- 69.000	- 57.421	11.579
50.	49.49	317.46	15.	.014281	- 69.000	- 58.364	10.636
45.	55.05	333.33	15.	.012837	- 69.000	- 59.328	9.672
40.	60.60	333.33	15.	.011539	- 69.000	- 60.312	8.688
35.	66.16	333.33	15.	.010372	- 65.444	- 58.952	6.492
30.	71.71	333.33	15.	.009323	- 47.667	- 46.334	1.332
25.	77.27	333.33	15.	.008380	- 29.889	- 31.279	- 1.390
20.	82.83	333.33	15.	.007533	- 12.111	- 13.797	- 1.686
15.	88.38	333.33	15.	.006771	5.666	3.936	- 1.730
10.	93.94	333.33	15.	.006086	23.444	21.690	- 1.754
5.	99.49	333.33	15.	.005471	41.222	39.446	- 1.776

TABLE III

TRANSDUCER TEMPERATURE vs AIR TEMPERATURE

Simulated Flight: Ascent on Balloon

Ascent Rate = 1000 Ft/Min., Transducer Emissivity = .000

ALTITUDE MSL (THSND FT)	ELAPSED TIME (MIN)	BOUNDARY LAYER (FEET)	AIR DENSITY (LB/CU FT)	AIR TEMPERATURE (DEGREES F)	TRANSDUCER TEMPERATURE (DEGREES F)	TEMPERATURE DIFFERENCE (DEGREES F)
0.	0.	.004665	.080000	59.000	60.000	1.000
5.	5.	.005190	.064639	41.222	46.030	4.807
10.	10.	.005774	.052228	23.444	28.866	5.421
15.	15.	.006424	.042200	5.666	11.682	6.015
20.	20.	.007146	.034097	- 12.111	- 5.443	6.667
25.	25.	.007950	.027550	- 29.889	- 22.501	7.387
30.	30.	.008844	.022260	- 47.667	- 39.484	8.182
35.	35.	.009839	.017986	- 65.444	- 56.386	9.058
40.	40.	.010947	.014533	- 69.000	- 66.708	2.292
45.	45.	.012178	.011742	- 69.000	- 68.381	.618
50.	50.	.013548	.009487	- 69.000	- 68.827	.172
55.	55.	.015072	.007666	- 69.000	- 68.948	.051
60.	60.	.016768	.006194	- 69.000	- 68.983	.017
65.	65.	.018654	.005004	- 69.000	- 68.994	.006
70.	70.	.020752	.004043	- 69.000	- 68.998	.002
75.	75.	.023087	.003267	- 69.000	- 68.999	.001
80.	80.	.025684	.002640	- 69.000	- 69.000	.000
85.	85.	.028573	.002133	- 64.083	- 67.670	- 3.586
90.	90.	.031787	.001723	- 55.889	- 64.022	- 8.133
95.	95.	.035363	.001392	- 47.694	- 58.765	- 11.071
100.	100.	.039341	.001125	- 39.500	- 52.791	- 13.291
105.	105.	.043766	.000909	- 31.306	- 46.520	- 15.214
110.	110.	.048689	.000734	- 23.111	- 40.147	- 17.036
115.	115.	.054167	.000593	- 14.917	- 33.774	- 18.857
120.	120.	.060260	.000479	- 6.722	- 27.456	- 20.734
125.	125.	.067038	.000387	1.472	- 21.227	- 22.699
130.	130.	.074580	.000313	9.666	- 15.108	- 24.774
135.	135.	.082970	.000252	17.862	- 9.112	- 26.974
140.	140.	.092303	.000204	26.056	- 3.264	- 29.320
145.	145.	.102690	.000165	34.250	2.442	- 31.807
150.	150.	.114240	.000133	42.444	8.002	- 34.442
155.	155.	.127090	.000107	49.000	13.350	- 35.650

TABLE IV

TRANSDUCER TEMPERATURE vs AIR TEMPERATURE

Simulated Flight: Ascent on Balloon

Ascent Rate = 1000 Ft/Min., Transducer Emissivity = .100

ALTITUDE MSL (THSND FT)	ELAPSED TIME (MIN)	BOUNDARY LAYER (FEET)	AIR DENSITY (LB/CU FT)	AIR TEMPERATURE (DEGREES F)	TRANSDUCER TEMPERATURE (DEGREES F)	TEMPERATURE DIFFERENCE (DEGREES F)
0.	0.	.004665	.080000	59.000	60.000	1.000
5.	5.	.005190	.064639	41.222	48.585	7.362
10.	10.	.005774	.052228	23.444	31.955	8.510
15.	15.	.006424	.042200	5.666	15.311	9.644
20.	20.	.007146	.034097	- 12.111	- 1.219	10.892
25.	25.	.007950	.027550	- 29.889	- 17.621	12.268
30.	30.	.008844	.022260	- 47.667	- 33.883	13.784
35.	35.	.009839	.017986	- 65.444	- 49.992	15.452
40.	40.	.010947	.014533	- 69.000	- 59.435	9.565
45.	45.	.012178	.011742	- 69.000	- 60.316	8.684
50.	50.	.013548	.009487	- 69.000	- 59.917	9.082
55.	55.	.015072	.007666	- 69.000	- 59.118	9.882
60.	60.	.016768	.006194	- 69.000	- 58.147	10.853
65.	65.	.018654	.005004	- 69.000	- 57.060	11.940
70.	70.	.020752	.004043	- 69.000	- 55.866	13.134
75.	75.	.023087	.003267	- 69.000	- 54.564	14.436
80.	80.	.025684	.002640	- 69.000	- 53.147	15.853
85.	85.	.028573	.002133	- 64.083	- 50.288	13.796
90.	90.	.031787	.001723	- 55.889	- 44.972	10.917
95.	95.	.035363	.001392	- 47.694	- 37.995	9.699
100.	100.	.039341	.001125	- 39.500	- 30.255	9.244
105.	105.	.043766	.000909	- 31.306	- 22.140	9.165
110.	110.	.048689	.000734	- 23.111	- 13.843	9.268
115.	115.	.054167	.000593	- 14.917	- 5.465	9.451
120.	120.	.060260	.000479	- 6.722	2.934	9.657
125.	125.	.067038	.000387	1.472	11.322	9.849
130.	130.	.074580	.000313	9.666	19.669	10.003
135.	135.	.082970	.000252	17.862	27.956	10.094
140.	140.	.092303	.000204	26.056	36.163	10.107
145.	145.	.102690	.000165	34.250	44.274	10.023
150.	150.	.114240	.000133	42.445	52.271	9.826
155.	155.	.127090	.000107	49.000	60.100	11.100

DETERMINATION OF ATMOSPHERIC PARAMETERS BY ACOUSTIC MEANS

Progress Report No. 1

Section I:

SURVEY OF LITERATURE AND THEORETICAL INVESTIGATION

-5-

Thermal Boundary Layer Effects on the Sonotherm Acoustic Interferometer

Eyung-Wha Kang
Electrical Engineer

S C H E L L E N G E R R E S E A R C H L A B O R A T O R I E S
Texas Western College El Paso, Texas

C O N T E N T S

1. INTRODUCTION

1.1. General

The acoustic interferometer (See Section II-6) or Sonotherm is designed to measure atmospheric parameters from a moving platform. Since the motion of the transducer through the air is equivalent to the flow of a viscous fluid past a solid boundary, a boundary layer will be set up near the transducer faces. The structure of this layer is discussed in Section I-3. Of particular interest are the thickness of the layer and the behavior of the temperature and density gradients between the transducer face and the undisturbed medium since these factors have a great influence on the speed of sound as it is transmitted through the space between the faces.

This paper presents a study of acoustic wave transmission in the atmospheric medium by the electrical transmission line analogy. The transmission is described by a second order nonlinear differential equation with variable coefficients, whose solution in closed form does not exist. The best solutions are obtained by the WKBJ approximation method and Frobenius' method. The WKBJ method yields a solution in exponential form. This method involves a restricting condition over the application of the solution; however, a better comprehension of system behavior is possible due to the simpler and more descriptive solution. The solution by the Frobenius method is in the form of an infinite power series which is not of any known function. The accuracy of this method can be improved to any desired degree by inclusion of additional terms. Therefore, this method should be used when numerical accuracy is desired.

The solution obtained is combined with four-terminal electrical network

analysis in order to further the investigation of acoustic impedance across the transducer. The result of the theoretical analysis is an expression of the acoustic impedance across the transducer which related the characteristic impedance of the undisturbed medium whose temperature is to be determined to the characteristic impedance of the boundary layer and the frequency at which the pressure peaks are to be detected.

Finally the method of applying these results to the determination of the speed of sound in the undisturbed medium is presented.

1.2. Initial Concept and Object

Consider an ideal case of a plane wave generator and a parallel receiver/reflector separated by a distance. The temperature of the system is assumed to have reached equilibrium and the air medium between the plates is a homogeneous, isotropic, ideal gas in the direction of the propagation.

It is well known that the temperature of the medium can be determined based on the known dependence of the velocity of acoustic propagation upon the temperature of the medium,

$$c = \sqrt{\frac{\gamma R}{M} T}$$

where

γ = ratio of specific heat at constant pressure to that of at constant volume

R = universal gas constant
M = molecular mass of air
T = temperature of medium

The measurement of temperature by the acoustic wave transmission method is essentially reduced to the measurement of the velocity c. The velocity is of course dependent upon the acoustic impedance of the medium. The

actual situation in the atmsophere is far from the ideal. First, there would rarely be a temperature equilibrium between the instrument and the atmospheric medium; secondly, the medium would not be isotropic nor homogeneous because of the thermodynamic boundary layer formed due to the relative motion of the system with respect to the atmospheric medium. The effects of the viscosity of the medium are considered to be limited to the formation of this fluid boundary layer. Acoustically, the medium is still considered to be ideal, and viscous effects are neglected.

The immediate object of the investigation of the acoustic impedance of the atmospheric medium is the determination of the boundary layer characteristics and their effects on the wave transmission. The boundary layer characteristics, taking into consideration all possible variations of the parameters involved, dictate the variation of acoustic impedance and in turn the velocity c.

1.3. Physical Description and the Operations

Ideally, the acoustic interferometer (section II-6) consists of a plane wave generator and a receiver/reflector. The separation is some integral multiple of a half-wavelength.

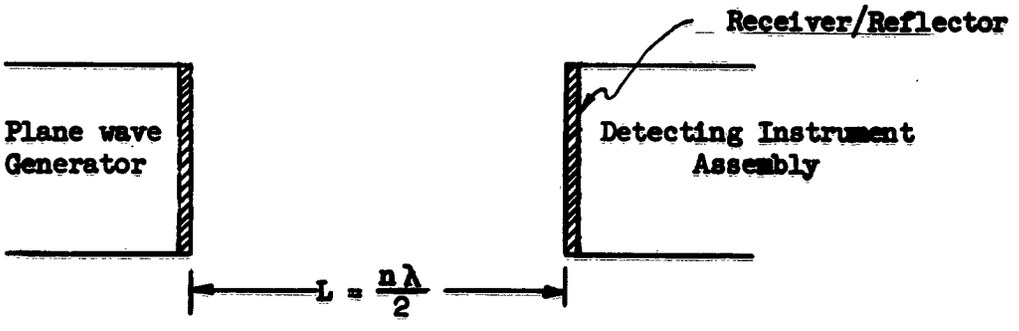

Figure 1.3-1

The operating frequency of the generator is 25-30 KC. The detecting instrument assembly continuously records the magnitude of the standing wave pressure on the face of the receiver/reflector as the generator varies its frequency. The maximum pressure exists only when the frequency is such that the separation is some integral multiple of a half-wavelength. The velocity c is determined on the basis of the relationship

$$L = \frac{n\lambda}{2} = \frac{n\pi c}{\omega_o} \qquad (1.3\text{-}1)$$

where λ = wavelength
ω_o = normal frequency (frequency at which the maximum acoustic pressure is detected.)

As was mentioned, the medium is not homogeneous nor isotropic. The above equation must be modified according to the boundary layer characteristics:

$$L = \frac{n\lambda}{2} = \frac{n\pi c}{\omega_o + \Delta\omega} \qquad (1.3\text{-}2)$$

The boundary layer is assumed to be parallel to the transducer faces. An investigation of the boundary characteristics has indicated that the temperature variation in the direction of propagation is given as [1]

$$T(x) = (T_o - T_w)\left[\frac{3}{2}\left(\frac{x}{\delta}\right) - \frac{1}{2}\left(\frac{x}{\delta}\right)^3\right] + T_w \qquad (1.3\text{-}3)$$

where T_w = temperature of generator and receiver/reflector,
T_o = temperature of undisturbed atmospheric medium, and
δ = thickness of boundary layer ($x \leq \delta$).

Then the velocity of acoustic wave propagation in the boundary is expressible as:

$$c(x) = c_o\left\{1 - \frac{\Delta T}{T_o}\left[1 + \frac{1}{2}\left(\frac{x}{\delta}\right)^3 - \frac{3}{2}\left(\frac{x}{\delta}\right)\right]^{\frac{1}{2}}\right\} \qquad (1.3\text{-}4)$$

c_o = velocity in the undisturbed medium
ΔT = temperature difference $T_o - T_w$.

1.4. Characteristic Impedance

The acoustic characteristic impedance is defined as the ratio of the effective sound pressure at a given point to the effective particle velocity at the point, and is equal to the product of the density of the medium and the velocity of sound c. The impedance of the boundary layer and the undisturbed mid-section are discussed below.

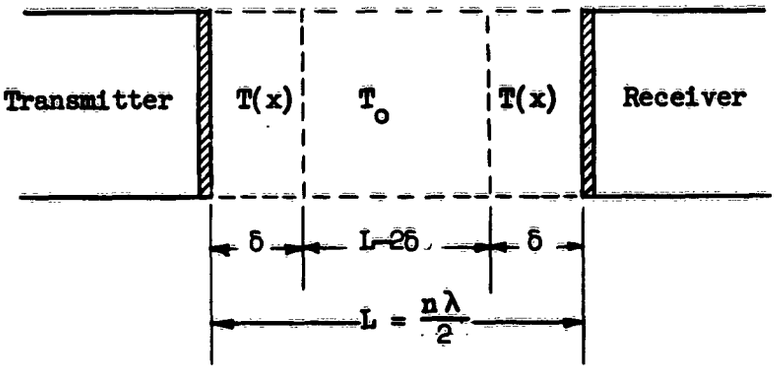

Figure 1.4-1

1.41. Undisturbed Mid-Section (L-2δ)

The characteristic impedance of this section (Z_o) is given as:

$$Z_o = \rho_o c_o .$$

Being undisturbed, this section is homogeneous and isotropic. Discussions given above under the ideal situation are applicable.

1.42. Boumdary Layer

The characteristic impedance of the boundary layer is dependent upon the position as Equation 1.42-1 shows. The characteristic impedance is a function of x, δ, and ΔT.

$$Z(x) = \rho(x)c(x) = f(x,\delta,\Delta T) \qquad (1.42\text{-}1)$$

Derivation of $f(x,\delta,\Delta T)$ is given in detail in section 4.

2.0. WAVE EQUATION AND ACOUSTIC IMPEDANCE

2.1. Solution for Undisturbed Medium

The propagation of plane waves in a homogeneous, isotropic nondissipating medium is governed by the following equations. [2]

$$-\frac{\partial p}{\partial x} = \rho \frac{\partial u}{\partial t}$$

$$-\frac{\partial u}{\partial x} = \frac{1}{B} \frac{\partial p}{\partial t} \qquad (2.1\text{-}1)$$

p = particle pressure
u = particle velocity
ρ = density of medium
B = bulk modulus (adiabatic)

With the particle pressure as a dependent variable, the wave equation is

$$\frac{\partial^2 p}{\partial x^2} = \frac{1}{c_o^2} \frac{\partial^2 p}{\partial t^2} \qquad (2.1\text{-}2)$$

The general solution to this equation assuming sinusoidal variation is

$$p(x) = Ae^{j(\omega t \pm \frac{x}{c_o})} \qquad (2.1\text{-}3a)$$

$$u(x) = \frac{j}{\omega \rho(x)} \cdot \frac{dp}{dx} \qquad (2.1\text{-}3b)$$

and the impedance as a function of position is

$$Z(x) = \frac{p(x)}{u(x)} = \rho_o c_o \qquad (2.1\text{-}3c)$$

2.2. Solution for the Disturbed Boundary Layer

The resultant differential equation after the variation of c is considered is of second degree, nonlinear, with variable coefficients.

$$\frac{\partial^2 p}{\partial x^2} = \frac{1}{[c(x)]^2} \frac{\partial^2 p}{\partial t^2} \qquad (2.2\text{-}1)$$

where

$$c(x) = c_o \left\{ 1 - \frac{\Delta T}{T_o} \left[1 + \frac{1}{2}\left(\frac{x}{\delta}\right)^3 - \frac{3}{2}\left(\frac{x}{\delta}\right) \right] \right\}^{\frac{1}{2}}$$

The solution to this equation is in form of

$$p(x) = Ae^{j(\omega t + \gamma_1 x)} + Be^{-j(\omega t + \gamma_2 x)} \qquad (2.2\text{-}2a)$$

$$u(x) = \frac{j}{\omega \rho(x)} \cdot \frac{dp}{dx} \qquad (2.2\text{-}2b)$$

$$Z(x) = \frac{p(x)}{u(x)} \qquad (2.2\text{-}2c)$$

γ_1 = forward propagation constant
γ_2 = backward propagation constant
A, B = constants
(γ is a complex quantity whose imaginary term is the absorption constant and the real term is the phase constant.)

Unlike in the undisturbed mid-section, the impedance Z(x) of the boundary is a function of x, δ, $\frac{\Delta T}{T_o}$. As it is seen, the velocity of c(x) in the boundary is most important in the determination of ambient temperature.

3. SOLUTION OF THE DIFFERENTIAL EQUATION

3.1 General

There are considerable advantages in finding an analytical solution for a differential equation when this is possible. The solution to Eq. (2.2-1) in analytic form contains such acoustic parameters as boundary thickness (δ), the temperature difference (ΔT), and the normal frequency (ω_o), whose interrelationship is important for the investigation of acoustic impedance.

There are several methods of solution to this type of nonlinear differential equation. As is true for virtually all methods of attacking nonlinear

problems, no one of these methods gives all the information desired. Often it is desirable to use several methods, each method providing certain information otherwise unobtainable by other methods. Considering the complications arising in each method and the accuracy of the solution in the final numerical value, a solution by the WKBJ approximation method and Frobenius' method are employed.

Mathematical procedures for Frobenius' method are tedious but the degree of accuracy can be improved by adding more terms in the power series. The WKBJ method provides a general descriptive solution from which the interrelationships among the parameters can be studied.

3.2. WKBJ Approximation Method [3]

Eq. 2.1-4 is rewritten in a slightly different form as shown.

$$p''(x) + \left[\frac{\omega}{c(x)}\right]^2 p(x) = 0 \qquad (3.2\text{-}1)$$

$$c(x) = c_o \left\{ 1 - \frac{\Delta T}{T_o} \left[1 + \frac{1}{2}\left(\frac{x}{\delta}\right)^3 - \frac{3}{2}\left(\frac{x}{\delta}\right) \right] \right\}^{\frac{1}{2}}$$

The magnitude of the mean value of $\frac{\omega}{c_o}$ is relatively large about which small variations take place. That is

$$0 < 1 - \frac{\Delta T}{T_o} \left[1 + \frac{1}{2}\left(\frac{x}{\delta}\right)^3 - \frac{3}{2}\left(\frac{x}{\delta}\right) \right] \leq 1$$

The solution contains only a complementary part, for the equation is free of a forcing function. Under the restricting condition mentioned below, the solution is

$$p(x) = \left[\frac{\omega}{c(x)}\right]^{-\frac{1}{4}} \left[c_1 e^{j\phi(x)} + c_2 e^{-j\phi(x)} \right] \qquad (3.3\text{-}2)$$

where

$$\phi(x) = \int \frac{\omega}{c(x)} \cdot dx$$

$$\left| \left[\frac{\omega}{c(x)} \right]^2 \right| \ggg \left| \frac{\ddot{c}(x)}{2c(x)} - \frac{3}{4}\left[\frac{\dot{c}(x)}{c(x)} \right]^2 \right|$$

The integration of the series is

$$\phi(x) = \frac{\omega}{c_o}\left(1-\frac{\Delta T}{T_o}\right)^{-\frac{1}{2}}\left\{x - \frac{3}{8}\left(\frac{\Delta T}{\delta T_o}\right)\left(1-\frac{\Delta T}{T_o}\right)^{-1}x^2 + \frac{9}{32}\left(\frac{\Delta T}{\delta T_o}\right)^2\left(1-\frac{\Delta T}{T_o}\right)^{-2}x^3 + \left[\frac{1}{16}\left(\frac{\Delta T}{T_o}\right)\left(1-\frac{\Delta T}{T_o}\right)^{-1} - \frac{45}{512}\left(\frac{\Delta T}{\delta T_o}\right)^3\left(1-\frac{\Delta T}{T_o}\right)^{-3}\right]x^4 - \left[\frac{9}{80}\left(\frac{\Delta T}{T_o}\right)^2\left(1-\frac{\Delta T}{T_o}\right)^{-2} - \frac{567}{1984}\left(\frac{\Delta T}{\delta T_o}\right)^4\left(1-\frac{\Delta T}{T_o}\right)^{-4}\right]x^5 + \ldots\ldots\ldots\ldots\ldots\ldots\ldots\ldots\right\} \quad (3.2\text{-}3)$$

The final form of the particle pressure is:

$$p(x) = \left[\frac{\omega}{c(x)}\right]^{-\frac{1}{2}}\left[c_1 e^{\left\{j\frac{\omega}{c_o}\left(1-\frac{\Delta T}{T_o}\right)^{-1}\left[x - \frac{3}{8}\left(\frac{\Delta T}{\delta T_o}\right)\left(1-\frac{\Delta T}{T_o}\right)^{-1}x^2+\ldots\right]\right\}} + c_2 e^{-j\left\{\frac{\omega}{c_o}\left(1-\frac{T}{T_o}\right)^{-1}\left[x - \frac{3}{8}\left(\frac{\Delta T}{\delta T_o}\right)\left(1-\frac{\Delta T}{T_o}\right)^{-1}x^2+\ldots\right]\right\}}\right]$$

After the constants C_1 and C_2 are evaluated and further simplification, the sound pressure p(x) is

$$p(x) = \left\{1-\frac{\Delta T}{T_o}\left[1+\frac{1}{2}\left(\frac{x}{\delta}\right)^3 - \frac{3}{2}\left(\frac{x}{\delta}\right)\right]\right\}^{1/4} \frac{p_o \sin\phi(x) - p_R\left(1-\frac{\Delta T}{T_o}\right)^{-1/4}\left\{\sin\left[\phi(x)-\phi(\delta)\right]\right\}}{\sin\phi(\delta)} \quad (3.2\text{-}4)$$

where p_o = pressure at temperature T_o
p_R = pressure on the face of receiver/reflector
$\phi(\delta) = \phi(x)\Big|_{x=\delta}$

As it can be seen the sound pressure is a function of the operating frequency, the ratio of the temperature difference to the atmospheric

temperature and the thickness of the boundary.

The particle velocity u(x) and the impedance Z(x) are obtained by Eqs. 2-5b and 2-5c (See 4. ACOUSTIC IMPEDANCE BY TRANSMISSION LINE ANALOGY.)

3.3 Frobenius' Method (Infinite Power Series)[4]

The solution of Eq. 2-4 is assumed to be a product of two functions as:

$$p(x,t) = F(x) \cdot e^{j\omega t}$$

and F(x) to be a power series of the form

$$F(x) = e^{a_1 x + a_2 x^2 + a_3 x^3 + a_4 x^4 + \cdots\cdots\cdots + a_n x^n \cdots\cdots}$$

when the second derivatives of p(x,t) with respect to x and t are substituted, the differential equation takes the following form, from which the coefficients a_1, a_2, a_3, a_4 ..... a_n ... must be found so that the original differential equation is satisfied.

$$\sum_{n=0} n(n-1)a_n x^{n-2} + \left\{\sum_{n=0} n a_n x^{n-1}\right\}^2 + \left(\frac{\omega}{c_o}\right)^2 \left\{\left(1-\frac{\Delta T}{T_o}\right)^{-1} + \right.$$

$$\left. \sum_{k=1} \sum_{p=1} \frac{p(p+1)(p+2)(p+3) \cdots (p+[k-1])}{k!} \left(\frac{\Delta T}{T_o}\right)^{p+[k-1]} (N-M)^k \right\} = 0$$

where

$$N = \frac{1}{2}\left(\frac{x}{\delta}\right)^3$$

$$M = \frac{3}{2}\left(\frac{x}{\delta}\right)$$

The following are samples of the first few terms. The expression for a general term is also given.

$$a_2 = \frac{-1}{2 \cdot 1}\left\{(1 \cdot a_1)^2 + \left(\frac{\omega}{c_o}\right)^2 \left(1-\frac{\Delta T}{T_o}\right)^{-1}\right\}$$

$$a_3 = -\frac{1}{3\cdot 2}\left\{(2)\ (1\cdot 2)a_1a_2 + \left(\frac{\omega}{c_o}\right)^2\left[-M\sum_{p=1}\frac{p}{1!}\left(\frac{\Delta T}{T_o}\right)^p\right]\right\}$$

$$a_4 = -\frac{1}{4\cdot 3}\left\{(2\cdot a_2)^2+(2)(1\cdot 3)a_1a_3+\left(\frac{\omega}{c_o}\right)^2\left[M^2\sum_{p=1}\frac{p(p+1)}{2!}\left(\frac{\Delta T}{T_o}\right)^{p+1}\right]\right\}$$

$$a_5 = -\frac{1}{5\cdot 4}\left\{(2)\left[(1\cdot 4)a_1a_4 + (2\cdot 3)a_2a_3\right] + \left(\frac{\omega}{c_o}\right)^2\left[-M^3\sum_{p=1}\frac{p(p+1)(p+2)}{3!}\left(\frac{\Delta T}{T_o}\right)^{p+2} + N\sum_{p=1}\frac{p}{1!}\left(\frac{\Delta T}{T_o}\right)^p\right]\right\} \ldots$$

$$a_{2n} = -\frac{1}{(2n)(2n-1)}\left\{(na_n)^2 + 2\sum_{k=1}^{j>k}\sum_{j=2n-1}^{} kja_ka_j \ldots\right.$$

$$+\left(\frac{\omega}{c_o}\right)^2\left[M^{2n-2}\sum_{p=1}\frac{p(p+1)(p+2)(p+3)\ \ldots\ (p+[2n-3])}{(2n-2)!}\left(\frac{\Delta T}{T_o}\right)^{p+[2n-3]}\right.$$

$$-(2n-4)NM^{2n-5}\sum_{p=1}\frac{p(p+1)(p+2)(p+3)\ \ldots\ (p+[2n-5])}{(2n-4)!}\left(\frac{\Delta T}{T_o}\right)^{p+[2n-5]}$$

$$+(n-3)(2n-7)N^2M^{2n-8}\sum\frac{p(p+1)(p+2)(p+3)\ \ldots\ (p+[2n-7])}{(2n-6)!}\left(\frac{\Delta T}{T_o}\right)^{p+[2n-7]}$$

$$\frac{-2(n-4)(n-5)(2n-9)}{3}N^3M^{2n-11}\sum\frac{p(p+1)(p+2)(p+3)\ \ldots\ (p+[2n-9])}{(2n-8)!}\left(\frac{\Delta T}{T_o}\right)^{p+[2n-9]}$$

$$\left.\left.+\ \ldots\right]\right\} \ldots$$

$$a_{2n} = -\frac{1}{(2n)(2n-1)}\left\{(na_n)^2+2\sum_{k=1}^{j>k}\sum_{j=2n-1}kja_ka_j+\left(\frac{\omega}{c_o}\right)^2\left[\sum_{k=1}(-1)^{k-1}G_kN^{k-1}M^{2n-3k+1}\right.\right.$$

$$\left.\left.\sum_{p=1}\frac{p(p+1)(p+2)(p+3)\ \ldots\ (p+2[n-k]-1)}{2(n-k)!}\left(\frac{\Delta T}{T_o}\right)^{p+2[n-k]-1}\right]\right\} \qquad (3.2\text{-}5)$$

$$a_{2n+1} = -\frac{1}{(2n+1)(2n)}\left\{2\sum_{k=1}^{j>k}\sum_{j=2n}kja_ka_j + \left(\frac{\omega}{c_o}\right)^2\left[-M^{2n-1}\right.\right. \ldots$$

$$\left.\left.\sum_{p=1}\frac{p(p+1)(p+2)(p+3)\ldots(p+[2n-2])}{(2n-1)\ !}\left(\frac{\Delta T}{T_o}\right)^{p+(2n-2)}\right.\right.$$

$$+ (2n-3)NM^{2n-4}\sum_{p=1} \frac{p(p+1)(p+2)(p+3)\ \ldots\ (p+[2n-4])}{(2n-3)!}\left(\frac{\Delta T}{T_o}\right)^{p+[2n-4]}$$

$$- (n-3)(2n-5)N^2M^{2n-7}\sum_{p=1} \frac{p(p+1)(p+2)(p+3)\ \ldots\ (p+[2n-6])}{(2n-5)!}\left(\frac{\Delta T}{T_o}\right)^{p+[2n-6]}$$

$$+ \frac{(n-4)(2n-7)(2n-9)}{3} N^3M^{2n-10}\sum_{p=1} \frac{p(p+1)(p+2)(p+3)\ \ldots\ (p+[2n-8])}{(2n-7)!}\left(\frac{\Delta T}{T_o}\right)^{p+[2n-8]}$$

$$- \frac{(n-5)(n-6)(2n-11)}{3!} N^4M^{2n-13}\sum_{p=1} \frac{p(p+1)(p+2)(p+3)\ \ldots\ (p+[2n-10])}{(2n-9)!}\left(\frac{\Delta T}{T_o}\right)^{p+[2n-10]}$$

$$+ \ldots\ldots\ldots\ldots\ldots\ldots\ ]\}$$

$$a_{2n+1} = -\frac{1}{(2n+1)(2n)}\left\{2\sum_{k=1}^{j>k}\sum_{j=2n} kja_ka_j + \left(\frac{\omega}{c_o}\right)\left[\sum_{k=1}(-1)^k H_k N^{k-1}M^{2n-3k+2}\right.\right.$$

$$\left.\left.\sum_{p=1} \frac{p(p+1)(p+2)(p+3)\ \ldots\ p-[2(n-k)]}{(2n-3k+2)!}\left(\frac{\Delta T}{T_o}\right)^{p-2(n-k)}\right]\right. \qquad (3.2\text{-}6)$$

In the above equation

$$N = \frac{1}{2}\left(\frac{x}{\delta}\right)^3$$

$$M = \frac{3}{2}\left(\frac{x}{\delta}\right)$$

$G_1 = 1$ $\qquad$ $H_1 = 1$

$G_2 = (2n-4)$ $\qquad$ $H_2 = (2n-3)$

$G_3 = (n-3)(2n-7)$ $\qquad$ $H_3 = (n-3)(2n-5)$

$$G_4 = \frac{(n-4)(n-5)(2n-9)}{3} \qquad H_4 = \frac{(n-4)(2n-7)(2n-9)}{3}$$

$$G_5 = \frac{(n-5)(n-6)(2n-11)(2n-13)}{3!} \qquad H_5 = \frac{(n-5)(n-6)(2n-9)(2n-11)}{3!}$$

The general expression given above includes up to sixteen terms. The degree of accuracy in numerical value can be improved by adding more terms in the series. An inevitable problem in the solution of power series is the rate of convergence. The convergence of the power series is such as to insure a maximum error of less than one five thousandth using sixteen terms.

3.4. Comparison of the Two Methods

The cumbersome mathematical operations and considerably long expressions (2-5 and 2-6) of the results often bury the physical meanings of the parameters and cloud clear interpretations of their relationships. The WKBJ method avoids mathematical involvement. Solution by this method leads at once to a picture of the process involved and allows a straightforward investigation of the results. For instance, it shows clearly that the amplitude of sound pressure is inversely proportional to sin ϕ (δ) and directly proportional to the one-fourth power of the ratio of temperature difference to the atmospheric ambient temperature; that the propagation constant is inversely proportional to the one-half power of the same; that the boundary thickness δ has increasing effects as it becomes thinner, etc. (3-4)

4. ACOUSTIC IMPEDANCE BY TRANSMISSION LINE ANALOGY

4.1. General

The following figure represents essential parts of the transducer,

a simplified equivalent electrical model for the study of acoustic impedance by transmission line analogy.

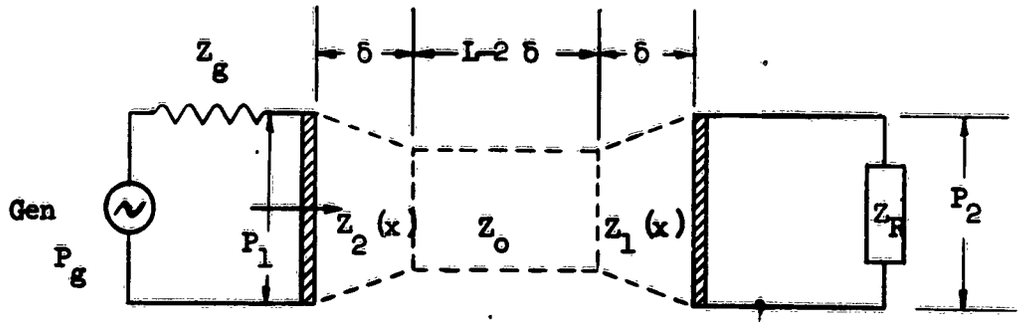

Figure 4.1-1

Z_o: characteristic impedance of nonuniform mid-section,
$Z_1(x), Z_2(x)$: characteristic impedance of nonuniform boundary layer,
Z_R: load impedance
Z_{1s}: total input impedance when load-end is short-circuited
Z_{1o}: total input impedance when load-end is open-circuited.

According to four-terminal network theory[5], the output pressure (P_2) is related to the input pressure (P_1) by:

$$p_2 = \frac{1}{Z_{1s}\left[\frac{1}{Z_R} + \frac{1}{Z_{2s}}\right]} \sqrt{1 - \frac{Z_{1s}}{Z_{1o}}} \quad (p_1)$$

When the circuit impedance is bilateral and the load impedance Z_R is much greater than the short-circuited impedance Z_{1s}, the above equation becomes

$$p_2 = \sqrt{1 - \frac{Z_{1s}}{Z_{1o}}} \; p_1 \qquad (4.1\text{-}1)$$

The above equation (4.1-1) shows the relation between the sound pressures at the generator and reflector plate. When the internal impedance of the generator Z_g is taken into consideration, (4.1-1) takes the following form.

$$p_2 = \frac{Z_s}{Z_g} p_1 \cong \frac{Z_{lo}}{Z_g} p_1 \qquad (4.1\text{-}2)$$

The output pressure P_2 is directly proportional to Z_{lo} when the internal impedance of the generator is a constant. In the following sections, the expression of the input impedance of the transducer is derived, and the condition that Z_{lo} becomes maximum is investigated using a simplified model, an approximate model, and the exact model.

4.2. CASE 1. Three Uniform Transmission Lines Cascaded

Three uniform transmission lines are cascaded. The characteristic impedance of the two end sections is Z_{o1}, which is different from that of the mid section Z_o.

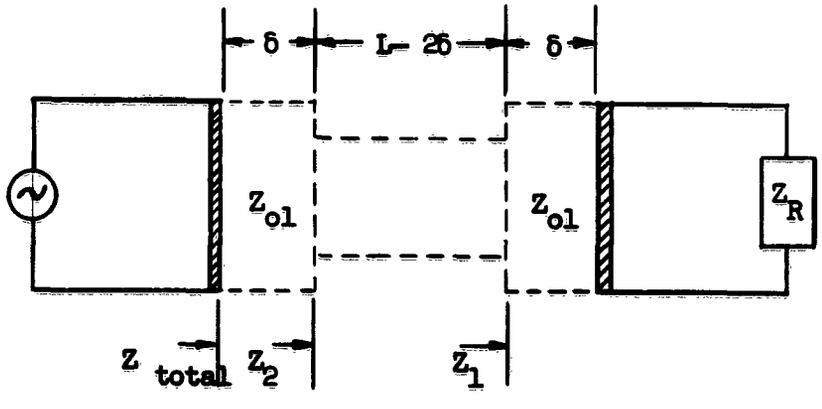

Figure 4.2-1

The impedance Z_1 at $x = \delta$ looking toward the load Z_R is

$$Z_1 = -jZ_o \cot \beta_1 \delta \tag{4.2-1}$$

$$\beta_1 = \frac{\omega}{c_{o1}}$$

When it is assumed that the load impedance is infinite (open-circuit) or very large compared with the characteristic impedance Z_{o1}. Likewise, the impedance Z_2 at $x = L - \delta$ is

$$Z_2 = Z_o \frac{Z_1 + jZ_o \tan \beta_o (L-2\delta)}{Z_o + jZ_1 \tan \beta_o (L-2\delta)} \tag{4.2-2}$$

The total input impedance Z_{total} at $x = L$ looking toward the load is

$$Z_{total} = Z_{o1} \frac{Z_2 + jZ_{o1} \tan \beta_1 \delta}{Z_{o1} + jZ_2 \tan \beta_1 \delta} \tag{4.2-3}$$

After successive substitutions of Z_1 and Z_2 into the last equation, the total input impedance with load-end Z_{lo} is

$$Z_{lo} = jZ_{o1} \frac{\left(\frac{Z_o}{Z_{o1}} + \frac{Z_{o1}}{Z_o} \right) \tan \beta_o (L-2\delta) + \tan \beta_1 \delta - \cot \beta_1 \delta}{\frac{Z_{o1}}{Z_o} \cot \beta_1 \delta \tan \beta_o (L-2\delta) - \frac{Z_o}{Z_{o1}} \tan \beta_1 \delta \tan \beta_o \delta (L-2\delta) + 2} \tag{4.2-4}$$

The condition for Z_{lo} to be maximum is

$$\tan (1-k)\theta = \frac{2}{\frac{Z_o}{Z_{o1}} \tan \beta_1 \delta - \frac{Z_{o1}}{Z_o} \cot \beta_1 \delta}$$

$$= \frac{Z_{o1}}{Z_o} \frac{2}{\tan \beta_1 \delta - \left(\frac{Z_{o1}}{Z_o} \right)^2 \cot \beta_1 \delta} \tag{4.2-5}$$

where

$$k = \frac{2\delta}{L}$$

$$\theta = \frac{\omega}{c_o} L$$

$$\beta_1 = \frac{\omega}{c_1}$$

The relation between k and θ is

$$L \approx \frac{n\pi}{1-k(1-A)} \cdot \frac{c}{\omega} \qquad (4.2\text{-}6a)$$

where $A = \frac{Z_o}{Z_{o1}}$ $\qquad \frac{Z_o}{Z_{o1}} \doteq \frac{T_\omega}{T_o}$

Comparing the above with Eq. (1.3-1), a correction term $\frac{1}{1-k(1-A)}$ is introduced. It is obvious that the ratio of the boundary thickness δ to the separation L and the ratio of the characteristic impedance of the undisturbed medium to that of the boundary have attributed a shift of the normal frequency by $\Delta\omega$ as the following equations show.

$$L = \frac{n\pi c}{\omega_o}$$

and

$$L \approx \frac{n\pi}{1-k(1-A)} \cdot \frac{c}{\omega_o + \Delta\omega}$$

then

$$\frac{\Delta\omega}{\omega_o} = \frac{1-k(1-A)}{k(1-A)} \qquad (4.2\text{-}6b)$$

4.3. CASE II. A Uniform Line and Two Nonuniform Lines at Ends (Approximation)

A uniform line of impedance Z_o and two nonuniform lines at the ends are cascaded as the following figure shows.

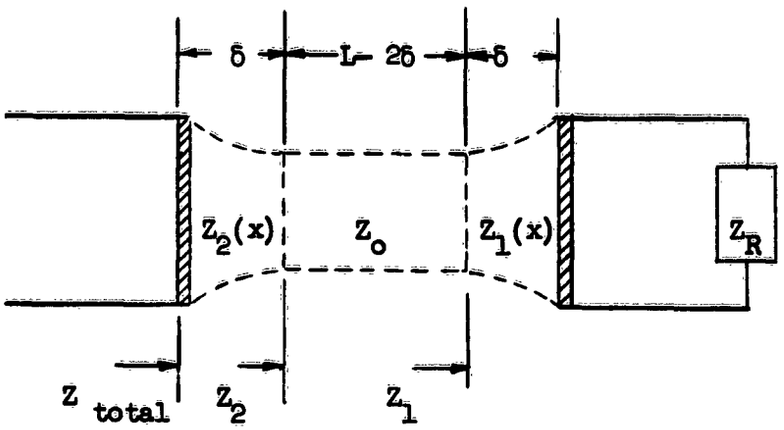

Figure 4.3-1a

In order to facilitate the investigation, the above transmission line is sectioned into three parts as follow:

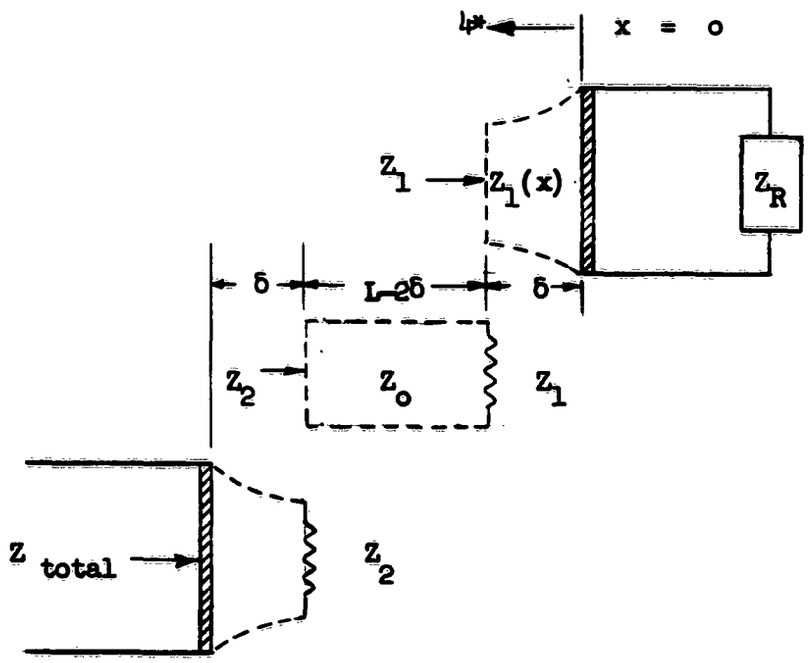

Figure 4.3-1b

4.31. Right-Hand Nonuniform Line

The particle pressure p(x), particle velocity u(x), and the impedance

Z(x) of the right-hand side non-uniform line are as follows according to the WKBJ approximate solution discussed previously.

$$p(x) = \left[\frac{c(x)}{\omega}\right]^{\frac{1}{2}} \left[c_1 e^{j\phi(x)} + c_2 e^{-j\phi(x)}\right] \qquad (3.2\text{-}2)$$

$$u(x) = \frac{j}{\omega p(x)} \cdot \frac{dp}{dx} \qquad (2.1\text{-}3a)$$

$$z(x) = \frac{p(x)}{u(x)} \qquad (2.1\text{-}3c)$$

When the constants C_1 and C_2 are evaluated having the load-end opened, the impedance of the nonuniform boundary becomes

$$Z(x) = j\omega\rho(x)c(x)\,\frac{\omega\cos\phi(x) - \beta_o \sin\phi(x)}{(\omega^2 + \beta_o\beta_x)\sin\phi(x) + (\omega\beta_o - \omega\beta_x)\cos\phi(x)}$$

where

ω = frequency

$$\phi(x) = \int \frac{\omega}{c(x)}\,dx$$

$$\beta_{o,x} = \left.\frac{c'(x)}{2}\right|_{x=0}$$

The input impedance Z_1 at x = is then:

$$Z_1 = Z(x)\Big|_{x=\delta} = -j\rho_o c_o\,\frac{\cos\phi(\delta) - \frac{c'(0)}{2\omega}\sin\phi(\delta)}{\sin\phi(\delta) + \frac{c'(0)}{2\omega}\cos\phi(\delta)}$$

$$= -j\rho_o c_o\,\frac{1 - \frac{c'(0)}{2\omega}\tan\phi(\delta)}{\tan\phi(\delta) + \frac{c'(0)}{2\omega}}$$

where

$$c'(0) = \left.\frac{d}{dx}\,c(x)\right|_{x=0} \qquad (4.31\text{-}1)$$

The above equation (4.31-1) is easily recognizable as a modified form of Eq. (4.2-1) which is discussed in CASE I. When $\frac{c'(0)}{2\omega} \ll 1$ and is negligible,

the expression is identical. The second terms in the numerator and the denominator are the supplementary terms added due to non-uniformity of the section. The magnitude of the correction terms is $\frac{c'(0)}{2\omega}$, enveloped by a sinusoidal variation whose argument is $\phi(\delta)$. The expression for $\phi(\delta)$ is given in Eq. (3.2-3).

4.32. Uniform Mid-Section

The impedance Z_2 at the left end of the uniform section is

$$Z_2 = Z_0 \frac{Z_1 + jZ_0 \tan\beta_0(L-2\delta)}{Z_0 + jZ_1 \tan\beta_0(L-2\delta)} \qquad (4.31\text{-}1)$$

where Z_1 is the load impedance discussed in (4.31-1).

.33. Left-Hand Side Nonuniform Section

When the constants C_1 and C_2 are evaluated in Eq. (3.2-2) with load impedance Z_2 at $x = L-\delta$, the input impedance looking to the right is

$$Z_{total} = \frac{1}{1 + \frac{c'(0)}{2\omega}\tan\phi(\delta)} \cdot \frac{Z_2 + jZ_0\tan\phi(\delta)}{Z_0 + jZ_2 \frac{1 - \frac{c'(\delta)}{2\omega}\cot\phi(\delta)}{\cot\phi(\delta) + \frac{c'(\delta)}{2\omega}}}$$

where

P_W = p at the generator

$$c_W = c(x)\Big|_{x = L}$$

$$c'(\delta) = \frac{d}{dx}[c(x)]\Big|_{x = \delta}$$

Summarizing the sectioned impedances,

$$Z_1 = -jZ_0 \frac{1 - \frac{c'(0)}{2\omega}\tan\phi(\delta)}{\tan\phi(\delta) + \frac{c'(0)}{2\omega}} \qquad (4.31\text{-}1)$$

$$Z_2 = Z_0 \frac{Z_1 + jZ_0\tan(L-2\delta)}{Z_0 + jZ_1\tan(L-2\delta)} \qquad (4.33\text{-}2)$$

$$Z_{total} = p_w c_w \frac{1}{1 + \frac{c'(\delta)}{2\omega}\tan\phi(\delta)} \cdot \frac{Z_2 + jZ_o\tan\phi(\delta)}{Z_o + jZ_2 \frac{1 - \frac{c'(\delta)}{2\omega}\cot\phi(\delta)}{\cot\phi(\delta) + \frac{c'(\delta)}{2\omega}}} \quad (4.33\text{-}3)$$

In the following section, the total impedance is discussed and compared with the results under CASE I.

4.34. Total Input Impedance

Total input impedance is obtained when the sectioned impedances are cascaded; Z_2 and Z_1 are substituted in successively.

$$Z_{total} = j \frac{p_w c_w}{1 + M_\delta} \frac{A - \tan\beta_o(L - 2\delta) - \tan\phi(\delta)[1 + A\tan\beta_o(L - 2\delta)]}{1 + A\tan\beta_o(L - 2\delta) + N_\delta[A - \tan\beta_o(L - 2\delta)]} \quad (4.34\text{-}1)$$

In the above equation

$$A = \frac{1 - \frac{c'(0)}{2\omega}\tan\phi(\delta)}{\tan\phi(\delta) + \frac{c'(0)}{2\omega}} \cong \cot\phi(\delta)$$

$$N_\delta = \frac{1 - \frac{c'(\delta)}{2\omega}\cot\phi(\delta)}{\cot\phi(\delta) + \frac{c'(\delta)}{2\omega}} \cong \tan\phi(\delta)$$

$$M_\delta = \frac{c'(\delta)}{2\omega}\tan\phi(\delta)$$

Equation (4.33-3) expresses the total input impedance when the load-end is considered opened. The equation is identical to the regular transmission line equation when $\frac{c'(0)}{2\omega} \lll 1$ is negligible. Similarity between (4-10b) and (4-5) is noticeable; the magnitude is modified by a factor of $\frac{1}{1 + \frac{c'(\delta)}{2\omega}\tan\phi(\delta)}$ due to nonuniformity of the end sections. The condition which makes the total input impedance maximum is as follows

$$\tan(1-k)\theta = \frac{1 + N_\delta A}{N - A} \qquad (4.34\text{-}2)$$

where

$$k = \frac{2\delta}{L}$$

$$\theta = \frac{\omega}{c_o} L$$

The above condition is a modified form of (4.2-5). The similarity is striking. Graphical solutions of the transcendental equation (4.34-2) are given as an illustration. Solutions are the intersections of the two curves. (Refer to figures 4.34-1, -2, -3, and 4.)

We can now easily comprehend the meaning of Eq. (4.34-2) and (4.34-1): there is more than one frequency, in the vicinity of, say, $\phi=\pi$, at which the magnitude of standing wave at the receiver reflector face is maximum. The separation of the two frequencies or the deviation of the frequencies from the normal frequency ($\phi = \pi$ in this example) is a function of the boundary layer thickness, the speed of sound, and the ratio T_w/T_o. Knowing the frequencies, ω_1 and ω_2, the boundary layer thickness and the temperature of the undisturbed medium can be determined.

Under an assumption that $\frac{c'(0)}{2\omega}$ is very small, the above condition (4.34-2) becomes

$$\tan(1-k)\theta \cong -\tan 2\phi(\delta)$$

or

$$\tan\theta = -\frac{2\omega\delta}{c_o}\sqrt{\frac{T_w}{T_o}} + \frac{2\omega\delta}{c_o}$$

from which

$$\frac{\omega}{c_o} L \cong \frac{n\pi}{1 - \frac{2\delta}{L}\left(1 - \frac{T_w}{T_o}\right)} \qquad (4.34\text{-}3)$$

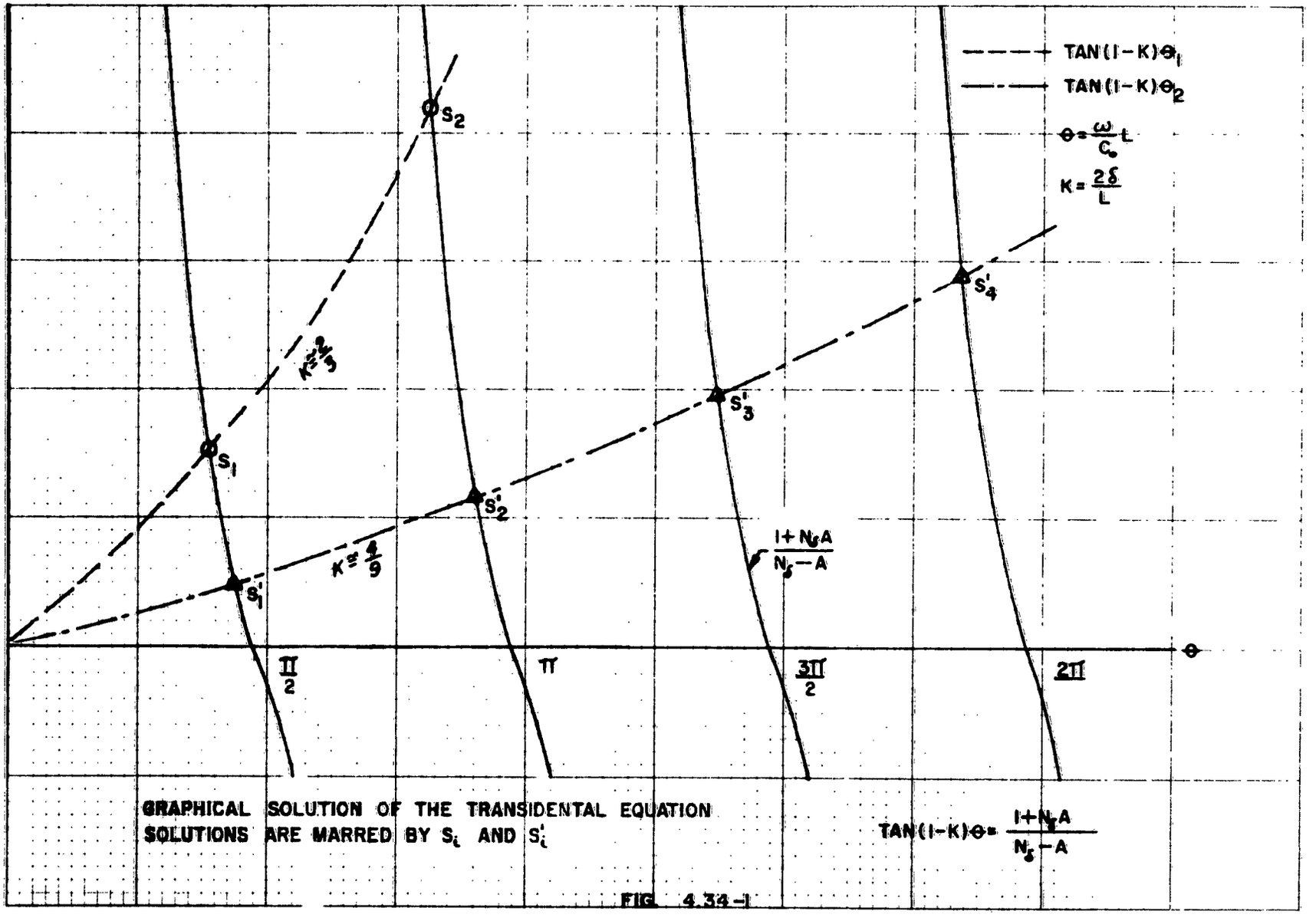

GRAPHICAL SOLUTION OF THE TRANSIDENTAL EQUATION
SOLUTIONS ARE MARRED BY S_i AND S'_i

$$\tan(1-K)\Theta = \frac{1+N_0 A}{N_0 - A}$$

FIG 4.34-1

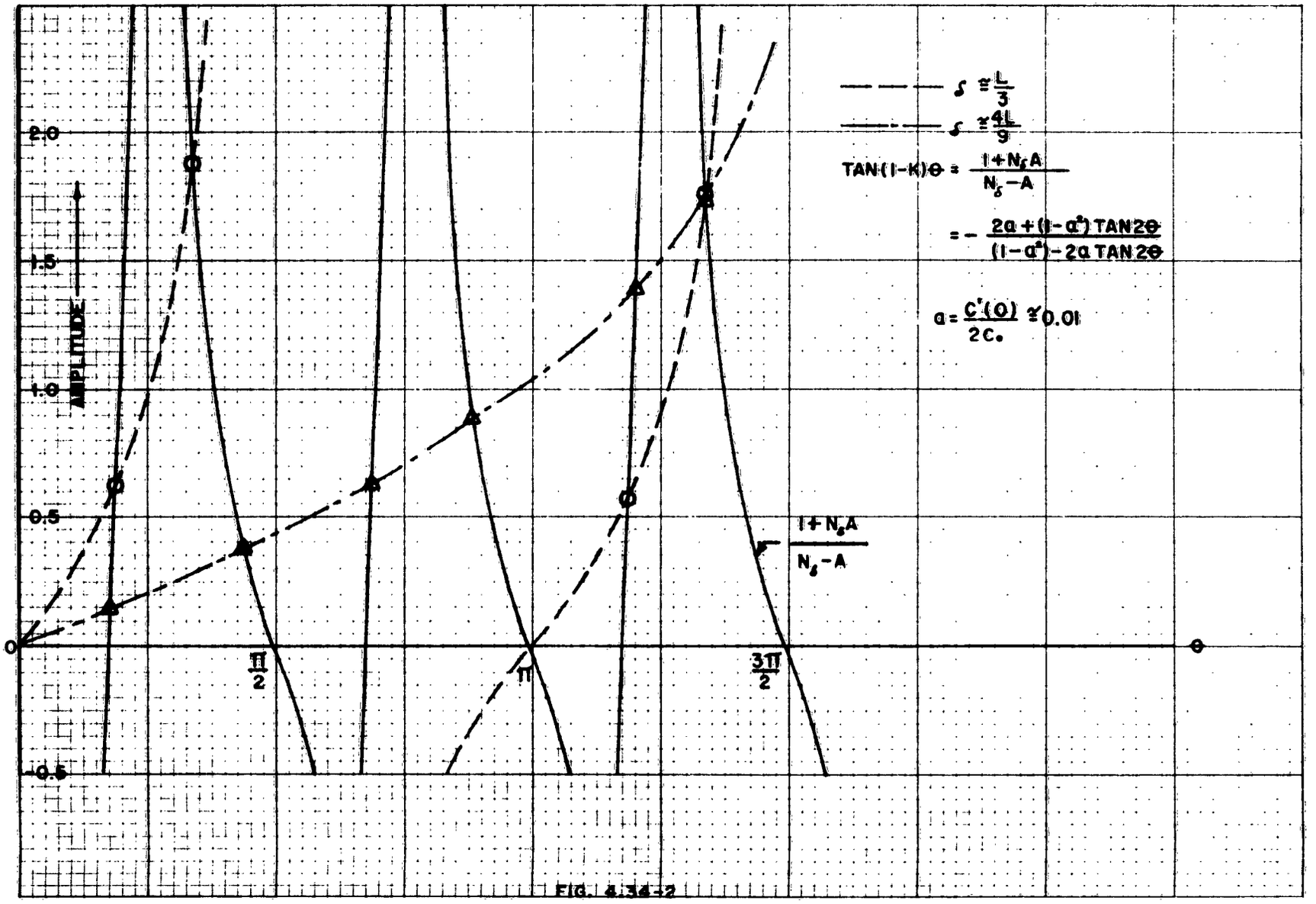
AMPLITUDE
2.0
1.5
1.0
0.5
0
-0.5
π/2
π
3π/2
θ
δ ≅ L/3
δ ≅ 4L/9
TAN(1-K)θ = (1+N_δA)/(N_δ-A)
= - (2a+(1-a²)TAN2θ)/((1-a²)-2a TAN2θ)
a = C'(0)/2C₀ ≅ 0.01
(1+N_δA)/(N_δ-A)

FIG. 4.34-2

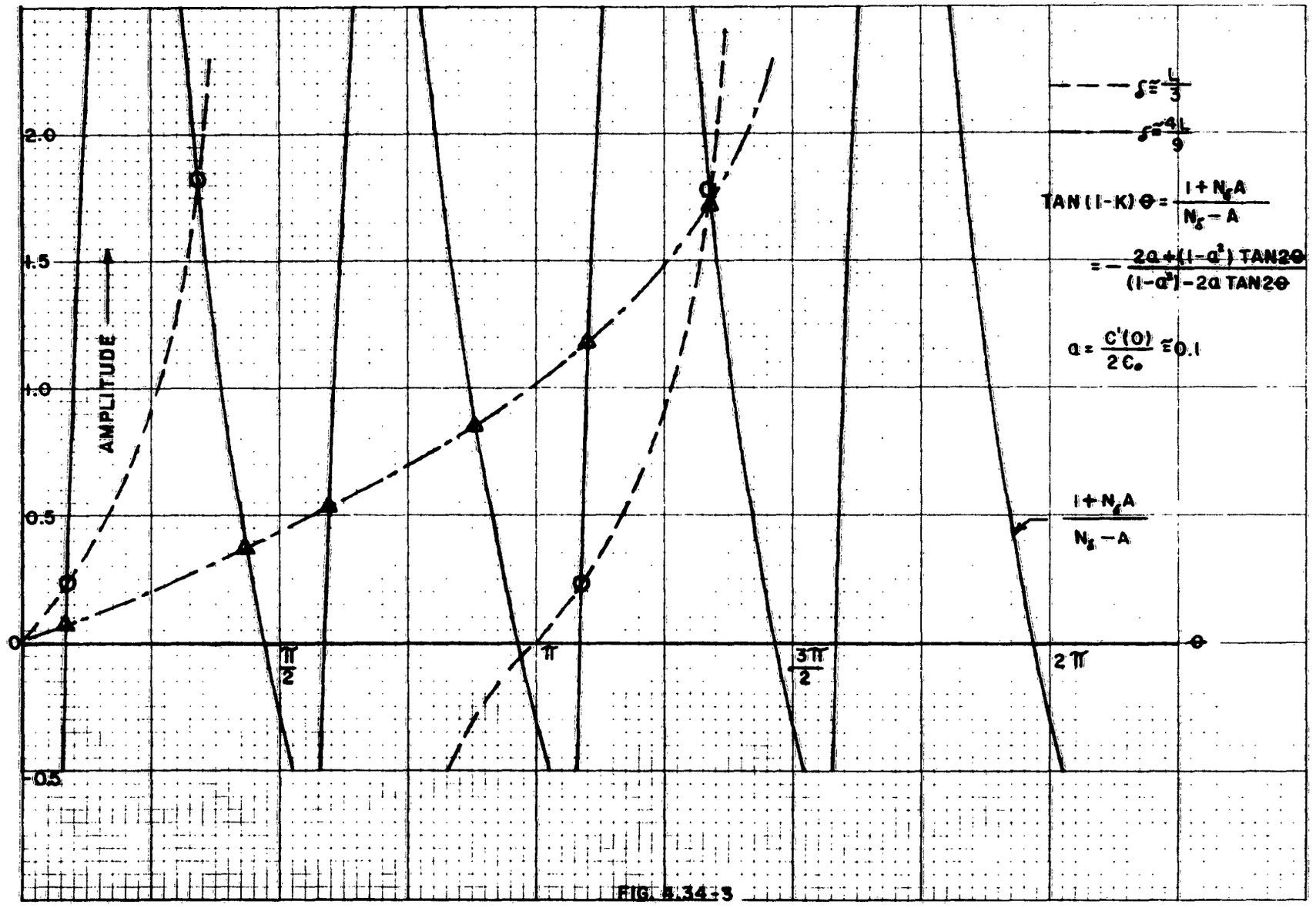
AMPLITUDE
2.0
1.5
1.0
0.5
0
-0.5
π/2
π
3π/2
2π
θ
δ = L/3
δ = 4L/9
TAN (1-K) θ = (1 + N_δ A) / (N_δ − A)
= − (2α + (1−α²) TAN2θ) / ((1−α²) − 2α TAN2θ)
α = C'(0) / 2C_0 ≅ 0.1
(1 + N_δ A) / (N_δ − A)

FIG. 4.34-3

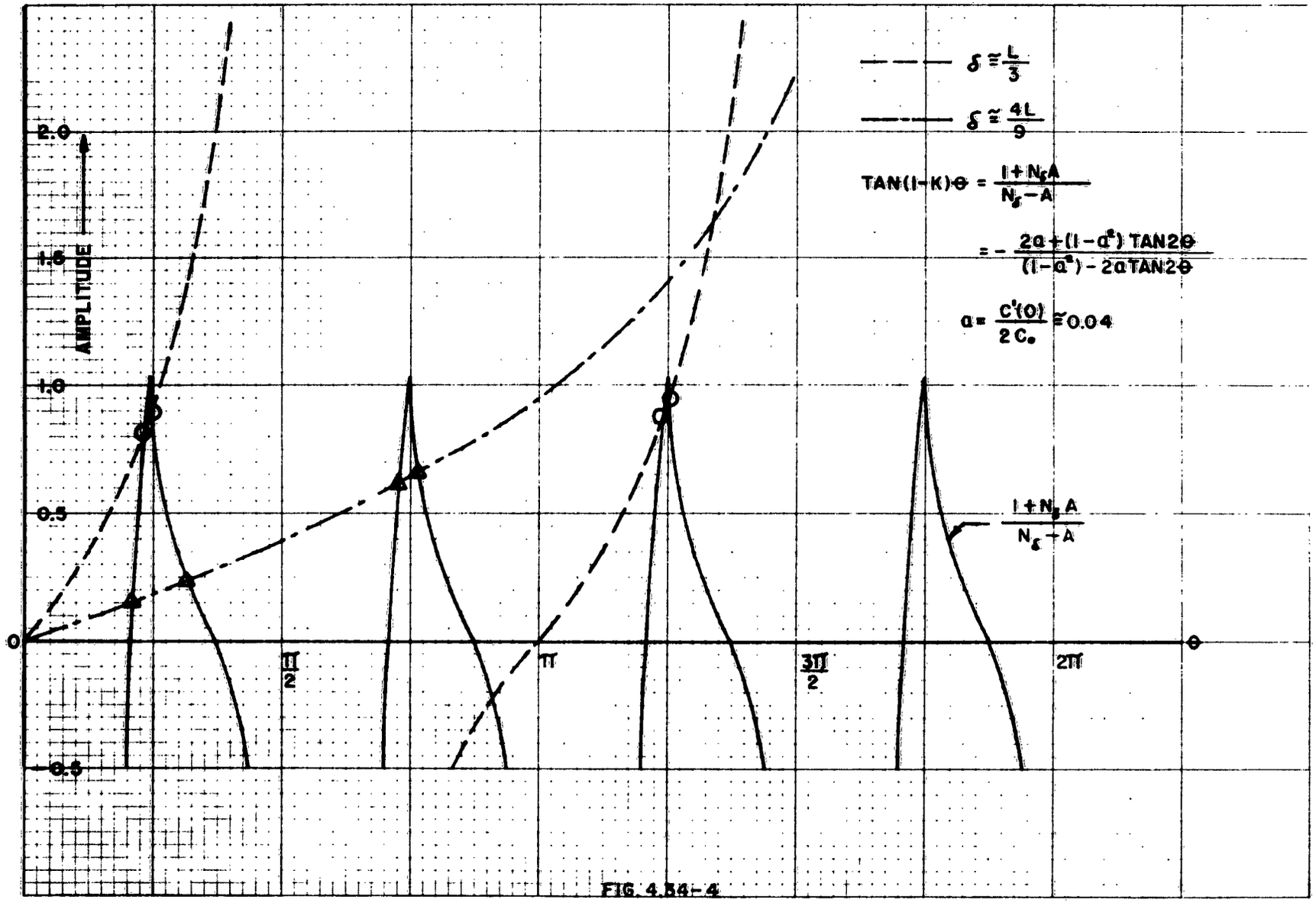
δ ≅ L/3
δ ≅ 4L/9
TAN(1-K)θ = (1+N_δA)/(N_δ-A)
= -(2α+(1-α²) TAN2θ)/((1-α²)-2α TAN2θ)
α = C'(0)/2C₀ ≅ 0.04
(1+N_δA)/(N_δ+A)
AMPLITUDE
2.0
1.5
1.0
0.5
0
-0.5
π/2
π
3π/2
2π
θ

FIG. 4.54-4

The result is the same as (4.2-6) as in CASE I; however, it is more clear and definite what effects T_w and δ have on the speed of sound c_o. The qualifying restriction is that the product $\left(\frac{\lambda}{\delta}\right)\left(\frac{\Delta T}{T_o}\right)$ be small.

4.4. CASE III. A Uniform Line and Two Nonuniform Lines at Ends (Exact)

4.41. General

The derivation of the exact expression for the total open-ended input impedance is presented. As it is noticed, the finite discontinuities of the acoustic impedances at the boundary are neglected in CASE I, and the forward and backward propagation constants are not considered separately in CASE II. The WKBJ approximation method does not disclose the difference between the two propagation constants.

The procedures for deriving the impedance are similar to those employed in CASE II. The total separation is sectioned into three parts as Fig. 4.3-1b shows. The particle pressure and velocity are expressed as follows, assuming sinusoidal variation of both, but separating the forward and backward propagation constants.

$$p(x) = Ae^{\gamma_1(x)} + Be^{\gamma_2(x)} \qquad (4.41\text{-}1)$$

$$u(x) = \frac{-\gamma_1(x)}{j\omega\rho(x)} Ae^{\gamma_1(x)} - \frac{\gamma_2(x)}{j\omega\rho(x)} \cdot Be^{\gamma_2(x)} \qquad (4.41\text{-}2)$$

where

$$\gamma_1(x) = a_1x + a_2x^2 + a_3x^3 + \ldots + a_nx^n + \ldots \quad \text{(forward propagation constant)}$$

$$\gamma_2(x) = A_1x + A_2x^2 + A_3x^3 + \ldots + A_nx^n + \ldots \quad \text{(backward propagation constant)}$$

$$\gamma_1'(x) = \frac{d}{dx}[\gamma_1(x)]$$

$$\gamma_2'(x) = \frac{d}{dx}[\gamma_2(x)]$$

It can be shown that a_1 and A_1; a_2 and A_2; are equal in magnitude but the subsequent terms a_3 and A_3; a_4 and A_4; .....are not, which indicates that the forward and backward propagation constant must be separately treated when the accuracy of the numerical value is to be improved.

4.42. Receiver Side; Nonuniform Boundary

When the constants A and B are evaluated in Eq. (4.41-1) at the load and the ratio of P(x) to u(x) is taken, the impedance Z(x) is expressible as:

$$Z'_R = Z_R \frac{A_1\left[e^{\gamma_1(\delta)} + e^{\gamma_2(\delta)}\right] + \frac{j\omega\rho_w}{Z_R}\left[e^{\gamma_1(\delta)} - e^{\gamma_2(\delta)}\right]}{\frac{-\gamma_1(\delta)}{j\omega\rho_o}\left(j\omega\rho_w + Z_R k_1\right)e^{\gamma_1(\delta)} + \frac{\gamma_2(\delta)}{j\omega\rho_o}\left(j\omega\rho_w - Z_R A_1\right)e^{\gamma_2(\delta)}} \qquad (4.42\text{-}1)$$

The load impedance Z_R is general. The results for the open-ended condition, $Z_R \sim \infty$, is discussed later.

4.43. Mid-Section: Uniform, Undisturbed

Being undisturbed, the impedance at $x = L - \delta$ is

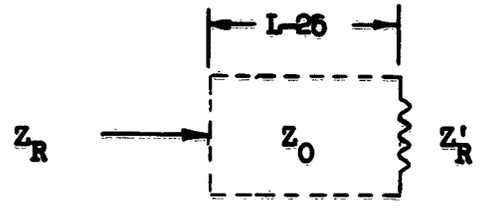

$$Z''_R = Z_o \frac{Z'_R + jZ_o \tan\beta_o(L - 2\delta)}{Z_o + jZ'_R \tan\beta_o(L - 2\delta)} \qquad (4.43\text{-}1)$$

where

$$\beta_o = \frac{\omega}{c_o}$$

$$Z_o = \rho_o c_o$$

4.44. Generator-Side: Nonuniform Boundary

The constants A and B are evaluated differently; the load is now Z''_R at $x = L - \delta$. The total impedance at the generator looking toward the receiver Z_{total} is

$$Z_{total} = Z''_a \frac{\left[\dot{\gamma}_2(L-\delta) + \frac{j\omega\rho}{Z''_R}\right] e^{\gamma_1(L)-\gamma_2(L-\delta)} - \left[\dot{\gamma}_1(L-\delta) + \frac{j\omega\rho_o}{Z_R}\right] e^{\gamma_2(L)-\gamma_1(L-\delta)}}{\frac{-j(L)}{j\omega\rho_w}\left[Z''_R\,\dot{\gamma}_2(L-\delta)+j\omega\rho_o\right] e^{\gamma_1(L)-\gamma_1(L-\delta)} + \frac{\dot{\gamma}_2(L)}{j\omega\rho_w}\left[Z''_R\,\dot{\gamma}_1(L-\delta)+j\omega\rho_o\right]}$$

$$\frac{}{e^{\gamma_2(L)-\gamma_2(L-\delta)}} \qquad (4.44\text{-}1)$$

Summarizing the sectioned impedances, (Refer to Figures given in the following page)

$$Z'_R = (j\omega\rho_o)\frac{A_1\left[e^{\gamma_1(\delta)} + e^{\gamma_2(\delta)}\right] + \frac{j\omega\rho_w}{Z_R}\left[e^{\gamma_1(\delta)} - e^{\gamma_2(\delta)}\right]}{-A_1\left[\gamma_1(\delta)e^{\gamma_1(\delta)} + \dot{\gamma}_2(\delta)e^{\gamma_2(\delta)}\right] + j\omega\rho_w\left[-\dot{\gamma}_1(\delta)e^{\gamma_1(\delta)} + \dot{\gamma}_2(\delta)e^{\gamma(\delta)}\right]}$$

(4.42-1)

$$Z''_R = Z_o \frac{Z'_R + jZ_o \tan\beta_o(L-2\delta)}{Z_o + jZ'_R \tan\beta_o(L-2\delta)} \qquad (4.43\text{-}1)$$

$$Z_{total} = j\omega\rho_w \frac{\left[\gamma_2(L-\delta)e^{\gamma_1(L)-\gamma_1(L-\delta)} - \dot{\gamma}_1(L-\delta)e^{\gamma_2(L)-\gamma_2(L-\delta)}\right] +}{\left[-\dot{\gamma}_1(L)\dot{\gamma}_2(L-\delta)e^{\gamma_1(L)-\gamma_1(L-\delta)} + \dot{\gamma}_2(L)\dot{\gamma}_1(L-\delta)e^{\gamma_2(L)-\gamma_2(L-\delta)}\right] +}$$

$$\frac{\frac{j\omega\rho_o}{Z''_R}\left[e^{\gamma_1(L)-\gamma_1(L-\delta)} - e^{\gamma_2(L)-\gamma_2(L-\delta)} \right]}{\frac{j\omega\rho_o}{Z''_R}\left[-\dot{\gamma}_1(L)e^{\gamma_1(L)-\gamma_1(L-\delta)} + \dot{\gamma}_2(L)e^{\gamma_2(L)-\gamma_2(L-\delta)} \right]} \qquad (4.44\text{-}1a)$$

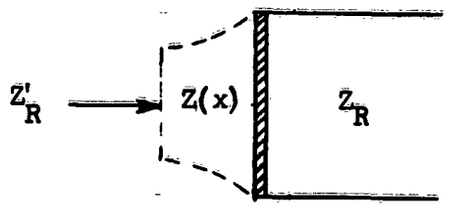

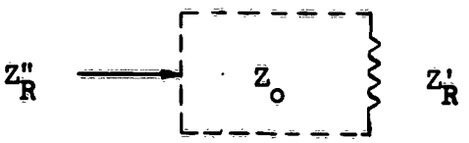

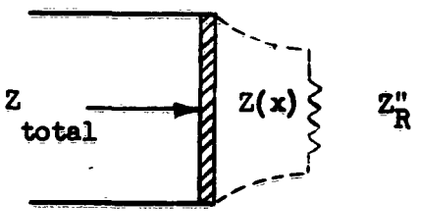

4.45. Total Input Impedance

Total input impedance in terms of the load impedance Z_R is obtained

when the three sectional impedances are cascaded. The open-ended impedance Z_{1o} is obtained when $Z_R = \infty$.

$$Z_{total} = j\omega\rho_w \frac{G\left[A+jZ_o\tan\beta_o(L-2\delta)\right]+\frac{j\omega\rho_o}{Z_o}P\left[Z_o+jA\tan\beta_o(L-2\delta)\right]}{H\left[A+jZ_o\tan\beta_o(L-2\delta)\right]+\frac{j\omega\rho_o}{Z_o}Q\left[Z_o-jC\tan\beta_o(L-2\delta)\right]} \quad (4.44\text{-}1b)$$

$$Z_{1o} = j\omega\rho_w \frac{G\left[-C+jZ_o\tan\beta_o(L-2\delta)\right]+\frac{j\omega\rho_o}{Z_o}P\left[Z_o-jC\tan\beta_o(L-2\delta)\right]}{H\left[-C+jZ_o\tan\beta_o(L-2\delta)\right]+\frac{j\omega\rho_o}{Z_o}Q\left[Z_o-jC\tan\beta_o(L-2\delta)\right]} \quad (4.45\text{-}1)$$

$$G = \dot{\gamma}_2(L-\delta)e^{\gamma_1(L)-\gamma_1(L-\delta)} - \dot{\gamma}_1(L-\delta)e^{\gamma_2(L)-\gamma_2(L-\delta)}$$

$$H = -\dot{\gamma}_1(L)\,\dot{\gamma}_2(L-\delta)e^{\gamma_1(L)-\gamma_1(L-\delta)} + \dot{\gamma}_2(L)\,\dot{\gamma}_1(L-\delta)e^{\gamma_2(L)-\gamma_2(L-\delta)}$$

$$P = e^{\gamma_1(L)-\gamma_1(L-\delta)} - e^{\gamma_2(L)-\gamma_2(L-\delta)}$$

$$Q = \gamma_1(L)e^{\gamma_1(L)-\gamma_2(L-\delta)} + \gamma_2(L)e^{\gamma_2(L)-\gamma_2(L-\delta)}$$

$$A = j\omega\rho_o \frac{\dot{\gamma}_2(0)\left[e^{\gamma_1(0)}+e^{\gamma_2(0)}\right]+\frac{j\omega\rho_w}{Z_R}\left[e^{\gamma_1(0)}-e^{\gamma_2(0)}\right]}{-\dot{\gamma}_2(0)\left[\dot{\gamma}_1(\delta)e^{\gamma_1(0)}+\dot{\gamma}_2(\delta)e^{\gamma_2(\delta)}\right]+\frac{j\omega\rho_w}{Z_R}\left[-\dot{\gamma}_1(\delta)e^{\gamma_1(\delta)}+\dot{\gamma}_2(\delta)e^{\gamma_2(\delta)}\right]}$$

$$C = j\omega\rho_o \frac{e^{\gamma_1(\delta)}+e^{\gamma_2(\delta)}}{\dot{\gamma}_2(\delta)e^{\gamma_2(\delta)}+\dot{\gamma}_1(\delta)e^{\gamma_1(\delta)}}$$

The condition for which Z_{1o} becomes maximum is

$$\tan(1-k)\theta = \mathrm{Re}\left[\frac{HC-j\omega\rho_o Q}{\frac{\omega}{c_o}QC+jZ_oH}\right] \quad (4.45\text{-}2)$$

Equation (4.45-2) is an equivalent of (4.34-2) whose graphical solutions

are given. Accurate numerical values of the roots of the above equation will be obtained by aid of a computer. These values correspond to the interceptions of the curves discussed on page 5-22.

4.5. Summary

The total input impedance with load-end open in the three different cases is repeated below.

$$Z_{1o} = jZ_{o1} \frac{\left(\frac{Z_o}{Z_{o1}} + \frac{Z_{o1}}{Z_o}\right) \tan \beta_o(L-2\delta) + \tan \beta_1\delta - \cot \beta_1\delta}{\frac{Z_{o1}}{Z_o} \cot \beta_1\delta \tan \beta_o(L-2\delta) - \frac{Z_o}{Z_{o1}} \tan \beta_1\delta \tan \beta_o(L-2\delta) + 2} \qquad (4.24)$$

$$Z_{1o} = j \frac{\rho_w c_w}{1+M_\delta} \frac{A - \tan \beta_o(L-2\delta) - \tan\phi(\delta)[1 + A\tan \beta_o(L-2\delta)]}{1 + A\tan \beta_o(L-2\delta) + M_\delta [A - \tan \beta_o(L-2\delta)]} \qquad (4.34\text{-}1)$$

$$Z_{1o} = j\omega\rho_w \frac{G[-C+jZ_o\tan \beta_o(L-2\delta)] + \frac{j\omega\rho}{Z_o} P[Z_o - jC\tan \beta_o(L-2\delta)]}{H[-C+jZ_o\tan \beta_o(L-2\delta)] + \frac{j\omega\rho}{Z_o} Q[Z_o - jC\tan \beta_o(L-2\delta)]} \qquad (4.45\text{-}1)$$

The above three expressions are similar in form. For instance, a) the term $\tan \beta_1\delta$ (4.2-4) is equivalent to the term $\tan \phi(\delta)$ in (4.34-1) and in turn to P/Q in (4.45-1); b) $\cot \beta_1\delta$ is equivalent to A, and to H/G, etc.

The conditions for which Z_{1o} is maximum in three cases are also repeated for comparison and discussions.

$$\tan(1-k)\theta = \frac{2}{\frac{Z_o}{Z_{o1}} \tan \beta_1\delta - \frac{Z_{o1}}{Z_o} \cot \beta_1\delta} \qquad \text{Simplified} \qquad (4.2\text{-}5)$$

$$\tan(1-k)\theta = \frac{1 + M_\delta A}{M_\delta - A} \qquad \text{Approximated} \qquad (4.34\text{-}2)$$

$$\tan(1-k)\theta = \mathrm{Re}\left[\frac{HC - j\omega\rho_o Q}{\frac{\omega}{c_o} QC + jZ_o H}\right] \qquad \text{Exact} \qquad (4.45\text{-}2)$$

The interpretation and findings of each condition have already been given; however, they are repeated here.

1) Eq. (4.2-5) reveals that the deviation of the operating frequency from the normal frequency is affected more strongly by the ratio of $\frac{2\delta}{L}$ than the ratio of $\frac{T_w}{T_o}$ as is shown by (4.2-6a and 4.2-6b).

2) (4.34-2) is presented in a graphical form to facilitate understanding. Solutions are the interceptions. There are usually two frequencies in the vicinity of the normal frequency. The boundary layer thickness δ and the speed of sound c_o can be evaluated from these two frequencies at which the output reaches maximum.

3) (4.45-2) will be solved by computer technique in order to obtain acceptable accurate numerical values of δ and c_o. Approximate values of δ and c_o are already known from (4.34-2).

5.0. CONCLUSION

An exact expression of acoustic impedance across the transducer including the nonuniform boundary layer effects at both ends has been presented. An approximate theory has also been presented, applicable to cases in which the temperature difference between the transducer plates and the atmospheric ambient is small and the boundary layer thickness is comparatively large with respect to the wavelength.

The conditions for the maximum input impedance has been derived, and solutions for the maximum input impedance based on the approximated ex-

pression plotted in graphical form as an illustration. It is planned to employ computer technique when accurate numerical values are desired.

Fairly consistent agreement between the preliminary experimental measurements and the analysis substantiates the essential correctness of the results, and demonstrates the feasibility of the measurement of ambient temperature.

REFERENCES

1. Thermal and Radiation Effects on Acoustic Measurements in the Upper Atmosphere, Richard C. Montgomery

2. Leo L. Beranek, Acoustics, McGraw-Hill Book Co., N.Y. 1954.

3. W.J. Cunningham, Introduction to Nonlinear Analysis, McGraw-Hill Book Co., N.Y. 1958.

4. C.R. Wylie, Jr., Advanced Engineering Mathematics, McGraw-Hill Book Co., N.Y. 1959.

5. Walter C. Johnson, Transmission Lines and Networks, McGraw-Hill Book Co., N.Y. 1950.

DETERMINATION OF ATMOSPHERIC PARAMETERS BY ACOUSTIC MEANS

Progress Report No. 1

July, 1962

Section II

DESIGN AND DEVELOPMENT OF ACOUSTIC DEVICES

DETERMINATION OF ATMOSPHERIC PARAMETERS

BY ACOUSTIC MEANS

DA-SIG-36-039-62-G17

Progress Report No. 1

July, 1962

Section II

DESIGN AND DEVELOPMENT OF ACOUSTIC DEVICES

-6-

Air-Borne Acoustic Interferometer (Sonotherm)

for

Atmospheric Measurements

Carlos McDonald
Research Physicist

S C H E L L E N G E R R E S E A R C H L A B O R A T O R I E S

Texas Western College El Paso, Texas

CONTENTS

1.0 - INTRODUCTION

An airborne acoustic interferometer (Sonotherm) for performing acoustic measurements in the upper atmosphere is described. The atmospheric temperature is determined through local speed of sound measurements. Relative measurements of air density and sound absorption can be accomplished by amplitude and frequency measurements.

Due to its compactness, the proposed acoustic interferometer is suitable for use with either meteorological rockets or balloons. Theoretical and experimental evidence indicates that local phase velocity measurements with an ARCAS meteorological rocket are possible up to altitudes of 65 km (Sec. 5.7).

1.1 - General Description

The proposed acoustic interferometer utilizes two, closely spaced, broad band, piston-type transducers. One transducer acts as a transmitter of sound, while the other acts as a receiver (microphone) and sound reflector. With proper transducer face dimensions (greater or comparable to a wavelength) and spacing, an acoustic standing wave is generated in the air space between the receiver and transmitter. However, unlike typical acoustic interferometers, the spacing between the transducers is held fixed, while the sound frequency is varied.

The receiver sound pressure is detected as a function of frequency. Ideally, at the antiresonant frequency where the receiver-transmitter spacing corresponds to an integral number of half wavelengths, the receiver sound pressure is maximum. At this condition, the antiresonant frequency f_o is related to the phase velocity of sound c (Sec. 4.6) by

$$c = \frac{2\ell}{n} f_o \qquad (1\text{-}1)$$

where ℓ is the receiver-transmitter spacing, and n is the number of half wavelengths. Since the spacing ℓ is known and the antiresonant frequency f can be measured, the phase velocity of sound can be determined.

A frequency bandwidth measurement, about the antiresonant frequency, can be related to the absorption coefficient of sound, and the magnitude of the receiver sound pressure can be related to the air density.

1.2 – Basic Relationships

The relationship between the acoustic interferometer measurements and the physical parameters of the atmosphere are summarized.

1.21 – Speed of Sound – Virtual Temperature

Under the assumption that the atmosphere behaves like an ideal gas (Sec. I–2) and that the propagation of sound is an adiabatic process in certain frequency and atmospheric pressure ranges, the kinetic air temperature T can be expressed (Sec. 4.2) by

$$c = \sqrt{\gamma T \left(\frac{R}{M}\right)} \qquad (1\text{–}2)$$

where R is the gas constant per mole, M is the molecular mass of air, and γ is the ratio of specific heat at constant pressure to that at constant volume. The virtual temperature T^* is determined by the defining relation

$$T^* = \frac{T}{M} M_o$$

where M_o is the standard molecular weight of dry air. Since γ varies slowly with changes in temperature and composition (Sec. I–2), a measurement of the speed of sound yields the virtual temperature.

1.22 – Sound Absorption

The acoustic energy losses of the interferometer can be determined by a measurement of the Q of the acoustic standing wave (Sec. 4–8) as defined by

$$Q = \frac{f_o}{2\Delta f}$$

where f_o is the antiresonant frequency corresponding to the maximum receiver sound pressure, and $2\Delta f$ is the frequency bandwidth, about f_o, where the sound pressure is reduced by a factor of $1/\sqrt{2}$.

When the acoustic energy losses due to transducer geometry, wind, and non-rigidity of the transducer faces are small compared to sound absorption losses, the Q of the standing wave can be related to the sound absorption coefficient α by (Sec. 4.10)

$$Q = \frac{\omega_o}{2\alpha c}$$

where ω is the angular antiresonant frequency, $2\pi f_o$, and c is the speed of sound. Consequently, the absorption coefficient can be determined by a measurement of the Q of the acoustic standing wave, the frequency corresponding to a maximum receiver sound pressure, and the speed of sound. At low atmospheric pressures and for high frequencies, the absorption coefficient can be related to the air viscosity (Sec. 4.3).

1.23 - Air Density

The maximum receiver sound pressure is proportional to the product of the air density, the speed of sound, and Q of the acoustic standing wave (Sec. 5.41). Consequently, the variation of air density or atmospheric pressure with respect to altitude can be determined by a knowledge of the variation of the speed of sound and the Q of the standing wave.

1.3 - Sensitivity

From Eq. (1-1), the change Δf in the antiresonant frequency, corresponding to an incremental change in the speed of sound c_o, is given by

$$\frac{\Delta c}{c_o} = \frac{\Delta f}{f_o} . \qquad (1\text{-}3)$$

The change Δc in the speed of sound results from change ΔT in the air temperature. From equations (1-2) and (1-3), the change Δf in the antiresonant frequency is

$$\Delta f = \frac{f_o}{2} \frac{\Delta T}{T_o} \qquad (1\text{-}4)$$

where T_o is the air temperature corresponding to the speed of sound c_o. From the above expression, it can be seen that a small deviation in air temperature results in a large deviation of frequency if high frequencies are used. For example, using typical values from an experimental model (Sec. II-7),

$$f_o = 23\text{kC},$$

$$T_o = 300^\circ\text{k}.$$

The resulting change in antiresonant frequency when the temperature varies by 1° is

$$\Delta f \cong 38 \text{ cps}.$$

Electronically, it is possible to detect antiresonant frequency to within 2 cps (Sec. II-8). Consequently, it is possible to detect temperature variations of less than 0.1°C.

1.4 – Advantages

For upper atmospheric measurements, the proposed acoustic interferometer has the following advantages over other techniques:

1. Since the basic measurement is frequency, a very sensitive speed of sound measuring system is possible. In laboratory measurements, variations in the speed of sound within one part in 10,000 were easily detectable. This corresponds to temperature variations of approximately 0.1°C.

2. Acoustic standing waves generated between the fixed, closely spaced transducers produce such intense levels that the signal-to-noise ratio is greatly improved at high altitudes.

3. Close spacing and relatively large transducer surfaces minimizes wind effects.

4. Close receiver-transmitter spacing can be utilized without loss of accuracy if heating and cooling effects of the transducer faces are taken into account (Sec. 3.4).

5. Fixed, closely spaced transducers make a compact flight package suitable for rocketsonde applications.

6. The method of obtaining the information results in a flight unit with light, non-critical instrumentation.

7. Air density, sound absorption, and other acoustic measurements are also possible.

2. GENERAL SYSTEM DESCRIPTION

For balloon or rocketsonde operations, the Sonotherm system will consist of: a) the airborne unit housing the acoustic interferometer and an RF Transmitter; b) the ground station for receiving the telemetered signal; c) a detection system for demodulating the acoustic interferometer output (Sec. II-8).

2.1 Airborne Unit

Figure 2.1 shown a block diagram of the essential elements of the airborne unit. It consists of a variable frequency oscillator, the sound transmitter amplifier, two sound transducers which act as the receiver and transmitter of sound, the receiver amplifier, an automatic gain control, and the RF transmitter

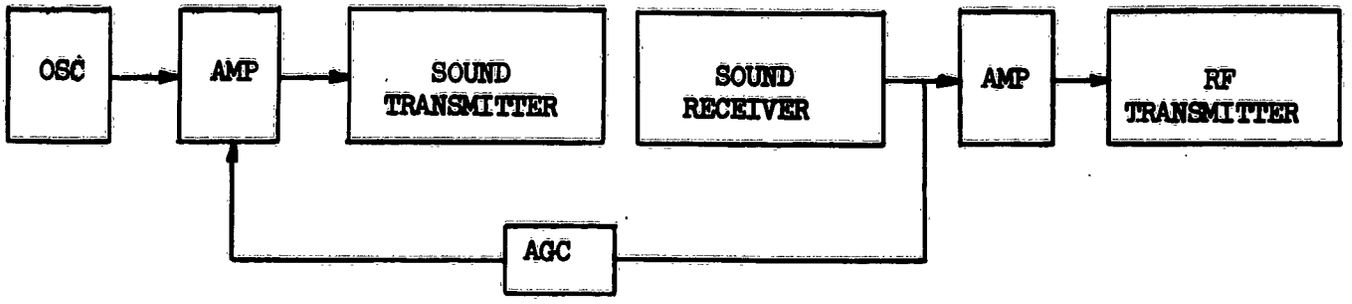

Figure 2-1

(see Sec. II-7 for more details).

The transducer faces are positioned parallel and at a fixed distance from each other. In order to minimize wind effects (Sec. 3.1), the transducers are mounted in an air channel (Fig. 2-2) with their faces flush to the channel surface and thermally insulated.

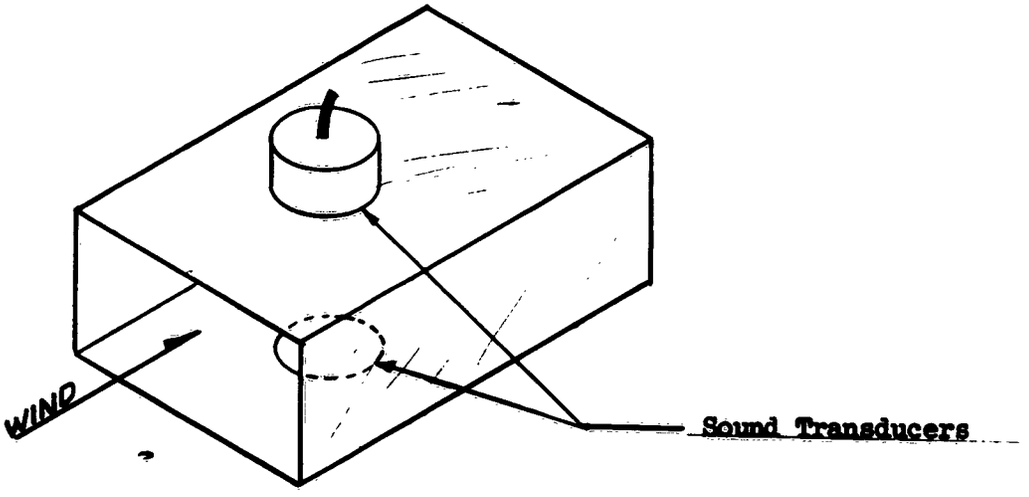

Figure 2-2

In actual practice, the frequency of the oscillator driving the transmitter-transducer is varied periodically similar to the manner shown in Fig. 2-3a where the frequency of the oscillator is plotted as a function of time.

With this type modulation, the receiver output voltage consists of a frequency-amplitude modulated waveform with respect to time as shown in Fig.2-3b.

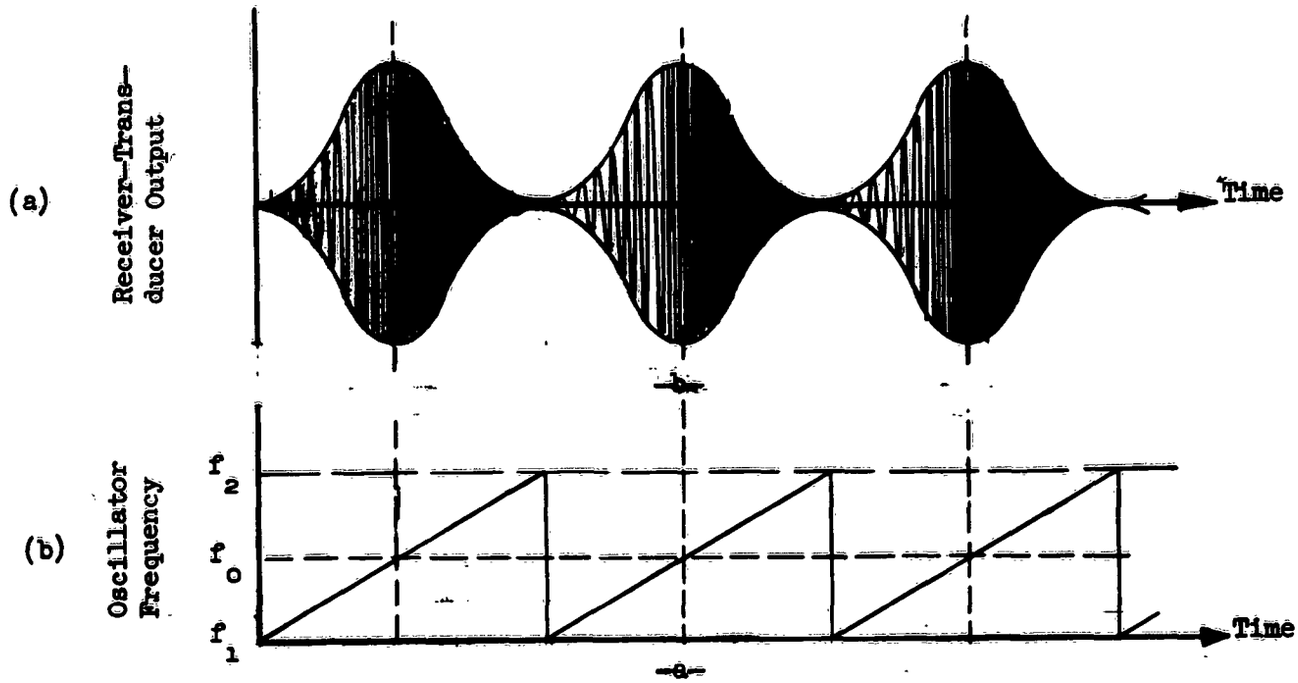

Figure 2-3

Ideally, maximum output occurs at the frequency f_o when the spacing between the transducers corresponds to an integral number n of half wavelengths at a particular speed of sound c_o (Eq 1-1).

As the frequency or the speed of sound varies, the transducer spacing will not correspond to a multiple half wavelength; and if the acoustical Q is high, the receiver output is reduced sharply.

Due to the method of detection (Sec. II-8) the rate at which the oscillatory frequency changes does not necessarily have to be a linear function with respect to time. In order to eliminate loss of amplitude and ringing effects, the rate of change of the frequency is kept slow enough to allow sufficient time for the acoustic standing wave with the highest Q to reach its maximum amplitude.

In practice as the speed of sound varies, the spacing between the transducer faces is set to correspond to an integral number of half wavelengths so that the frequencies are within the bandwidth of the transducers (sec. 5.6).

2.2 Detection

The frequency-amplitude modulated signal from the receiver-transducer is telemetered by conventional means (such as the Rawin Set AN/GMD-1) from the airborne unit to a ground station.

The virtual air temperature is then determined by measuring the frequency f_o corresponding to the maximum amplitude of the received signal. Since the spacing between the transducers is known, the phase velocity of sound and the virtual temperature can be calculated once the frequency f_o is measured.

There are various electronic techniques that can be used to measure accurately the frequency f_o at which the maximum output of the receiver-transducer occurs (Sec. II-8).

3. ACOUSTIC MEASUREMENTS IN THE UPPER ATMOSPHERE

Various factors have to be considered when performing accurate measurements on moving platforms in the upper atmosphere. The factors include:

a. Wind effects.

b. Dispersion of sound.

c. Sound pressure reduction.

d. Thermal effects.

A study of the above effects on the proposed acoustic interferometer indicates that they can be minimized under certain conditions, or the magnitude of the effects can be measured in the process of varying the frequency.

3.1 Wind Effects

The rate of flow of air or wind with respect to the acoustic interferometer is determined primarily by its rate of ascent or descent through the atmosphere. Wind, of course, affects the speed of sound measurement, removes

acoustic energy, results in aerodynamic effects which can lead to turbulence and noise, and strongly dictates the extent of the thermal effects on the operation of the acoustic interferometer.

3.11 Effect on Phase Velocity

In the case of the acoustic interferometer, wind effects on the measurement of the phase velocity of sound are minimized. This is based on the fact that for the case of a sound plane wave, wind flowing parallel to the wave fronts has no effect on the phase velocity. With proper construction and orientation of the transducer faces with respect to the direction of motion (Fig. 2-2), the wind present between the transducer faces will be the component parallel to their faces. Since plane waves exist between the transducer faces, the phase velocity measurement will not be affected.

3.12 Aerodynamic Effects

As the transducers move through the air, viscosity causes a layer of stagnant air to form on the vibrating surfaces of the transducers. This layer forms at the leading edge of the air intake (Fig. 3-1) and increases as a

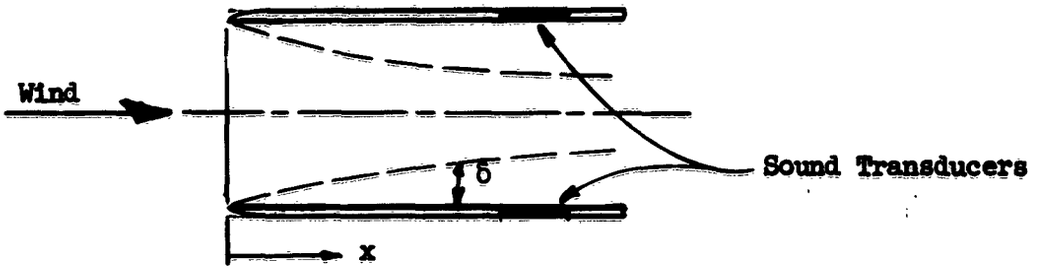

Figure 3-1

function of the distance x. Within this boundary layer, the velocity of the wind varies from zero at the surfaces to the undisturbed stream velocity. Assuming a flat plate, the boundary layer thickness, δ, is approximately[1]

$$\delta = \frac{5x}{\sqrt{R_e}} . \qquad (3\text{-}1)$$

R_e is the Reynolds number,

$$R_e = \frac{\rho_o}{\mu} xv ,$$

where ρ_o is the air density, μ is the coefficient of viscosity, and v is the stream velocity of the wind. Consequently, the thickness of the layer is an inverse function of the air density and the wind speed.

The stagnant layer results in two effects:

1. If a temperature difference exists between the transducer faces and the air, the stagnant air layer tends to be heated or cooled by the transducer faces. This effect is discussed in Sec. 3.4.

2. Under certain conditions, wind turbulence can result which in turn can lead to acoustic noise.

3.13 Acoustic Noise

If the flow of air between the transducer faces is laminar, the noise detected by the receiver will be mainly due to the thermal agitation of the air molecules.[2] This noise is extremely small (.0002 dyne/cm^2, 20Kc bandwidth; sea level atmospheric conditions) and decreases with density and temperature. However, if a critical Reynolds number of approximately 500,000 is exceeded (assuming a flat plate), the wind flow becomes turbulent, and the noise increases as a function of velocity (Sec. III-10). Consequently, the Reynolds number (Eq. 3-1) must be kept below its critical value in order to maintain a high signal-to-noise ratio.

A Reynolds number below the critical value can be accomplished quite easily in practice by locating the transducers near the air intake (Fig. 3-1) and controlling the wind velocity. Since the Reynolds number decreases with density and the coefficient of viscosity varies rather slowly with density and temperature, the wind velocity can be increased as a function of altitude while maintaining laminar flow. As a result, initial high velocities of descent, as those encountered with meteorological rocketsondes, are possible with proper areodynamic design of the acoustic package.

3.14 - Sound Energy Losses

Since the area of the transducer is finite, the air flow relative to the transducer faces removes some of the acoustic energy. The effect is the same as if the receiver face rigidity was reduced so that part of the acoustic energy is absorbed in moving the face instead of being reflected. As a result, the magnitude of the receiver sound pressure and the Q of the acoustic standing wave are reduced. This in turn reduces the accuracy of determining the frequency corresponding to a maximum reciever output (Sec. 5.7).

However, with proper dimensions of the acoustic interferometer, wind velocities of the order of 300 ft/sec can be tolerated. This can be shown by expressing the acoustic energy loss due to wind in terms of a quality factor Q_w, the ratio of the acoustic energy stored between the transducer faces to the acoustic energy lost per wavelength (Sec. 4.91). Assuming transducers of rectangular dimensions, the quality factor Q_w is given by Eq. 4-69:

$$Q_w = 2\pi n \left(\frac{L}{\ell}\right)\left(\frac{c}{v}\right),$$

where L is the width of the transducers in the direction of the wind, ℓ is the transmitter spacing, v is the wind velocity, and n is the number of half

wavelengths between receiver and transmitter. Typical dimensions can be a width to receiver-transmitter separation ratio of 2, and a receiver-transmitter separation corresponding to 3/2 wavelengths (Sec. III-7). For a wind velocity of 200 feet per sec, the quality factor would be approximately 270. With the above dimensions, if overall acoustic Q at zero wind velocity would be in the order of 120, the resulting Q with a wind velocity of 200 feet per sec would be in the order of 80. Hence, the change in the acoustical Q in increasing the wind velocity from 0 to 200 feet per sec would amount to 33 percent.

3.2 Sound Dispersion

It is necessary to consider the dispersion effects (See Sec. I-2 and 4.3) of sound when accurate determination of the air temperature is desired. In general, dispersion of sound at high altitudes is mainly due to viscous energy losses which are proportional to the sound frequency and inversely proportional to the atmospheric pressure. As a result, the phase velocity of sound is not simply related to the undisturbed speed of sound as given by Eq. (1-2).

The temperature correction, in calculating the virtual air temperature from the simple speed of sound expression (Eq. 1-2), can be kept small if sound frequencies below 30,000 cps are used. Table 6-2 of Sec. I-2 shows the temperature corrections and the error in calculating the correction as determined by a knowledge of the parameters upon which sound dispersion depends. Without any corrections, the air temperature can be determined from a phase velocity measurement within 1° at altitudes up to 50 km if sound frequencies below 20,000 cps are used, and within 2° up to 60 km at frequencies below 10,000 cps.

However, since sound dispersion is also associated with acoustical energy losses, the temperature corrections can also be determined by a measurement of the Q of the standing wave.

3.3 Sound Pressure Reduction

The sound pressure generated by piston-type transducers is proportional to the air density. As a result, the output sound pressure reduces with altitude if the operating conditions of the transducer are held constant. Furthermore, the sound intensity is inversely proportional to the square of the distance from the transducer in the far field.

In the case of the acoustic interferometer, due to the loading effect on the transducer by the standing wave, the output sound pressure is increased by a factor corresponding to the Q of the acoustic standing wave (Sec. 5.3). Furthermore, since the receiver transducer is located in the near field, an intense sound pressure can be generated with minimum power requirements. As a result, a high signal-to-noise ratio is maintained at high altitudes.

3.4 Thermal Effects

Thermal effects on the acoustic interferometer can be classified under:

a. Thermal boundary layer effects.

b. Heat radiation.

c. Thermal expansion.

3.41 Thermal Boundary Layer Effects

As mentioned in Sec. 3.22, the motion of the acoustic interferometer through the atmosphere causes a stagnant layer of air to form adjacent to the transducer faces.

If a temperature difference exists between the air and the transducer faces, it is found (Sec. I-3) that a thermal boundary layer forms which is about the same thickness and functional dependence as the velocity boundary layer. Therefore, a decrease in density or in wind velocity increases the thermal boundary layer. The air within the thermal boundary layer is cooled or heated by the transducer faces, and the temperature within the layer varies from the face temperature to the undisturbed air temperature.

The thermal boundary layer has two effects on the operation of the acoustic interferometer:

1. Since the air in the thermal boundary layer is not at the same temperature as that of the undisturbed region, the apparent phase velocity of sound as measured by the acoustic interferometer will be different from that of the undisturbed air medium. However, as long as the thermal boundary layers do not intersect within the transducer faces, it is possible to determine not only the speed of sound in the undisturbed region, but also the magnitude of the thermal boundary layer (Sec. I-5). In this case, it is necessary to measure the frequencies corresponding to two successive pressure maximums on the receiver face and the transducer face temperature.

When the receiver-transmitter separation is large compared to the thermal boundary layer, and the difference between the face and air temperature is small compared to the absolute temperature, the apparent error ΔT_E of the temperature measurement is approximately (Sec. I-5)

$$\Delta T_E = \frac{\delta}{\ell} \Delta T , \qquad (3-5)$$

where δ = thermal boundary layer thickness

ℓ = receiver-transmitter separation

ΔT = temperature difference between the air and transducer surfaces.

Consequently, the error can be minimized by maintaining a large receiver-transmitter spacing compared to the thermal boundary layer, and by maintaining a small temperature difference between the air and the transducer surfaces. In general, this temperature difference can be minimized by thermal insulation of the transducer faces from the rest of the device, increasing the ratio of the surface area to the volume of the transducer faces, and by controlling the thickness of the thermal boundary layer.

The error can also be calculated from a knowledge of the transducer face temperature, the rate of ascent or descent of the acoustic thermometer through the atmosphere, the air density, and the coefficient of viscosity.

2. The second effect relates to the fact that, for a constant air velocity, the velocity and thermal boundary layer thicknesses vary with distance from the air intake (Fig. 3-1). As a result, since the isotherms within the boundary layer will not be parallel to the surface of the transducer, the sound waves passing through the thermal boundary layer will be refracted. The refraction of the sound wave will in general lead to a lowering of the effective Q of the standing wave and can affect the measurement of the phase velocity.

The above effect, however, can be eliminated by maintaining a uniform thermal boundary layer over the transducer surfaces. This can be accomplished by increasing the air velocity with respect to the distance x from the air intake (Fig. 3-1) so that a constant Reynolds number is maintained (Eq. 3-1). For wind velocities less than 300 feet per sec, the air acts like an in compressible fluid[3]. Consequently, the wind velocity can be increased by reducing the cross sectional area of the channel (Fig. 3-2) with respect to the distance from the air intake.

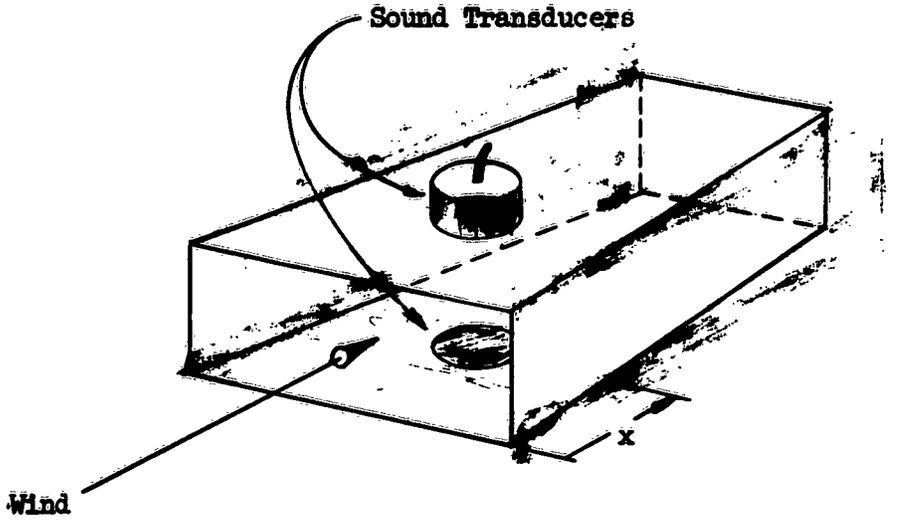

Figure 3-2

By locating the transducers as far as possible from the air intake and by reducing their dimension along the direction of the wind, the change in the air velocity can be kept small. In this manner, heating effects due to compression, which are a function of the difference in the squares of the initial and final velocity, will be minimized even with high subsonic wind velocities encountered by instrumentation packages ejected from meteorological rockets at high altitudes.

3.42 Heat Radiation

Although heat radiation has a negligible direct effect on acoustic measurements (Sec. I-2), it does tend to heat the transducer faces. As a result, the temperature difference between the air and the transducer faces tends to increase. However, from theoretical calculations on the temperature difference expected between the air and transducer faces (Sec. I-3,4), the effect due to heat radiation in the atmosphere is slight.

3.43 Thermal Expansion

As the air temperature varies, the spacing between the transducers tends to change due to the thermal expansion or contraction of the exposed mounting

holding the transducers. From Eq. (1-1) the speed of sound error, Δc, resulting from a change in separation, $\Delta \ell$, is

$$\frac{\Delta c}{c} = \frac{\Delta \ell}{\ell_o}, \tag{3-6}$$

where c and ℓ_o correspond to the actual speed of sound and the receiver-transmitter separation, respectively.

Assuming that the mounting holding the transducers determines the separation ℓ, it can be expressed approximately by

$$\ell = \ell_o (1 + \alpha T), \tag{3-7}$$

where α is the coefficient of linear thermal expansion, ℓ_o is the initial separation at 0°C and T is the temperature in °C.

From equations 3-6 and 3-7 the error in the speed of sound as a function of the separation due to thermal expansion is

$$\frac{\Delta c}{c} = \alpha (T_2 - T_1), \tag{3-8}$$

where $T_2 - T_1$ is the difference between the initial and final temperatures of the mounting in °C. In the extreme case, if a measurement of the speed of sound is to be made within one part in ten thousand (corresponding to an error in the temperature measurement of less than 0.1°C), and if the difference between the initial and final temperature of the bracket corresponds to 100°C, the linear coefficient of thermal coefficient of the bracket would have to be less than

$$\alpha \leq 10^{-6}. \tag{3-9}$$

Invar (nickle steel, 36 percent), with a coefficient of linear thermal expansion of 0.9×10^{-6} easily meets this requirement. Of course, mechanical

techniques, such as pivot points, can reduce the effective separation due to thermal expansion considerably.

4. ACOUSTICAL RELATIONSHIPS

The various acoustical relationships of the air medium between the sound transducers of the acoustic interferometer are derived. It is assumed that the transducer faces are parallel and vibrate with a uniform velocity, and that a plane sound is generated by the transmitter and reflected by the receiver. The wind flow is assumed parallel to the transducer faces and its only effect is assumed to be removal of acoustic energy (Sec. 3.11).

Viscosity effects are only included since they are the major effect at high altitudes. However, the results are general so that secondary effects, such as thermal conductivity, molecular absorption, and heat radiation can also be included.

4.1 Acoustic Equations

Assuming that the air medium between the receiver and transducer is a non-turbulent homogeneous, isotropic, adiabatic viscous fluid, the small signal acoustic equations are[2]

$$\frac{\partial \rho'}{\partial t} + \rho_o \nabla \cdot \underline{u} = 0 \qquad (4\text{-}1)$$

$$\rho_o \frac{\partial \underline{u}}{\partial t} + \frac{K_s}{\rho_o} \nabla \rho' - \frac{4}{3} \eta \nabla(\nabla \cdot \underline{u}) = 0$$

where ρ' = instantaneous change in density

ρ_o = static air density

$\underline{u}$ = instantaneous particle velocity

η = coefficient of viscosity

K_s = isentropic bulk modulus of elasticity

t = time.

The first equation arises from the equation of continuity, and the second corresponds to Newton's Second Law.

From the definition of bulk modulus, the sound pressure p is related to the change in density ρ' by

$$p = \frac{K_s}{\rho_o} \rho' .$$

Substituting the above expression for ρ', and assuming sound propagation along the x-axis, equations 4-1 reduce to

$$-\frac{\partial p(x,t)}{\partial x} = \rho_o \frac{\partial u(x,t)}{\partial t} - \frac{4}{3}\eta \frac{\partial^2 u(x,t)}{\partial x^2}$$

$$-\frac{\partial u(x,t)}{\partial x} = \frac{1}{K_s} \frac{\partial p(x,t)}{\partial t} . \qquad (4-2)$$

4.2 Ideal Air Medium

For the ideal case where viscosity effects are negligible, Eqs. (4-2) reduce to

$$-\frac{\partial p(x,t)}{\partial x} = \rho_o \frac{\partial u(x,t)}{\partial t}$$

$$-\frac{\partial u(x,t)}{\partial x} = \frac{1}{K_s} \frac{\partial p(x,t)}{\partial t} . \qquad (4-3)$$

Differentiating the first of Eqs. 4-3 and substituting the second for $\frac{\partial u}{\partial x}$, the wave equation in terms of sound pressure is

$$\frac{\partial^2 p(x,t)}{\partial x^2} = \frac{1}{c^2} \frac{\partial^2 p(x,t)}{\partial t^2} \qquad (4-4)$$

$$c = \sqrt{\frac{K_s}{\rho_o}} . \qquad (4-5)$$

Assuming an adiabatic process and that the air medium is an ideal gas,

$$K_s = \gamma p_o$$
$$\rho_o = \frac{p_o}{T}\left(\frac{M}{R}\right) \qquad (4\text{–}6)$$

where p_o = static atmospheric pressure

γ = ratio of specific heat at constant pressure to that at constant volume

M = molar mass of air

R = gas constant per mole

T = atmospheric temperature in degrees Kelvin.

From the above expressions, the speed of sound reduces to

$$c = \sqrt{\gamma T\left(\frac{R}{M}\right)} \; . \qquad (4\text{–}7)$$

Assuming that the sound pressure varies sinusoidally at the angular frequency ω, it can be expressed by the real part of

$$p(x,t) = A(x)e^{j\omega t} \; . \qquad (4\text{–}8)$$

The general solution of the wave equation, eq. 4–4, is

$$p(x,t) = Ae^{j(\omega t + kx)} + Be^{j(\omega t - kx)} \qquad (4\text{–}9)$$

where k, the phase constant, is

$$k = \frac{\omega}{c} \; . \qquad (4\text{–}10)$$

The solution for the particle velocity, obtained by substituting Eq. (4–9) for p in the first of eqs. (4–3), is

$$u(x,t) = -\frac{A}{z_o} e^{j(\omega t + kx)} + \frac{B}{z_o} e^{j(\omega t - kx)} \qquad (4\text{–}11)$$

where $z_o = \rho_o c$, the specific acoustic impedance of the air medium.

From eqs. 4-9 and 4-11, it follows that the instantaneous sound pressure at any point x is the sum of two plane sinusoidal waves traveling in opposite directions. The constants A and B are determined by the boundary conditions, i.e., the value of the sound pressure and particle velocity at the transducer faces.

4.3 Viscous Air Medium

When viscous effects are not negligible, sound energy losses will result, and consequently, the traveling plane waves are attenuated as they travel. For sinusoidal sound pressure variations, the general solutions of Eqs. 4-2 for small losses will be of the form

$$p(x,t) = Ae^{j\omega t} e^{(\alpha + jk)x} + Be^{j\omega t} e^{-j(\alpha + jk)x}$$

$$u(x,t) = Ce^{j\omega t} e^{(\alpha + jk)x} + De^{j\omega t} e^{-j(\alpha + jk)x} \qquad (4\text{-}12)$$

where α is the attenuation constant or the sound absorption coefficient. Due to the dissipative losses, the phase constant k will be different from the non-dissipative case, and as a result, sound dispersion occurs.

The attenuation and phase constants can be determined by substituting Eqs. 4-12 in Eqs. 4-2. On performing the above operation, the following result is obtained:

$$\gamma^2 = \frac{-k_o^2}{\alpha + jx} \qquad (4\text{-}13)$$

where $\gamma = \alpha + jk$, the propagation constant, and

$$x = \frac{4}{3} \eta \frac{\omega}{\rho c^2} \qquad (4\text{-}13a)$$

$$k_o = \frac{\omega}{c} \ .$$

Assuming small losses, the approximate solutions for the attenuation and phase constants are*

$$k^2 = \left(\frac{\omega}{c}\right)^2 \cong \left(\frac{k_o^2}{1 + x^2}\right)\left(1 + \frac{x^2}{4}\right) \cong \frac{k_o^2}{1 + \frac{3}{4}x^2}$$

$$\alpha = k_o \frac{x}{2}\left[1 + \frac{x^2}{4}\right]^{-1} \cong \frac{x}{2} k_o \qquad (4\text{–}14)$$

The phase velocity $\underline{c}$, from the first of Eqs. 4–14 is approximately

$$(\underline{c})^2 \cong (\underline{c})^2\left[1 + \frac{3}{4} x^2\right] . \qquad (4\text{–}15)$$

In terms of the absorption coefficient, Eq. 4–15 can be as expressed by

$$(\underline{c})^2 \cong (c)^2\left[1 + 3\left(\frac{\alpha}{k_o}\right)^2\right] \qquad (4\text{–}16)$$

From the above expressions, it can be seen that the speed of sound increases due to viscosity, and the attenuation constant is proportional to the ratio of the sound frequency to the air density or atmospheric pressure.

The particle velocity, $u(x,t)$, obtained by substituting the first of Eqs. 4–12 for $p(x,t)$ in the first of Eqs. 4–2, is

$$u(x,t) = -\frac{A}{z_o} e^{j\omega t} e^{(\alpha + jk)x} + \frac{B}{z_o} e^{j\omega t} e^{-(\alpha + jk)x} \qquad (4\text{–}17)$$

where z_o, the specific acoustic impedance of the medium is given by

$$z_o = \frac{(j\omega\rho_o - \frac{4}{3}\eta\gamma^2)}{\gamma} \ .$$

Substituting Eq. 4–13 for γ, z_o reduces to

$$z_o = \rho_o c\left[\left(1 - j\frac{\alpha}{k}\right)^{-1} - jx\left(\frac{c}{\underline{c}}\right)^2\left(1 - j\frac{\alpha}{k}\right)\right] . \qquad (4\text{–}18)$$

* See F. Hunt[2] for a more detailed description.

Consequently, the sound pressure and particle velocity of the traveling wave are not in time phase.

The above results are general since if secondary effects are included, such as thermal conductivity, molecular absorption and heat radiation, only the expressions regarding the propagation constant and specific acoustic impedance have to be modified.

4.4 Acoustic Transmission Line

As shown in section 4.2 and 4.3, the sound field between the transmitter and receiver of the acoustic interferometer can be ideally described by two plane sound waves traveling in opposite directions. These two plane waves can be assumed to be the transmitted and reflected sound waves.

In general, the instantaneous sound pressure and particle velocity, for the case when the air medium is uniform, are given by the first of Eqs. 4–12 and Eq. 4–17:

$$p(x,t) = Ae^{j\omega t + \gamma x} + Be^{j\omega t - \gamma x} \qquad (4\text{–}19a)$$

$$u(x,t) = \frac{A}{z_o} e^{j\omega t + \gamma x} + \frac{B}{z_o} e^{j\omega t - \gamma x} \qquad (4\text{–}19b)$$

where x is the distance measured from the transmitter face (Fig. 4–1), γ is the propagation constant, and z_o is the specific acoustic impedance of the air medium. Eqs. 4–19 are analogous equations for the voltage and current of air electrical transmission line with distributive parameters. Therefore, we can treat the air space between the receiver and transmitter as an acoustic transmission line.

The constants A and B are determined by the boundary conditions of the particle velocity and sound pressure on the receiver face. However, since

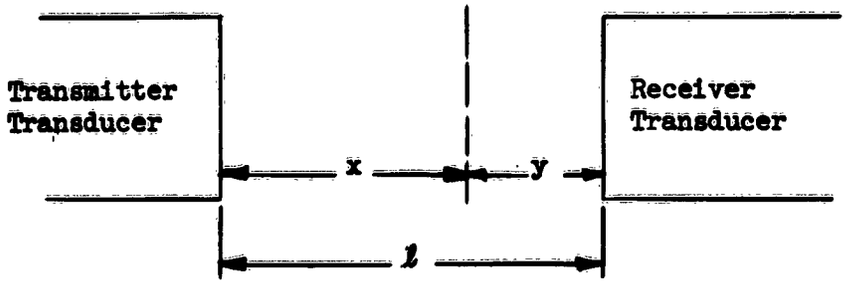

Figure 4-1

the sound field is ideally restricted within the volume defined by the transducer faces and their separation, it is necessary to work with volume velocity, and acoustic impedance[4]. The volume velocity, U(x,t), and the acoustic impedance, z_o, of the air medium are approximately,

$$U(x,t) = u(x,t)S \tag{4-20}$$

$$Z_o = \frac{z_o}{S}$$

where S is the effective surface area of the transducers.

From Eqs. 4-19b and 4-20, the volume velocity U(x,t) is then

$$U(x,t) = -\frac{A}{z_o} e^{j\omega t + \gamma x} + \frac{B}{z_o} e^{j\omega t - \gamma x} . \tag{4-21}$$

To determine the constants A and B, let $p(\ell, t) = P_r e^{j\omega t}$ and $U(\ell, t) = U_r e^{j\omega t}$ be the sound pressure and uniform volume velocity on the receiver face, located at $x = \ell$ (Fig. 4-1). The acoustic impedance Z_r at the receiver face is

$$Z_r = \frac{P_r}{U_r} . \tag{4-23}$$

At the above conditions, Eqs. 4-19 and 4-21 reduce to

$$P_r = Ae^{\gamma \ell} + Be^{-\gamma \ell} \tag{4-24}$$

$$U_r = -\frac{A}{Z_o} e^{\gamma \ell} + \frac{B}{Z_o} e^{-\gamma \ell}. \qquad (4\text{-}25)$$

Solving the above simultaneous equations for A and B,

$$A = (p_r - U_r Z_o) \frac{e^{-\gamma \ell}}{2} \qquad B = (p_r + U_r Z_o) \frac{e^{+\gamma \ell}}{2} . \qquad (4\text{-}26)$$

The acoustic impedance $Z(x)$ at a distance x from the receiver face (looking toward the receiver face) is defined by the ratio of the instantaneous sound pressure $p(x,t)$ (Eq. 4-19a) to the volume velocity (Eq. 4-21):

$$Z(x) = Z_o \frac{Ae^{\gamma x} + Be^{-\gamma x}}{-Ae^{\gamma x} + Be^{-\gamma x}} . \qquad (4\text{-}27)$$

Referring to Eq. 4-27, if Eqs. 4-26 are substituted for A and B; the numerator and denominator is divided by U_r; the ratio p_r/U_r is substituted for Z_r (Eq. 4-23); and the definitions of the hyperbolic sine, cosine, and tangent are utilized; the acoustic impedance reduces to:

$$Z(x) = Z_o \frac{Z_r + Z_o \tanh \gamma y}{Z_o + Z_r \tanh \gamma y} \qquad (4\text{-}28)$$

where $y = \ell - x$, the distance measured from the receiver face.

The sending end acoustic impedance Z_S (the acoustic impedance that the transmitter "sees") is obtained by evaluating Eq. 4-28 at $x = \ell$, the location of the transmitter face with respect to the receiver:

$$Z_S = Z_o \frac{Z_r + Z_o \tanh \gamma \ell}{Z_o + Z_r \tanh \gamma \ell} . \qquad (4\text{-}29)$$

Since $\tanh \gamma \ell = \tanh (\alpha + j \frac{\omega \ell}{c}) = \frac{\tanh \alpha \ell + j \tan \frac{\omega \ell}{c}}{1 + j \tanh \alpha \ell \tan \frac{\omega \ell}{c}}$, the sending end impedance can be expressed by

$$Z_S = Z_o \frac{(Z_r + Z_o \tanh \alpha\ell) + j(Z_o + Z_r \tanh \alpha\ell) \tan \frac{\omega}{c}\ell}{(Z_o + Z_r \tanh \alpha\ell) + j(Z_r + Z_o \tanh \alpha\ell) \tan \frac{\omega}{c}\ell} . \quad (4-30)$$

The sending end acoustic impedance determines the radiation impedance of the transmitter resulting from the reaction of the sound pressure on the transmitter face (see Fig. 5-1). If the transducer face dimensions are greater or comparable to a wavelength of sound, the mechanical radiation impedance Z_R (Sec. 5.3) is

$$Z_R = S^2 Z_S . \quad (4-31)$$

4.5 Transmitter Sound Pressure

The sound pressure at the transmitter face is

$$p_S = Z_S U_S \quad (4-32)$$

where Z_S is the sending end acoustic impedance (Eq. 4-29 or Eq. 4-30), and U_S is the air volume velocity adjacent to the transmitter face. This volume velocity is related to the effective velocity u_1 of the transmitter face by

$$U_S = u_1 S, \quad (4-33)$$

where S is the surface area of the transmitter face. Since the acoustic loading on the transmitter is small compared to its mechanical impedance, the face velocity u_1 is determined primarily by the transmitter mechanical-electrical characteristics (See Sec. 5.3).

Consequently, the transmitter sound pressure is maximum at the frequency where Z_S is maximum. From Eq. 4-30, Z_S is maximum at the acoustic antiresonant frequency, ω_o,

$$\frac{\omega_o}{c}\ell = n\pi \qquad n = 1,2,3, \ldots . \quad (4-34)$$

which corresponds to a receiver-transmitter spacing of an integral number of half wavelengths:

$$\ell = \frac{n\lambda}{2} , \qquad (4\text{-}35)$$

where λ is the wavelength of sound.

At the antiresonant frequency, the sending end impedance has value of

$$Z_S = Z_o \frac{Z_r + Z_o \tanh \alpha\ell}{Z_o + Z_r \tanh \alpha\ell} . \qquad (4\text{-}37)$$

From Eqs. 4-31 and 4-37, the transmitter sound pressure at the antiresonant frequency, is

$$p_S = Z_o \frac{Z_r + Z_o \tanh\alpha\ell}{Z_o + Z_r \tanh \alpha\ell} U_S . \qquad (4\text{-}38)$$

If the sound absorption losses are small,

$$p_S \cong Z_r U_S . \qquad (4\text{-}39)$$

As shown in section 4.6, the sound pressure on the receiver face is also maximum at the antiresonant frequency given by Eq. 4-34.

4.6 Receiver Sound Pressure

The sound pressure acting on the receiver face consists of the sum of the incident and reflected sound waves. In order to determine this sound pressure, the constants A and B (Equations 4-19) , can be evaluated in terms of the boundary conditions at receiver and transducer faces. However, if the impedance analogy[3] is used, the sound pressure on the receiver face can also be determined by treating the air space between the receiver and transmitter as a one-dimensional transmission line, and utilizing network theory. In this case, the acoustic transmission line can be treated as a four-terminal network terminated by the equivalent acoustic impedance of the receiver (Fig. 4-2), where

Figure 4-2

p_S and p_r correspond to the sound pressure at the transmitter and receiver faces, respectively.

From four-terminal network theory[5], the ratio of the sound pressure at the receiver face to that at the transmitter face is

$$\frac{p_r}{p_S} = \frac{Z_r}{Z_S} \frac{\sqrt{Z_{20}(Z_{10} - Z_{1S})}}{(Z_r + Z_{20})} \qquad (4\text{-}40)$$

where (refer to Fig. 4-2):

Z_r = the acoustic impedance of the receiver.

$Z_S = Z_{10} \frac{Z_r + Z_{2S}}{Z_r + Z_{20}}$, the sending end impedance of the acoustic transmission line terminated by Z_r.

Z_{1S} = the acoustic impedance looking into terminals No. 1 with $Z_r = 0$.

Z_{10} = the acoustic impedance looking into terminals No. 1 with $Z_r = \infty$.

Z_{2S} = the acoustic impedance looking into terminals No. 2 with a short circuit at terminals No. 1.

Z_{20} = the acoustic impedance looking into terminals No. 2 with an open circuit at terminals No. 1.

Since the acoustic transmission line is symetrical,

$$Z_{1o} = Z_{2o}$$

$$Z_{1S} = Z_{2S} .$$

(If thermal boundary layer effects are included, this requires the transducer faces to be at the same temperature.)

Substituting the above expressions in Eq. 4-40, and simplifying, the sound pressure acting on the receiver face can be expressed by

$$p_r = \left[\left(\frac{Z_r}{Z_r + Z_{1s}} \right) \sqrt{1 - \frac{Z_{1S}}{Z_{1o}}} \right] p_S \cdot \quad . \tag{4-41}$$

From Eq. 4-29, Z_{1S} and Z_{1o} can be evaluated by letting $Z_r = 0$ and $Z_r = \infty$ respectively:

$$Z_{1S} = + Z_o \tanh \gamma \ell$$

$$Z_{1o} = + Z_o \coth \gamma \ell .$$

Substituting in Eq. 4-41 the above expressions for Z_{1S} and Z_{1o} and simplifying,

$$p_r = \left(\frac{Z_r}{Z_r + Z_o \tanh \gamma \ell} \right) \left(\frac{p_S}{\mathrm{Cosh}\, \gamma \ell} \right) . \tag{4-42}$$

The receiver sound pressure (Eq. 4-42) is also maximum at the same frequency corresponding to a maximum transmitter sound pressure (Sec. 4-7):

$$\frac{\omega \ell}{c} = n \pi \qquad n = 1,2,3,.....$$
$$\ell = \frac{n\lambda}{2} . \tag{4-43}$$

At this frequency, since the receiver acoustic impedance is much greater than the acoustic impedance of the air medium, the receiver sound pressure is approximately

$$p_r = \frac{p_S}{\cosh \gamma \ell} \tag{4-44}$$

where p_S is given by Eqs. 4-32 or 4-38, and Z_S is given by Eq. 4-37.

If sound absorption losses are small, the above expression reduces to

$$P_r = Z_s U_s \qquad (4\text{-}44a)$$

where p_S was substituted for Eq. (4-39).

4.7 Receiver Sound Pressure Versus Frequency

In order to determine the speed of sound, the maximum receiver output (corresponding to a maximum sound pressure on the receiver face) has to be correlated with the antiresonant frequency. Consequently, the accuracy of the measurement will depend on the change of the receiver sound pressure magnitude near the antiresonant frequency.

A measure of the variation of the receiver sound pressure with respect to frequency is the quality factor Q_A (acoustical Q) of the acoustic standing wave:

$$Q_A = \frac{\omega_o}{\omega_2 - \omega_1} \qquad 4\text{-}45$$

where ω_o is the antiresonant frequency corresponding to a maximum receiver sound pressure; ω_1 and ω_2 are the frequencies, above and below the antiresonant frequency, where the receiver sound pressure reduces to $1/\sqrt{2}$ of its maximum value. As shown in Sec. 4.9, the quality factor Q_A is related to the overall acoustic energy losses.

The maximum receiver sound pressure (Eq. 4-44) is determined by maximizing Z_S of Eq. 4-30, the sending end impedance,

$$Z_S = Z_o \frac{Z_r' + jZ_o' \tan \frac{\omega \ell}{c}}{Z_o' + jZ_r' \tan \frac{\omega \ell}{c}} \qquad (4\text{-}46)$$

where

$$Z_r' = Z_r + Z_o \tanh \alpha\ell \qquad (4\text{–}47)$$

$$Z_o' = Z_o + Z_r \tanh \alpha\ell$$

Z_r = acoustic impedance of receiver

Z_o = acoustic impedance of the air medium.

At the antiresonant frequency,

$$\frac{\omega_o \ell}{c} = n \ , \qquad n = 1,2,3 \ldots \qquad (4\text{–}31)$$

The maximum value of Z_S is

$$(Z_S)_{max} = Z_o \left(\frac{Z_r'}{Z_o'}\right).$$

At the frequency where the receiver sound pressure reduces by a factor of $1/\sqrt{2}$, the value of Z_S is approximately

$$Z_S = \frac{1}{\sqrt{2}} (Z_S)_{max} = \frac{1}{\sqrt{2}} Z_o \left(\frac{Z_r'}{Z_o'}\right). \qquad (4\text{–}48)$$

When the above condition occurs, the frequency can be determined by substituting Eq. 4–48 for Z_S in Eq. 4–46, and solving for $\tan^2 \omega\ell/c$:

$$\tan^2 \frac{\omega\ell}{c} = \frac{(Z_r')^2 (Z_o')^2}{(Z_r')^4 - 2(Z_o')^4} \ . \qquad (4\text{–}49)$$

Since Z_r is much greater than Z_o if dissipation losses are small, the above expression is approximately

$$\tan \frac{\omega\ell}{c} = \frac{Z_o'}{Z_r'} = \frac{Z_o}{Z_r} + \alpha\ell \ . \qquad (4\text{–}50)$$

The angular frequency ω is close to the antiresonant frequency ω_o so that

$$\omega = \omega_o + \Delta\omega \ , \qquad (4\text{–}51)$$

and

$$\frac{\omega \ell}{c} = n\pi + \frac{\Delta\omega \ell}{c} \quad .$$

Substituting the above expression for $\omega\ell/c$, Eq. 4–50 reduces to

$$\tan\left(n\pi + \frac{\Delta\omega\ell}{c}\right) \cong \tan\frac{\Delta\omega\ell}{c} \cong \frac{\Delta\omega\ell}{c} \cong \frac{Z_o'}{Z_r'} \cong \frac{Z_o}{Z_r} + \alpha\ell. \qquad (4\text{–}52)$$

In terms of $\Delta\omega$, the quality factor Q_A (Eq. 4–45) is approximately

$$Q_A = \frac{\omega_o}{2\Delta\omega} \quad . \qquad (4\text{–}53)$$

From Eqs. 4–52 and 4–53, the quality factor can be expressed by

$$Q_A = \frac{n\pi}{2}\frac{Z_r'}{Z_o'} = \frac{1}{\frac{2}{n\pi}\frac{Z_o}{Z_r} + \frac{2\alpha c}{\omega_o}} \quad . \qquad (4\text{–}54)$$

Near the antiresonant frequency, ω_o, the sending end impedance can be expressed in terms of the acoustical Q by first substituting Eq. (4–52) for $\tan \omega\ell/c$ in Eq. 4–46:

$$Z_S = Z_o \frac{Z_r' + jZ_o'\left(\frac{\omega - \omega_o}{\omega_o}\right) n\pi}{Z_o' + jZ_r'\left(\frac{\omega - \omega_o}{\omega_o}\right) n\pi} \qquad (4\text{–}55)$$

where ℓ/c was substituted in terms of ω_o (Eq. 4–34). Multiplying Eq. 4–55 by its complex conjugate, dividing the numerator and denominator by $(Z_o')^2$, and substituting the ratio Z_r'/Z_o' in terms of the quality factor Q_A given by Eq. 4–54, the resulting expression is

$$Z_S^2 = Z_o^2 \left[\frac{\left(\frac{2Q_A}{n\pi}\right)^2 + \left(\frac{\omega - \omega_o}{\omega_o}\right)^2 (n\pi)^2}{1 + \left(\frac{2(\omega - \omega_o)}{\omega_o}\right)^2 Q_A^2}\right] . \qquad (4\text{–}56)$$

Near the antiresonant frequency ω_o, the magnitude of the acoustic sending end impedance is approximately

$$\left|Z_S\right| = \frac{2Z_o\, Q_A}{n\pi\sqrt{1 + (Q_A)^2\left[\frac{2(\omega - \omega_o)}{\omega_o}\right]^2}} \quad . \qquad (4\text{–}57)$$

Substituting the above expression for Z_S in Eq. 4–44a, the receiver sound pressure near or at the antiresonant frequency is

$$p_r = \frac{2Z_o\, U_S\, Q_A}{n\pi\sqrt{1 + (Q_A)^2\left[2\frac{(\omega - \omega_o)}{\omega_o}\right]^2}} \quad . \qquad (4\text{–}58)$$

Consequently, if the Q of the acoustic standing wave is high, the receiver sound pressure variation will be large near the antiresonant frequency.

4.8 Acoustical Q

Physical resonant systems, such as the acoustic interferometer, exhibit an exponential loss in energy with respect to time due to their inherent losses. If the system is driven, the source supplies an amount of energy equal to that lost so that energy of the system remains constant. On the other hand, if the energy source is removed from the system, the energy content reduces exponentially with respect to time. For this latter case, the energy content can be expressed in form,

$$W(t) = W_o e^{-\frac{\omega t}{Q}} \qquad (4\text{–}59)$$

where W_o is the initial energy stored by the system at $t = 0$, $W(t)$ is the energy content at a time, $t > 0$, and Q represents the quality factor of the system. The power loss, P_L, of the system is

$$P_L = \frac{dW(t)}{dt} = \frac{\omega_o}{Q} e^{-\omega/Q^t} . \qquad (4\text{–}60)$$

The ratio of Eq. (4–59) to that of (4–60) yields the defining equation of the Q of a resonant system:

$$Q = \frac{\omega_o W(t)}{\left(\frac{dW}{dt}\right)} = \frac{\omega_o \text{ Energy stored}}{\text{Power loss}} = \frac{2\pi \text{ Energy stored}}{\text{Energy lost /cycle}} . \qquad (4\text{–}61)$$

For small losses, the Q of the acoustic standing wave, as defined above, is in accordance with the previous definition stated in Sec. 4.7, Eq. 4–45:

$$Q = \frac{\omega_o}{\omega_1 - \omega_2} \qquad (4\text{–}45)$$

where ω_o is the antiresonant frequency; ω_1 and ω_2 are the frequencies where the sound pressure reduces by a factor of $1/\sqrt{2}$ of its maximum value at ω_o, assuming a constant power input.

The equivalency of the above definitions of Q can easily be shown for the case of the acoustic interferometer. It can be assumed that the transducer faces are perfectly reflecting, and that at t = 0, the transmitter input is reduced to zero. Since the energy density is proportional to the square of sound pressure or particle velocity, the acoustic energy stored, W(t) as a function of time is:

$$W = W_o e^{-2\alpha x} = W_o e^{-2\alpha c t}$$

where W_o is the acoustic energy stored at t = 0. The power loss is then

$$\frac{dW}{dt} = -2\alpha c\, W_o e^{-2\alpha c t} .$$

Substituting the two preceeding expressions in Eq. 4–61, the Q resulting from sound absorption is

$$Q = \frac{\omega_o}{2\alpha c} .$$

The above expression for the acoustical Q is the same as that obtained in Eq. 4-54 when the transducer faces are assumed rigid.

From Eq. 4-54, the Q of the standing wave can be written in the form,

$$Q_A = \frac{1}{\frac{1}{Q_r} + \frac{1}{Q_\alpha}} \qquad (4\text{-}62)$$

where

$$Q_r = \frac{n}{2} \frac{Z_r}{Z_o}, \qquad (4\text{-}62a)$$

is a quality factor related to the receiver face rigidity, and

$$Q = \frac{\omega_o}{2\alpha c} \qquad (4\text{-}63)$$

is a quality factor related to the attenuation constant α.

4-9 Energy Losses and Acoustical Q

The sound energy losses of the acoustic interferometer can be grouped under:

a) Losses due to sound absorption resulting from viscothermal, molecular or heat radiation effects.

b) Losses due to the non-rigidity of the transducer faces.

c) Losses due to the removal of sound energy by the wind or air flow relative to the transducers.

d) Losses due to the transducer geometry (divergence of the sound field).

The energy losses in a) and b) above have been described in the previous section in terms of their respective quality factors. The energy losses resulting from the wind and transducer geometry can be associated with an effective decrease in the receiver face rigidity and is based on the following reasoning: When the receiver face is not perfectly rigid, the incident sound

wave causes the receiver face to be displaced. As a result, part of the sound energy associated with the incident sound wave is absorbed, and the magnitude of the reflected sound wave is reduced. Consequently, the magnitude of the standing wave is reduced.

The end effect of the wind (assumed parallel to the transducer faces) and the divergence of sound field (neglecting phasing effects) is essentially the same: part of the sound energy of the incident sound wave on the receiver face is removed; the magnitude of the reflected wave is reduced; and as a result, the magnitude of the standing wave is also reduced.

The above energy losses can be related to an overall acoustical quality factor, Q_A, by defining the following power losses:

$\left(\frac{dW}{dt}\right)_\alpha$ = acoustic power loss due to absorption

$\left(\frac{dW}{dt}\right)_r$ = acoustic power loss due to receiver face rigidity

$\left(\frac{dW}{dt}\right)_W$ = acoustic power loss due to the wind effect

$\left(\frac{dW}{dt}\right)_g$ = acoustic power loss due to transducer geometry

where W is the acoustic energy in the receiver-transmitter region. From Eq. 4-62, the overall quality factor, Q_A, is

$$Q_A = \frac{\omega W}{\left(\frac{dW}{dt}\right)_\alpha + \left(\frac{dW}{dt}\right)_r + \left(\frac{dW}{dt}\right)_W + \left(\frac{dW}{dt}\right)_g} \qquad (4\text{-}64)$$

where $Q_\alpha = \frac{\omega W}{\left(\frac{dW}{dt}\right)_\alpha}$ = quality factor related to absorption, (4-65)

$$Q_r = \frac{\omega W}{\left(\frac{dW}{dt}\right)_r} = \text{quality factor related to receiver face rigidity.}$$

$$Q_W = \frac{\omega W}{\left(\frac{dW}{dt}\right)_W} = \text{quality factor related to the wind effect.}$$

$$Q_g = \frac{\omega W}{\left(\frac{dW}{dt}\right)_g} = \text{quality factor related to the transducer geometry.}$$

Referring to Sec. 4–8, the quality factors Q_α and Q_r are given by Eqs. 4–62a and 4–63, respectively.

An expression for the quality factor Q_W is derived in the following section from energy considerations.

4.91 Wind Q

The quality factor Q_W, related to wind energy losses, can be determined from a knowledge of the acoustic energy stored between the transducer faces, and the acoustic energy lost due to wind flow relative (and parallel) to the transducer faces. For simplicity, it is assumed that the transducer faces are rectangular. Referring to Fig. 4–3, the dimensions of the transducers are of length L (along the direction of the wind), width S, and the receiver–transmitter spacing is ℓ.

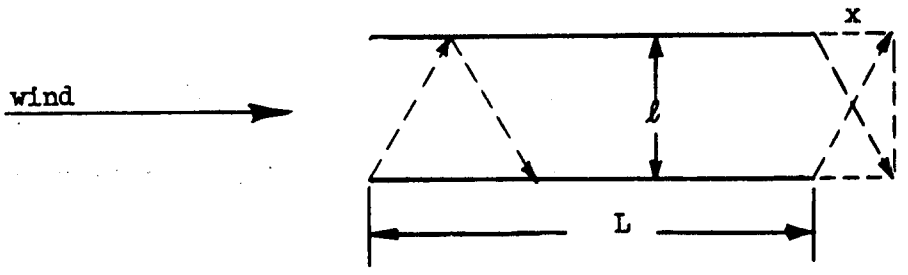

Figure 4–3

The wind flow will cause the transmitted plane wave to be displaced laterally, along the wind, as it travels toward the receiver. Upon reaching the receiver face, a portion x of the wavefront will be located outside the receiver face, resulting in an energy loss. In the same manner, the reflected wave will be displaced a distance x upon reaching the transmitter face. The standing wave is generated by the transmitted and reflected sound waves, and the transmitter supplies the energy loss.

Let the average energy density $\bar{E}$ in the receiver–transmitter region be

$$\bar{E} = \bar{E}_t + \bar{E}_r$$

when $\bar{E}_t$ and $\bar{E}_r$ are the energy densities associated with the transmitted and reflected waves, respectively. The total energy stored in the receiver–transmitter region is then

$$W = S\ell L\,(\bar{E}_t + \bar{E}_r) = S\ell L\bar{E}. \qquad (4\text{–}66)$$

The total energy lost (see Fig. 4–3) is

$$W_L = \frac{S}{2}\,\ell x\,(\bar{E}_t + \bar{E}_r) = \frac{S}{2}\,\ell x\bar{E},$$

and the energy lost per cycle is

$$(W_L)_{\sim} = \frac{S}{2}\,\ell x\bar{E}\left(\frac{\lambda}{\ell}\right). \qquad (4\text{–}67)$$

At the antiresonant frequency,

$$\ell = n\frac{\lambda}{2}, \qquad n = 1,2,3 \ldots$$

and the distance x can be expressed by

$$x = v\left(\frac{\ell}{c}\right)$$

where v and c are wind and phase velocities, respectively. Substituting the above expressions in Eq. 4–67, the energy lost per cycle is

$$(W_L)_{\sim} = \frac{S}{n} \ell^2 \left(\frac{v}{c}\right) E . \qquad (4\text{-}68)$$

From Eqs. 4-65, 4-66, and 4-68, the quality factor Q_W is

$$Q_W = 2\pi n \left(\frac{L}{\ell}\right) \left(\frac{c}{v}\right) . \qquad (4\text{-}69)$$

Consequently, the quality factor Q_W will be large if the wind velocity is small compared to the speed of sound, and or the receiver-transmitter spacing corresponds to a large number of half-wavelengths and is small compared to the transducer face dimensions.

4.10 Sound Absorption Measurement

If the acoustic energy losses due to sound absorption are much greater than the energy losses related to the transducer geometry, wind and non-rigidity of the transducer faces the Q of the acoustic standing wave, Eq. 4-64, reduces

$$Q_A = Q_\alpha \qquad (4\text{-}70)$$

where Q_α, the quality factor related to sound absorption, is given by Eq. 4-63,

$$Q_\alpha = \frac{\omega_o}{2\alpha c} . \qquad (4\text{-}63)$$

Consequently, the absorption coefficient α can be determined by a measurement of the Q of the standing wave, the antiresonant frequency and the speed of sound.

At low atmospheric pressures and or high frequencies the sound absorption coefficient can be related to the air viscosity (Sec. 4-3).

4.11 Air Density Measurement

Substituting Eqs. 4-20 for Z_o and U_s, and assuming that sound absorption losses are small, the receiver sound pressure can be expressed by (Eqs. 4-58, 4-18):

$$P_r = \frac{2\rho_o c_o Q_A \mu_1}{n\pi \sqrt{1 + Q_A^2 \left[2\left(\frac{\omega - \omega_o}{\omega_o}\right)\right]^2}} \qquad (4\text{-}71)$$

where μ_1 is the transmitter face velocity. At the antiresonant frequency, the maximum receiver sound pressure is

$$P_r = \frac{2\rho_o c_o Q_A \mu_1}{n\pi} \quad . \qquad (4\text{-}72)$$

The transmitter face velocity can be treated as a constant since it can be mainly determined by the electro-mechanical characteristics of the transmitter transducer. Therefore, the variation of air density with respect to altitude can be determined by a knowledge of the maximum receiver sound pressure, the acoustical Q and the speed of sound.

5. CHARACTERISTICS

The essential characteristics and requirements of the acoustic interferometer are summarized. For purposes of illustration, electrostatic-type transducers are assumed.

5.1 Electro-Mechanical-Acoustical Circuit

It is necessary to relate the electrical input and output of the sound transducers to their electro-mechanical characteristics and the acoustic standing wave generated between the receiver and transmitter faces.

The above relationships can be established by the use of dynamical analogies between the electrical, mechanical and acoustical quantities, and by the application of electrical network theory[4]. With this approach, an electro-mechanic-acoustical system can be represented by an equivalent circuit.

A simplified equivalent circuit (impedance type) for the acoustic interferometer is shown in Fig. 5-1,

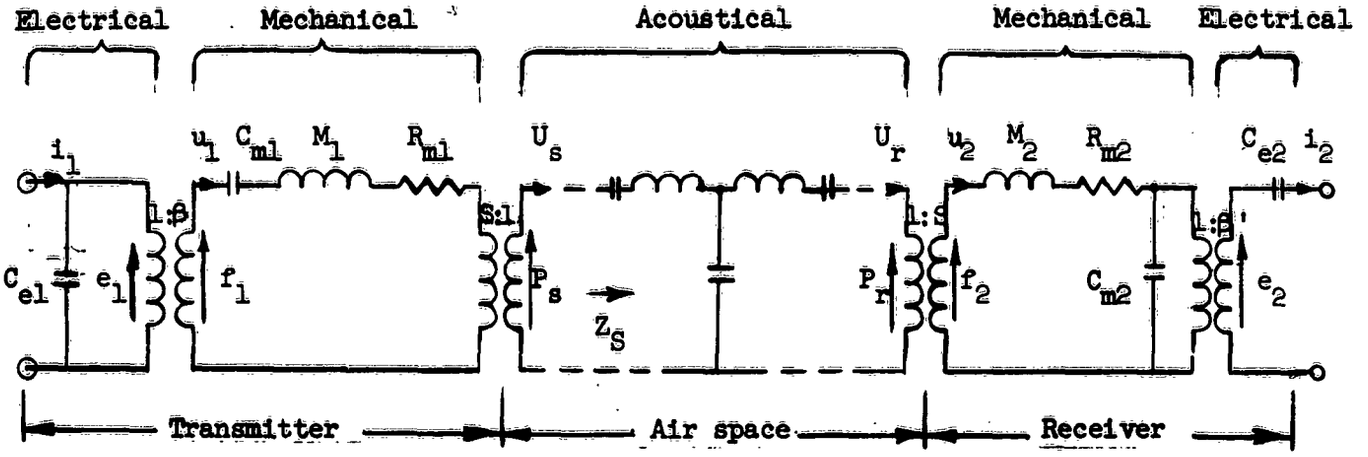

Figure 5-1

where

e_1, e_2 = instantaneous input and output voltages of the transmitter and receiver.

i_1, i_2 = instantaneous input and output current of the transmitter and receiver transducers.

u_1, u_2 = instantaneous mechanical velocities of the transmitter and receiver.

f_1, f_2 = force acting on the transmitter and receiver.

U_S, U_r = instantaneous volume velocity at the transmitter and receiver faces.

p_S, p_r = instantaneous sound pressure at the transmitter and receiver faces.

C_{el} = clamped electrical capacitance of the transmitter-transducer.

C_{ml} = effective mechanical compliance of the transmitter-transducer measured with the electrical terminals short-circuited.

β = electro-mechanical transformation factor of the transmitter-transducer.

M_1 = effective mechanical mass of the transmitter-transducer.

R_{m1} = effective mechanical resistance of the transmitter-transducer.

S = surface area of the transducer vibrating surfaces.

M_2 = effective mechanical mass of the receiver-transducer.

R_{m2} = effective mechanical resistance of the receiver-transducer.

C_{m2} = effective mechanical compliance of the receiver-transducer measured with the electrical terminals open circuited.

β' = electro-mechanical transformation factor of the receiver-transducer.

C_{e2} = electrical capacitance of the transducer measured with the transducer operating into a zero mechanical impedance.

Z_S = acoustical impedance as seen by the transmitter-transducer.

It has been assumed that the transducers are of the electrostatic or piezoelectric type, that the transducer faces vibrate with uniform velocities, that the receiver is located in the near field of the transmitter, and that the dimensions of the transducer faces are comparable or greater than a wavelength. If electromagnetic type transducers are used, their equivalent circuit can be reduced to the electrostatic type.[4]

Referring to Fig. 5-1, the transducers are represented by lumped electrical and mechanical networks. The air space between the receiver and transmitter faces is represented by an acoustic transmission line since plane sound waves propagate between the receiver and transmitter faces (Sec. 4.4). Conversion between electrical, mechanical, and acoustical quantities is accomplished by ideal transformers, and the transformation factors are determined from the physical relationships linking the electrical, mechanical and acoustical quantities.

5.2 General Transducer Characteristics

The proposed acoustic interferometer requires the piston-type transducers to be as directional as possible and to have a sufficient frequency bandwidth in order to cover the variation of the speed of sound with altitude (Sec. 5.5).

In general, highly directional characteristics can be obtained by designing the vibrating surfaces with dimensions comparable or greater than the wavelength of sound in the air medium[6]. For maximum directivity and higher sound intensities, it is desirable to place the receiver in the near sound (Fresnel diffraction zone) of the transmitter where there is little or no divergence of the sound field (diffraction effects have to be considered).

Since the receiver-transmitter spacing has to be well defined, and the operating frequency is low, it is necessary to use a clamped plate or a diaphragm under tension which can be driven by electromagnetic, electrostatic, magnetostriction, or by piezoelectric means. For maximum efficiency, the plate or diaphragm can be tuned in the operating frequency range and the frequency bandwidth can be increased by mechanical or acoustical damping. A commercial transducer (Massa Tr-21) consisting of a tuned clamped plate driven by piezoelectric means was used successfully in an experimental model (Sec. II-7).

5.3 Transmitter Characteristics

The electro-mechanical relations of the transmitter are analyzed in terms of the frequency bandwidth requirements. An expression for the sound pressure magnitude is derived in terms of the transmitter electro-mechanical characteristics and the acoustical loading on the transmitter.

5.31 Electro-Mechanical Relations.

From the equivalent circuit shown in Fig. 4-1, the electro-mechanical equivalent circuit of the transmitter transducer can be simplified to that shown

in Fig. 5-2.

Z_R, the mechanical radiation impedance, is (see Fig. 5-1)

$$Z_R = S^2 Z_S \tag{5-1}$$

where Z_S, the acoustic sending end impedance at the transmitter face, is determined by acoustic standing wave (Sec. 4.4). Near the acoustic anti-resonant frequency, corresponding to a maximum sound pressure on the receiver, the acoustic impedance Z_S is given by Eq. 4-57. Consequently, for small dissipation losses, the mechanical radiation impedance can be expressed by

$$\left|Z_R\right| = \frac{2\rho_o c_o S Q_A}{n\pi \sqrt{1 + \left[2 \frac{(\omega - \omega_o)}{\omega_o}\right]^2 Q_A^2}} \tag{5-2}$$

where ρ_o = air density

c = speed of sound

ω_o = acoustic antiresonant angular frequency

Q_A = Q of the acoustic standing wave (Sec. 4.9).

Referring to Fig. 5-2, the mechanical impedance of the moving face (excluding the radiation impedance) is

$$Z_{m1} = R_{m1} + j\left(\omega M_1 - \frac{1}{\omega c_{m1}}\right) \tag{5-3}$$

where ω is the angular frequency of the input voltage.

For maximum efficiency, it is desirable to drive the transmitter near its mechanical resonance. Since the mechanical bandwidth is important, it is advantageous to express the mechanical impedance in terms of the mechanical Q of the transmitter, Q_{m1}:

$$Q_{m1} = \frac{\omega_1 M_1}{R_{m1}} = \frac{\omega_1}{2\Delta\omega} \tag{5-4}$$

ELECTRO-MECHANICAL EQUIVALENT CIRCUIT
of
TRANSMITTER-TRANSDUCER

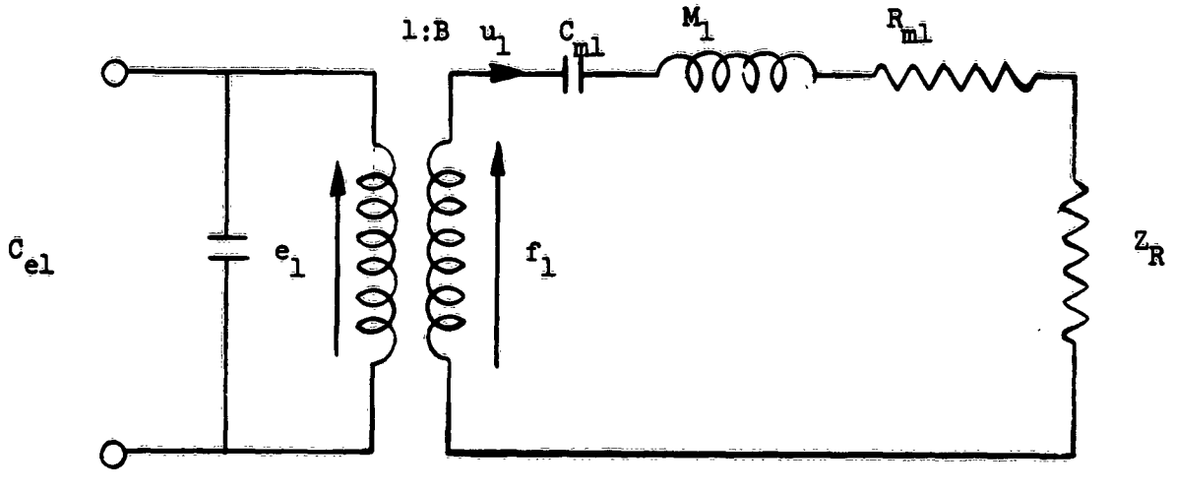

Fig. 5-2

where ω_1 is the angular frequency defined by

$$\omega_1 = \frac{1}{\sqrt{M_1 C_{m_1}}} \tag{5-5}$$

and $2\Delta\omega$ corresponds to mechanical frequency bandwidth.

The frequency bandwidth requirements (see Sec. 5.5) determine the value of the mechanical Q.

Substituting Eqs. 5-4 and 5-5 for C_{m1} and R_{m1} in Eq. 5-3, the absolute value of the mechanical impedance can be expressed by

$$\left|Z_{m1}\right| = \frac{\omega_1 M_1}{Q_{m1}} \left[1 + Q_{m1}^2 \left(\frac{\omega^2 - \omega_1^2}{\omega_1 \omega}\right)^2\right]^{\frac{1}{2}} . \tag{5-6}$$

The mechanical Q, and consequently the mechanical frequency bandwidth, can be adjusted by controlling the magnitude of the equivalent mechanical resistance R_{m1} either by mechanical or acoustic damping.

5.32 Sound Pressure

Referring to the equivalent circuits of Figs. 5-1 and 5-2, the sound pressure at the face of the transmitter is

$$P_S = \frac{Z_R}{S} u_1 \tag{5-7}$$

where u_1, the transmitter face velocity, is

$$u_1 = \frac{\beta e_1}{Z_R + Z_{m1}} . \tag{5-8}$$

Z_R and Z_{m1} are the radiation and mechanical impedances of the transmitter, respectively. If the driving frequency lies within the mechanical bandwidth of the transmitter and is near the acoustic antiresonant frequency, the radiation and mechanical impedances are given by Eqs. 5-2 and 5-6, respectively.

Since Z_R is proportional to the air density, it can be neglected in comparison to the mechanical impedance (especially at high altitudes). With the above assumptions, the sound pressure at the transmitter face is approximately

$$p_S = \frac{2 \rho_o c \beta e_i Q_{mi} Q_A}{n\omega_1 M_i \left\{ 1 + \left[2 \frac{(\omega - \omega_o)}{\omega_o} \right]^2 Q_A^2 \right\}^{\frac{1}{2}} \left\{ 1 + \left[\frac{\omega^2 - \omega_1^2}{\omega_1 \omega} \right]^2 Q_{mi}^2 \right\}^{\frac{1}{2}}} \qquad (5\text{-}9)$$

near or at the acoustic antiresonant frequency ω_o.

Within the mechanical bandwidth of the transducer, since the acoustical Q is much greater than the mechanical Q, the sound pressure is maximum at the acoustic antiresonant frequency ω_o.

From Eq. 5-9, it can be seen that the output sound pressure is directly proportional to the air density and the acoustical Q. As long as the sound energy losses are small, the value of the acoustic Q will be high. Consequently, an intense sound pressure can be obtained with this type of acoustic interferometer. Also, since the radiation impedance is mostly reactive for this case, very little acoustic power is required. For example, with the experimental model of the acoustic interferometer, sound pressure magnitudes of 3,000 dyne/cm^2 were obtained with a total power input of only .1 watts input to the transducer (Sec. II-7).

5.4 Receiver Characteristics

5.41 Receiver Sound Pressure

The sound pressure acting on the receiver face is determined by the incident and reflected sound on the receiver face. In general, the magnitude of the sound pressure is inter-related with the transmitter characteristics, the air space acting as an acoustic transmission line, and the properties of the receiver face as a reflecting surface (Sec. 4.6).

Referring to Eq. 4-44, the receiver sound pressure, p_r, near or at the acoustic antiresonant frequency, is

$$p_r = \frac{p_s}{\cosh \alpha \ell} \tag{5-10}$$

where p_s is the sound pressure generated by the transmitter (Eq. 4-9), α is the sound absorption coefficient, and ℓ is the receiver-transmitter spacing. Except for sound absorption losses, the receiver sound pressure is of the same magnitude as that generated at the transmitter face.

5.42 Receiver Output

Referring to the equivalent circuit shown in Fig. 5-1, the receiver output voltage (open circuit) is

$$e_2 = \frac{S \, X \, \beta' \, p_r}{Z_{m2}} \tag{5-11}$$

where p_r is the receiver sound pressure, Z_{m2} is the mechanical impedance of the receiver,

$$Z_{m2} = R_2 + j\left(\omega M_2 - \frac{1}{\omega c_{m2}}\right) \tag{5-12}$$

and X is the mechanical impedance of the compliance c_{m2},

$$X = \frac{1}{j \omega c_{m2}} \quad . \tag{5-13}$$

The mechanical impedance Z_{m2} can also be expressed in terms of the mechanical Q of the receiver, Q_{m2},

$$\left|Z_{m2}\right| = \frac{\omega_2 M_2}{Q_{m2}} \left\{ 1 + \left[\frac{\omega^2 - \omega_2^2}{\omega_2 \omega} \right]^2 Q_{m2}^2 \right\}^{\frac{1}{2}} \tag{5-14}$$

where ω_2 is angular frequency defined by

$$\omega_2^2 = \frac{1}{M_2 c_{m2}} \quad .$$

Substituting Eqs. 5-13 and 5-14 for X and Z_{m2} respectively, the receiver output near or at the acoustic antiresonant frequency is

$$|e_2| = \frac{S \beta' Q_{m2} P_S}{\cosh \alpha \ell \; \omega \; \omega_2 \; M \; c_{m2} \sqrt{1 + \left(\frac{\omega^2 - \omega_2^2}{\omega_2 \omega} \right)^2 Q_{m2}^2}} \quad . \qquad (5\text{-}15)$$

If the acoustical Q is much greater than the mechanical Q of the receiver and transmitter, the receiver output will be maximum at the acoustic antiresonant frequency ω_o where the transmitter sound pressure is maximum. With a high acoustical Q, a large rate of change of the receiver output occurs when the frequency approaches the acoustic antiresonant frequency.

5.43 Signal-to-Noise Ratio

The indeterminateness in correlating the maximum receiver output to the acoustic antiresonant frequency is dependent on two factors:

a) the change in receiver output as the frequency approaches the antiresonant frequency.

b) the noise present in the receiver and in the detection system.

Referring to Eq. 5-15, the change in the receiver output is dependent on the magnitude of the output voltage, the acoustical Q, and how close the frequency is to the antiresonant frequency. Neglecting the variation in the mechanical impedance of the transducers, the receiver output can be expressed by

$$e_2 = \frac{e_o}{\sqrt{1 - \left[\frac{2(f - f_o)}{f_o}\right]^2 Q_A^2}} \qquad (5\text{-}16)$$

where f is the frequency in cps, and e_o is the maximum receiver output at the acoustic antiresonant frequency, f_o. As the frequency varies slightly from f_o, the product of the variables inside the radical of Eq. 5-16 will be much less than one. Consequently, the receiver output can be expressed by expanding the radical in a power series and neglecting all terms except the first two:

$$e = e_o \left[1 - 2\left(\frac{\Delta f}{f_o}\right)^2 Q_A^2\right]$$

where $\Delta f = f - f_o$. From the above expression, if the antiresonant frequency is to be determined within a frequency bandwidth Δf for a specified acoustical Q, the required signal-to-noise ratio, SNR, is

$$\text{SNR} = \frac{e_o}{e_o - e} = \frac{1}{2Q_A^2}\left(\frac{f_o}{\Delta f}\right)^2. \qquad (5\text{-}17)$$

Referring to Eq. 1-4, the SNR can be written in terms of the corresponding error ΔT (neglecting sound dispersion and thermal effects) in determining the actual kinetic or virtual temperature T_o:

$$\text{SNR} = \frac{2}{Q_A^2}\left(\frac{T_o}{\Delta T}\right)^2 . \qquad (5\text{-}18)$$

Thus, for a specified degree of accuracy in determining the air temperature, the acoustical Q determines the required signal-to-noise ratio. For example, if air temperature is to be determined within one degree when the air temperature is 250°K, the required signal-to-noise ratio, for an acoustical Q of 25, is 200.

5.5 Transducer Frequency Bandwidth

Since the speed of sound varies with altitude, the sound frequency is varied within a frequency range periodically in order that the fixed receiver-transmitter spacing correspond to an integral number of half wavelengths. Consequently, the transducer's frequency bandwidth must be sufficiently wide in order to respond within the required frequency range.

If thermal effects are negligible, the frequency can be varied within a frequency range so as to obtain only one sound pressure maxima on the receiver face as the speed of sound varies. For this case, the frequency range is determined by the maximum variation of the speed of sound with respect to altitude. From Eq. 1-2, the speed of sound as a function of the absolute air temperature T can be expressed by

$$c = c_o \sqrt{\frac{T}{T_o}} \tag{5-19}$$

where c_o and T_o correspond to speed of sound and the temperature, respectively, at some reference altitude. From Eqs. 4-43 and 5-19, the antiresonant frequency (cps) at a temperature T is

$$f = f_o \sqrt{\frac{T}{T_o}} \ . \tag{5-20}$$

If the temperature extremes are T_o (highest) and T (lowest), the required frequency bandwidth is

$$\Delta f = f_o \left(1 - \sqrt{\frac{T}{T_o}} \right) \ . \tag{5-21}$$

Consequently, the required transducer Q is

$$Q = \frac{f_o - \frac{\Delta f}{2}}{\Delta f} = \frac{1}{2} \frac{1 + \sqrt{\frac{T}{T_o}}}{1 - \sqrt{\frac{T}{T_o}}} \ . \tag{5-21a}$$

When thermal boundary layer effects are to be measured, it is necessary to obtain two successive maxima as the frequency is varied. For this case, let f_o be the antiresonant frequency at the highest temperature T_o and speed of sound c:

$$f_o = \frac{n_o c_o}{2\ell} \tag{5-22}$$

At the speed of sound c, the next lowest antiresonant frequency f', is approximately

$$f' = \frac{(n_o - 1)}{n_o} f_o \quad .$$

At the lowest temperature T, the antiresonant frequency, f", corresponding to the same number of half wavelengths as f', is

$$f'' = \sqrt{\frac{T}{T_o}}\, f' = \left(\frac{n_o - 1}{n_o}\right)\sqrt{\frac{T}{T_o}}\, f_o \; . \tag{5-23}$$

From Eqs. 5-22 and 5-23 the required frequency bandwidth is

$$\Delta f = f_o - f'' = f_o \left[1 - \left(\frac{n_o - 1}{n_o}\right)\sqrt{\frac{T}{T_o}}\right]. \tag{5-24}$$

As shown in Sec. 5.6 it is necessary to limit the receiver-transmitter spacing if only one or two receiver maxima are to be detected.

5.6 Receiver-Transmitter Separation

As shown in the previous section, the frequency bandwidth is primarily determined by the variation of the speed of sound with respect to altitude. Consequently, it is necessary to restrict the receiver-transmitter spacing. Otherwise, since the antiresonant frequencies are determined by the number of half-wavelengths between the receiver-transmitter spacing, it is possible to obtain more than the desired number of pressure maxima at the receiver face.

If only one receiver sound pressure maximum is desired, it is necessary to adjust the receiver-transmitter separation so that the required frequency bandwidth (Eq. 5-21) is less than the frequency difference between two successive maxima. For this case, let f_o be the highest acoustic antiresonant frequency (within the required frequency bandwidth):

$$f_o = \frac{n_o c_o}{2 \ell} \quad . \tag{5-25}$$

The next lowest antiresonant frequency is

$$f' = \frac{n_o - 1}{2\ell} c_o = \frac{n_o - 1}{n_o} f_o \quad . \tag{5-26}$$

In order to eliminate one of the maxima, the frequency bandwidth, Δf, should be limited so that

$$\Delta f < f_o - f' . \tag{5-27}$$

From Eqs. 5-25 and 5-26, the number of half-wavelengths between the receiver and transmitter must then be

$$n_o < \frac{f_o}{\Delta f} \quad . \tag{5-28}$$

Substituting Eq. 5-21 for Δf,

$$n_o < \frac{1}{1 - \sqrt{\frac{T}{T_o}}} \tag{5-29}$$

where n_o is an integer.

For the case when only two receiver sound pressure maxima are desired, it is necessary to adjust the receiver-transmitter separation so that the frequency bandwidth given by Eq. 5-24 is less than the frequency difference between three successive maxima. If f_o is again the highest acoustic antiresonant frequency (Eq. 5-25), the second lowest antiresonant frequency, f", is

$$f'' = \frac{n_o - 2}{2\ell} c_o = \frac{n_o - 2}{n_o} f_o . \qquad (5\text{-}30)$$

The frequency range should be limited so that

$$\Delta f < f_o - f'' = \frac{2f_o}{n_o} . \qquad (5\text{-}31)$$

Substituting Eq. 5-24 for Δf in the above expression, and solving the resulting inequality for n_o, the number of half wavelengths at the frequency f_o has to be less than

$$n_o < \frac{2 - \sqrt{\frac{T}{T_o}}}{1 - \sqrt{\frac{T}{T_o}}} . \qquad (5\text{-}32)$$

5.7 Maximum Operating Altitude

The maximum operating altitude of the acoustic interferometer is primarily determined by the reduction of the acoustical Q resulting from viscosity losses (Sec. 4.3). Another important factor to consider is the minimum required signal-to-noise ratio for a specified degree of accuracy in determining the speed of sound or the air temperature.

5.71 Acoustical Q - High Altitudes

At high altitudes, the acoustical Q is mainly determined by the loss of acoustic energy resulting from viscosity effects. From Eqs. 4-14, 4-13a, and 4-63, it can be seen that the quality factor due to viscosity losses, Q_α, is proportional to the product of the air density and inversely proportional to the angular sound frequency:

$$Q = \frac{3\rho c^2}{4\omega\eta} . \qquad (5\text{-}34)$$

Consequently, the quality factor Q_α at high altitudes is a small number, and the overall acoustical Q (Eq. 4-56) is approximately Q_α:

$$Q_A \cong Q_\alpha . \tag{5-35}$$

In order to correlate the the acoustic antiresonant frequency with the maximum receiver sound pressure, or the maximum receiver output, the minimum acoustical Q cannot be less than twice the transducers' Q. From Eq. 5-21a, if thermal boundary layer effects are neglected, the minimum acoustic Q is therefore,

$$Q_A = \frac{1 + \sqrt{\frac{T}{T_o}}}{1 - \sqrt{\frac{T}{T_o}}} , \tag{5-36}$$

where T_o and T are the air temperature extremes to be measured.

5.72 Signal-to-Noise Ratio

The second factor to consider is the required signal-to-noise ratio for a specified degree of accuracy in the measurement of the phase velocity of sound or the air temperature. If the phase velocity of sound is to be determined within a range Δc or the air temperature to within ΔT degrees (neglecting sound dispersion), the minimum signal-to-noise ratio, SNR, is given by Eq. 5-18,

$$SNR = \frac{2}{Q_A^2} \left(\frac{T_o}{\Delta T} \right)^2 . \tag{5-18}$$

Consequently at high altitudes, for a specified degree of accuracy in determining the speed of sound or the air temperature, the required SNR is increased due to the reduction of acoustical Q.

As shown in Sec. 5.4, the maximum receiver sound pressure at the acoustic antiresonant frequency is proportional to the product of the air density and

the acoustical Q. From Eq. 5-34 it follows that at high altitudes, the sound pressure will vary proportionally to the square of the air density. If the input to the transmitter remains constant, the sound pressure P at any altitude can be written in terms of the sea level sound pressure P_o, the acoustical Q, Q_o, and the air density ρ_o:

$$P = P_o \left(\frac{\rho}{\rho_o}\right)\left(\frac{Q}{Q_o}\right) \qquad (5\text{-}37)$$

where ρ and Q correspond to the air density and the acoustical Q at the particular altitude where the sound pressure is P.

Following the discussion of Sec. 3.13, the acoustical noise at high altitudes can be neglected as long as the air flow past the transducer faces is laminar. Consequently, only the electrical noise arising in the receiver or detecting system has to be considered.

5.73 Example

As an example in calculating the highest operating range with the acoustic interferometer, assume that the Arcas meteorological missile is utilized. To minimize viscosity effects, the lowest possible frequency is to be used. However, due to space considerations, a nominal operating frequency of 9000 cps is assumed. Referring to Eq. 5-21a, and assuming that the acoustic interferometer is to measure air temperatures ranging from 300°K to 190°K, the required transducer Q is approximately 5.

Consequently, the minimum acoustical Q is twice the above value:

$$Q_A = 10$$

at high altitudes, the quality factor Q_α will primarily determine the Q of the standing wave.

Referring to Eq. 5-34 and to the values of the international reference atmosphere[7], the altitude corresponding to a quality factor Q_α of 10 is approximately 65 Km. This is theoretically the highest altitude possible assuming the above conditions.

In order to obtain an idea on the order of magnitude of the receiver sound pressure and the signal-to-noise ratio at this maximum altitude, assume that the receiver sound pressure and the acoustical Q at sea level is

$$P_o = 3000 \text{ dynes}$$

$$Q_o = 50$$

which are realizable values obtained experimentally (Sec. II-7).

From Eq. 5-37, the sound pressure at the maximum altitude of 65 Km would be 0.07 dynes/cm^2. At this altitude, the air temperature is approximately 234°K. If the air temperature is to be measured within 2°K (assuming sound dispersion corrections), the minimum signal-to-noise ratio, from Eq. 5-18 is

$$\text{SNR} = 275 .$$

Since the sound pressure is 0.07 dynes/cm^2, there is no problem in obtaining the above signal-to-noise ratio if the air flow past the transducer faces is laminar.

LITERATURE CITED

1. Schlichting, H. Boundary Layer Theory. 9th Ed. McGraw-Hill, 1960, p. 107.

2. Hunt, H. V. "Propagation of Sound in Fluids." American Institute of Physics Handbook, D. E. Grey, Coord Ed. New York: McGraw-Hill, 1957.

3. Roberts, R. C. "Compressible Flow of Gases." American Institute of Physics Handbook, D. E. Grey, Coord ed. New York: McGraw-Hill, 1957.

4. Berenk, L. L. Acoustics. New York: McGraw-Hill, 1954, Chapter 3.

5. Johnson, W. C. Transmission Lines and Networks. New York: McGraw-Hill, 1950, Chapter 11.

6. Kinsler, L. E. Fundamentals of Acoustics, New York: John Wiley and Sons, Inc., 1950.

7. CIRA 1961. (Cospar International Reference Atmosphere) New York: Interscience Publishers, Inc.

DETERMINATION OF ATMOSPHERIC PARAMETERS
BY ACOUSTIC MEANS

DA-SIG-36-039-62-G17

Progress Report No. 1

July, 1962

Section II:

DESIGN AND DEVELOPMENT OF ACOUSTIC DEVICES

-7-

Preliminary Design and Development of the Sonotherm Flight Unit

Paul Dano, Physicist

S C H E L L E N G E R R E S E A R C H L A B O R A T O R I E S

Texas Western College El Paso, Texas

Table of Contents

1. Introduction

In the design and development of the preliminary circuitry for the Sonotherm (Sec II-6) two objectives were combined: (a) the construction of a prototype flight unit, and (b) a testing system. Therefore, certain compromises such as that between simplicity of circuitry for flight unit application and versatility for laboratory and environmental testing were necessary in order to accomplish both objectives.

The primary elements of the Sonotherm device are the transducers. Once suitable transducers were found, the necessary circuitry was developed and adapted for environmental testing.

2. General Description

The proposed Sonotherm flight unit (see Sec II-6) is basically an airborne acoustic interferometer for performing acoustic measurements in the upper atmosphere. In operation, the flight unit performs the following functions: an acoustic standing wave is generated between a sound source (transmitter) and a microphone (receiver) separated by a fixed distance. The sound frequency is varied periodically between two prescribed frequency limits, and the receiver sound pressure is detected as a function of frequency. The receiver output is then telemetered to a ground station. A frequency measurement corresponding to the maximum receiver output yields information on the phase velocity of sound; sound absorption and other acoustic losses can be determined by a frequency bandwidth measurement; and an amplitude measurement can be related to the air density.

BLOCK DIAGRAM: SONOTHERM SYSTEM

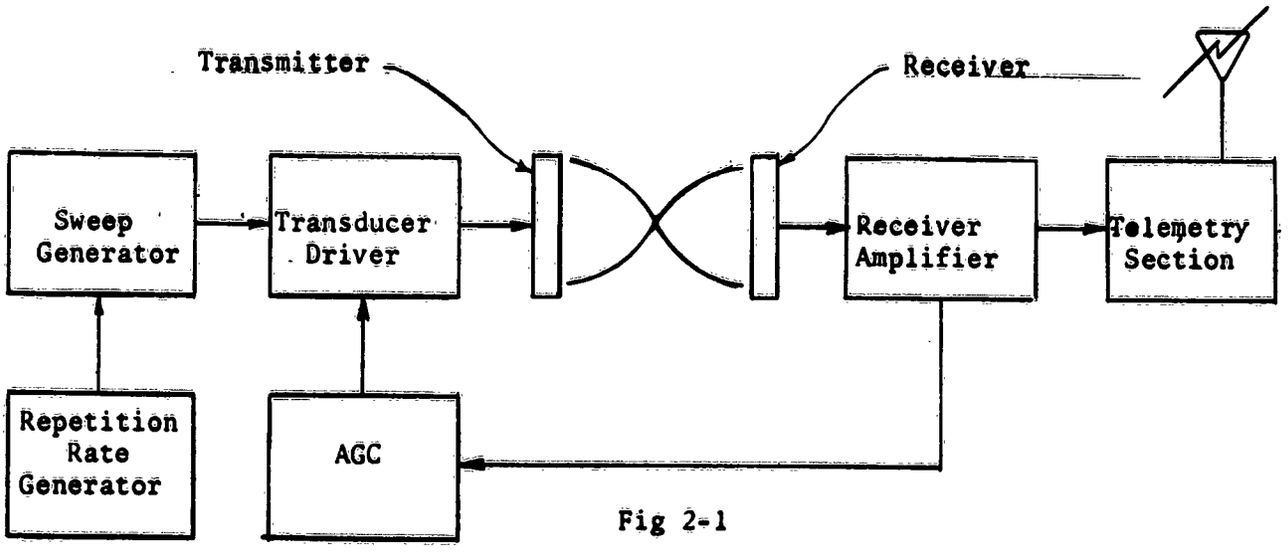

Fig 2-1

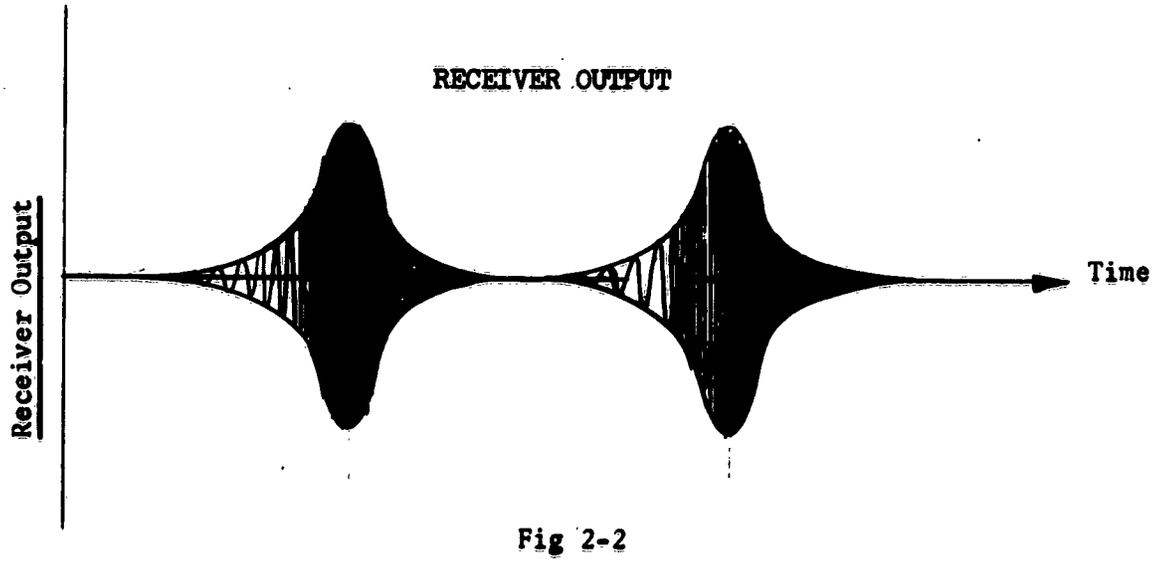

Fig 2-2

A block diagram of the flight unit is shown in Figure 2-1. Two piston-type sound transducers are positioned with their vibrating faces parallel, facing each other, and separated by a fixed distance. The transmitter-transducer generates a plane wave which is reflected at the face of the receiver-transducer. Interference between the transmitted and reflected sound waves results in a standing wave in the air medium between the transducer's faces.

Ideally, at the acoustic antiresonant frequency where the receiver-transmitter spacing corresponds to an integral number of half wavelengths, the receiver sound pressure and the receiver output is maximum. Consequently, the speed of sound can be determined by a measurement of the frequency corresponding to the maximum receiver output. The kinetic or virtual temperature can then be determined since it is a function of the speed of sound (Sec II-6).

Since the receiver-transmitter spacing is fixed and the speed of sound varies, a sweep generator (Fig. 2-1) scans the sound frequency, periodically, within a specified frequency range. During each period of frequency scanning, the receiver-transmitter spacing corresponds to the same integral number of half wavelengths at a particular frequency depending on the magnitude of the speed of sound. The repetition rate generator controls the frequency and the sampling rate of the sweep generator, and drives the transmitter-transducer.

The sound pressure acting on the receiver face is detected by the receiver-transducer and its output voltage consists of a frequency and amplitude modulated waveform as shown in Figure 2-2. The receiver-trans-

ducer output is then amplified by the receiver amplifier, and the amplified signal is applied to the telemetry section where the signal is transmitted to a ground station. An automatic gain control, located between the receiver and the transmitter driver, compensates for the amplitude variation of the sound pressure with respect to altitude.

The receiver-transducer signal is recovered at the ground station. Correlation of the signal amplitude with respect to frequency is accomplished by the Ground Detection System (Sec II-8).

At the present time, since environmental t ting has been emphasized, the telemetry system and the AGC control have not been designed. However, a standard Rawin Set AN/GMD-1 easily meets the telemetry system requirements with little or no modification.

The various elements of the flight unit will now be considered in detail.

3. The Transducers

The sound transducers are the primary elements of the Sonotherm flight unit. Various requirements had to be met by the sound transducers in order to be applicable for use with the Sonotherm device. In order to save time, commercially available sound transducers were utilized.

3.1 - General Requirements

The main requirements of the sound transducers were (see Sec II-6, pt. 5.2):

a) the sound transducers had to be of the piston-type with highly

directional characteristics and good sound reflecting properties.

b) the frequency bandwidth had to be sufficiently wide in order to cover the variation of the speed of sound with respect to altitude.

c) the operating frequency had to be sufficiently low (below 30 KC) in order to minimize sound dispersion effects (Sec I-2).

d) the sound intensity and receiver sensitivity had to be such that a good signal-to-noise ratio was maintained at high altitudes.

e) the sound transducers had to be as light and as compact as possible.

Highly directional characteristics were obtained by using transducers whose vibrating face dimensions were at least 2 wavelengths of sound, and by placing the receiver in the near field of the transmitter. For maximum efficiency at low frequencies, and since the receiver-transmitter spacing had to be well defined, it was decided to utilize transducers with a clamped vibrating flat plate or a stretched diaphragm which could be driven near its resonant frequency by electrostatic or magnetostrictive means.

Various types of commercial sound transducers were tested, such as small electromagnetic compression tweeters and crystal-type transducers. Most of these devices were rejected primarily because they either lacked a sufficient frequency bandwidth or were inefficient in generating an intense acoustic standing wave. Finally, the MASSA TR-21 sound transducer was selected because it met most of the desired characteristics and was was commercially available.

3.2 - TR-21 Transducer

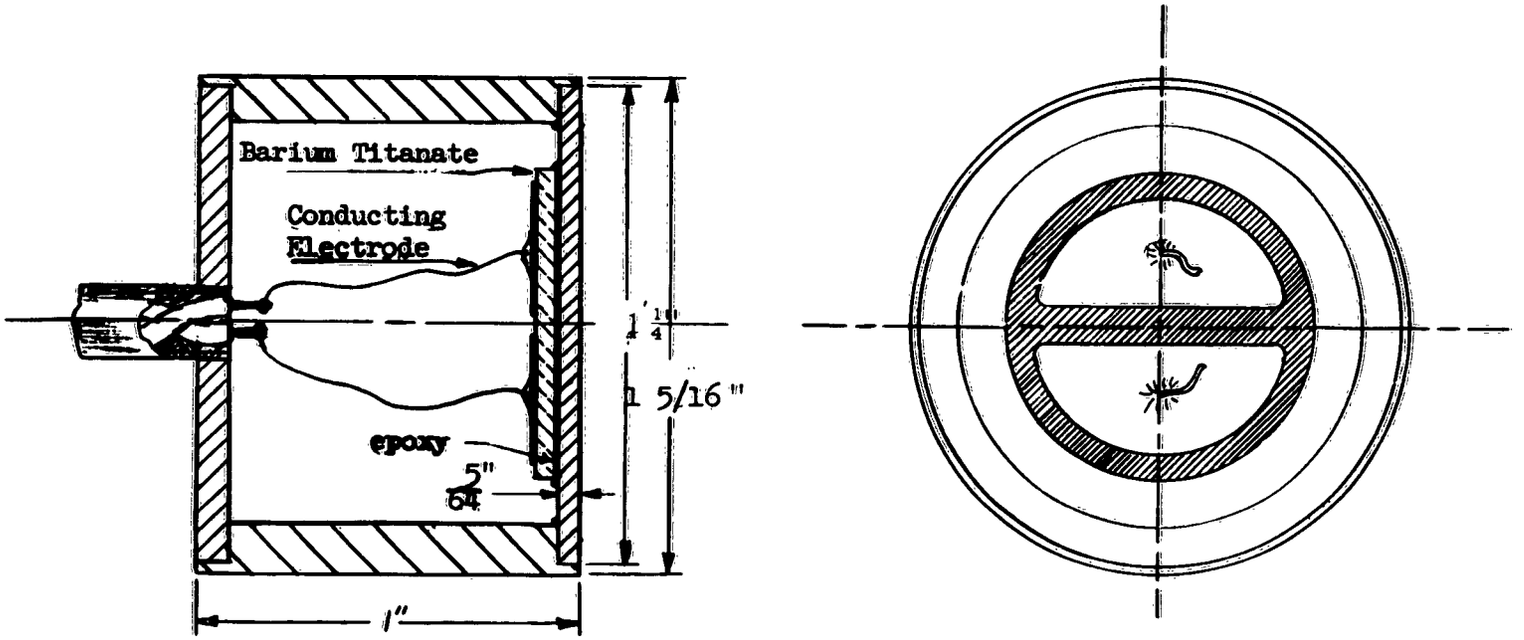

MASSA TR-21 SOUND TRANSDUCER

Fig 3-1

The MASSA TR-21 (Fig. 3-1) sound transducer is basically a clamped vibrating plate resonating at 23 KC and driven by piezoelectric means. The vibrating clamped plate is a flat aluminum circular disk 5/16" thick. Coated on the back side of the clamped plate is a barium titanate ceramic. Two semicircles of conductor material are bonded atop the barium titanate, to which the lead-ins are connected.

The electrical signal, via the characteristics of the barium titanate, causes the front plate to warp. Maximum efficiency is obtained at the fundamental resonant frequency, 23 KC, of the composite aluminum and barium titanate plate. The face diameter is slightly over 3 centimeters, which is approximately twice the wavelength of the resonant frequency of the transducer, 23 kilocycles.

Transmitting Characteristics

The TR-21's far field Transmitting Sensitivity is +34db (ref one microbar) at 1 ft. (100 milliwatts available power), and its beam width is 70^{o} where the sound intensity of the major lobe reduces by 1/2 of its axial intensity.

Receiving Characteristics

The sensitivity of the transducer as a receiver is -60 db (23 KC) (reference 1 volt per microbar) when untuned, with a bandwidth of 200 cycles. The bandwidth can be greatly increased (up to about 2350 cycles) by electrical tuning with a shunt or series low Q coil.

Electrical Characteristics

An approximate electrical equivalent circuit of the transducer is shown in Figure 3-2. Except at its resonant points, the TR-21 transducer appears as a capacitive impedance of approximately 8000 ohms.

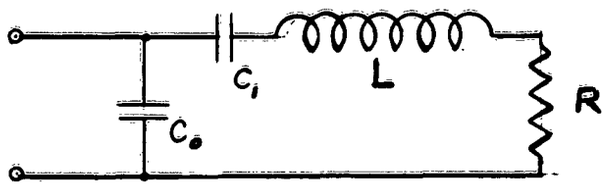

Figure 3-2

C_o is the clamped capacitance of the transducer, approximately 880 picofarads, and C_1 L, and R are the electrical equivalent elements of the mechanical characteristics.

Two resonant points occur; one is the parallel resonance of C_o, C_1 and L and the second resonance is the series resonance of C_1 and L.

Except at these resonance points, the impedance of the transducer is absolutely constant.

4. Electronic Circuitry

The flight unit circuitry (Fig. 2-1) was developed as its need appeared and initially was of bread-board construction. As refinement of the circuitry was developed, the circuitry was consolidated, as much as possible, into a unit. At present, the circuitry is not in a form for actual flight, but the basic construction and functional problems have been

solved.

4.1 - The Sweep Frequency Generator

Of primary importance was an oscillator which could sweep through a set of frequencies at a given rate. The frequency modulation of such a low set of frequencies proved to be difficult. Several types of oscillators were tried but with the same results: the amplitude of the output would vary with frequency or the frequency range was too limited. After several failures to get the desired results, it was decided that a biased multivibrator would be used with the bias controlled by a repetition rate generator.

Referring to Fig. 4-1, the sweep generator is a straight forward biased multivibrator V-5 working into a cathode follower V-4b, for matching the high output impedance of the multivibrator to the low input impedance of the RC integrating network which was used to eliminate some of the harmonics of the square wave output of the multivibrator. The output of the integrator is applied to a cathode follower V-6a to match the output of the integrator to the input of a harmonic filter. This filter was designed to pass the fundamental, but to reject all harmonics. The signal is then passed through a cathode follower, V-6b, to the input terminals of the transducer driver.

4.2 - The Repetition Rate Generator

The repetition rate generator is a multivibrator operating at 10 cps (Fig. 4-1). The output signal is fed into an amplifier, V-2a, which is driven from cutoff to saturation in order to produce a better square wave. The signal is then integrated, added to the original square wave signal through a differential amplifier, V-3, then fed into a clipping amplifier, V-2b, and

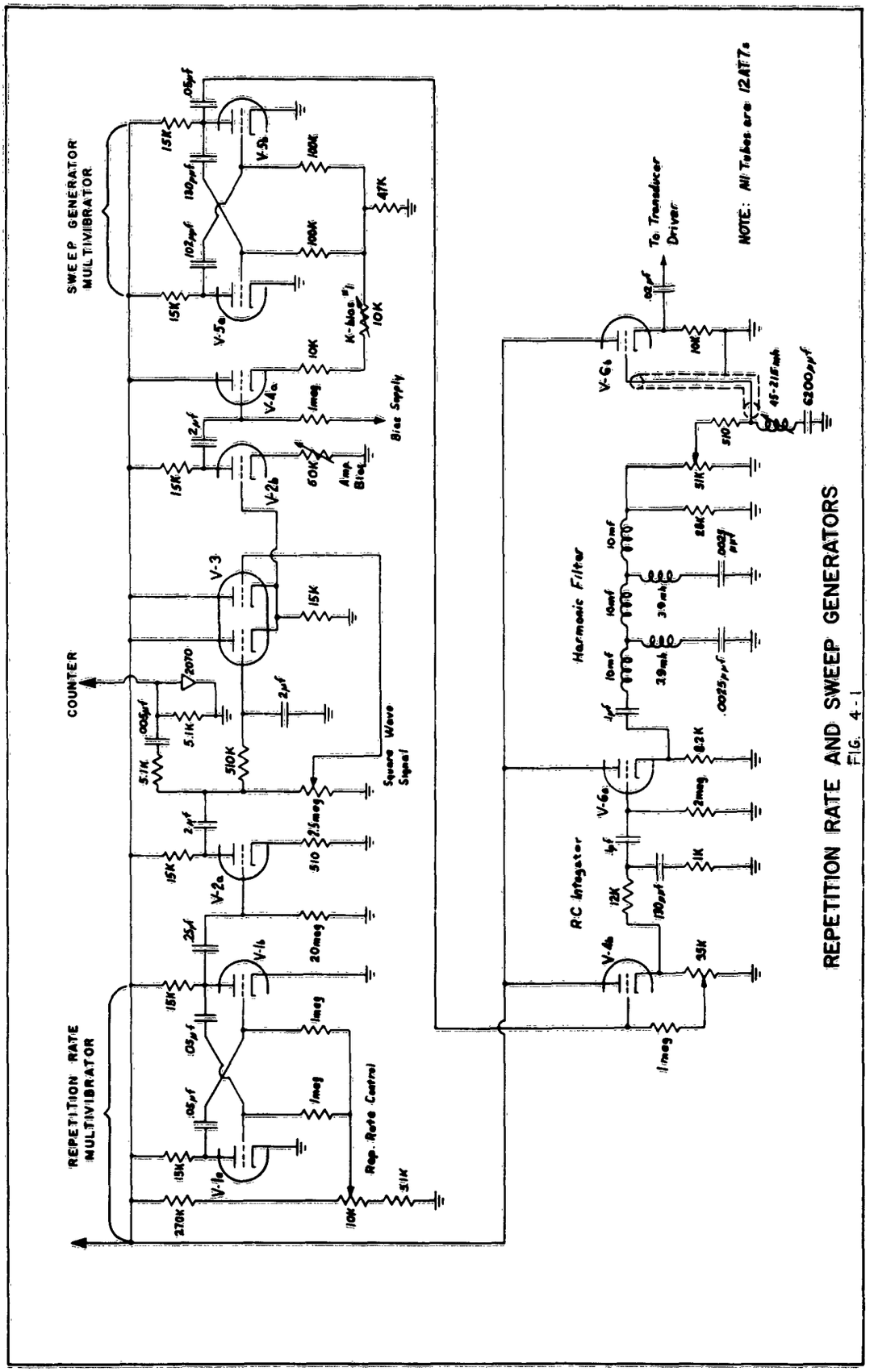

REPETITION RATE AND SWEEP GENERATORS

FIG. 4-1

on to a cathode follower, V-4a, which controls the multivibrator bias. The resultant waveform is a signal which rises linearly for 100 milliseconds then drops sharply to the base and stays at the base for 100 milliseconds. This gives five sweeps a second at the ten cycles per second repetition rate, leaving a 100 millisecond time interval between each sweep for possible telemetry of other information.

4.3 - Transducer Driver

Tests were conducted to determine the parameters of the circuit components necessary for properly driving the TR-21. It was found that a low impedance generator operated the best at the frequencies finally used in the chamber tests, and a commercial amplifier was used.

In order to increase the transducer's frequency bandwidth, the driver signal was reduced at and near the transducer's resonant frequency by a series tuned circuit, which was added to the grid of the output stage V-6b. This attenuated the resonant frequency driving signal 9 db and reduced the peak signal at resonance, thereby increasing the bandwidth.

Before tests could be conducted in the climate chamber, the effect of the long lead-in chamber lines on the operation of the transducers was determined in order to minimize the effect on the transducer response.

4.4 - Receiver Amplifier

The receiver amplifier (Fig. 4-2) amplifies and converts the balanced output of the TR-21 receiver to a single-ended output for monitoring purposes. The TR-21 receiver output was balanced in order to reduce stray electrostatic pick-up while operating in the vicinity of the TR-21 transmitter.

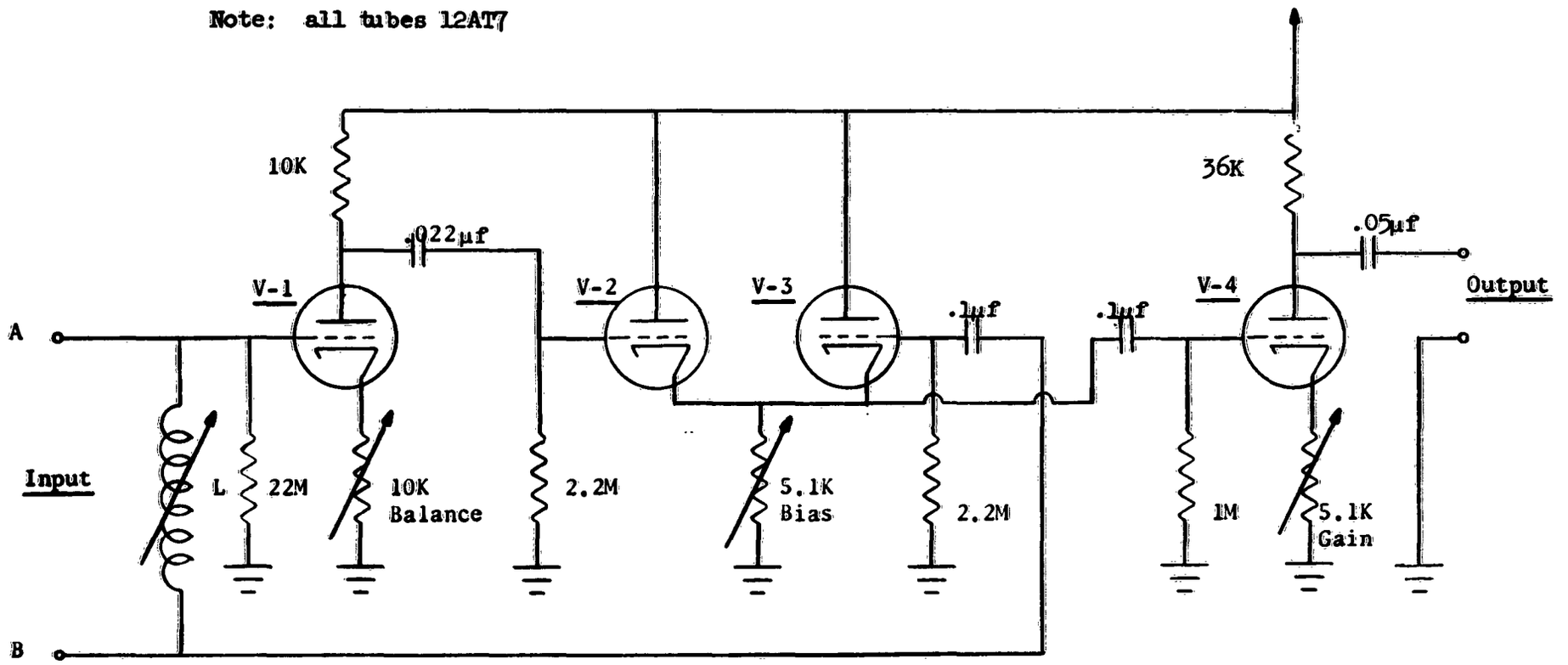

RECEIVER AMPLIFIER

Fig. 4-2

Referring to Fig. 4-2, one side of the balanced signal is fed into a phase inverter, V-1; the two balanced signals are then added by differential amplifiers consisting of V-2 and V-3. The output of the differential amplifier is then amplified by the triode V-4 where the signal is detected. The inductance L electrically tunes the receiver-transducer in order to obtain a broader frequency bandwidth.

5. Characteristics

The dynamic characteristics of the prototype flight unit were determined by laboratory and environmental tests (conducted in a climate chamber available at Schellenger Research Laboratories). The various tests included:

(a) Variation of the acoustic antiresonant frequency with respect to air temperature or speed of sound.

(b) sound pressure variation with respect to altitude.

(c) measurement of the Q of the acoustic standing waves.

(d) thermal, wind, and density effects on the accuracy and operation of the acoustic interferometer.

The results of part (d) are described in detail in Sec III-10. A description of the test procedure is given in part 7 of this report.

5.1 - Temperature-Measurement

Various tests were performed in the climate chamber in order to determine the variation of the acoustic antiresonant frequency with respect to altitude. Figure 5-1 shows the theoretical and expected variation of the acoustic antiresonant frequency (corresponding to the maximum amplitude of

Fig. 5-1
FREQUENCY VS TEMPERATURE

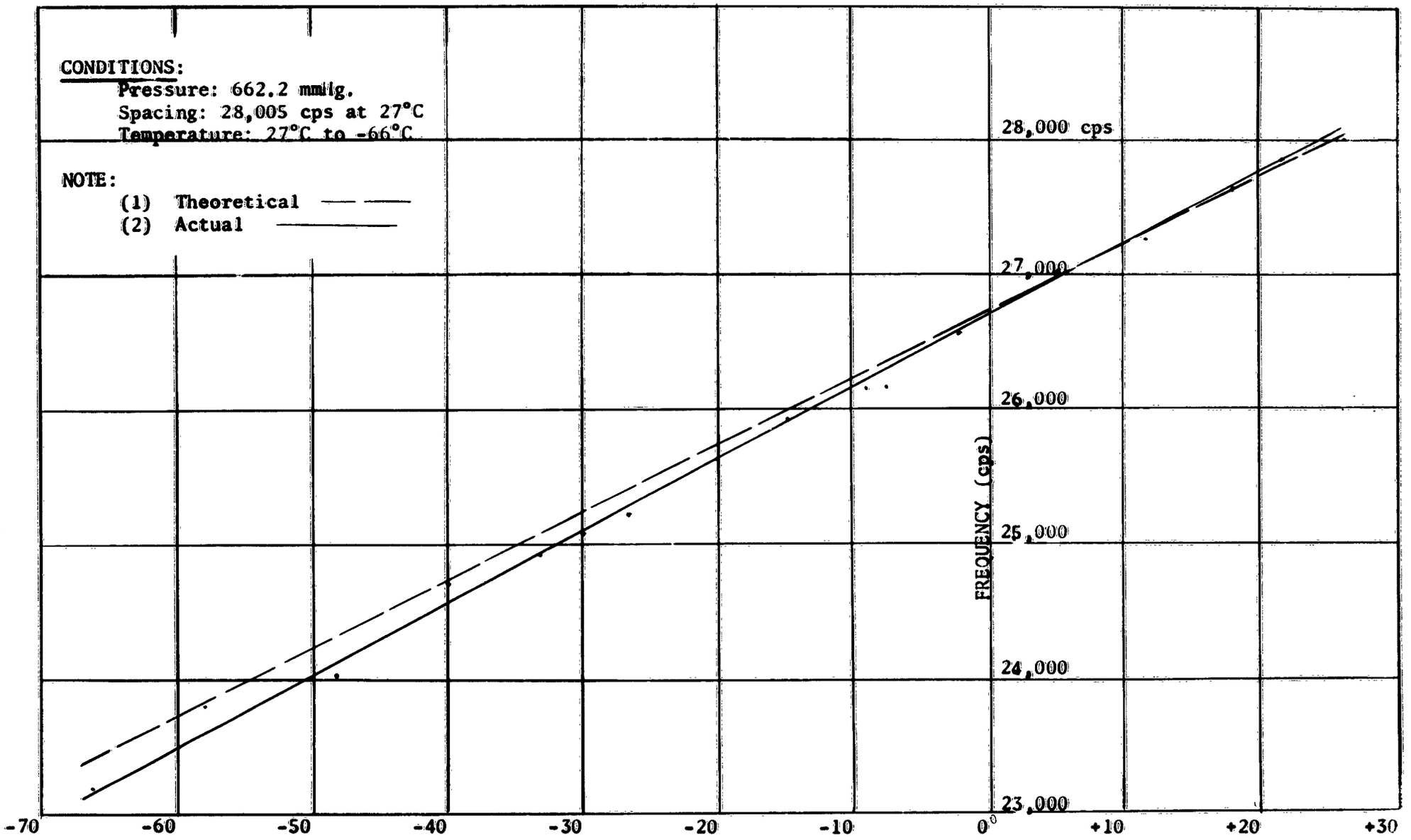

of the receiver sound pressure) plotted as a function of air temperature. For this case, the atmospheric pressure was held constant and the air temperature was varied. Thermal effects were eliminated by keeping the transducer faces in equilibrium with the air temperature.

The discrepancy between the theoretical and actual frequency variation with respect to the air temperature was found to be related to the contraction of the transducer mounting holding the transducers.

5.2 - Sound Pressure

Intense sound pressures of the order of 3000 dynes/cm^2 (100 mw/ input power, room pressure) were generated at the receiver-transducer when the acoustic antiresonant frequency was within the mechanical bandwidth of the transducers. However, with proper tuning of the transmitter and receiver transducers, an operating frequency range of only 1500 cps, about the mechanical resonance of the transducers, was obtained (Fig. 5-3). Since a wider operating frequency range was desirable (6000 cps) in order to cover the extreme variation of air temperature with respect to altitude, it was decided to operate above the mechanical resonant frequency of the transducers.

Figure 5-2 shows the receiver sound pressure plotted as a function of the acoustic antiresonant frequency (room pressure temperature). The receiver-transmitter spacing was adjusted so that the receiver-transmitter spacing corresponded to 3/2 wavelengths at each frequency. Presently, the frequency range of 25 KC to 31 KC is used since a nearly constant sound pressure of 400 dynes/cm^2 is obtained (room pressure) at the frequency

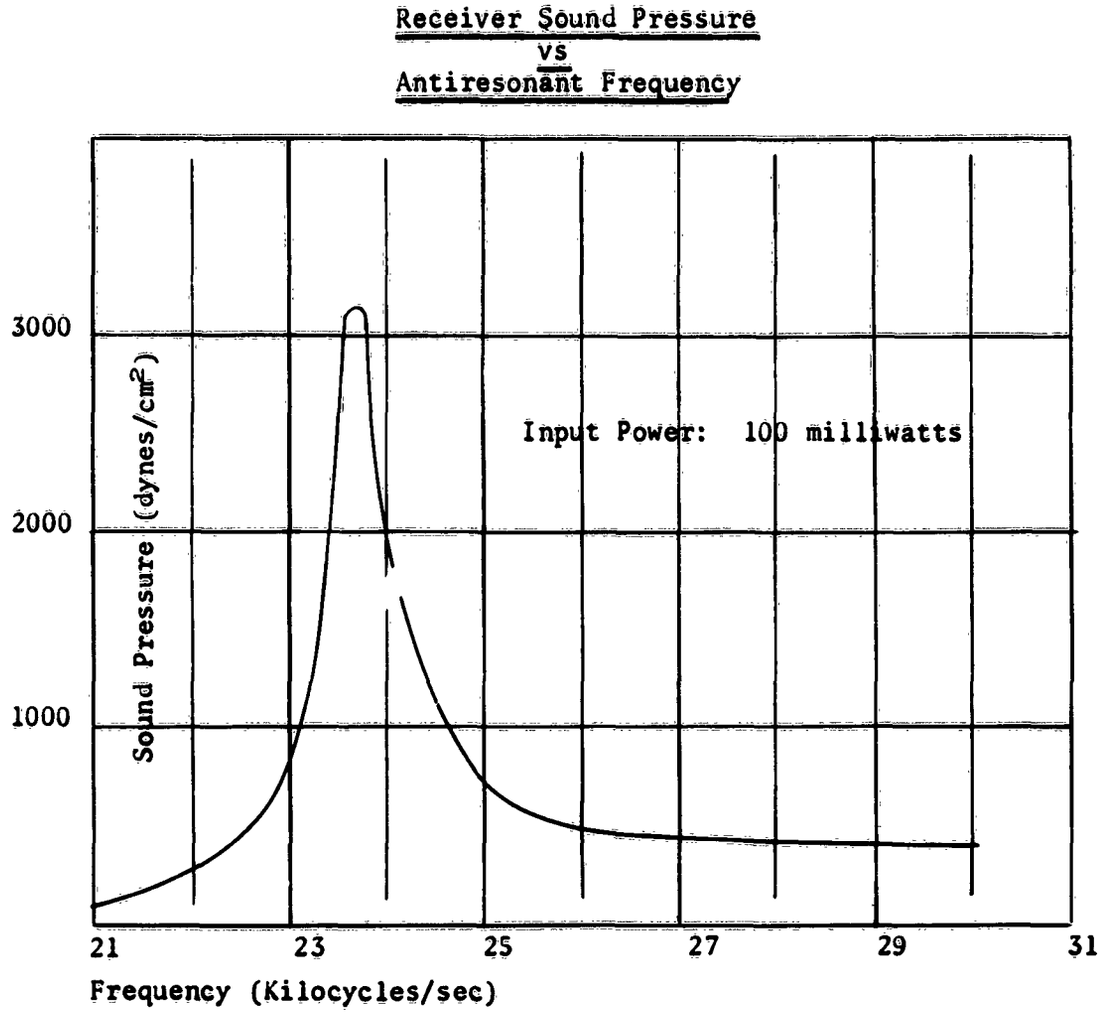
Receiver Sound Pressure
vs
Antiresonant Frequency
3000
2000
1000
Sound Pressure (dynes/cm²)
Input Power: 100 milliwatts
21
23
25
27
29
31
Frequency (Kilocycles/sec)

Fig. 5-2

where the receiver-transmitter spacing corresponds to 3/2 wavelengths.

The sound pressure decreases with altitude as shown experimentally in Fig. 3-1, sec. III-10. This reduction in sound pressure is primarily due to the fact that it is proportional to the air density and the Q of the acoustic standing wave (Sec II-6, Pt. 5.4).

5.3 Acoustical Q

The accuracy of the speed of sound measurement is dependent on the magnitude of the Q of the acoustic standing wave since the frequency corresponding to the maximum receiver output has to be determined. The acoustical Q is a function of the acoustic losses in the receiver-transmitter air region, the transducer geometry, and the transducer face rigidity (Sec II-6, pt. 4.9).

Figure 5-3 shows the relative receiver output (room pressure and temperature) plotted as a function of frequency for the case when an acoustic standing wave is generated between the TR-21 sound transducers. The dashed line corresponds to the combined electrical and mechanical frequency response of the receiver and transmitter. The receiver-transmitter spacing was adjusted at 3/2 wavelengths corresponding to 23.25, 24 and 24.75 kilocycles. At the various frequencies where the receiver-transmitter separation corresponded to 3/2 wavelengths, the receiver sound pressure and the receiver output were maximum. The acoustical Q ranged from approximately 77 to 135. For this case, the acoustical Q was primarily a function of the transducer geometry and rigidity since other acoustical losses were small. At high altitudes the acoustical Q reduces due to sound absorption resulting mainly from

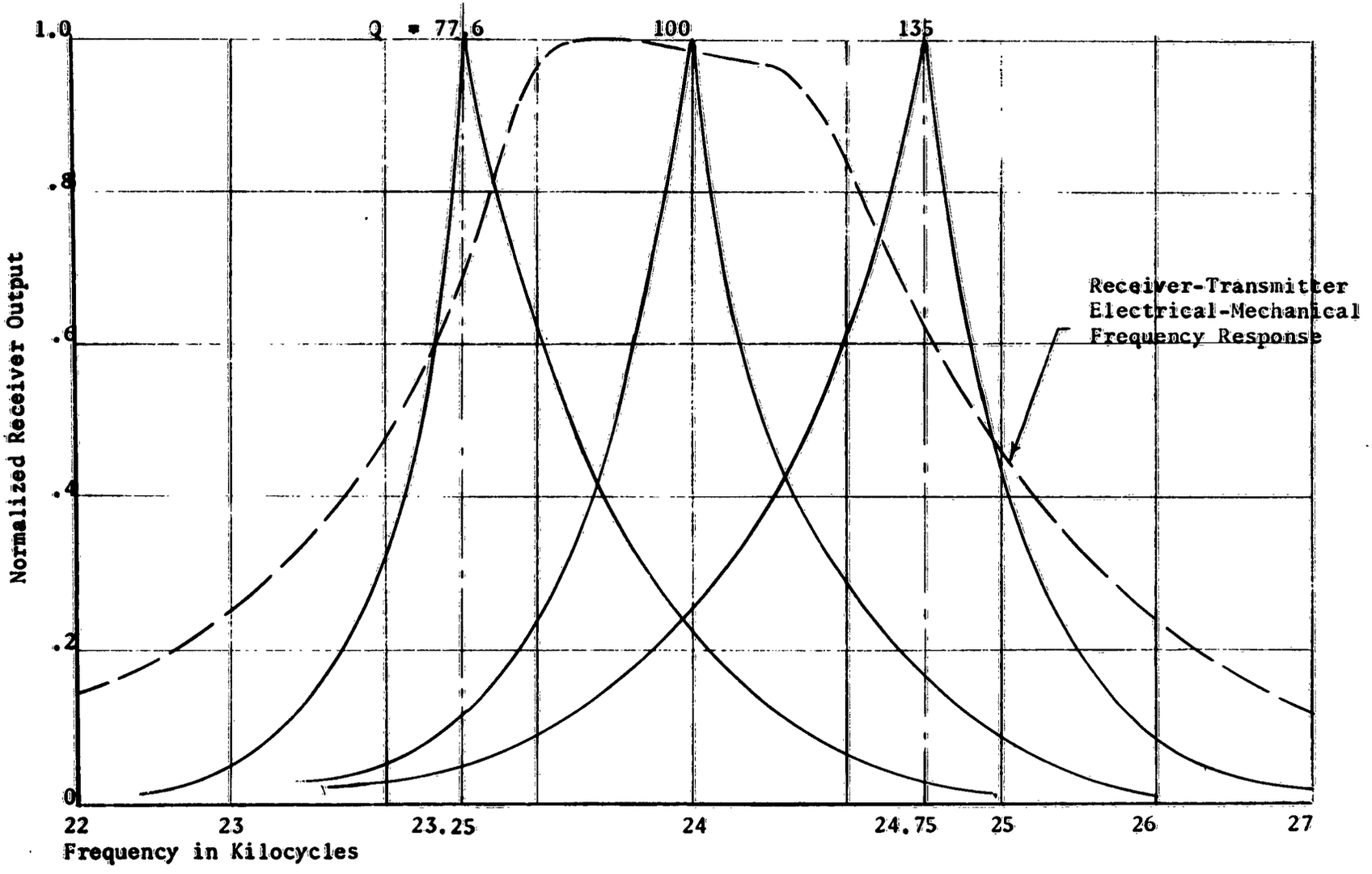

ACOUSTIC FREQUENCY RESPONSE

Fig. 5-3

viscosity effects (Sec II-6, pt. 4.9; and sec III-10, pt. 3.2).

5.4 Accuracy

As was indicated previously in section I-5 and II-6, the accuracy of the speed of sound measurements is primarily determined by the temperature difference or lag between the air and the transducer faces. If such a temperature difference exists, the stagnant layer of air adjacent to the transducers (caused by the effect of air viscosity) tends to be heated or cooled. As a result, the speed of sound measurements will be in error.

Simulated balloon flights of Sonotherm flight unit, performed in the climate chamber, (Sec III-10, pt. 4) indicated that the above thermal effect could result in errors up to 5°C in the determination of the air temperature. However, proper corrections are possible if the temperature of the transducer faces are known (Sec II-6, pt. 3.4).

At altitudes of over 150,000 feet, another source of error is related to the dispersion of sound due primarily to viscous effects on the propagation of sound (Sec I-2).

5.5 Range

The results from the environmental tests indicate that speed of sound measurements are possible up at least 150,000 feet. The maximum operating altitude is determined by the receiver sensitivity, the decrease in the acoustical Q due to sound absorption, the reduction of sound pressure with air density and acoustical Q, and by the desired accuracy of the speed of sound measurement (See Sec II-6, pt. 5.7).

6. Testing Program

The Sonotherm flight unit was tested in the climate chamber under the various environmental conditions expected in the upper atmosphere. Various environmental tests were conducted where the sound transducers were subjected to the varying environmental conditions as would be encountered by the flight unit when ascending to the upper atmosphere on a balloon. The experimental results are summarized in Section III-10.

6.1 Testing Procedure

A block diagram of the testing apparatus is shown in Fig. 6-1. Only the sound transducers, on an adjustable rack were placed inside the environmental chamber. This was necessary since it was desirable to subject the sound transducers to known conditions in order to determine their characteristics without the influence of circuitry performance resulting from environmental changes.

After the initial spacing of the transducers was set, the chamber sealed, and the desired environmental conditions attained, the output of the flight unit receiver was observed on channel A of an oscilloscope which was synchronized by the repetition rate signal supplied by the flight unit circuitry. The signal from the sweep generator was applied to the transducer driver and to a simulator whose output was observed on channel B of the oscilloscope. The simulator is a high Q variable bandpass amplifier and provides an adjustable narrow bandpass at a selected frequency within the operating frequency range of the Sonotherm device. The center frequency of the simulator was then adjusted until the simulator's maximum output coincided with the acoustic peak signal. The

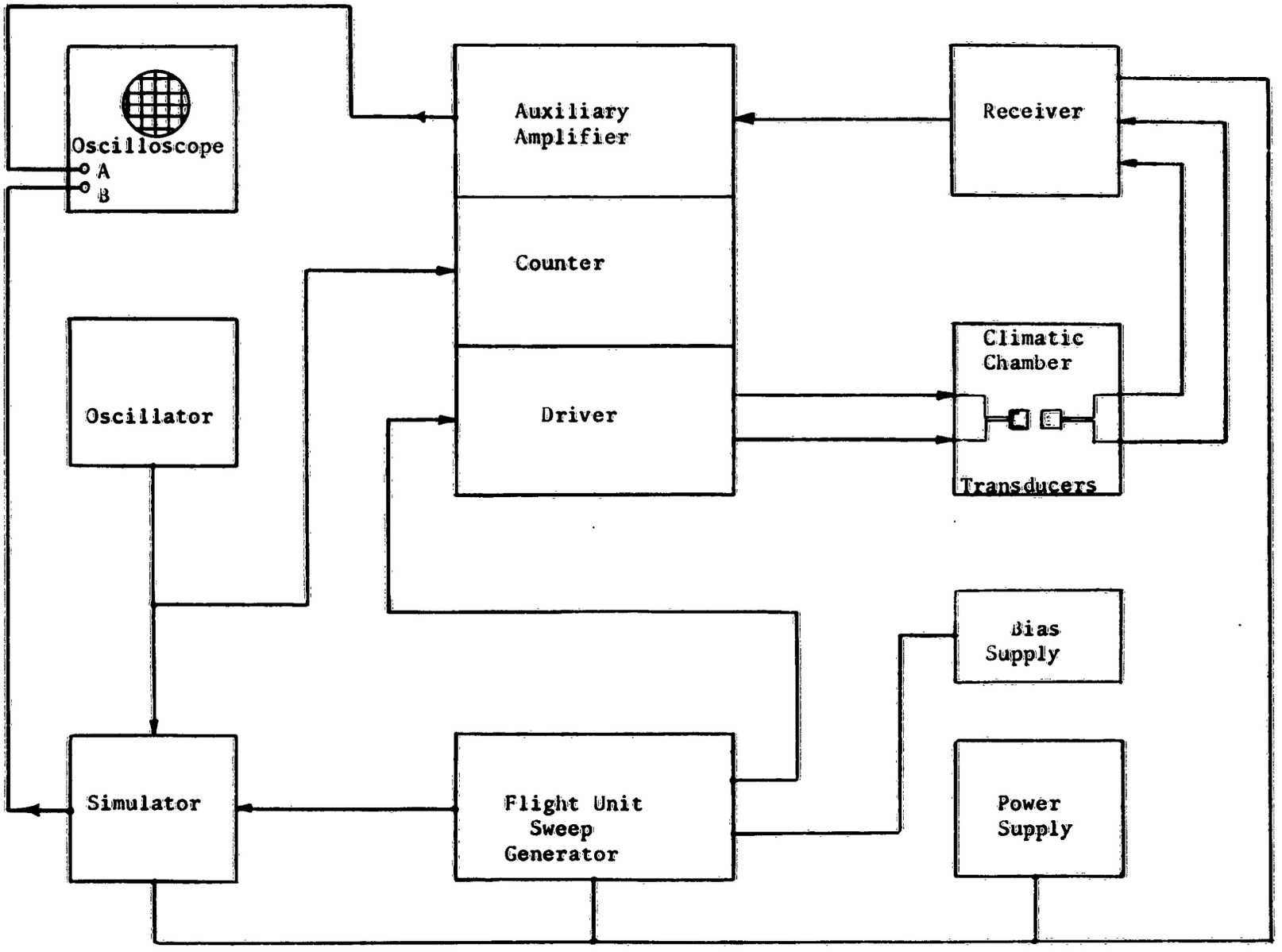

Fig. 6-1
SONOTHERM FLIGHT UNIT

TEST SETUP

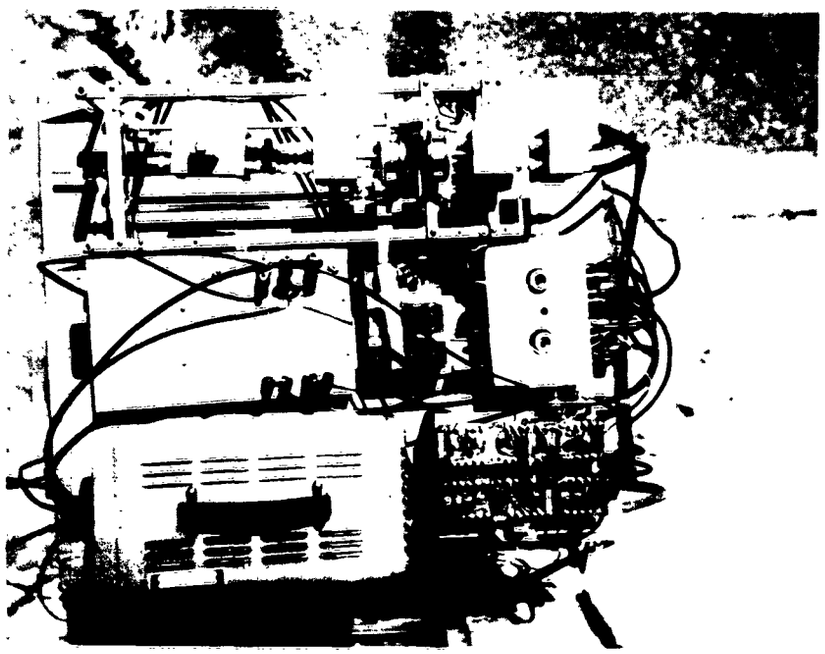

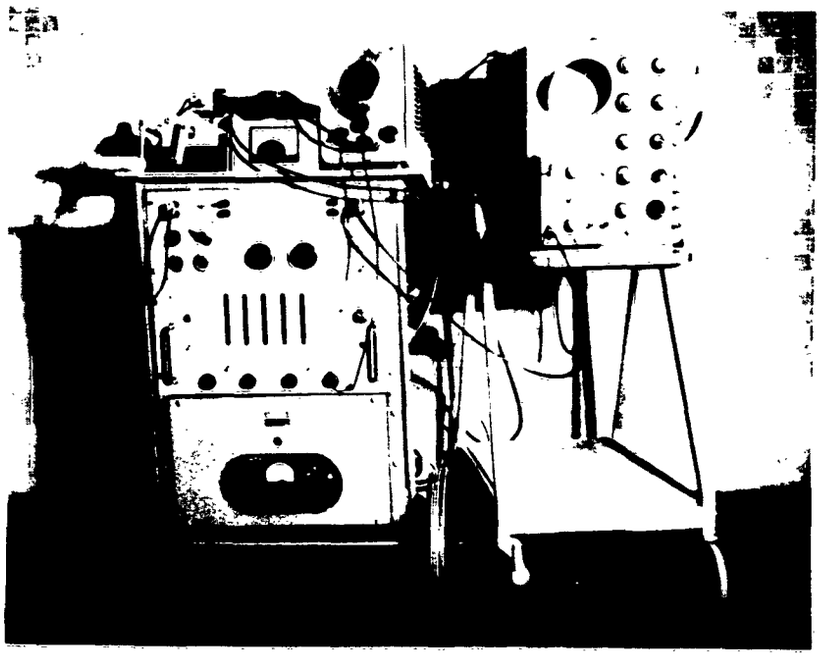

Experimental Sonotherm Flight Unit
and
Associated Test Equipment

input to the simulator was then switched over to the standard oscillator signal. The frequency of the oscillator was adjusted for a maximum output of the simulator and the frequency read directly by a frequency counter. In this manner, the frequency corresponding to the maximum of the receiver-transducer output was determined. The accuracy of the above method of reading the frequency of the acoustic peak signal was within the accuracy of the thermocouple temperature readings.

The complete test flight unit was consolidated on a mobile rack along with its associated test equipment and power supplies (Fig. 6-2).

7. Conclusion

The experimental results obtained with the experimental Sonotherm flight unit, together with theoretical evidence, indicates that speed of sound and other acoustic measurements by such a device can be accomplished in the upper atmosphere up to altitudes of at least 150,000 feet. The present system can be improved by utilizing sound transducers with a wider frequency bandwidth, reducing the heat capacity of the transducers in order to reduce the error due to thermal lag of the transducer faces with respect to the air temperature (sec III-10, pt. 4), and improving the transducer mounting in order to eliminate errors due to thermal contraction.

Since close spacing between compact sound transducers and simple, non-critical circuitry can be utilized, a light, compact, acoustic package can result for balloon-borne or rocketsonde applications.

DETERMINATION OF ATMOSPHERIC PARAMETERS BY ACOUSTIC MEANS

DA-SIG-36-039-62-G17

Progress Report No. 1

July, 1962

Section II

-8-

Design and Development of the Sonotherm Detection System

Terry L. Henderson
&
Carlos McDonald

SCHELLENGER RESEARCH LABORATORIES
Texas Western College El Paso, Texas

CONTENTS

1. Introduction

The design and development of the Sonotherm Detection system (Sec II-6) is summarized. Various techniques, under development, are discussed which correlate the antiresonant frequency corresponding to the maximum of the Sonotherm signal telemetered from the flight unit. Once this frequency is measured, information regarding the air temperature can be determined.

1.1 Problem Defined

The telemetered signal from the Sonotherm flight unit (Fig. 1-1) consists of a frequency-amplitude modulated waveform

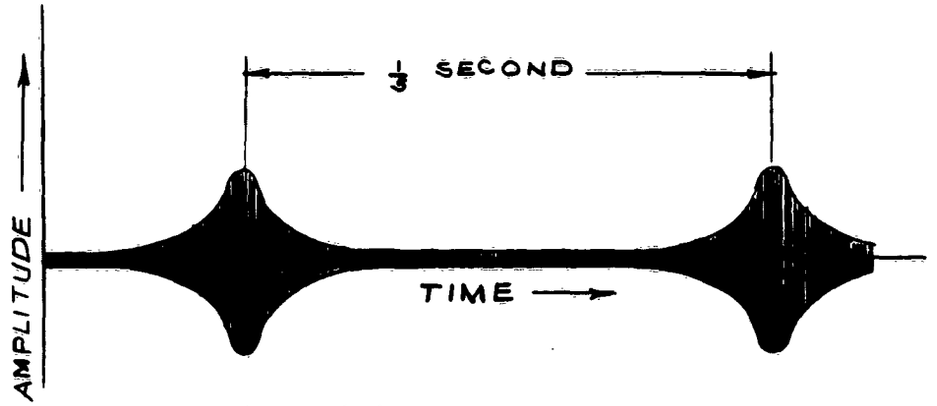

Figure 1-1

which repeats with respect to time. During each sample or sweep (represented by a single envelope), the frequency is varied in a linear manner between two frequency limits.

At the antiresonant frequency, lying between the two frequency limits, the amplitude of the envelope is maximum. In the present exper-

imental model, the frequency is varied between 26 to 31 Kc, and the sampling rate is approximately 5 cps. (Sec II-7).

The primary objective of the Detection System is to determine the frequency corresponding to maximums of the Sonotherm signal.

1.2 Detection Systems

There are several methods for determining the antiresonant frequency of the Sonotherm signal. The simplest is a visual technique (see Fig. 1-2) which utilizes a CRT to determine the antiresonant frequency.

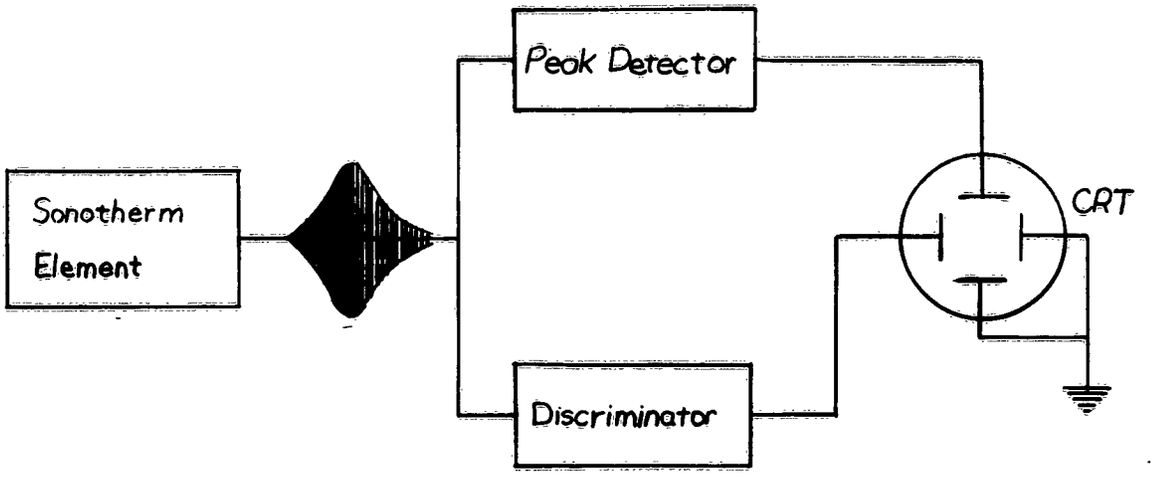

Figure 1-2

The Sonotherm signal is applied to a peak detector circuit whose output is a pulse which occurs at the maximum amplitude of each sweep signal, and to a frequency discriminator (see Sec. 3). The pulses from the peak detector circuit are applied to the vertical deflection plates of

the CRT and the voltage output of the discriminator is applied to the horizontal deflection plates. Since the output voltage of the discriminator is proportional to the frequency of the incoming signal, the horizontal deflection of the trace on the CRT can be calibrated with respect to frequency of the incoming signal. The antiresonant frequency is determined by measuring the horizontal deflection when the pulse occurs. A digital readout device can be used in place of the CRT to give more precise measurements.

A more elaborate system is shown in Figure 1-3. In this system

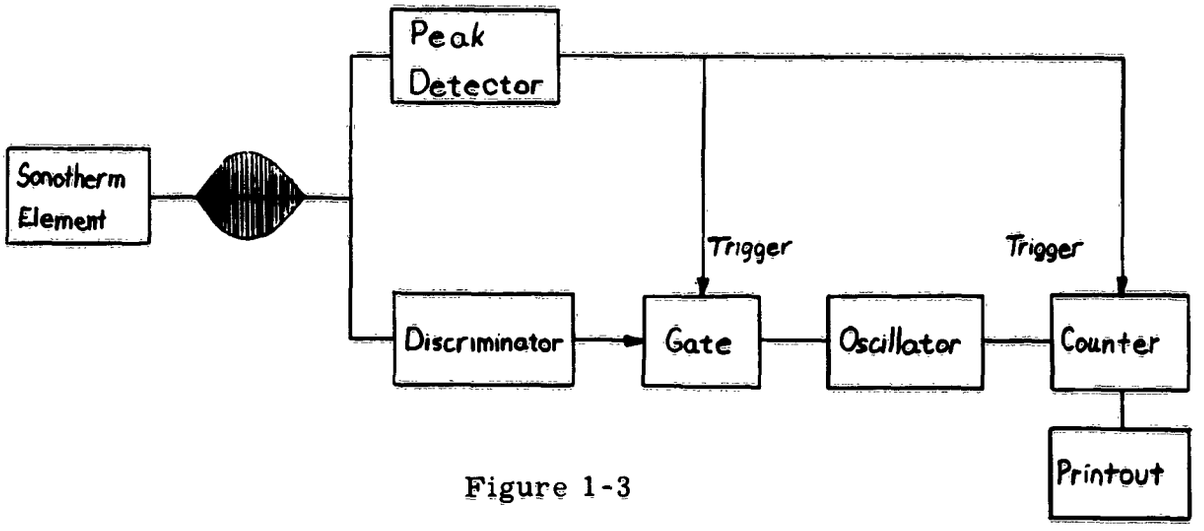

Figure 1-3

the output signal from the Sonotherm element is again applied to a peak detecting circuit and a frequency discriminator. The outputs of the discriminator and peak detector are applied to a gate circuit, where each pulse from the peak detector triggers a square gate signal whose voltage is determined by the discriminator output voltage at the time of the

triggering pulse (hence the voltage of the gate circuit output for each sweep signal is proportional to the antirosonant frequency). The voltage of the gate controls the frequency of an oscillator. The output of the oscillator is applied to a counter, and the pulse from the peak detector is used to trigger the counter for each sweep signal. The oscillator frequency is printed by a digital print-out machine and can be related to the antiresonant frequency of the Sonotherm signal.

The aforementioned methods are just two of many conceivable schemes for detecting antiresonant frequencies. In nearly all resonant frequency detection schemes the peak detector plays a very important part; it was for this reason the development of a peak detector circuit was emphasized.

1. 3 Sonotherm Simulator

In order to facilitate experimentation, a device was developed to simulate the Sonotherm signal. The simulator (Fig. 1-3a) utilizes a simple transistor circuit to produce the required waveform (see Fig. 1-1). A 30 Kc sine wave with a battery bias control between the collector and base is used to generate an envelope similar in shape to the Sonotherm signal. The 10 cps sine wave controls the bias on the base and hence the 30 Kc current through the transistor and the ac voltage on the load resistor. The output, taken from the emmiter, is base limited at plus one and a half volts by a biased IN2070 diode and is then applied to a pentode amplifier. The output from the pentode

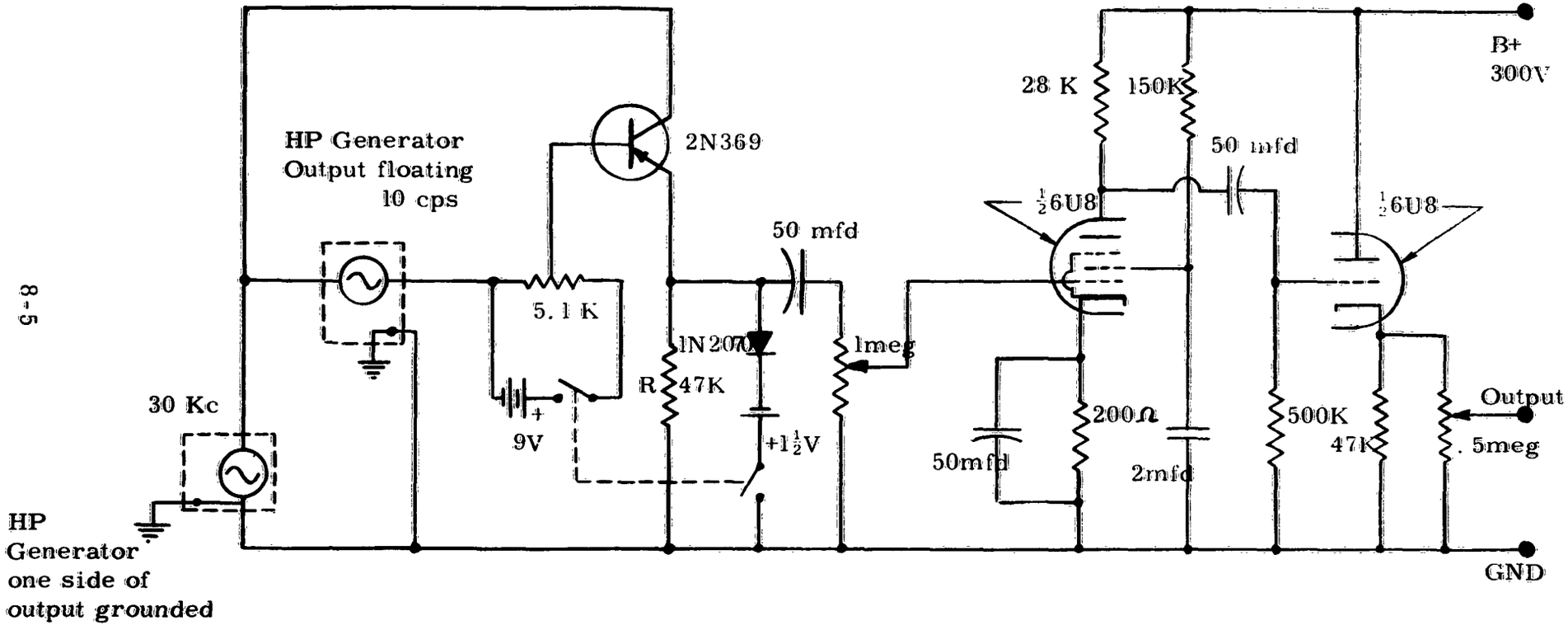

Fig. 1-3a Sonotherm Element Simulator

amplifier is then fed to a cathode follower from which the final output is taken. The output appeared (on an oscilloscope) as a straight line with positive sinusoidal envelopes of 30 Kc repeating every 1/10 of a second. The maximum output signal amplitude of the simulator was 80 volts peak, and the envelope width was controllable by adjusting the input signals.

The main differences between the Sonotherm signal and the simulator output are as follows: (1) the output of the Sonotherm element varies in frequency from approximately 26Kc to 31Kc during each sweep, while the frequency of the simulator remains at a constant 30Kc frequency, (2) whereas the output of the Sonotherm element appears as a straight line with repeating envelopes of equally positive and negative high frequency signal, the output of the simulator consists of the positive portions of the sinusoidal envelopes and therefore approximates the Sonotherm signal when rectified, (3) the period of the simulator output is 1/10 sec while that of the Sonotherm element output is 1/5 second. These differences did not affect the usefulness of the simulator since it is primarily used in the development of the peak detectors.

It was found that the amplitude of the output of the simulator varied slightly from signal to signal; however, this variation was less than that found in the Sonotherm signal itself. The simulator proved

quite useful and met all of its objectives.

2. Peak Detectors

All of the proposed detection systems require a pulse corresponding to the peak of the Sonotherm sweep signals. For this reason, the development of a peak detector was emphasized. The main requirements imposed on the peak detection device were: (1) It must detect the maximum of the Sonotherm sweep signals to at least within about 80 μsec or 2 cycles of the true peak; (2) has to be unaffected by variations in input signal strength. With this accuracy the virtual temperature can be determined within 0.1°C (see Sec II-6). The various types of peak detectors developed are discussed below.

2.1 The Differentiator Peak Detector

This device generates a pulse corresponding to the maximum of the Sonotherm sweep signal. The envelope of the Sonotherm signal is differentiated, and the zero crossover point (zero slope) of the differentiated wave form is detected since it corresponds to the maximum point (peak) of the envelope.

The circuit for this device is shown in Figure 2-1 and its block diagram is shown in Figure 2-2. Referring to Figure 2-2, the Sonotherm sweep signal is applied to a low pass filter network in order to obtain the envelope of the incoming signal. The envelope is then amplified (first amplifier) and then limited by a Zener diode (first base

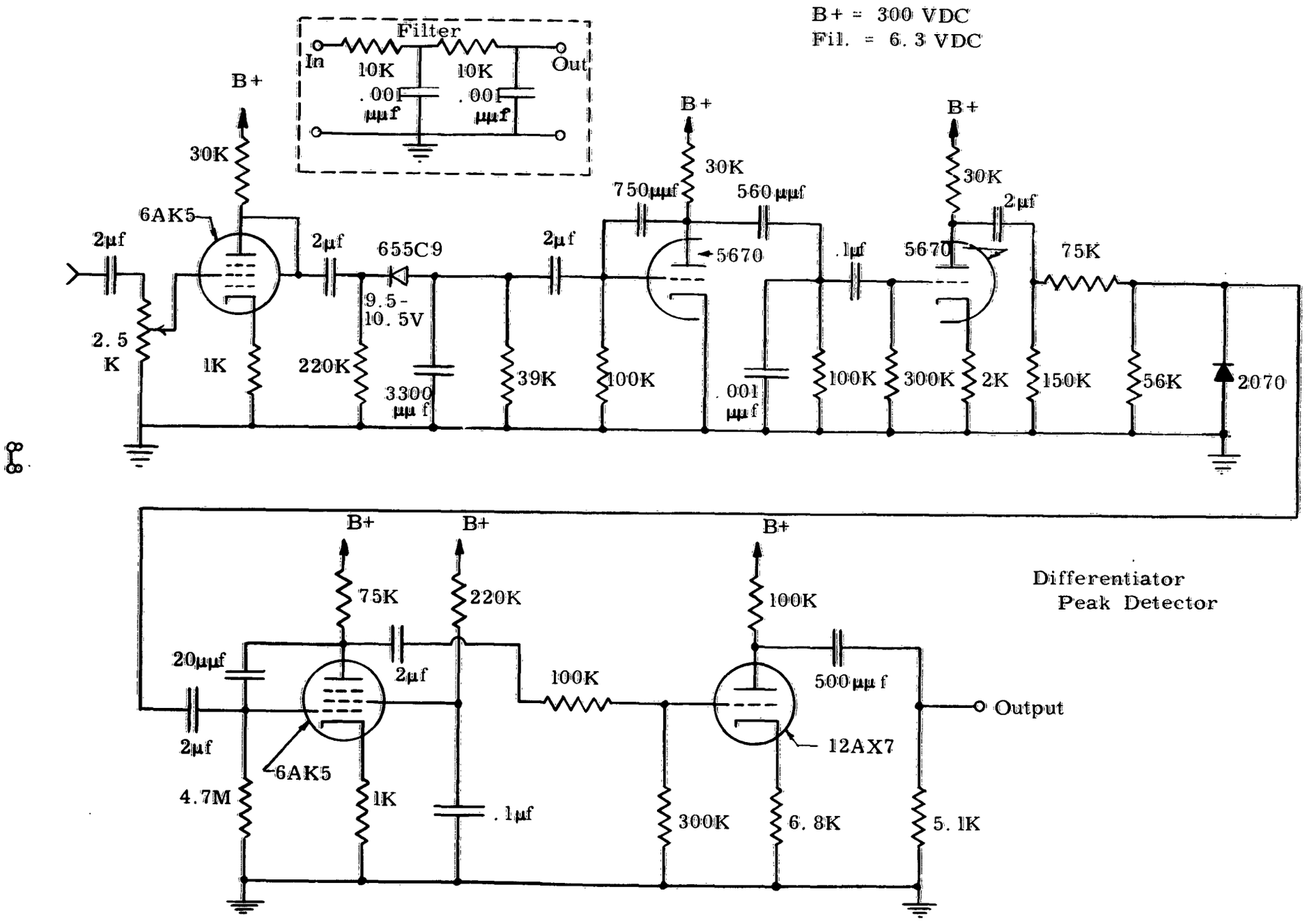
B+ = 300 VDC
Fil. = 6.3 VDC
Filter
In
Out
10K
10K
.001 µµf
.001 µµf
B+
30K
6AK5
2µf
2.5 K
1K
2µf
655C9
9.5-10.5V
220K
3300 µµf
2µf
39K
B+
750µµf
30K
560 µµf
100K
5670
.001 µµf
.1µf
100K
B+
30K
2µf
5670
300K
2K
75K
150K
56K
2070
B+
75K
20µµf
2µf
6AK5
4.7M
1K
B+
220K
2µf
.1µf
100K
B+
100K
500 µµf
12AX7
300K
6.8K
5.1K
Output
Differentiator
Peak Detector

Fig. 2-1

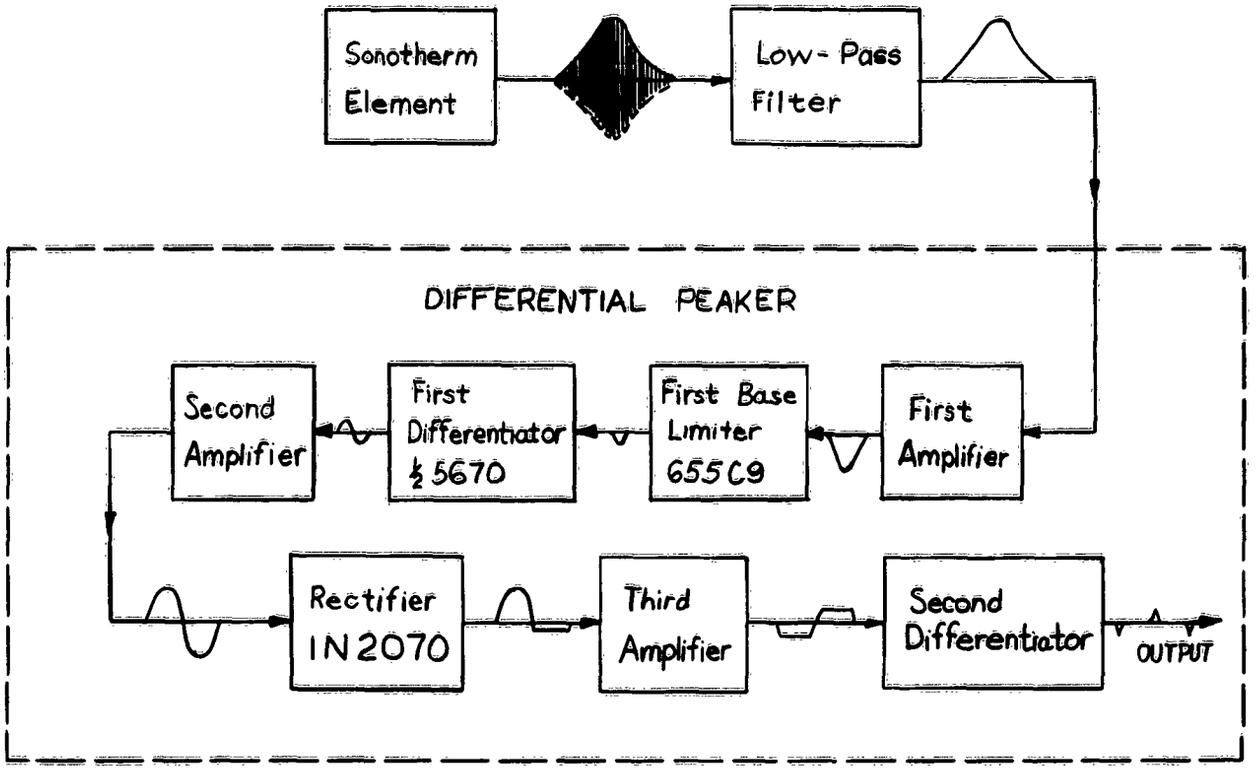

Figure 2-2
Peak Detector Block Diagram

limiter) leaving only the upper portion of the wave. This signal is then fed to an electronic differentiator (first differentiator) whose output can be seen in the figure. The output of the differentiator was then applied to a second amplifier and is then rectified by a IN2070 diode. The positive output from the diode is fed to a pentode and triode amplifiers (third amplifier) which greatly amplifies the signal). In fact, since the input signal to the pentode was of such a large magnitude, the output appears as a square wave, limited at top and bottom. The output from the last triode amplifier is then differentiated (second differentiator). The center pulse of the output corresponds

in time to the peak of the incoming sweep signal.

Various problems were encountered with this device. For one thing, it was very hard to keep track of the all-important zero level of the differentiated signal. It was also found that the incoming sweep signals had to be base limited very close to their peaks in order to have a sharp output pulse. However, since the amplitude of the Sonotherm signal varied and the limiting levels were constant, it was difficult to obtain reliable results.

It was decided that some sort of automatic amplitude control would have to be developed in order to minimize the signal's amplitude variations before this circuit would be successful.

2.2 Expander Peak Detector

The purpose of this device was to exaggerate the peak of the incoming signal so as to detect it more easily. The heart of the device is a variable amplification factor pentode; the amplification factor is controlled by the grid bias, and hence controlled by the instantaneous voltage of the incoming signal. As the signal goes more and more positive, the gain increased and hence the peak of the input signal is amplified more than the lower portion.

The circuit (Fig. 2-3) employs a 6BA6 variable μ tube which is operated with a 300 volt B+ supply through a 33K load resistor. The screen voltage is controlled by a Zener diode at 110 volts. The

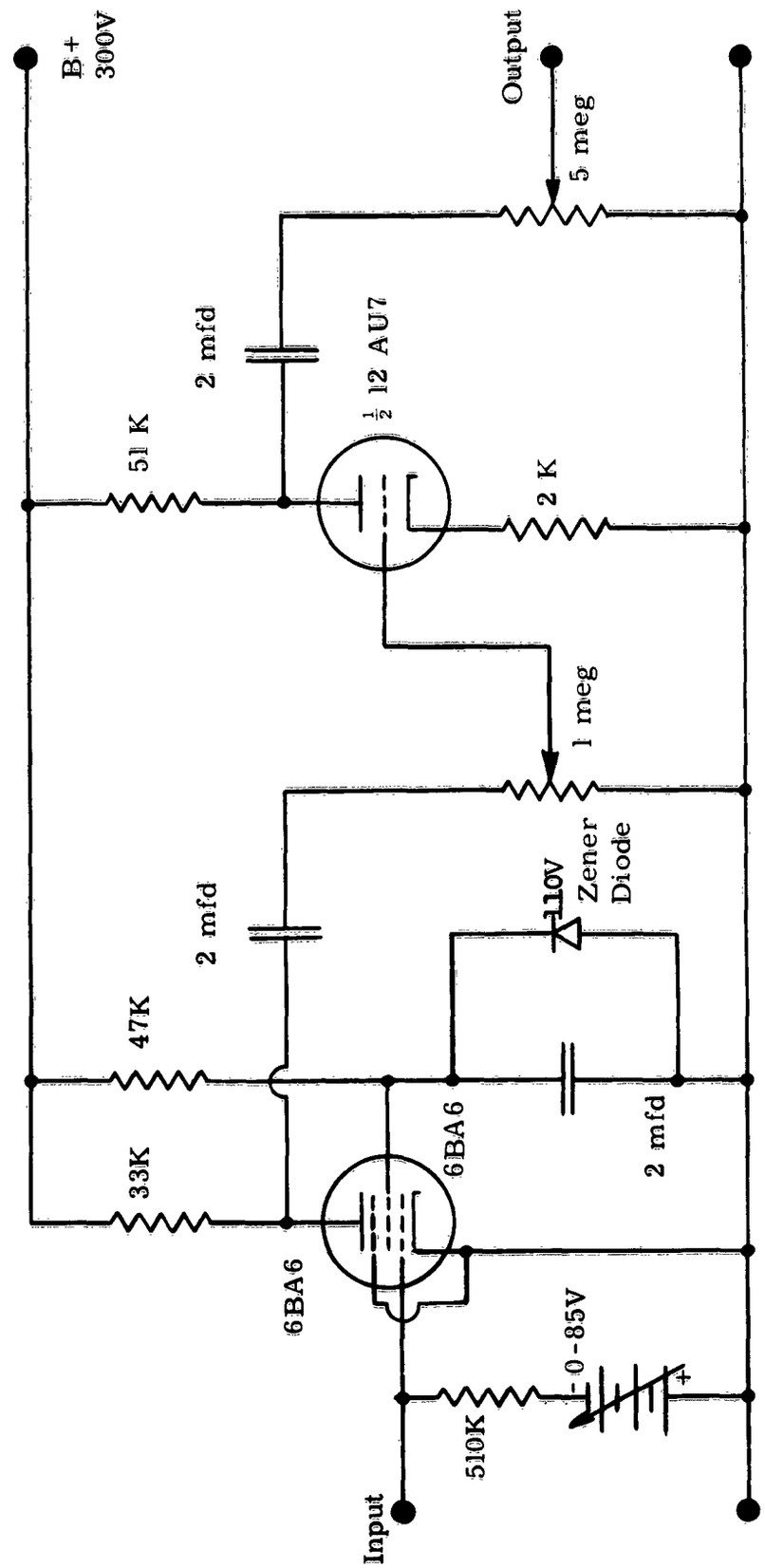

Fig. 2-3 Expander Peak Detector

grid is negatively biased at a voltage whose magnitude is slightly greater than that of the incoming positive signal. As a result, the tube is at cutoff until the signal is applied. The most positive portion of the signal is amplified non-linearly producing much sharper peaks than those of the input. The output signal is then amplified by a 12AU7 triode. The circuitry was constructed in module form and four stages of expanders were used.

The expander performed very well. By cascading 3 stages, a signal with a base width of 20 ms and a width of 12.5 ms at the 75% mark was reduced to a signal with a base width of 3 ms and a width of approximately 0.3 ms at the 75% mark. (See Fig. 2-4). However, it was found that adding a fourth stage was of little value. The small variations in the input from the Sonotherm signal or simulator are greatly amplified that after three stages the signal amplitude varied considerably. When this signal was fed to a fourth stage the bias level could not be adjusted to obtain a steady signal output. Only when the input to the fourth stage happened to fall within a certain range (determined by the bias) was there any output. Since the output from only three stages of expansion was not yet narrow enough for accurate detection it was decided that work on the expander should be discontinued until some sort of automatic amplitude control could be developed so that more stages could be added to the expander.

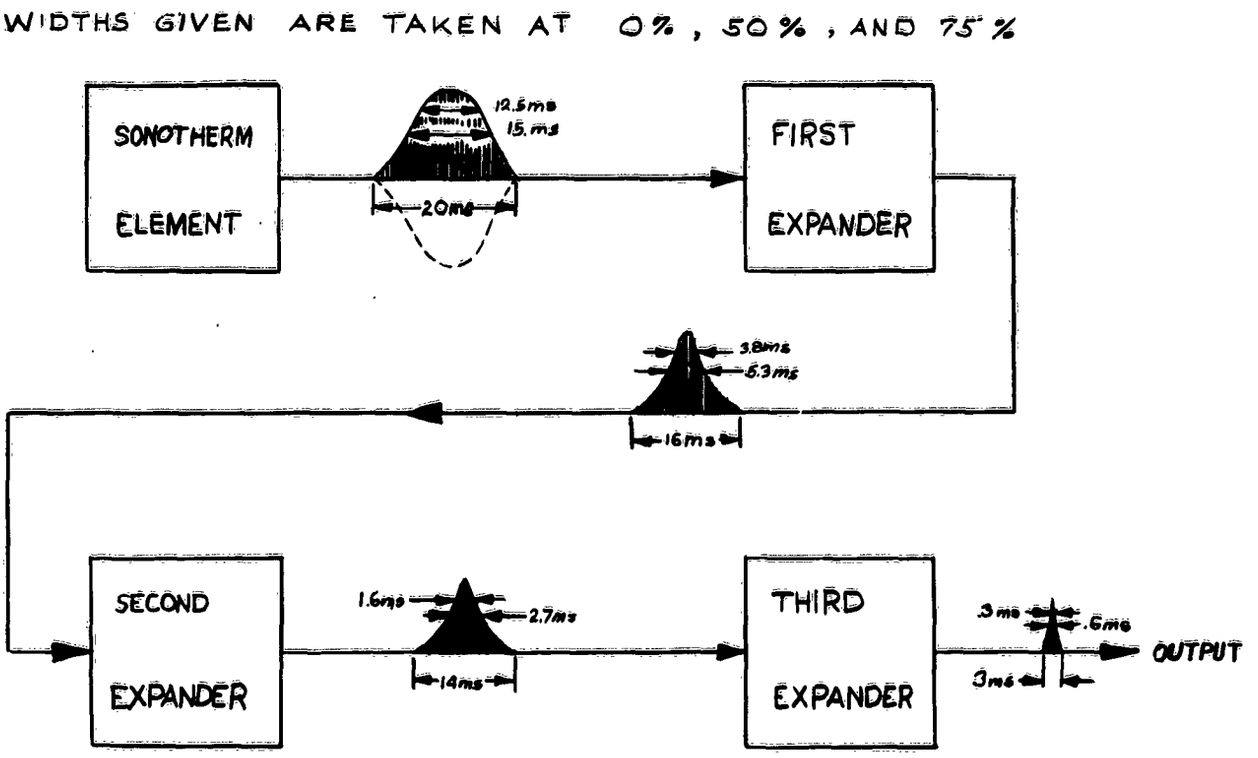

Figure 2-4
Cascaded Expander Peak Detectors

2.3 Staircase Peak Detector

This device was designed to be used in conjunction with a differentiator to detect the maximum of the Sonotherm signal (Fig. 2-5a). As the individual cycles of the Sonotherm signal are applied to the staircase detector, its output follows each cycle to its peak and then remains at that level until an input cycle of higher magnitude increases the output voltage (Fig. 2-5b). After the highest input cycle is applied, no other cycles are high enough to affect the output so it remains at the dc level of the peak cycle of the input signal. The output signal can then feed to a differentiator which results in a pulse for every rise in dc level of the input (Fig. 2-5c). The last such pulse for each

sweep signal corresponds to the peak of the Sonotherm sweep signal.

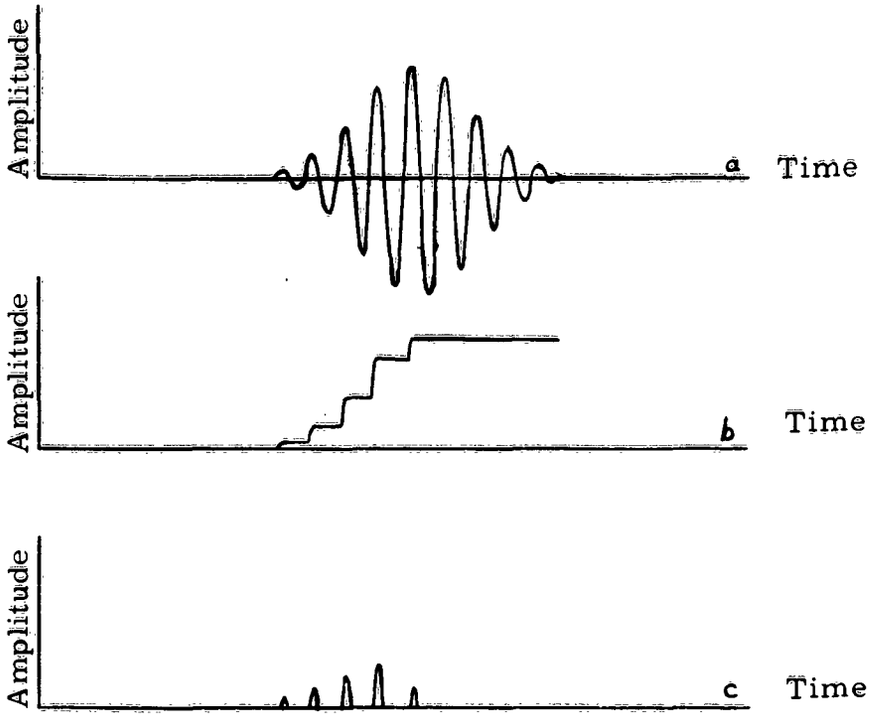

Figure 2-5
Effect of Staircase Peak Detector

The circuitry of the staircase detector is shown in Figure 2-6. The signal from the Sonotherm is applied through an input cathode follower to the diode D in series with the grounded capacitor C. The voltage across the capacitor C is applied to the floating grid of the output cathode follower. When a cycle of the input signal (Fig. 2-5a) is positive, the diode is forward biased resulting in the fast charging (5 μsec) of the capacitor C through the equivalent resistance of the diode and input cathode follower. Consequently, the capacitor C charges up to peak voltage of the input cycle. When the input cycle voltage decreases from its peak value, the diode is

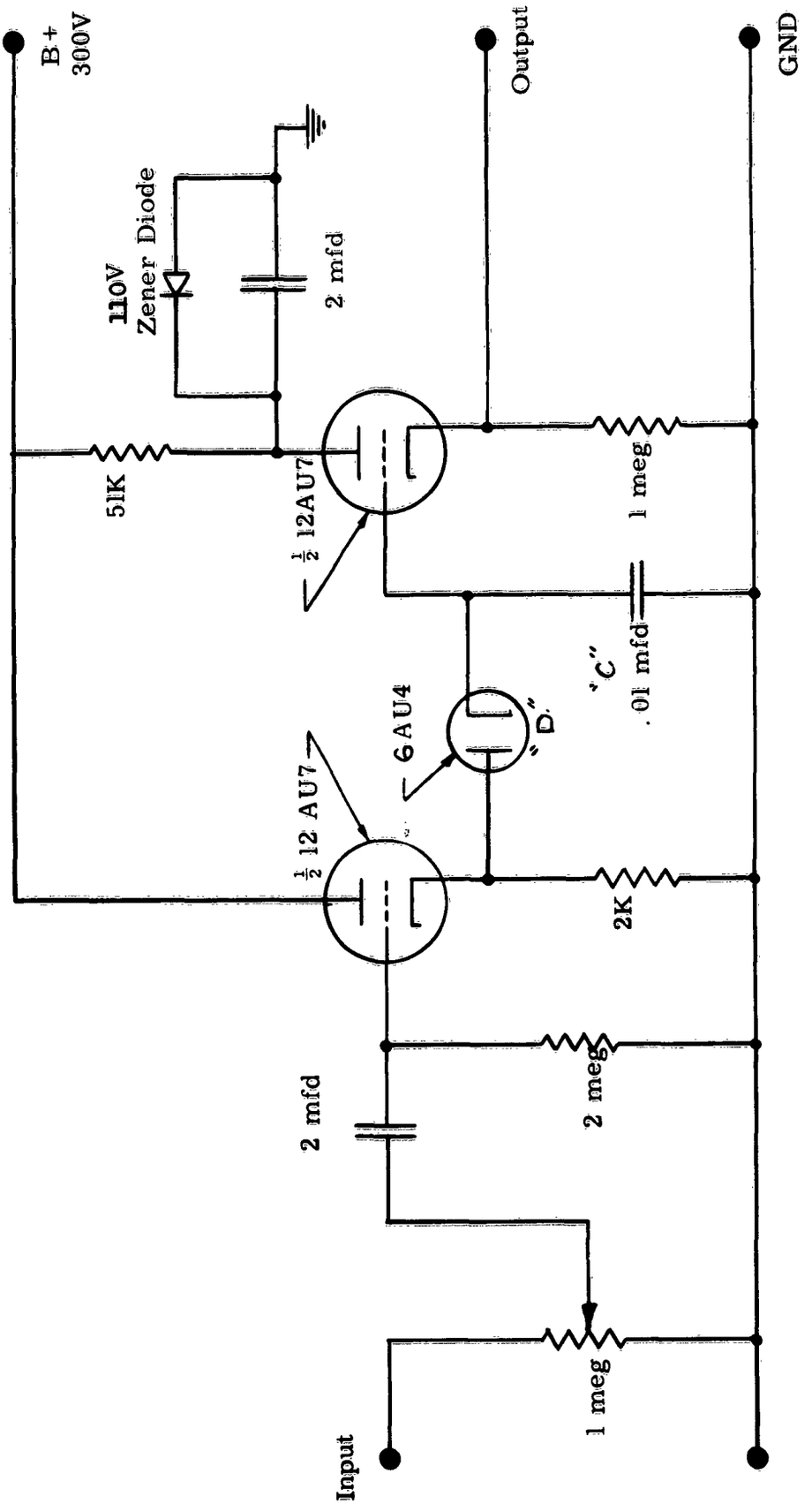

Fig. 2-6 Staircase Peak Detector

back biased, and the discharging time of the capacitor is much larger (1-10 sec) since it has to discharge through the large grid impedance of the output cathode follower. As a result, the voltage across the capacitor and the output cathode follower remains essentially constant. If the next input cycle is of a greater magnitude, the diode is forward biased only during the time interval when the input cycle voltage is of a higher magnitude than the voltage across the capacitor. The capacitor then charges up to the peak voltage of this input cycle.

In the above manner, the voltage across the capacitor and of the output cathode follower increases or "steps" to the voltage corresponding to the peak of the Sonotherm sweep signal (Fig. 2-5b). The cycles that follow after the peak of the Sonotherm sweep signal are of a lower magnitude, and consequently, the output voltage remains constant since the diode is in a back biased condition. If this output is differentiated (Fig. 2-5c), the last pulse will correspond to the peak of the Sonotherm signal.

The staircase detector was found to be very promising since it is independent of amplitude variations of the Sonotherm signal. Its main disadvantage was that the magnitude of the differentiated pulses (Fig. 2-5c) near the peak of the Sonotherm signal were of such small magnitude that it was a major problem to detect the last pulse unless the output signal was amplified excessively. However, this disad-

vantage is eliminated when the staircase detector is used in conjunction with several proposed types of peaking circuits discussed in Section 2-6.

2.4 Base Limiting Peak Detector

The purpose of this device was to isolate the extreme top portion of each incoming sweep signal from the Sonotherm element. This was accomplished by base limiting each sweep signal (Fig. 2-7a) at a level very near to its peak positive voltage, leaving only the top 1 or 2% of the sweep signal (Fig. 3-7b). The level at which each sweep signal is base limited is determined and set by the peak voltage amplitude of the output of the peaker from the preceeding sweep signal. Because the base limiting level was dependent on the magnitude of the input signal, this peaker operated over a wide range of input signal amplitudes.

The circuitry of this peaker (see Fig. 2-7) can be divided into 3 main sections:

1. LIMITER -AMPLIFIER SECTION: This section consists of the triode limiter T_1 and the output amplifier T_2. The triode limiter is normally biased to cutoff by its cathode voltage which determines the limiting level.

2. AUTOMATIC FEEDBACK LEVEL SECTION: This portion of the circuit samples the peak output voltage of the peaker in order

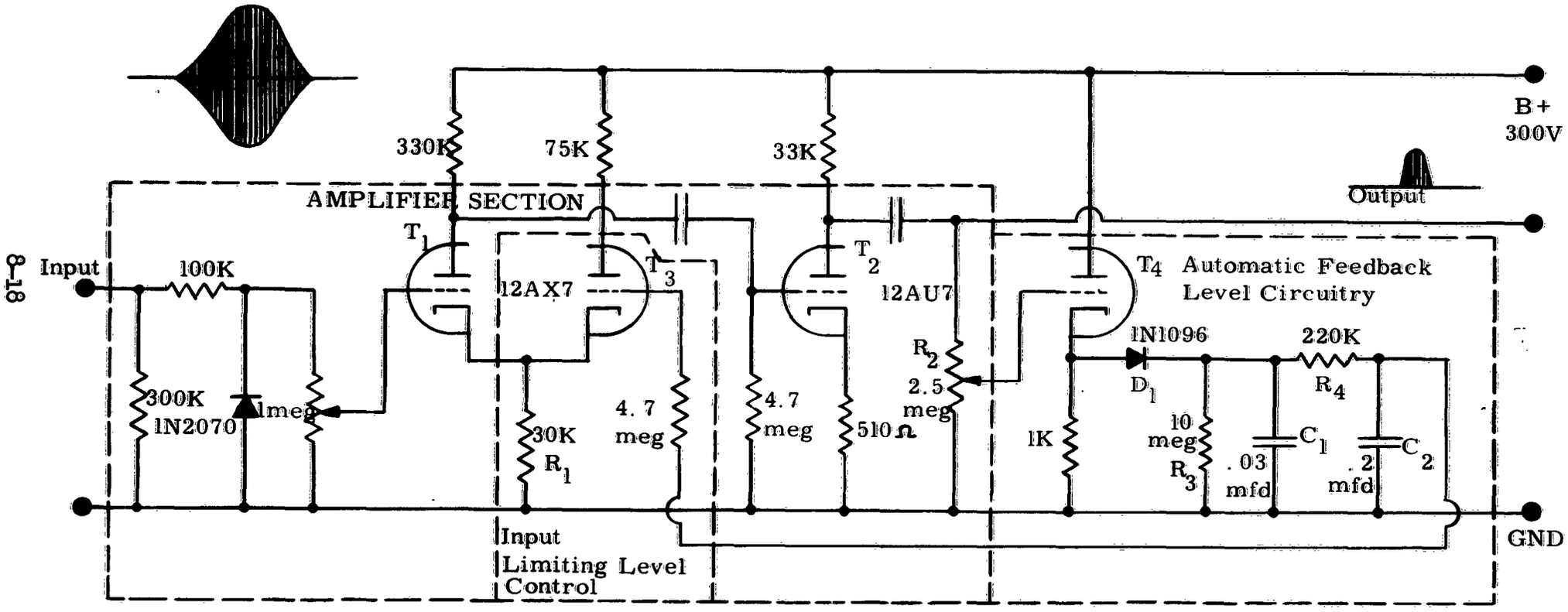

Fig. 2-8 Base Limiting Peak Detector

to set the limiting level of the triode amplifier. The circuitry includes a 12AU7 cathode follower (T_4) a diode-capacitor circuit (D, C_1) where the capacitor C_1 charges to a feedback voltage proportional to the peak of the output signal, and a filter circuit (R_4, C_2) to delay the feedback voltage until the sweep signal has passed through the triode limiter.

3. INPUT LIMITING LEVEL CONTROL: This section consists of a cathode follower (T_3) whose cathode is connected in common to that of the triode limiter, T_1. The automatic feedback level (dc) voltage is applied to the grid T_3 and determines the limiting level of the triode amplifier. Each sweep signal is used to set the limiting level of the triode-limiter T_1 for the next signal.

In order to explain the operation of the peaker, assume that there is no variation in peak voltage from sweep signal to sweep signal. When the first sweep signal is applied, it is base limited and amplified by the triode amplifier T_1. If there is no automatic limiting level control voltage (there is none since this is the first signal and feedback is delayed until the signal has passed), the voltage (with respect to ground) at which the limiting action occurs can be represented by a constant value K. Until the incoming signal reaches this level, no output will be seen on the plate of the first amplifier. Hence, if we represent the voltage of the peak of the incoming signal by S and the limiting voltage by K, the peak output voltage of T_1 will be $-G_1(S-K)$ where G_1 is its effective gain. This

signal is then fed to an ordinary triode amplifier T_2 with a gain G_2. The peak voltage of its output, which is the final output, for the first signal will be $-G_2\left[-G_1(S-K)\right]$ The final output signal (positive) is then fed to the cathode follower T_4 and charges the capacitor C through the equivalent forward resistance of the diode and the cathode follower T_4. The capacitor charges up to the peak voltage of the sweep signal and remains at approximately this value since the diode will be back-biased when the amplitude of the sweep signal decreases. The RC circuitry (R_4, C_2) will delay this rise in voltage so that it will not be fed back to the grid of T_3 immediately. The feedback dc voltage will soon appear on the grid causing the voltage of its cathode to rise. This will raise the base limiting level of the triode-limiter to a value ($K + F_1$) where K is the original level set by the cathode resistor and F_1 is the increase in this level due to the feedback from the first signal output. Hence, F_1 can be said to equal $G_F \times E_{out}$ where E_{out} is the output peak voltage of T_2 and G_F is the gain of the automatic feedback level circuitry. When the next sweep signal is applied it is limited at a voltage $K + G_F \times E_{out}$ and hence the peak voltage output for the second signal is much smaller than for the first. (In fact, if G_F, which is controlled by R_2, is made larger, the cathode voltage of T_1 may be so high that the following signals will not get through at all until the automatic level control voltage on capacitor C_1 decays).

This causes a decrease in the feedback limiting level since the peaker's peak output voltage is smaller, and the next incoming signal will be base limited at a lower level resulting in an increased output. The process will continue until the peak voltages of the output signals become constant. At this point, the voltages will be related by the following equations:

$$E_{out} = \left[S-(K + E_{out}G_F)\right] G_A$$

where E_{out} = peak voltage of output signal

S = peak voltage of the input signal

K = the grid cutoff clamping level for 0 feedback

G_F = the gain of the automatic feedback level circuitry

G_A = the gain of the first signal amplifiers T_1 and T_2.

Solving for E_{out},

$$E_{out} = \frac{G_A(S - K)}{1 + G_A G_F}$$

If G_A is kept constant and the output is decreased, the input signal is limited closer to the peak. This can be accomplished by increasing the values of K, G_F or decreasing the magnitude of the input signal. (However, K cannot become greater than S or there will be no output). It was found that it was practical to control the base clipping level by varying the potentiometer R_1 so as to vary the magnitude of G_F. In this manner, it was possible to control the limiting level signal input.

The peaker performed very well. The main disadvantage was that the peaker could not handle large variations in amplitude from one sweep signal to the next. However, it was concluded that this peaker would be reliable if the feedback circuit controlling the base limiting level was modified in such a manner that the limiting level would be determined by the preceeding cycle within the same sweep signal.

2.5 Evaluation

The various peak detectors discussed previously were capable of meeting the requirement of generating a sharp pulse at the maximum of the Sonotherm signal. Except for the staircase case, their main disadvantage was their sensitivity to amplitude variations of the Sonotherm signal. An automatic gain control could solve the above difficulty. However, as discussed in the next section, various other peak detectors have been proposed which not only are insensitive to amplitude variations of the Sonotherm signal, but also have promise of being much more accurate in detecting the maximums of the Sonotherm signal.

2.6 Proposed Peak Detectors

A number of peak detectors, discussed below, show promise of not only being insensitive to amplitude variations of the Sonotherm signal, but also capable of detecting the signal maximums to a great degree of accuracy.

2.61 Constant Level Peak Detector

This device utilizes a time delay system to, in effect, determine amplitude of the peak of each incoming sweep signal before it arrives. Then the sweep signal is base limited at a level relative to the peak, hence the output is the peak portion of the incoming signal and is independent of signal amplitude variations.

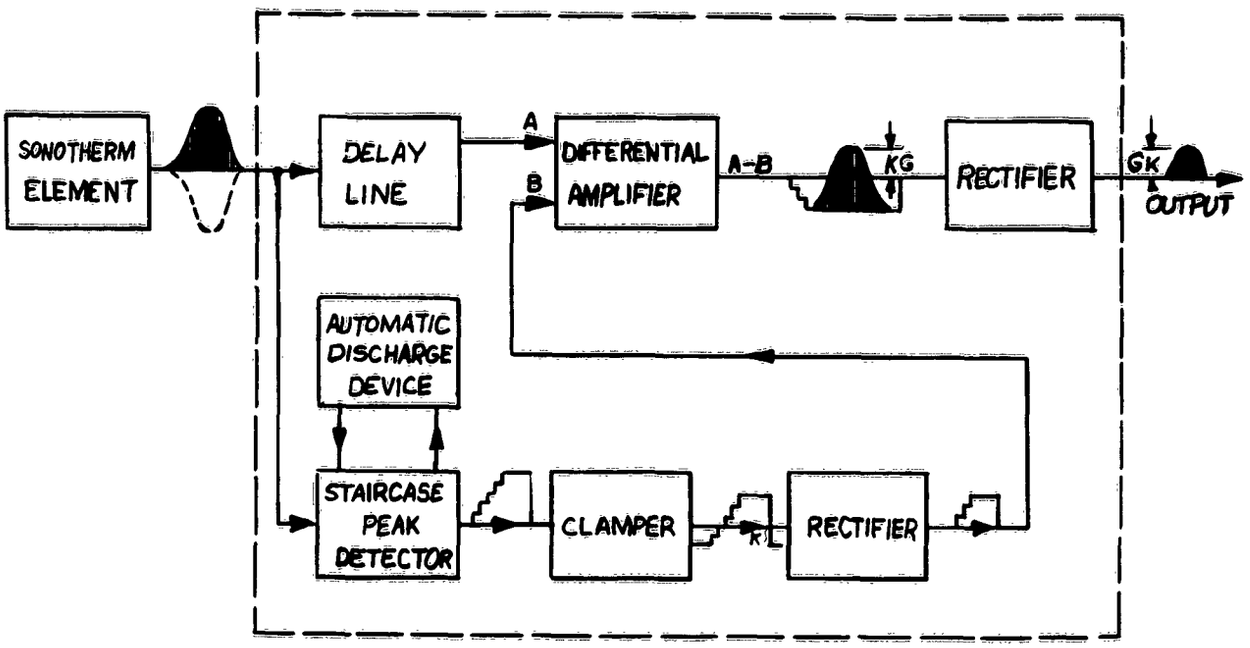

Figure 2-9
The Constant Level Peak Detector

A block diagram (Fig. 2-9) illustrates how this method might be utilized. The sweep signal from the Sonotherm element is fed to a delay line and to a dc level setting circuit. In the level setting circuit the signal is first fed to the staircase peak detector (see Sec. 2-3). Connected to

this peak detector is a device to automatically discharge the capacitor (see Fig. 2-9) after each sweep signal has passed through. From the staircase peak detector, the signal is fed to a clamper. Here the signal is merely displaced downward on the y-axis a distance of K volts. The purpose of this device is to create a difference between the magnitude of the dc level of the peak detector and the amplitude of the peak of the delayed sweep signal. If the difference were zero, the output of the differential amplifier would be zero at the peak of the delayed sweep signal. From the clamper the signal goes through a rectifier to bring the base line of the signal back to zero volts so that the baseline of the differential amplifier output will not lie on the same level as the peak of the delayed sweep signal.

The outputs from the delay device and the dc level setting circuit are fed into a differential amplifier. The output voltage of the differential amplifier (Fig. 2-9) will step down to the dc level setting device voltage and then peak back up when the delayed sweep signal comes through. The peak of the delayed sweep signal will lie above the zero volts line by a distance (K) (G) volts where K is the voltage displacement in the clamper and G is the gain of the differential amplifier. The output of the differential amplifier is then rectified leaving only the top portion of the sweep signal. The main advantage of this device is that the amplitude of the output signal will always remain

constant no matter what the signal input is (unless it falls below K volts).

This device can either be used as a peaker, in which case K would be set very low, or as an automatic level control. In the latter case, the peak detector's output would be sent to any one of the foregoing types of peakers, which would then work quite well since there would be no variation in input signal amplitude.

The main disadvantage of the device is that its output does not correspond in time to the peak of the incoming sweep signal. However, this disadvantage can be eliminated by applying the input signal to a similar delay line.

2.62 Short Delay Peak Detector

This type of peaker would be somewhat similar to the previous peak detector. Its objective would be to subtract each positive cycle of the Sonotherm signal from the next cycle.

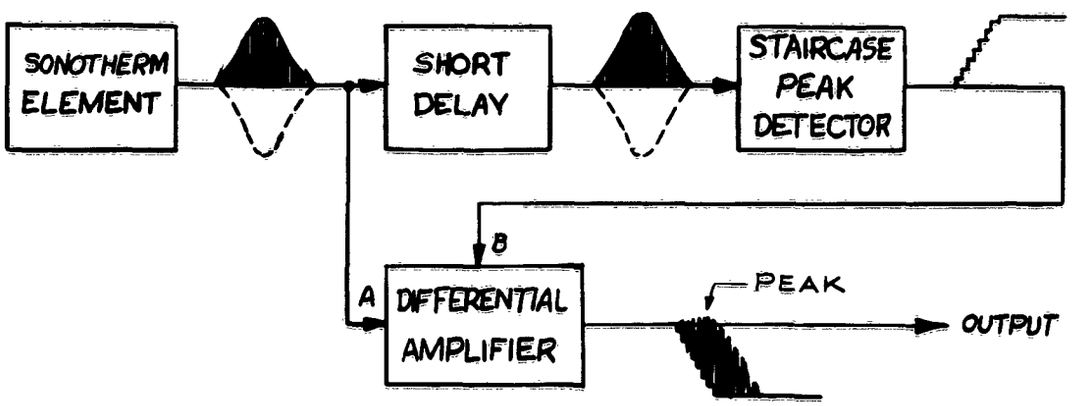

Figure 2-10
Short Delay Peak Detector

Referring to Fig. 2-10 the sweep signal is fed through a delay device (approximately 20 μsec) to the staircase peak detector. The output of the diode stepper is then fed to the differential amplifier along with the original sweep signal. The last positive cycle corresponds to the peak of the incoming sweep signal. The zero crossover point after the signal output is filtered corresponds approximately to the peak.

2.63 Alternator Peak Detector

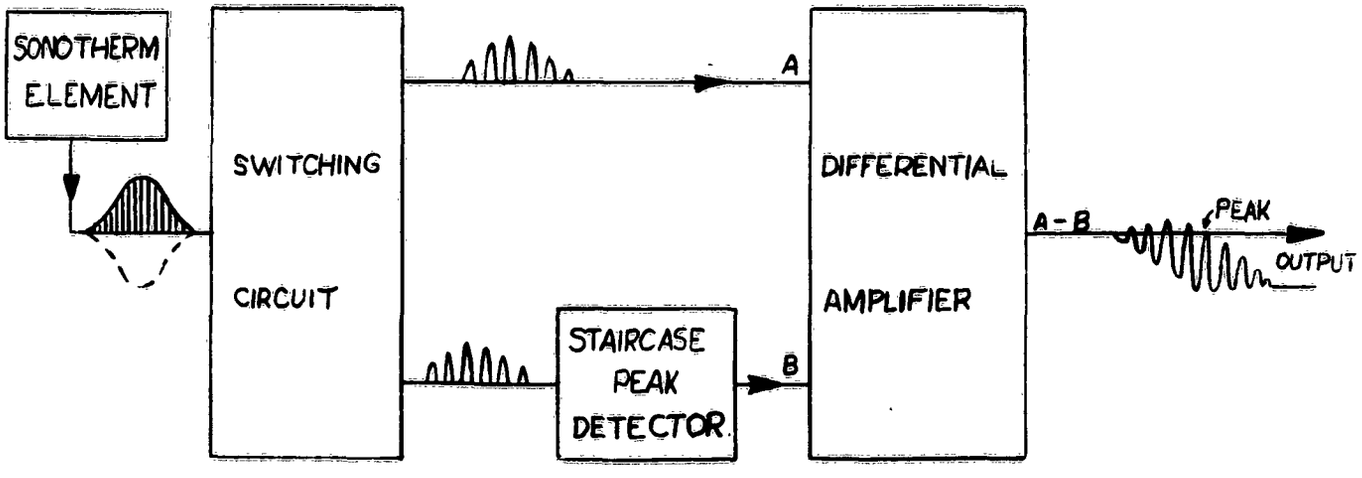

Figure 2-11
Alternator Peak Detector

This type of peaker (Fig. 2-11) is quite similar to the short delay peaker except that instead of using a delay device to delay the signal fed to the staircase peak detector, a switching circuit is used to alternately channel the individual pulses of the sweep envelope first to one channel of the differential amplifier, then to the staircase peak

detector. The staircase detector output is connected to the other channel of the differential amplifier. Here the peak voltage of each odd pulse is subtracted from each even pulse. Again, the last positive pulse corresponds to the peak.

2.64 Full-Wave Peak Detector

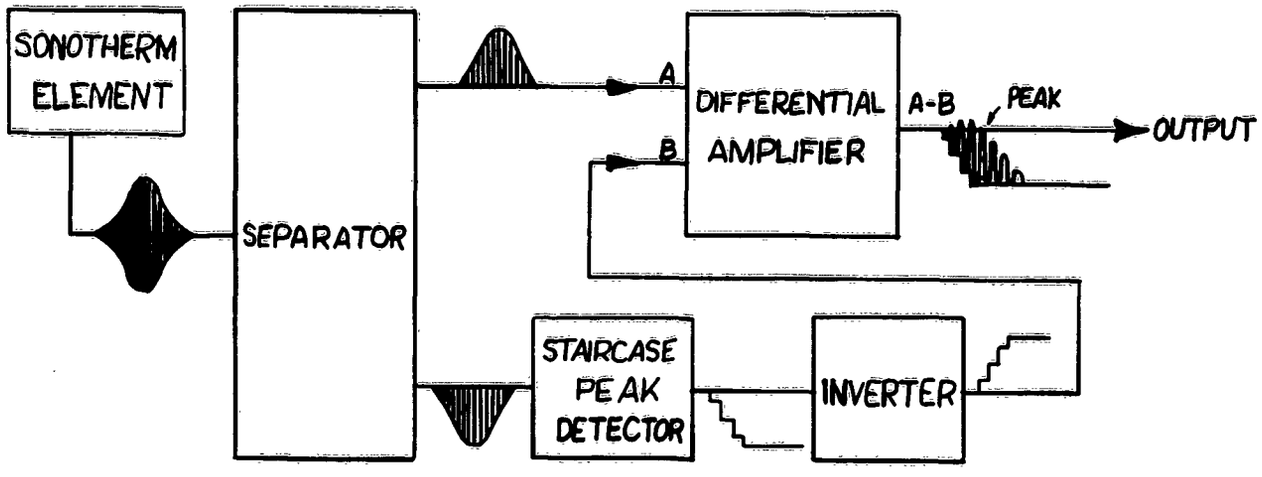

Figure 2-12
Full Wave Peaker

This peaker (Fig. 2-12) is similar to the aforementioned peakers (alternator, short delay) except that the full sweep signal (positive and negative) is used. In this case, the signal is separated at the 0 volts line, the top half is applied to the differential amplifier, the bottom half to the staircase peak detector and then through an inverter to the differential amplifier. This circuit then subtracts the voltage of each negative going cycle from that of the following positive cycle.

3. Discriminator

In conjunction with work done on detection, experimentation was done with a discriminator circuit in order to obtain an output voltage proportional to the frequency of the Sonotherm signal.

The circuit for the discriminator is shown in Fig. 3-1. The frequency-amplitude modulated signal from the Sonotherm element is amplified and then limited by the action of a dual Zener diode. This signal is then applied to a cathode-coupled gate circuit whose output is a square wave signal of constant amplitude and width for each cycle of the input signal. This constant width-amplitude square wave is then integrated by a low pass filter where output voltage is proportional to frequency of the Sonotherm signal. The above circuit proved to be ideal since a large voltage variation with respect to frequency can be obtained at the relative low frequencies of the Sonotherm signal.

4. Conclusion

The techniques of correlating the frequency to the maximum of the Sonotherm signal have been basically determined. Even though further research and development is necessary, theoretical and preliminary experimental evidence indicates that the above techniques will be reliable and capable of performing the desired measurements to the degree of accuracy required.

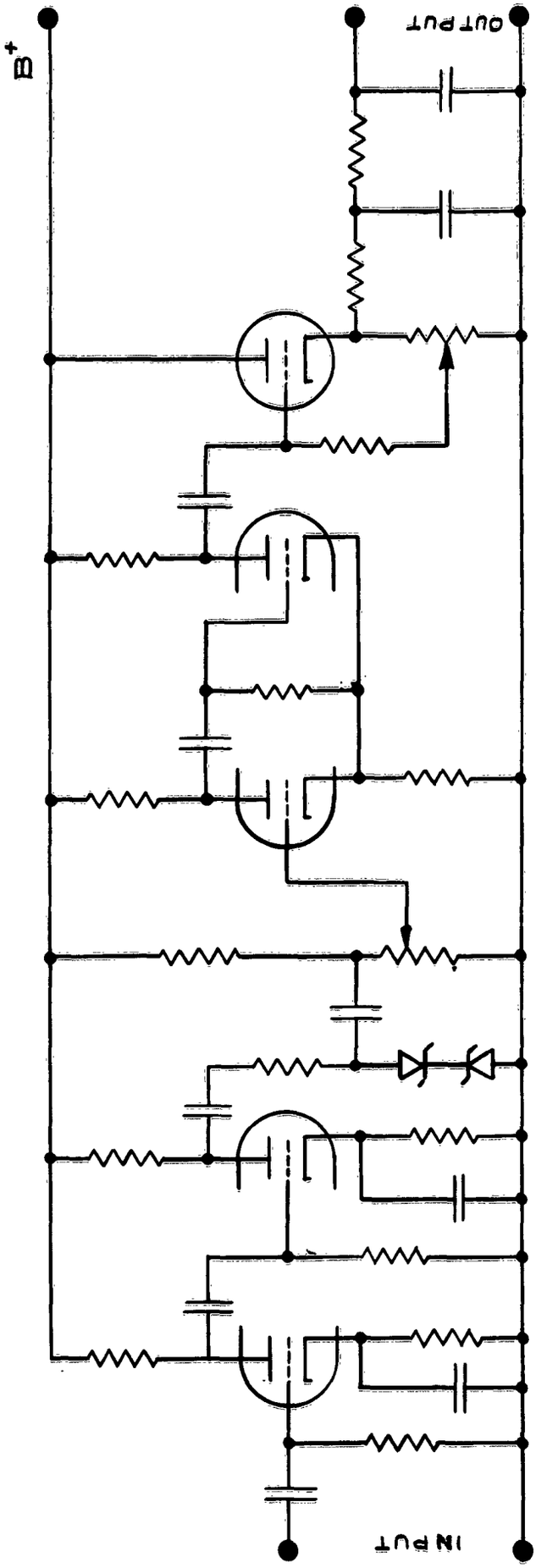

Fig. 3-1 Discriminator

DETERMINATION OF ATMOSPHERIC PARAMETERS
BY ACOUSTIC MEANS

DA-SIG-36-039-62-G17

Progress Report No. 1

July, 1962

Section II:

DESIGN AND DEVELOPMENT OF ACOUSTIC DEVICES

-9-

An Acoustic Thermometer for Enviromental Testing

Harold N. Ballard
Mike Izquierdo
Fred Salvatti, Jr.
Kerry Wilson

S C H E L L E N G E R R E S E A R C H L A B O R A T O R I E S
Texas Western College El Paso, Texas

Table of Contents

Section 9

AN ACOUSTIC THERMOMETER FOR ENVIRONMENTAL TESTING

1. Introduction

An acoustic thermometer was discussed in a Schellenger Research Laboratories publication, Response Time of and Effects of Radiation on the VECO Bead Thermistor, April 7, 1961. It was noted in this report that thermocouples and thermistors placed within an environmental chamber failed to monitor the air temperature correctly, the failure being brought about by radiation effects from the walls of the chamber. The acoustic thermometer was developed in an attempt to make air temperature determinations within the chamber which were free from these wall radiation effects. The acoustic thermometer discussed in the above SRL report was capable of measuring the chamber air temperature with an accuracy of $\pm$ 5°C over a temperature range from -90°C to +25°C and over a pressure range from 1 mm Hg to 670 mm of Hg. The accuracy of not better than $\pm$ 5°C was caused by the uncertainty in the determination of the elapsed time between the initiation of the sound pulse by the speaker and the arrival of the sound pulse at the receiving microphone.

To improve the accuracy of the thermometer, electronic circuitry has been introduced such that the uncertainty in the determination of the time of travel of the sound between the speaker and the microphone has been reduced to $\pm$1μsec, corresponding to an accuracy of $\pm$0.5°C in the determination of the air temperature over a range from -85° to+25°C and at a pressure of 670 mm Hg.

2. Principle of Operation

The speed of sound is given by the equation

$$v_o = \sqrt{\frac{\gamma P}{\rho}}$$

where the quantities ρ , P, and γ are the ratio of the specific heats, pressure, and density of the medium, respectively. If it is assumed that the equation of state of the medium is that corresponding to a perfect gas,

$$\frac{P}{\rho} = \frac{RT}{M} ,$$

and the expression for the speed of sound becomes

$$v = \sqrt{\frac{\gamma RT}{M}} = \sqrt{\frac{\gamma RT_o}{M}\frac{T}{T_o}} = v_o\sqrt{\frac{T}{T_o}}$$

where $v_o = \sqrt{\frac{RT_o}{M}}$ is the speed of sound at zero°C (273°K).

The equation

$$v = v_o\sqrt{\frac{T}{T_o}}$$

may be written

$$\frac{S}{t} = \frac{S}{t_o}\sqrt{\frac{T}{T_o}}$$

where S is the effective distance between the source of sound and the receiving microphone. If the distance S is held fixed, then the equation

$$\frac{S}{t} = \frac{S}{t_o}\sqrt{\frac{T}{T_o}}$$

becomes

$$\frac{t_o}{t} = \sqrt{\frac{T}{T_o}}$$

and the absolute temperature is given by the equation

$$T = T_o\left(\frac{t_o}{t}\right)^2$$

where t_o is the time of travel over the fixed distance S at 273°K and t is the time of travel at T°K. Thus the temperature determinations is reduced to the

determination of the terms t_o and t.

3. Calibration

The speaker acting as the source of sound and a microphone were placed within the test chamber. Thermocouples were mounted on each wall of the chamber. Two thermocouples were placed along the sound path between the speaker and the microphone. The test chamber was brought to a temperature of 0°C and allowed to reach a thermal equilibrium such that the thermocouples on the walls of the chamber and those mounted in the air all recorded 0°C. The time t_o was then determined. From this value of t_o and the equation

$$T = T_o\left(\frac{t_o}{t}\right)^2$$

or

$$t = t_o\left(\frac{T}{T_o}\right)^{\frac{1}{2}}$$

times of travel corresponding to temperature between +25°C and -85°C were calculated and compared with measured travel times over the same temperature ranges, the temperature being determined by the air thermocouples. These data are presented in Fig. 1 and Table I, respectively.

TABLE I

Pressure-670 mm Hg

Acoustic Measurements		Thermocouples (Observed)	Average
t(μ sec)	T°C (Calculated)	Air(°C)	Wall(°C)
1308	25.2	25.0	25.0
1367	0.0	0.0	0.0
1445	-28.7	-28.5	28.0
1501	-46.7	-46.3	46.1
1582	-69.3	-68.8	-66.5
1650	-85.7	-84.1	-82.0

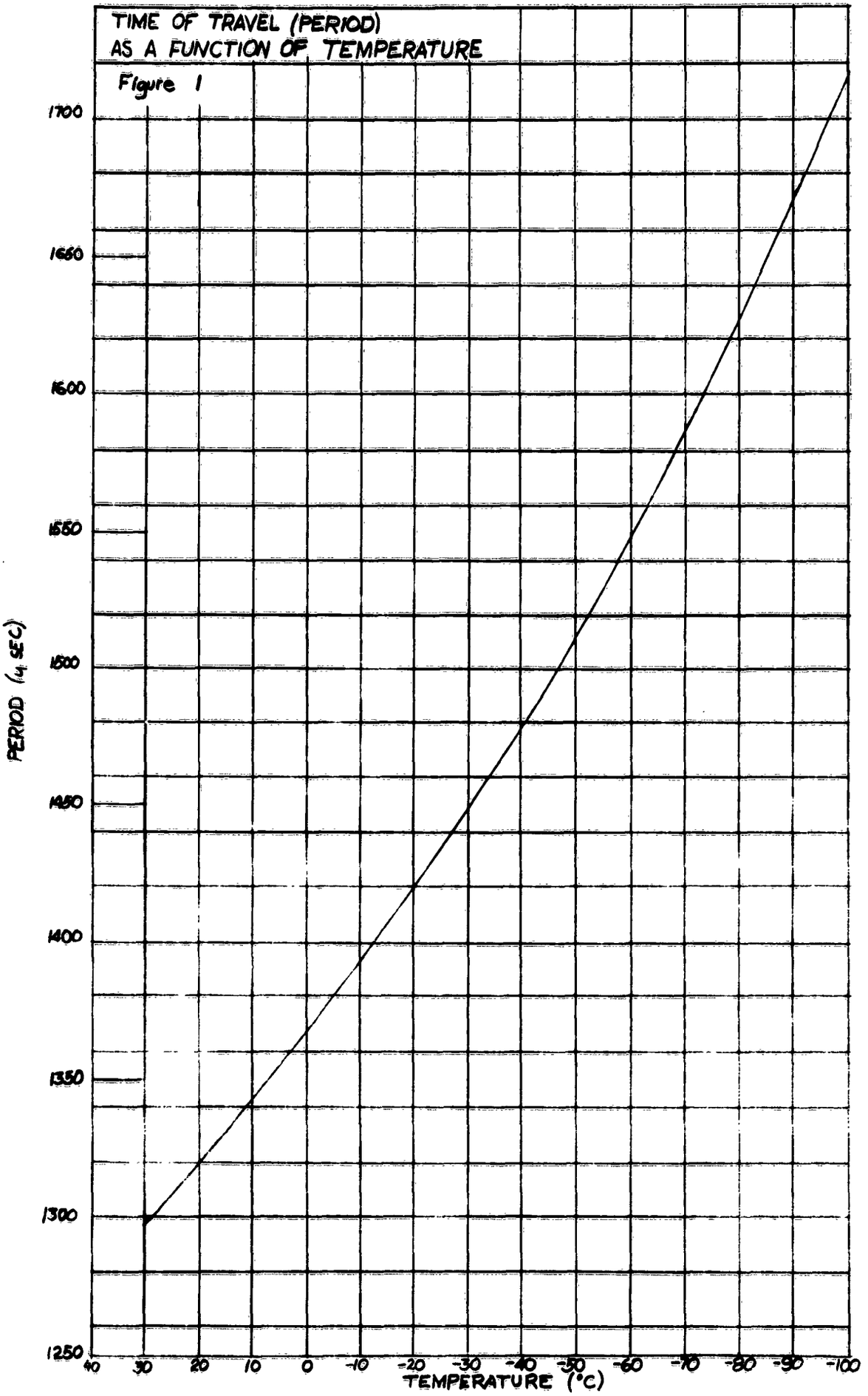
TIME OF TRAVEL (PERIOD)
AS A FUNCTION OF TEMPERATURE
Figure 1
PERIOD (4 SEC)
1700
1650
1600
1550
1500
1450
1400
1350
1300
1250
40
30
20
10
0
-10
-20
-30
-40
-50
-60
-70
-80
-90
-100
TEMPERATURE (°C)

Fig. 1

4. Acoustic Thermometer Circuits

A block diagram of the acoustic thermometer is shown in Fig. 2.

5. Remarks

The acoustic thermometer performs satisfactorily at a pressure of 670 mm Hg; however, when a pressure of the order of 1 mm of mercury is reached, the operation becomes unstable and erratic. It is hoped that these difficulties will be eliminated and that the acoustic thermometer will give accurate air temperature measurements within the chamber with an accuracy of $\pm 0.5^{\circ}C$ over the entire range of chamber temperatures at pressures ranging from 670 mm Hg to 1 mm Hg.

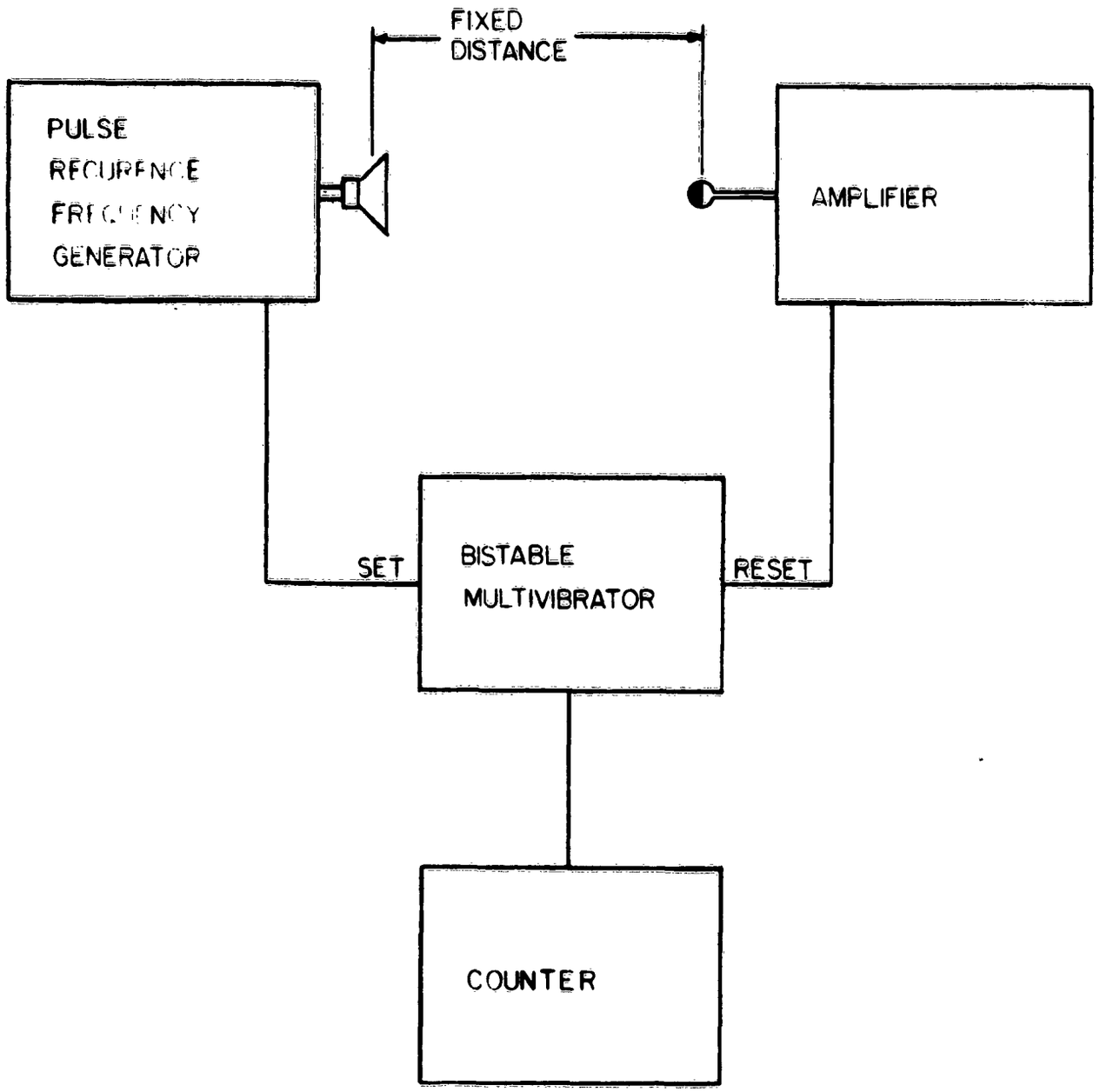
FIXED
DISTANCE
PULSE
RECURRENCE
FREQUENCY
GENERATOR
AMPLIFIER
SET
BISTABLE
MULTIVIBRATOR
RESET
COUNTER

Figure 2

DETERMINATION OF ATMOSPHERIC PARAMETERS

BY ACOUSTIC MEANS

DA-SIG-36-039-62-G17

Progress Report No. 1

July 1962

Section III

LABORATORY TESTING

Environmental Testing of the Sonotherm System

Paul K. Dano, Carlos McDonald,

Physicists

TEXAS WESTERN COLLEGE
EL PASO, TEXAS

SCHELLENGER RESEARCH LABORATORIES

TABLE OF CONTENTS

1. Introduction

The Sonotherm Flight Unit (Sec. II-6,7) in the upper atmosphere will encounter air density, thermal and wind effects (Sec. II-6, part 3) which can effect the range and accuracy of the acoustic measurements. This report summarizes the experiments performed in a climatic chamber in order to determine the magnitude of the above effects, and relates the experimental results with the theoretical predictions.

2. General Testing Procedure

Almost all of the environmental tests had the same general set-up; only the variation of environmental conditions such as pressure, temperature and wind velocity differentiated the experiments. Normally only the detection device consisting of the transducers and an adjustable rack mounting (Fig. 2-1) was subjected to the changing environment. The only other equipment in the chamber served to monitor temperature and wind.

The initial transducer spacing was set to a standard distance as measured by the standing wave frequency. The chamber was then sealed and the conditions varied. Thermocouples monitored the temperature of the air blast, the transducer face, the air directly behind the transducers, the air in other parts of the chamber and the chamber walls. A thermistor was used to monitor rapid changes in the air blast temperature, and a pitot tube was developed in order to monitor the wind velocity of the air blast.

The chamber set-up was continually refined to improve the reading accuracy and the actual conditions within the chamber.

The air blast was controlled and directed by a funneling system and directed perpendicularly to the propagation path of the sound between the transducers. Cams were designed to automatically control the temperature and pressure to simulate changing environmental conditions such as would be

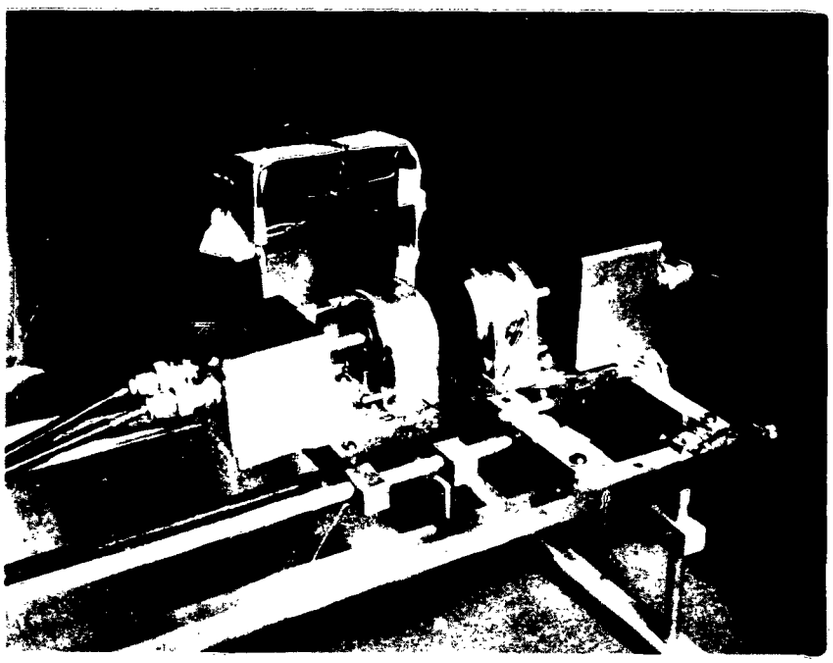

Sound Transducers on Mounting Rack

Fig. 4-1

encountered by a balloon moving upward through the atmosphere at a certain rate.

Section II, part 7, summarizes electronic circuitry and general testing procedure.

3. Air Density Effects

As described in Sec. II-6, part 5.4, the sound pressure detected by the receiver transducer is a function of the air density (or atmospheric pressure), the speed of sound, and the acoustical Q of the standing wave generated between the receiver-transmitter spacing. At high altitudes, the acoustical Q also reduces due to viscosity effects. As a result, the receiver sound pressure decreases with respect to altitude.

In the following sections, the expressions for the receiver sound pressure and acoustical Q as a function of density and atmospheric pressure are summarized. The theoretical predictions are then compared with the actual experimental results.

3.1 Receiver Sound Pressure

Referring to Section II-6, part 5.41, the sound pressure P_r, acting on the receiver face is given

$$P_r = \frac{P_s}{\cosh \alpha \ell} \qquad (3-1)$$

where P_s is the sound pressure generated at the transmitter face, α is the [illegible] absorption coefficient and ℓ is the receiver-transmitter spacing.

As shown in Sec. II-6, part 5.32, the transmitter sound pressure can be expressed by

$$P_s = k \rho_o c_o Q_A \qquad (3-2)$$

where

k is a proportionality constant,

ρ_o is the air density,

c_o is the local speed of sound, and

Q_A is the quality factor or Q of the acoustic standing wave. From equations 3–1 and 3–2, the receiver sound pressure can be expressed in terms of the acoustical Q and air density by

$$P_r = \frac{k\rho_o c_o Q_A}{\cosh \alpha \ell} \qquad (3\text{–}3)$$

The above expression can be written in terms of the atmosphere pressure if it is assumed that the propagation of sound in air is an adiabatic process. For this case (see Sec. II–6, part 4.2),

$$c_o = \sqrt{\frac{\gamma P_o}{\rho_o}} \qquad (3\text{–}4)$$

where P_o is the atmospheric pressure and γ is the ratio of specific heat at constant pressure to that at constant volume. Substituting equation 3–4 for ρ_o in equation 3.3, the receiver pressure can be expressed by

$$P_r = \frac{kQ_A\gamma P_o}{c_o \cosh \alpha \ell} \qquad (3\text{–}5)$$

3.2 Acoustical Q.

In the Sonotherm system, the receiver sound pressure amplitude is detected as a function of frequency. The acoustical Q or the quality factor is defined by (see Sec. II–6, part 4.9)

$$Q_A = \frac{f_o}{2\Delta f} \qquad (3\text{–}6)$$

where f_o is the acoustic antiresonant frequency corresponding to a maximum receiver sound pressure, and $2\Delta f$ is the frequency bandwidth about the frequency f_o, where the amplitude reduces by a factor of $1/\sqrt{2}$.

Referring to Sec. II–6, part 4.10, the quality factor Q_A is a measure of the sound energy losses related to the transducer geometry, wind, receiver face rigidity or loading, and sound absorption losses. It was also shown that the over–all quality factor, Q_A, could be expressed in terms of quality factors

related to the above individual energy losses by the expression (Sec. II-6, part 4.9)

$$Q_A = \frac{1}{\frac{1}{Q_g} + \frac{1}{Q_w} + \frac{1}{Q_r} + \frac{1}{Q_\alpha}} \qquad (3\text{-}7)$$

where Q_g, Q_w, Q_r, and Q_α are the quality factors related to the transducer geometry, wind, receiver loading, and sound absorption losses, respectively. Only the quality factors Q_r and Q_α vary with density or pressure (Sec II-6, Part 4.8):

$$Q_\alpha = \frac{\omega_o}{2c_o \alpha} \qquad (3\text{-}8)$$

$$Q_r = \frac{n \pi Z_r}{2\rho_o c_o S} \qquad (3\text{-}9)$$

where

ω_o = acoustic antiresonant angular frequency,

α = sound absorption coefficient,

Z_r = mechanical impedance of the receiver-transducer,

S = effective surface area of the receiver face.

The sound absorption coefficient at high altitudes is primarily determined by viscosity (Sec. II-6, part 4.1) and thermal conductivity effects. Referring to Hunt*, a good approximation for the sound absorption coefficient is

$$\alpha = \frac{\omega_o}{2\rho_o c_o^3} \left[\frac{4}{3}\eta + \frac{(\gamma - 1)k}{c_p} \right] \qquad (3\text{-}10)$$

where

η = coefficient of air viscosity,

k = thermal conductivity of air

c_p = specific heat at constant pressure.

*F. V. Hunt. "Propagation of Sound in Fluids." American Institute of Physics Handbook. D. E. Gray Co-ed. McGraw-Hill, 1957.

From equations 3-9 and 3-10, it follows that Q_α is proportional to the air density which decreases with altitude. The expression for α, equation 3-10, can be written in terms of the atmospheric pressure, P_o, by substituting equation 3-4 for P_o:

$$\alpha = \frac{\omega^2}{2\gamma P_o c_o} \left[\frac{4}{3}\eta + \frac{(\gamma-1)\, k}{c_p} \right] \qquad (3\text{-}11)$$

3.3 Predicted Variation

The expected variation of the receiver sound pressure and acoustical Q as a function of air density or atmospheric pressure are determined from the expressions given in Sec. 3.1 and 3.2, and from known reference values at a given altitude.

3.31 Acoustical Q

Assuming a constant descent or ascent rate the acoustic Q will only vary as a function of Q_α and Q_r. Consequencly Q_A (Eq. 3-7) can be expressed by

$$Q_A = \frac{1}{\frac{1}{Q_s} + \frac{1}{Q_\alpha} + \frac{1}{Q_r}} \qquad (3\text{-}12)$$

where

$$\frac{1}{Q_s} = \frac{1}{Q_g} + \frac{1}{Q_w} \qquad (3\text{-}13)$$

is a constant value. The expected values of Q_r, Q_α, and Q_s will now be calculated. The values of Q_α as a function of atmospheric pressure are shown in Table I as calculated from equations 3-8, 3-10 or 3-11 and from the typical conditions of the experiments (room temperature, variable pressure): *

$\gamma = 1.415$

$c_p = 0.2$ cal/g°C

$\eta = 1.83 \times 10^{-4}$ dynes/sec/cm^2

*L. L. Berenck. "Acoustic Properties of Gases." American Institute of Physics Handbook. D. E. Gray Co-ed. McGraw-Hill, 1957.

$k = 5.48 \times 10^{-5}$ cal/cm sec °C

$\omega = 2\pi f$

$f = 2.38 \times 10^{4}$ cps

$c_o = 3.4 \times 10^{4}$ cm/sec

TABLE I

P_o (mm Hg) Atmospheric Pressure	Q_α
664	2.28×10^{4}
100	3.43×10^{3}
10	3.43×10^{2}
1	3.43×10^{1}
0.1	3.43

It should be noted that the value of Q near room pressure (664 mm Hg) is approximate since molecular absorption has to be included.

Q_r (Eq. 3-9), the quality factor related to the receiver loading, can be determined from Eq. 3-9 if the mechanical impedance of the receiver is known. Referring to Sec. II-6, part 5.52, within the receiver mechanical bandwidth, tne mechanical impedance is approximately,

$$Z_r = \frac{\omega M}{Q_m} \qquad (3\text{-}14)$$

where ω is the angular frequency, M is the mass of the vibrating face and Q_m is its mechanical Q. The mass of the vibrating face is approximately

$$M = S\rho t \qquad (3\text{-}15)$$

where

S = surface area of the receiver face,

ρ = mass density of the vibrating face,

t = thickness of the vibrating face.

Substituting equations 3-14, 3-15 in equation 3-9, the expression for Q_r reduces to

$$Q_r = \frac{n\pi\rho\omega t}{2\rho_o c_o Q_m} \qquad (3\text{-}16)$$

where the measured receiver constants were

$$\rho = 2.7\ g_m/cm^3$$

$$t = .078\ \text{in.}$$

$$Q_m = 10.5$$

Table II shows the predicted values of Q_r with respect to atmospheric pressure (room temperature).

Table II

Po (mm Hg)	Qr
664	300
100	2×10^3
10	2×10^4
1	2×10^5
.1	2×10^6

Q_s, the constant quality factor as determined by the transducer geometry and wind effects (Eq. 3-13), can be calculated by a knowledge of the over-all acoustical Q (Q_A) at some given altitude. The measured value of Q_A at room pressure (667 mm Hg) was 73 (Sec. 3.4). Substituting this measured value for Q_A and the predicted values of Q_α and Q_r at room pressure from Tables I and II in Eq. 3-12, the value of Q_s was approximately,

$$Q_s = 96.5 \qquad (3\text{-}17)$$

The expected values of Q_A with respect to atmospheric pressure (constant temperature) are shown in Table III. These values were calculated by substituting the value of Q_s (Eq. 3-17) and the corresponding values of Q_α and Q_r from Tables I and II. in eq. 3-12.

Table III

Po (mm Hg)	Q_A
664	73
100	89.6
10	75
1	25.4
.1	3.31

3.32 Sound Pressure

The expected receiver sound pressure variation with respect to altitude can be determined from Equation 3.5 and the expected values of Q_A shown in Table III. The relative values of the sound pressure (assuming a constant input to the transmitter-transducer) are shown in Table IV.

Table IV

Atmospheric Pressure (mm Hg)	Rel. Sound Pressure
664	1
100	.18
10	.015
1	5.2×10^{-4}
.1	6.8×10^{-6}

3.4 Experimental Results

Various experiments were performed in the climate chamber in order to determine the variation of the receiver sound pressure as a function of air pressure or density expected in the upper atmosphere. In these experiments, the air temperature was kept constant (27°C) and the atmospheric pressure was reduced. The receiver sound pressure was recorded as a function of frequency, and the acoustical Q was determined from these values. The receiver-transmitter separation corresponded to one-half wavelength at 23.8kc, and a constant input to the transmitter-transducer was maintained.

Figure 3-1 shows the experimental and theoretical variation of the acoustical Q plotted as a function of atmospheric pressure. The discrepancy near room pressure is believed to be due to the fact that molecular absorption was neglected in calculating the theoretical value of the expected Q.

The predicted and actual variation of the receiver sound pressure as a function of atmospheric pressure is shown in Fig 3-2. The sound pressure is plotted relative to that obtained at room pressure, 664 mmH_g. At room pressure, the sound pressure recorded was approximately 3000 dyne cm^2.

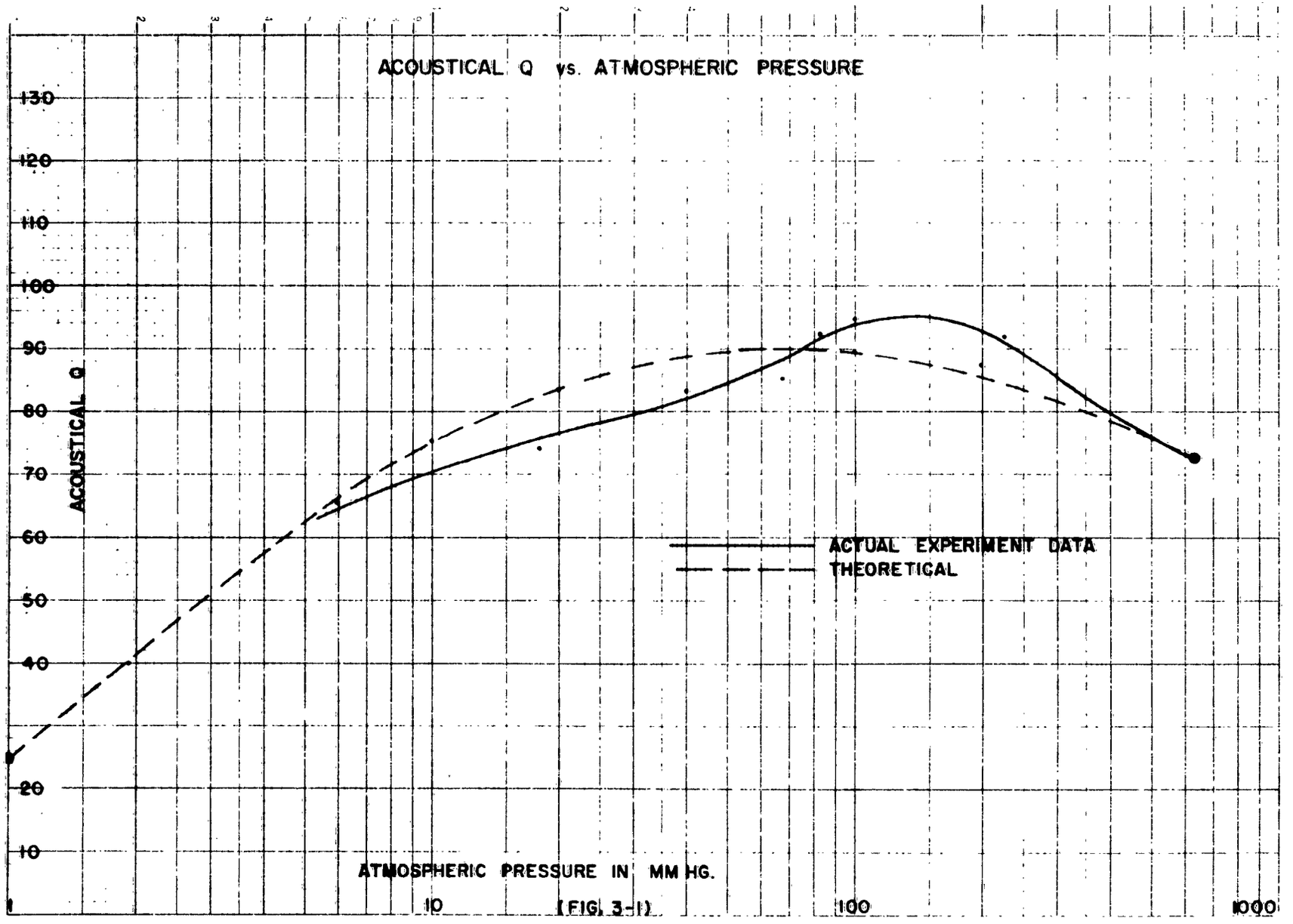
ACOUSTICAL Q vs. ATMOSPHERIC PRESSURE
ACOUSTICAL Q
130
120
110
100
90
80
70
60
50
40
20
10
ACTUAL EXPERIMENT DATA
THEORETICAL
ATMOSPHERIC PRESSURE IN MM HG.
1
10
100
1000

(FIG. 3-1)

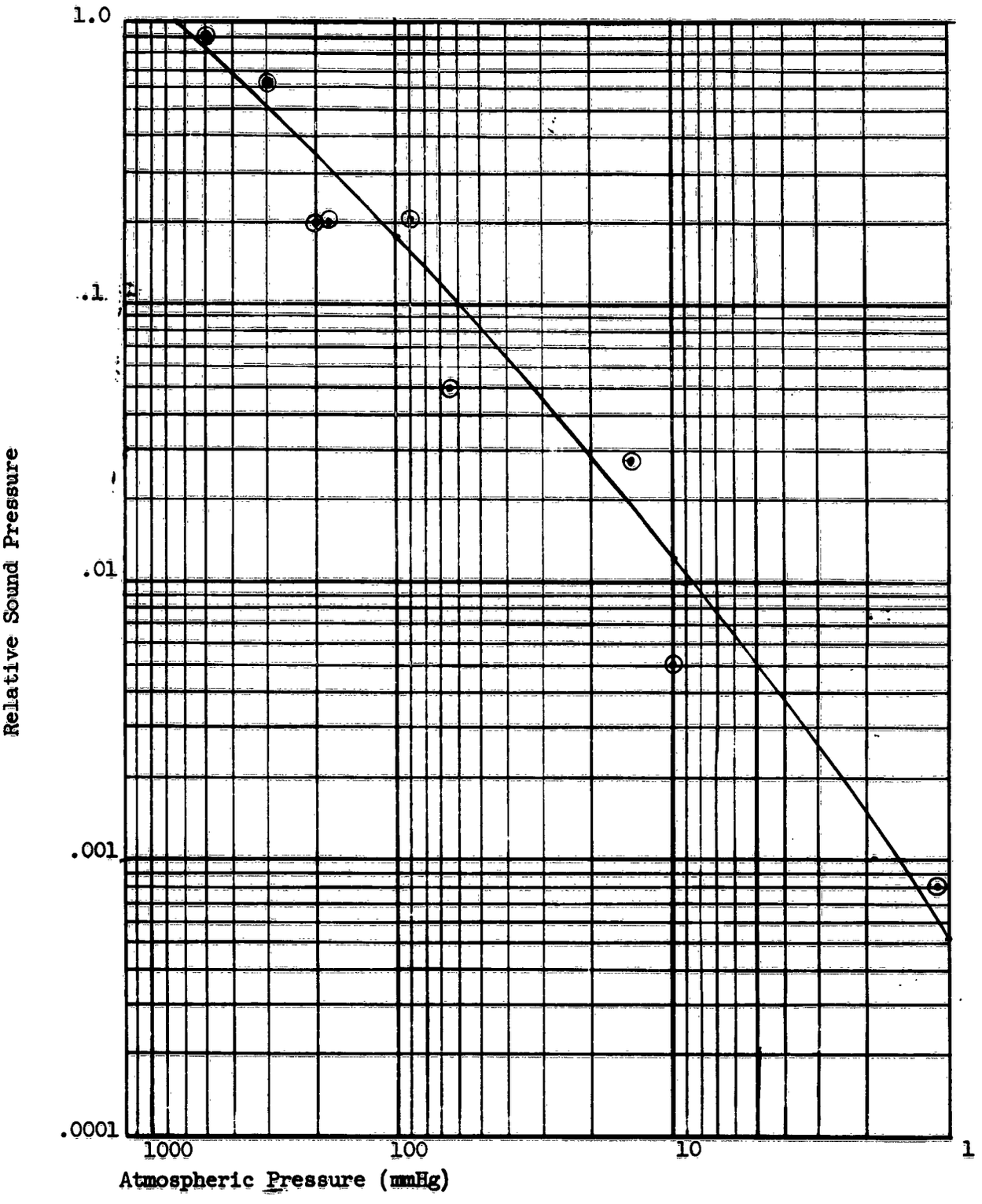

RELATIVE SOUND PRESSURE
vs.
ATMOSPHERIC PRESSURE

Fig. 3-2

4. Thermal Boundary Layer

The accuracy of the speed of sound measurements by the Sonotherm is primarily a function of the thermal effect related to the heating or cooling of stagnant layers of air, or thermal boundary layers, adjacent to the transducer faces. (Sec. II-6, part 3). Based on a theoretical description of the above effect (Secs. I-3, I-4, I-5), various experiments were performed in order to verify the functional dependence of the thermal boundary layer and to determine the error of the speed of sound measurements resulting from the thermal boundary layer.

4.1 General

As the transducers move through the atmosphere,

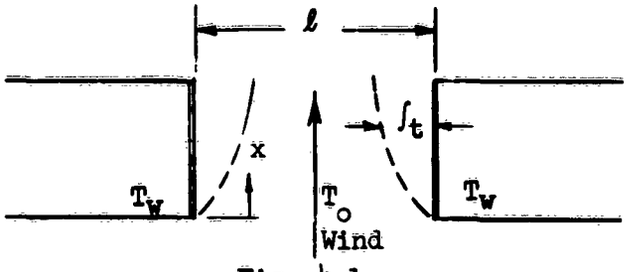

Fig. 4-1

a stagnant layer of air is formed adjacent to the transducer faces (Fig. 4-1) due to the effect of air viscosity. Since the temperature of the air medium will, in general, vary, a temperature difference between the air and the transducer faces will tend to exist, and its magnitude will depend on heat convection between the stagnant layer of air and the transducer faces (See Sections I-3, I-4). Due to this temperature difference, the stagnant layer tends to be heated or cooled, and its temperature will not correspond to that of air medium. Consequently, since the Sonotherm samples the speed of sound in the air medium between the transducer faces, an error will result in the speed of sound measurement.

4.2 Theoretical Relations

If the air between the transducer faces is at a uniform temperature corresponding to that of the undisturbed air medium, the acoustic antiresonant

frequency f_o, corresponding to a maximum receiver sound pressure and a maximum receiver output, is (Sec. II-6, part 4.7)

$$f_o = n \frac{C_o}{\ell} \qquad (4\text{-}1)$$

where n is the number of half wavelengths between the receiver-transmitter separation, ℓ, and C_o is the speed of sound of the undisturbed medium. However, as described in Section I-5, part 4.2, if a small temperature difference exists between the air and the transducer faces, and if the thermal boundary layer is less than the separation between the transducer faces, the acoustic antiresonant frequency will be

$$f = \frac{f_o}{1 - \frac{2 \int_t}{\ell} \sqrt{\frac{T_o}{T_w}}} \qquad (4\text{-}2)$$

where

$\int_t$ = thickness of the thermal boundary layer,

T_w = transducers' face temperature

T_o = air temperature

The thermal boundary layer corresponds approximately to the thickness of the stagnant layer of air where the temperature varies from the air temperature to the face of the transducer. Referring to Sec. I-3, the thermal boundary layer is given approximately by

$$\int_t = \frac{4.53}{\sqrt[3]{P_r}} \sqrt{\frac{\mu x}{\rho v}} \qquad (4\text{-}3)$$

Where μ is the dynamic viscosity, P_r is the prantle number, ρ is the air density, v is the stream velocity of the air medium with respect to the transducers, and x is the distance measured along the transducer face from the air intake (see Fig. 4-1).

From equations 4-1 and 4-2, the frequency error, $\Delta f = f_o - f$, resulting from the thermal boundary layer is

$$\Delta f = \frac{f_o K}{1-K} \qquad (4-4)$$

where

$$K = \frac{2\int_t}{\ell}\left(1 - \sqrt{\frac{T_o}{T_w}}\right)$$

If $\int_t < \ell$ and $T_o \cong T_w$, the frequency error is approximately,

$$\Delta f = \frac{\int_t \Delta T_g}{\ell T_o} f_o \qquad (4-5)$$

where $\Delta T_g = T_w - T_o$.

If f_o corresponds to the frequency of the actual undisturbed air temperature and f corresponds to the frequency of the apparent temperature T as determined by the uncorrected expression,

$$f = \eta \frac{c}{\ell} \quad , \qquad (4-6)$$

the temperature error measured by the Sonotherm is

$$\Delta T = T - T_o \qquad (4-7)$$

From equations 4-1 and 4-6, and since the speed of sound is proportional to the square root of the temperature, the frequency Δf is related approximately to the temperature error, ΔT, by

$$\Delta f = \frac{\Delta T}{2T_o} f_o \qquad (4-8)$$

if the temperature difference ΔT is small compared to T_o. From equations 4-5 and 4-8, it follows that the temperature error ΔT, resulting from the temperature difference between the air and the transducer faces, ΔT_g, is

$$\Delta T = \left(\frac{2\int_t}{\ell}\right) \Delta T_g \qquad (4-9)$$

Consequently, the temperature error measured by the Sonotherm is small if the thermal boundary layer is small compared to ℓ, the receiver-transmitter separation, and/or by decreasing the temperature difference ΔT_g (temperature lag) between the air and the transducer faces.

4.3 Test Description and Procedure

Various experiments were performed in the environmental chamber not only to verify the theoretical relationships described in the previous section, but also to determine the actual error of the experimental Sonotherm device resulting from the thermal boundary layer.

In order to accomplish the above objectives, the Sonotherm device was tested at various atmospheric pressures, and wind velocities. The air temperature was rapidly varied in order to establish a temperature difference between the transducer faces and the air temperature, and the acoustic antiresonant frequency was recorded as a function of the transducer face and air temperatures.

Figure 4-2 shows the experimental setup in the environmental chamber. In order to supply a steady air flow between the transducer faces, the air supply sent to the chamber was completely sealed off except for an area covered with an air duct. The air duct directed the air flow (generated by a fan capable of operating at two speeds) parallel to the transducer faces and normal to the sound propagation, and a pitot tube was used to measure the air velocity.

In order to produce large temperature differences between the air and the transducers, the transducers were covered with an insulating cover while the outside air temperature was rapidly varied. When the desired temperature difference was established, the cover on the transducers was lifted mechanically. Measurements were then performed as a function of the temperature difference between the air and the transducer faces. Various thermocouples and a thermistor were used to measure the transducer face and air temperatures.

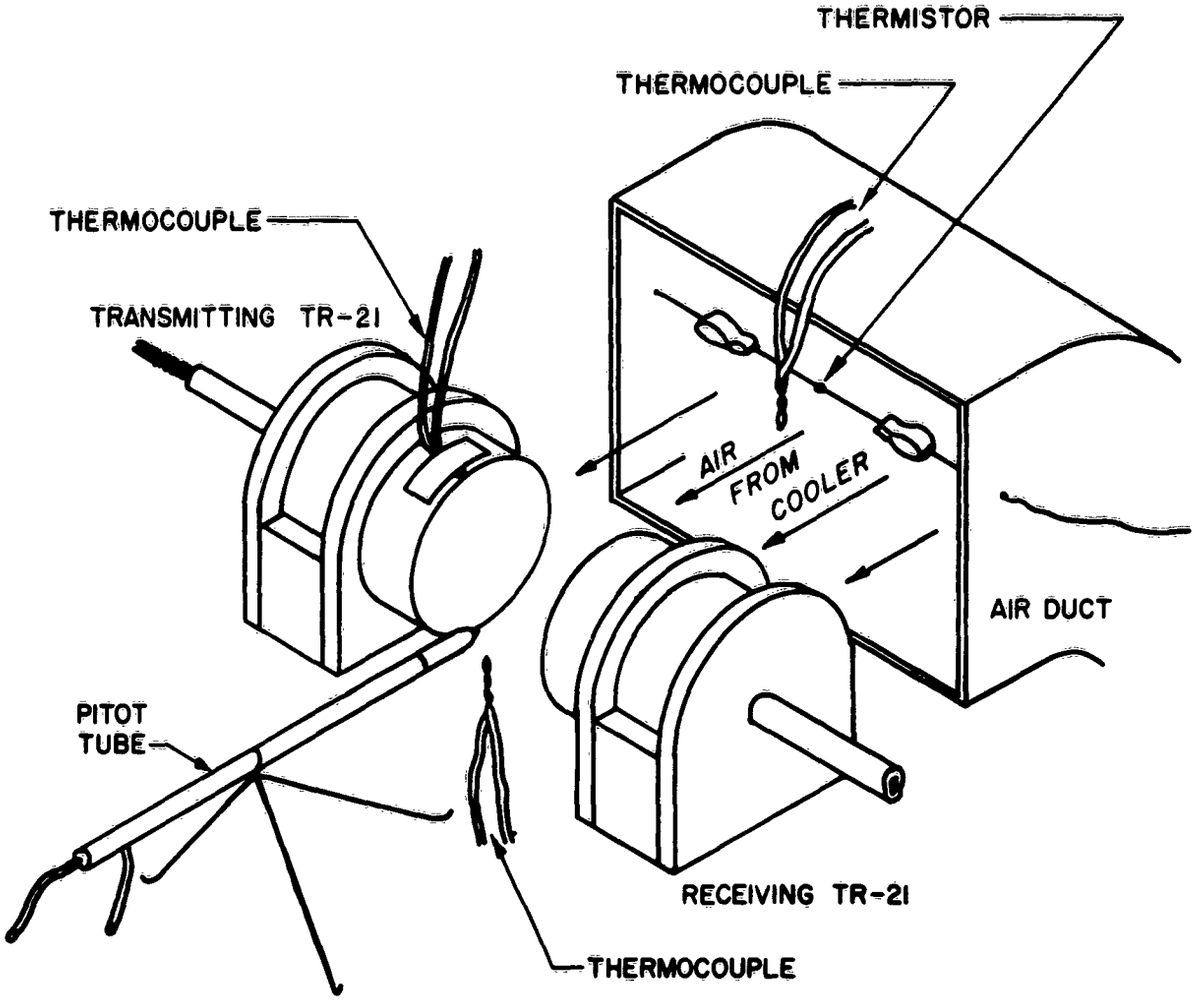

SONOTHERM TR-21 STANDING WAVE TRANSDUCERS AND ASSOCIATED TEST EQUIPMENT

FIG. 4-2

4.4 Experimental results and verification.

A series of experiments were first performed in order to verify the functional dependence between the acoustic antiresonant frequency error, Δf, the air density, wind velocity, and the temperature difference, ΔT_g, between the air and the transducer faces. From equation 4-5 this functional dependence can be expressed by the proportionality,

$$\frac{\Delta f}{\Delta T_g} \propto \frac{\int_{t_o}^{t}}{\ell}$$

If the receiver-transmitter spacing and air temperature are approximately constant, the above proportionality reduces to

$$\frac{\Delta f}{\Delta T_g} \propto \frac{1}{\sqrt{P_o v}} \qquad (4\text{-}10)$$

where P_o is the atmospheric pressure and v is the wind velocity. The above expression follows from equation 4-3, the ideal gas law, and the fact that the air viscosity is only a function of the air temperature which is assumed constant.

The proportionality given by equation 4-10 was verified by recording the frequency error Δf as function the temperature difference ΔT_g under different conditions of atmospheric pressure and wind velocity. Table V shows a summary of the experimental results.

Table V

EXP No.	Air Velocity (Ft/sec)	Atmospheric Pressure (mmHg)	$\Delta f/\Delta T_g$
1012	4.5	100	26.2
1011	11	100	16
1008	6.6	664	8.60
1010	40	664	3.65

The resulting ratios $\Delta f/\Delta T_g$ are in fair agreement with equation 4-10. For example, comparing the experiments at different wind velocities and

constant atmospheric pressure, the ratio of $\Delta f/\Delta T_g$ at 6.6 ft/sec to that at 40 ft/sec and 664 mmHg was

$$\left[\frac{\left(\Delta f/\Delta T_g\right)_{6.6}}{\left(\Delta f/\Delta T_g\right)_{40}}\right]_{664\text{mmHg}} = 2.36 \qquad (4\text{–}11)$$

At 100 mmHg, the ratio was

$$\left[\frac{\left(\Delta f/\Delta T_g\right)_{4.54}}{\left(\Delta f/\Delta T_g\right)_{11}}\right]_{100\text{ mmHg}} = 1.64$$

According to equation 4–10 and the values of the air velocities shown on Table V, the above corresponding ratios should theoretically be

$$\left[\frac{\left(\Delta f/\Delta T_g\right)_{6.6}}{\left(\Delta f/\Delta T_g\right)_{40}}\right]_{664\text{ mmHg}} = 2.46 \qquad (4\text{–}12)$$

$$\left[\frac{\left(\Delta f/\Delta T_g\right)_{4.54}}{\left(\Delta f/\Delta T_g\right)_{11}}\right]_{100\text{ mmHg}} = 1.56$$

Thus, the theoretical and actual results are in fair agreement. In the same manner, the effect of atmospheric pressure can be determined by comparing the ratio of $\Delta f/\Delta T_g$ of exp. No. 1012 to that of exp. No. 1008, and the ratio of of $\Delta f/\Delta T_g$ of exp. No. 1011 to that of exp. No. 1010. The actual ratios were:

$$\frac{\left(\Delta f/\Delta T_g\right)_{100\text{mmHg, }4.54\text{ ft/sec}}}{\left(\Delta f/\Delta T_g\right)_{664\text{mmHg, }6.6\text{ ft/sec}}} = 3.05 \qquad (4\text{–}13)$$

$$\frac{\left(\Delta f/\Delta T_g\right)_{100\text{mmHg, }11\text{ ft/sec}}}{\left(\Delta f/\Delta T_g\right)_{664\text{mmHg, }40\text{ ft/sec}}} = 4.38$$

From equation 4–10, the theoretical ratios are

$$\frac{\left(\Delta f/\Delta T_g\right)_{100\ \text{mmHg},\ 4.54\ \text{ft/sec}}}{\left(\Delta f/\Delta T_g\right)_{664\ \text{mmHg},\ 6.6\ \text{ft/sec}}} = 3.12$$

$$\frac{\left(\Delta f/\Delta T_g\right)_{100\ \text{mmHg},\ 11\ \text{ft/sec}}}{\left(\Delta f/\Delta T_g\right)_{664\ \text{mmHg},\ 40\ \text{ft/sec}}} = 4.92 \qquad (4\text{–}14)$$

Comparing the ratios given by equations 4–3 and 4–14, it can be seen that the actual results are in fair agreement with the theoretical results.

A second series of experiments were performed in order to determine the temperature error of the Sonotherm device as a function of thermal boundary layer and the temperature difference between the air and the transducer faces. A typical result is shown in Fig. 4–3. The actual temperature error at (the difference between the air temperature and the temperature predicted from acoustic antiresonant frequency) is plotted as a function of the temperature difference, or lag, between the air and the transducer faces, ΔT_g, for the conditions specified in the figure. The average slope, $\Delta T/\Delta T_g$, is approximately

$$\Delta T/\Delta T_g = 0.43 \qquad (4\text{–}15)$$

Since the temperature difference ΔT_g is small compared to the absolute air temperature, the above ratio is related to the thermal boundary layer $\int_t$ and the receiver–transmitter separation, ℓ, by equation 4–9:

$$\frac{\Delta T}{\Delta T_g} \doteq \frac{2 \int_t}{\ell} \qquad (4\text{–}16)$$

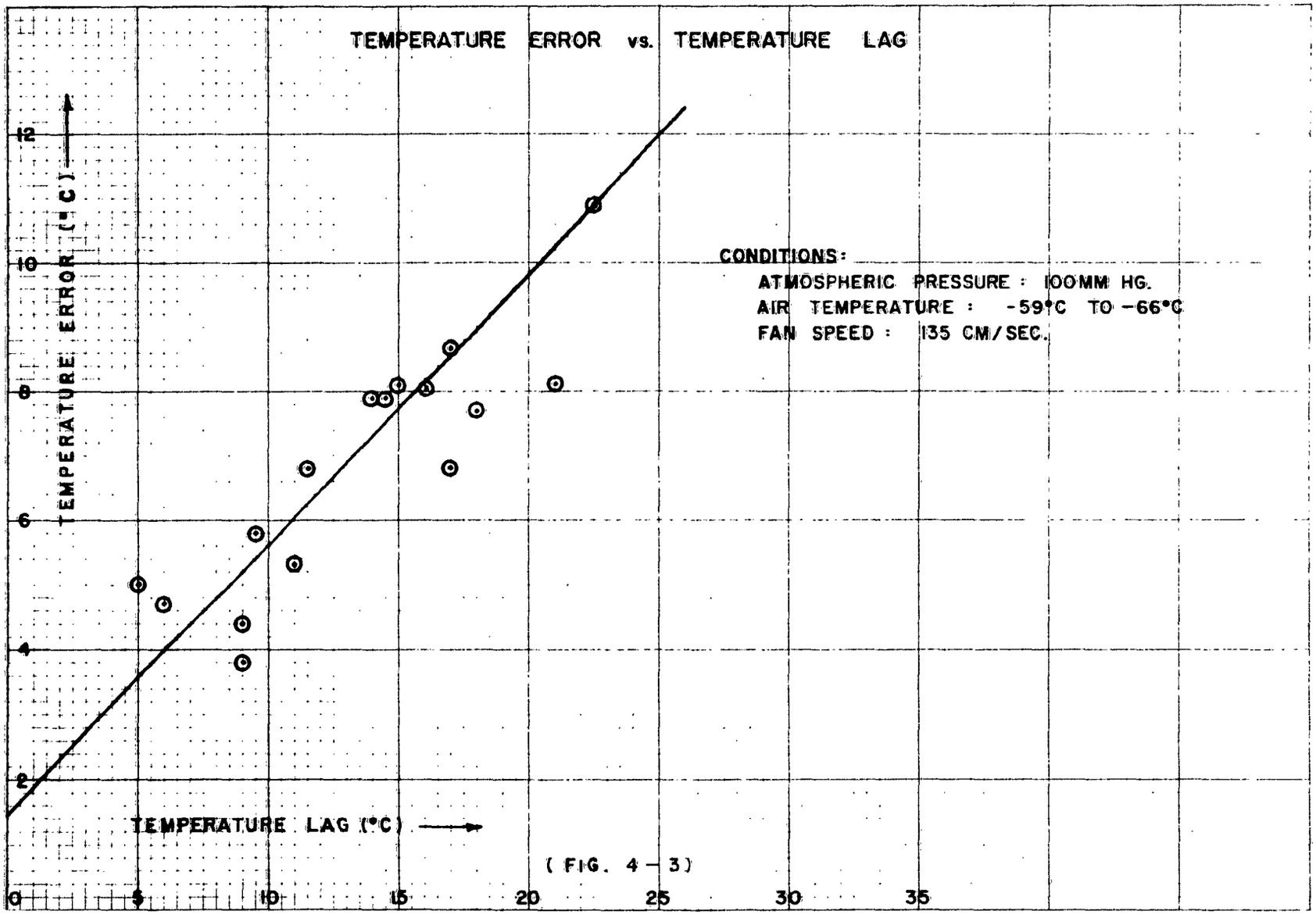
TEMPERATURE ERROR vs. TEMPERATURE LAG
TEMPERATURE ERROR (°C)
TEMPERATURE LAG (°C)
CONDITIONS:
ATMOSPHERIC PRESSURE : 100MM HG.
AIR TEMPERATURE : -59°C TO -66°C
FAN SPEED : 135 CM/SEC.
0
5
10
15
20
25
30
35
2
4
6
8
10
12

(FIG. 4 – 3)

The above ratio can be calculated since the boundary layer can be approximately determined from equation 4-3 and the separation ℓ was known. From the actual conditions of the experiment,

$$*u = 1.4174 \times 10^{-4} \text{ dyne sec/cm}^2$$

$$*Pr = 0.739$$

$$x = 3.18 \text{ cm}$$

$$v = 135 \text{ cm/sec}$$

$$\ell = 1.59 \text{ cm}$$

$$\rho = 1.9317 \times 10^{-4} \text{ gr/cm}^3$$

where the value of x was assumed to correspond to the diameter of the transducer face. From the above values and equation 4-3

$$\int_t = 0.657 \text{ cm}$$

Substituting the above value of $\int_t$ and ℓ in equations 4-15 and 4-16, the calculated value of $\Delta T/\Delta T_g$ is 0.413, which is in fair agreement with the actual measured values.

4.5 Temperature Lag of Transducers

As seen in the previous section, the temperature error of the Sonotherm resulting from the thermal boundary layer is dependent on the magnitude of the temperature lag of the transducers or the temperature difference between the air and the transducer faces. The temperature lag is a function of the thermal properties of the air and of the transducers, and the rate of ascent or descent (see Sections I-3, I-4). In order to determine the magnitude of the temperature lag, the transducers where subjected in the environmental chamber to the temperatures and pressures encountered by a balloon-borne instrument ascending at a rate of

*R. J. List. "Meteorological Data." American Institute of Physics Handbook, D. E. Gray Co-ed. McGraw Hill, 1957.

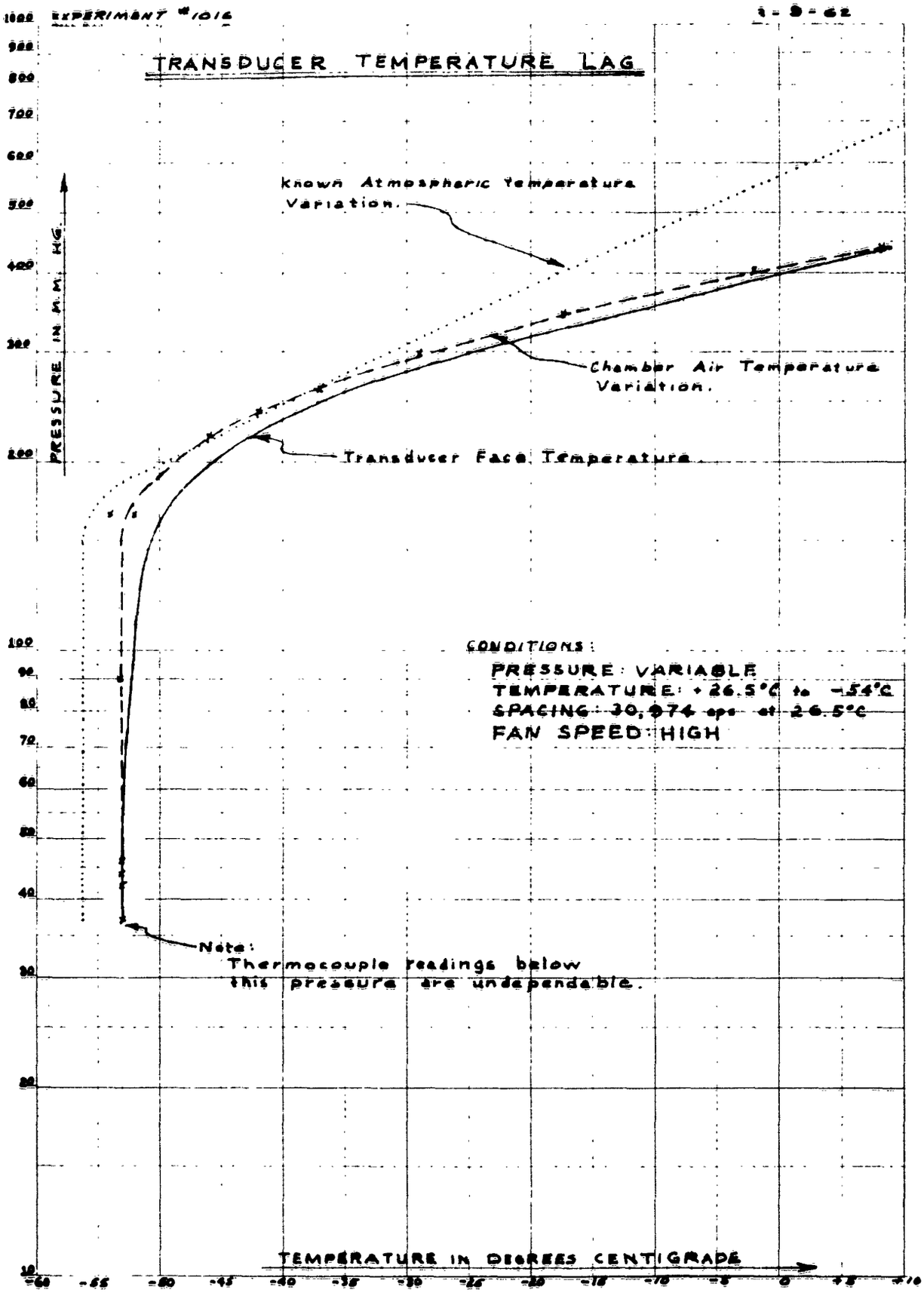
EXPERIMENT #1016
1-9-62
TRANSDUCER TEMPERATURE LAG
PRESSURE IN M.M. HG.
1000
900
800
700
600
500
400
300
200
100
90
80
70
60
50
40
30
20
10
known Atmospheric Temperature Variation.
Chamber Air Temperature Variation.
Transducer Face Temperature.
CONDITIONS:
PRESSURE: VARIABLE
TEMPERATURE: +26.5°C to -54°C
SPACING: 30,074 cps at 26.5°C
FAN SPEED: HIGH
Note:
Thermocouple readings below this pressure are undependable.
TEMPERATURE IN DEGREES CENTIGRADE
-60
-55
-50
-45
-40
-35
-30
-25
-20
-15
-10
-5
0
+5
+10

figure 4-4

1000 ft/min.

Figure 4-4 presents the results of such a test. The air and the transducer face temperature is plotted as function of atmospheric pressure. The maximum temperature difference between the air and the transducer faces was about 3°C up to atmospheric pressures of 37 mmHg (60,000 feet). This would result in a calculated temperature error of approximately 1 degree. The results are in fair agreement with theoretical calculations (Section I-4), although the air velocity in this experiment could not be controlled exactly.

The thermal lag at lower atmospheric pressures, corresponding to altitudes above 60,000 feet, was not investigated since the temperature readings of the thermocouples become undependable due to radiation effects. A more reliable acoustic method for temperature measurements inside the climatic chamber is presently under development (Section II-9).

As mentioned in Section I-4, the temperature lag of the transducer faces can be minimized by reducing their heat capacity by increasing the ratio of their surface area to thickness dimension.

5. Wind Effects

Two wind effects (Section II-6, part 3) on the Sonotherm were investigated: (a) The variation of acoustic Q with respect to wind velocity and (b) the variation of the noise level as a function of wind velocity. These experiments were conducted in a wind tunnel (located at White Sands Missile Range) where the wind velocity could be varied and accurately measured.

5.1 Acoustical Q

As shown previously in part 3.2, the acoustical Q of the standing wave, Q_A, varies as (equation 3-7)

$$Q_A = \frac{1}{\frac{1}{Q_g} + \frac{1}{Q_w} + \frac{1}{Q_r} + \frac{1}{Q_\alpha}} \qquad (3\text{-}7)$$

where Q_g, Q_w, Q_r and Q_α are the quality factors related to the acoustic energy losses resulting from the transducer geometry, wind, receiver loading and sound absorption losses, respectively.

The acoustic energy losses resulting from the wind stem from the fact that the air flow (assumed parallel to the transducer faces) removes part of the acoustic energy (Section II-6, part 4.9). As a result, the Q of the acoustic standing wave is reduced.

In the experiments performed, all parameters were kept constant except the magnitude of the wind velocity. Referring to equation 3-7, the variation of the acoustic Q can be assumed to be

$$Q_A = \frac{1}{\frac{1}{Q_c} + \frac{1}{Q_w}} \qquad (5\text{-}1)$$

where

$$\frac{1}{Q_c} = \frac{1}{Q_g} + \frac{1}{Q_r} + \frac{1}{Q_\alpha}$$

is constant. The variation of Q_w with respect to wind velocity can be determined from the basic definition of Q (Section II-6, part 4.9)

$$Q_w = 2\pi \cdot \frac{\text{Energy stored}}{\text{Energy lost/ cycle}} \qquad (5\text{-}2)$$

Assuming that the energy loss to be small,

$$\begin{aligned} \text{Energy stored} &= EV_t \\ \text{Energy lost} &= EV_\ell \end{aligned} \qquad (5\text{-}3)$$

where

E = energy density between the faces

V_t = volume between the faces of the transducers, and

V_ℓ = displaced volume containing energy lost due to the wind.

Figure 5-1 shows the volume V_t enclosed by the circular faces of the TR-21 transducers, and the Volume V_ℓ (the difference between the solid and dashed volumes) of acoustic energy displaced by

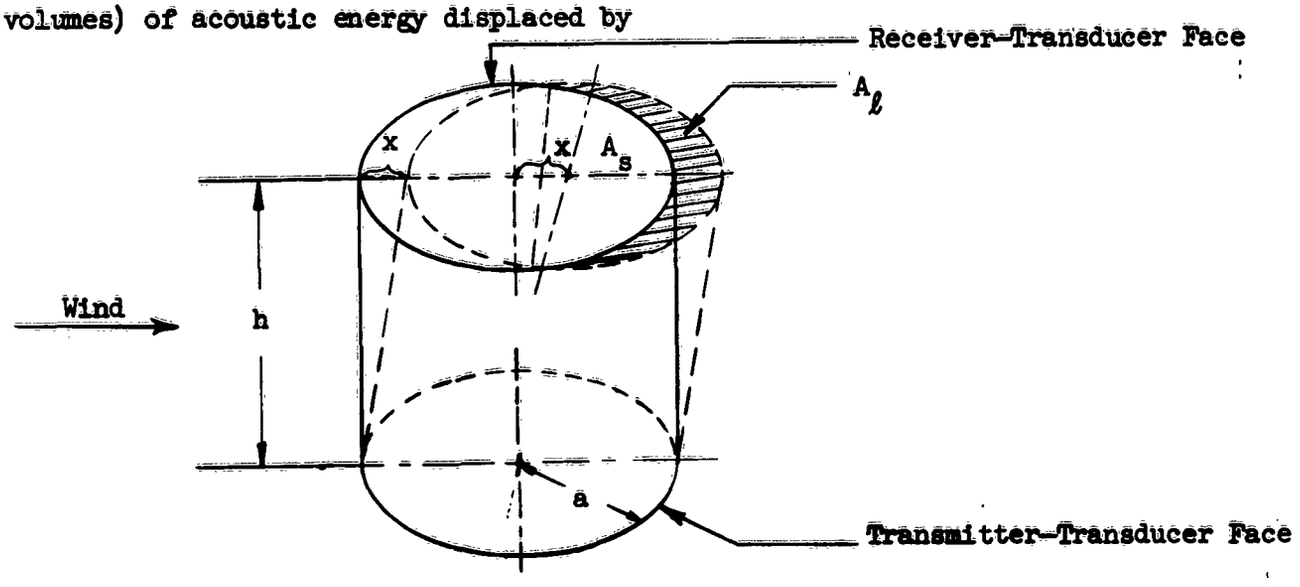

Fig. 5-1

the air flow assumed parallel to the transducer faces. The distance x corresponds to the lateral displacement of the plane wave by the wind during the time interval when it is propagating from the transmitter to the receiver. If c is the speed of sound and v is the wind velocity, the displacement x is

$$x = hv/c \qquad (5\text{-}4)$$

where h is the separation between the transducers. The volume V_t is

$$V_t = A_t h \qquad (5\text{-}5)$$

where A_t is surface area of the transducer faces:

$$A_t = \pi a^2, \qquad (5\text{-}6)$$

and "a" is the radius of the face. V_ℓ, the volume containing the energy lost is

$$V_\ell = A_\ell \, h/2 \qquad (5\text{-}7)$$

and

$$A_\ell = A_t - 2A_s \qquad (5\text{-}8)$$

where A_ℓ is the shaded area (Fig 5-1) outside the receiver face and A_s is the area of the segment defined by the intersection of the dashed and solid circles. The area of the segment is*

$$A_s = a^2\cos^{-1}(x/2a) - 1/2\ x\sqrt{a^2-(x/2)^2} \qquad (5\text{-}9)$$

From equations 5-3, 5-5, and 5-7 the energy stored is

$$\text{Energy stored} = EA_t h \qquad (5\text{-}10)$$

the energy lost is

$$\text{Energy lost} = \frac{EA_\ell h}{2} \qquad (5\text{-}11)$$

If λ is the wavelength of sound, the energy lost per cycle is

$$\text{Energy lost per cycle} = \frac{EA_\ell h}{2}\left(\frac{\lambda}{h}\right) = EA_\ell hn \qquad (5\text{-}12)$$

since h, the receiver transmitter separation, corresponds to an integral number n of half-wavelengths.

From equations 5-2, 5-10 and 5-11, the quality factor Q_w is

$$Q_w = 2\pi n\frac{A_t}{A_\ell} \qquad (5\text{-}13)$$

Substituting equations 5-6, 5-8 and 5-9 for A_t and A_ℓ, and equation 5-4 for x, the quality factor as a function of wind velocity is

$$Q_w = 2\pi n\ \frac{\pi a^2}{a^2 - 2a^2\cos^{-1}\frac{hv}{2ac} + \frac{hv}{c}\sqrt{a^2-\left(\frac{hv}{2c}\right)^2}} \qquad (5\text{-}14)$$

If the wind velocity is less than the speed of sound, the above expression reduces to

$$Q_w = 2\pi n^2\left(\frac{ac}{hv}\right) \qquad (5\text{-}15)$$

*Rinehart Mathematical Tables, "Formulas and Curves", Rinehart and Co., Inc. New York, 1957.

The values used in the experiment were as follows:

$a = 0.651$ in.

$h = 3/2\lambda$ at 22615 cps

$n = 3$

$c = 716$ mph

Substituting the above values in equation 5-15, the value of Q_w as a function of wind velocity was

$$Q_w = \frac{3.37 \times 10^4}{v} \qquad (5\text{-}16)$$

Where v is in mph. At zero wind velocity, the overall Q, Q_A was 43. Therefore, from equations 5-1 and 5-16, the variation of the overall acoustic Q was

$$Q_A = \frac{1}{\frac{1}{43} + \frac{v}{3.3 \times 10^4}} \qquad (5\text{-}17)$$

Figure 5-2 shows the actual and theoretical variation of the acoustic Q

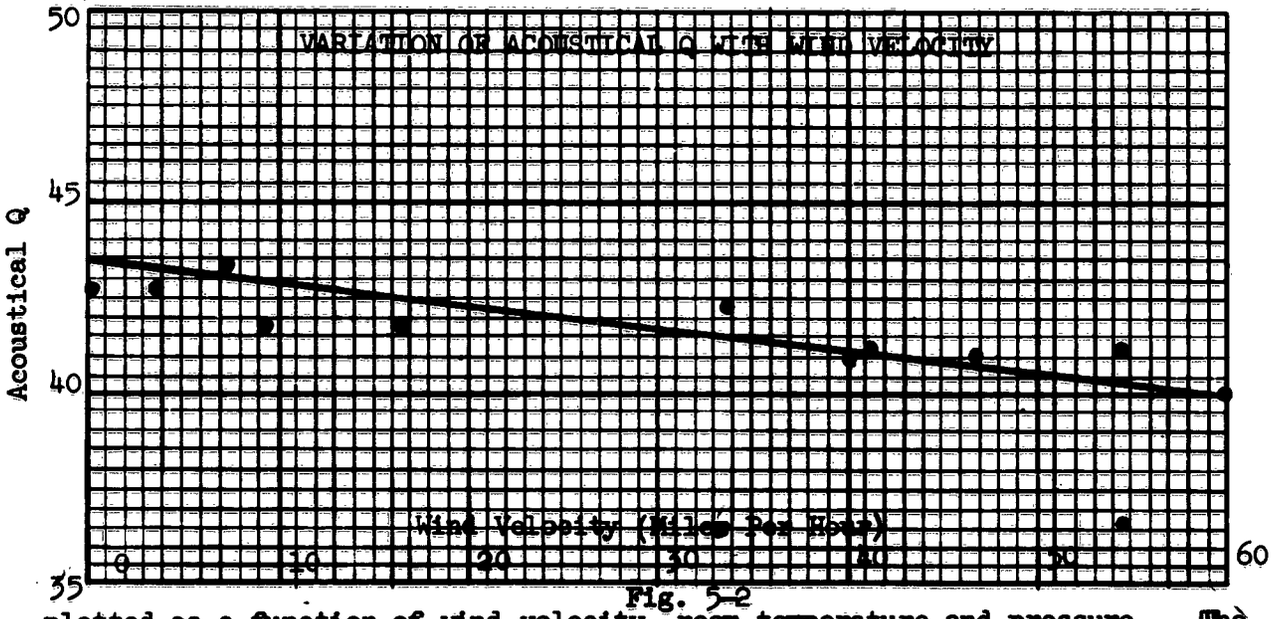

Fig. 5-2

plotted as a function of wind velocity room temperature and pressure . The theoretical variation corresponds to the solid curve as determined by equation 5-17. Good agreement was obtained between the theoretical and measured results except for wind velocities greater than 45 mph where turbulence occurred.

5.2 Noise

In conjunction with the above experiments where the variation of the acoustical Q was measured as a function of wind velocity, the receiver noise was also measured.

As previously mentioned in Section II-6, part 3.2, if the wind flow past the transducer faces is laminar, the noise detected by the receiver will be due mainly to the thermal agitation of the air molecules. However, once the air flow becomes turbulent, the noise increases rapidly as a function of wind velocity.

Figure 5-3 shows the noise (dynes/cm^2) detected by the TR-21 receiver transducer as a function of wind velocity (room temperature and pressure). Above 45 mph, the wind flow became turbulent and receiver noise increased rapidly. Below this velocity, the noise was negligible as theoretically predicted. Besides the degree of surface roughness, the transition wind velocity

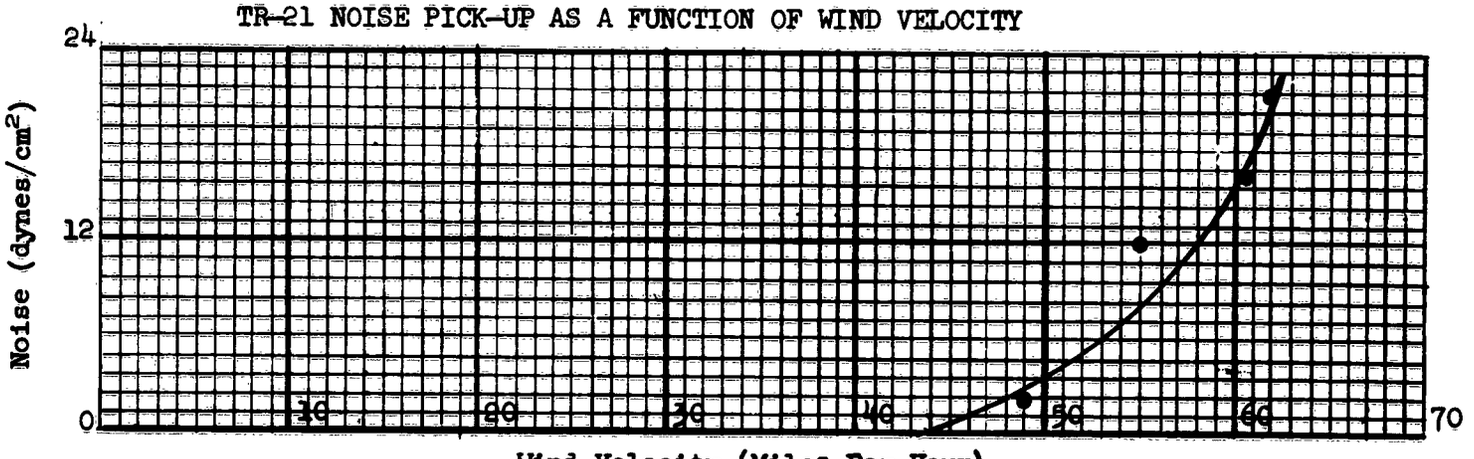

Fig. 5-3

is related to the Reynolds number which is proportional to the air density and the distance from the leading edge of the air intake (Section II-6, parts 3.22, 3.23). Therefore, the Sonotherm is capable of operating under high wind velocities in the upper atmosphere where the air density is reduced.

6. Conclusion:

The overall system meets the theoretical expectations as evident in the preceding discussion. Various improvements which will improve its operation are: (a) increasing the mechanical-electrical bandwidth of the transducers in order to insure the predominance of the acoustical signal variation with respect to frequency; (b) development of a more sensitive, wide-band receiver in order to increase the operating altitude range; (c) decreasing the operating frequency range in order to reduce sound absorption and dispersion effects; (d) mounting the transducers such that their separation is not effected by temperature changes; and (e) reducing the heat capacity of the transducer faces in order to minimize thermal boundary layer effects.

As indicated from the experimental results, the ultimate objective of the Sonotherm system - performing acoustic measurements in the upper atmosphere - is feasible, and indications thus far do not point to any serious obstacles in its future development.

DETERMINATION OF ATMOSPHERIC PARAMETERS BY ACOUSTIC MEANS

Progress Report No. 1

July, 1962

Section IV

FUTURE RESEARCH AND DEVELOPMENT PLANS

Carlos McDonald

IV. Future Research and Development Plans

The major effort will be concentrated toward the completion of the Sonotherm system utilizing balloon-borne instrumentation. Completion of the Sonotherm system will require:

1. Final design and construction of the Sonotherm flight unit;
2. Adapting the flight unit to the meteorological Rawin set GMD-1 telemetry system available at Schellenger Research Laboratories;
3. Final design and construction of the Ground Detection System;
4. Calibration and environmental testing of the flight unit;
5. Actual flight tests up to altitudes of 90,000 feet.

At the same time, theoretical and experimental studies will continue with the aim of determining the maximum amount of information about the atmosphere from acoustic measurements, improving the accuracy and range of the Sonotherm system, and investigating other acoustic techniques and devices for performing accurate acoustic measurements in the upper atmopshere.